Mechanistic characterisation of Activin/Smad and PI3K/mTOR Crosstalk during the Specification of Definitive Endoderm from Human Embryonic Stem Cells

Jason Shu Lim Yu

Thesis submitted towards the fulfilment of the degree of

Doctor of Philosophy

Institute of Reproductive and Developmental Biology

Department of Surgery and Cancer

Faculty of Medicine

Imperial College London

June 2015

Abstract

During the course of development, specification of the three embryonic germ layers, ectoderm, mesoderm and definitive endoderm (DE), is a critical process by which pluripotent cells acquire the temporal and spatial information needed to form specialised tissues. Of these initial germ layers, the DE arises during gastrulation, which latterly gives rise to the liver, pancreas, lung and epithelial lining of the digestive tract. Elucidation of the molecular mechanisms that govern DE specification not only facilitates our understanding of developmental biology but also aids in the differentiation of human pluripotent stem cells to specific cell types for disease modelling and regenerative therapies. DE formation is largely driven by the cooperation of Activin/Nodal and Wnt/β-catenin signalling, however recent evidence has additionally implicated PI3K/Akt signalling in modulating this process. Although it has been previously reported that PI3K activation acts to antagonise the *in vitro* differentiation of DE, the molecular mechanisms responsible for this effect remains unclear. To address this issue, this study utilises pluripotent human embryonic stem cells (hESCs) as an *in vitro* model to interrogate the molecular underpinnings of DE formation through a fully defined differentiation protocol. Modulation of PI3K activity was found to reciprocally downregulate the activation of Smad2/3, which was mitigated in the presence of the PI3K inhibitor LY294002 (LY). Suppression of PI3K/Akt signalling prolongs the activation of Smad2/3 in response to Activin, promoting their nuclear accumulation and the enhancement of transcriptional activity, resulting in the upregulation of mesendoderm and DE gene expression. Activation of PI3K negatively impacts the activity of Smad2/3 via phosphorylation of the Smad2/3 linker T220/T179 residue, which is fully independent of Erk and CDK activity. Phosphorylation of this residue induces the recruitment of the E3 ubiquitin ligase Nedd4L to activated Smad2/3, which in turn promotes their ubiquitin-mediated degradation and attrition of activity. Inhibition of mTORC2 activity by both inhibitor supplementation and genetic manipulation, rather than modulation of Akt or mTORC1 activity, recapitulates the LY-mediated reduction of T220/T179 phosphorylation and increases the duration of Smad2/3 transcriptional activity, promoting a more robust mesendoderm and endoderm differentiation. These findings reveal a new and novel connection between the PI3K/mTOR and TGFβ/Activin pathways, which will greatly impact our understanding of both cell fate determination and the preservation of normal cellular functions. Notably, identification of mTORC2 as a key player in the regulation of this differentiation provides new avenues through which hESCs differentiation protocols can be improved for both regenerative and biomedical applications.

Statement of Originality

I hereby certify that I am the sole author of this thesis and that all the experiments presented here were conducted by me unless otherwise stated below.

Specifically, Dr. Thamil Ramasamy performed all the experiments presented as part of the introduction to Chapter 3 (Figure 3.1) with the exception of Figure 3.1D which was performed by myself. Mr. Nick Murphy performed site-directed mutagenesis of Flag-Smad2-WT to Flag-Smad2-T220V under the supervision of Dr. Rafal Czapiewski, Dr. Wei Cui and myself. Dr. Rafal Czapiewski also conducted the cloning and synthesis of recombinant GST-Flag-Smad2-WT/T220V for use in kinase assays. Mr. Shikhai Wei assisted in the experiment interrogating the effect of Smad2 activation upon Nedd4L recruitment (Figure 5.5), whilst Miss Marie Holt performed immunoblotting to assess the response of PC-3 cells to Activin and LY treatment (Figure 5.1F) under my supervision.

Copyright Declarations

Acknowledgements

Firstly, I am eternally grateful to my supervisor, Dr. Wei Cui, who has provided me with the very best supervision, training and advice throughout the course of my PhD. Her passion for scientific excellence and boundless enthusiasm throughout this this project is something I will do my utmost to aspire to emulate. Secondly, I would like to extend my gratitude to past and present members of the lab who have contributory greatly to my scientific development, as well as providing much needed support in times of difficulty or trouble. Specifically, I would like to thank Dr. Thamil Ramasamy and Dr. Fiona Sewell (née Lamont) for their patience and excellent tuition upon my initial arrival at this lab, as well as Dr. Patrick Ovando-Roche and Shuchen Zhang for being the very best of companions throughout the course of this journey. I would also like to show my appreciation for Shikhai Wei, Marie Holt, and Nick Murphy, diligent and gifted students who I have had the pleasure of supervising, as well as Dr. Rafal Czapiewski for their consistent interest and critical contribution to this project, which would no doubt be less of a success in their absence. Thirdly, I would like to thank Dr. Nick Dibb, Dr. Robert Krypta, Dr. Tristan Rodriguez, Dr. Veronique Azuara, Prof. Eric Lam, and Prof. Vasso Episkopou for their insightful discussions and the valuable advice they have offered at various stages of the study, as well as the Medical Research Council UK (MRC-UK) for supporting me financially throughout the course of this study. I would also like to extend my thanks to my examiners Dr. Ana Costa-Pereira and Dr. Ludovic Vallier for providing remarkable insights and positive suggestions to improve the quality of this thesis.

Lastly, I would also like to thank my family and friends who have provided support in one form or another throughout this journey. To my parents, thank you both for always believing in the path I have chosen for myself no matter how different or difficult it may seem and to my sister, for being that constant companion whom I could always trust and confide in. Lastly and most importantly, I would like to thank my girlfriend, Ming-yee Li, who has always supported me through the good and difficult times, and who without I would not be the person I am today. Thank you for always trusting and assuring me of my success no matter how hard it gets.

Dedicated to the
Loving Memory of My Grandma

You left me beautiful memories,
your love is still my guide,
and though I cannot see you,
you're always by my side.

Table of Contents

Tables and Figures

Chapter 1

Chapter 3

Chapter 4

Chapter 5

Chapter 6

Chapter 7

Appendix

Abbreviations

AA	Activin A
AFP	Alpha-fetoprotein
APS	Ammonium persulphate
ATP	Adenosine triphosphate
bFGF	Basic fibroblast growth factor
BMP	Bone morphogenetic protein
bp	Base pair
BSA	Bovine serum albumin
CDK	Cyclin dependent kinase
°C	Celsius
cDNA	Complementary DNA
CK1	Caesin kinase 1
CMV	Cytomegalovirus promoter
Co-IP	Co-immunoprecipitation
Ct	Threshold cycle
DAPI	4',6-diamidino-2-phenylindole
DE	Definitive endoderm
DMEM	Dulbecco's modified eagle serum
DMSO	Dimethyl sulphoxide
DNA	Deoxyribonucleic acid
dNTP	Deoxynucleotide triphosphate
DPBS	Dulbecco's phosphate buffered saline
DTT	Dithiothreitol
E	Embryonic day
EDTA	Ethylenediaminetetraacetic acid
EGFP	Enhanced green fluorescent protein
EGTA	Ethylene glycol tetraacetic acid
EMT	Epithelial to mesenchymal transition
Eomes	Eomesdermin
EpiSCs	Epiblast-derived stem cells
FBS	Foetal bovine serum
FGF2	Fibroblast growth factor 2

FKBP	FK506 binding protein
Fox	Forkhead
G	Gauge
GSC	Goosecoid
GSK3	Glycogen synthase kinase 3
GST	Glutathione S-transferase
GTPase	Guanosine triphosphate hydrolase
H	Heregulin
HI	Heregulin and IGF-1 co-treatment
HA	Hemagglutinin tag
HAT	Histone acetyl transferase
HECT	Homologous to the E6-AP carboxyl terminus
HEPES	4-(2-hydroxyethyl)-1-piperazineethanesulfonic acid
hESC	Human embryonic stem cells
HGF	Hepatocyte growth factor
HNF	Hepatocyte nuclear factor
HRP	Horseradish peroxidase
I	LR3®-IGF
ICM	Inner cell mass
IGF	Insulin-like growth factor
IgG	Immunoglobulin
IP	Immunoprecipitation
iPSC	Induced pluripotent stem cell
JNK	c-Jun N-terminal kinase
kb	Kilobase
kDa	Kilodalton
Klf	Krüppel-like factor
KO-DMEM	Knockout DMEM
KSR	Knockout serum replacement
LB	Lysogeny broth
LIF	Leukaemia inhibitory factor
LY	LY294002
MAD	Mothers against decapentaplegic
MAPK/MEK	Mitogen activated protein kinase

MEF-CM/CM	MEF conditioned media
MEF	Mouse embryonic fibroblast
mESC	Mouse embryonic stem cell
MH1/2	Mad homology domain 1/2
Mix	Mixer
mRNA	Messenger ribonucleic acid
mTORC	Mammalian target of rapamycin complex
NEAA	Non-essential amino acids
NEB	New England Biolabs
Nedd4L	Neural precursor cell expressed developmentally downregulated gene 4-like
NP-40	Nonidet P40
OA	Okadaic acid
Oct4	Octamer-binding transcription factor 4
PDK1	Phosphoinositide-dependent kinase 1
PH	Pleckstrin homology domain
PI3K	Phosphatidylinositide 3-kinases
PKB	Protein kinase B or Akt
PKC	Protein kinase C
PMP	Protein metallophosphatase
PPM	Protein phosphatase Mg2+/Mn2+-dependent
PPP	Phospho-protein phosphatases
PtdIns	Phosphatidylinositide
PTEN	Phosphate and tensin homolog
PuroR	Puromycin resistance gene encoding for puromycin-*N*-acetyl-transferase
qRT-PCR	Quantitative real-time polymerase chain reaction
Ras	Rat sarcoma
RNA	Ribonucleic acid
ROCK	Rho associated protein kinase
rpm	Revolutions per minute
RPMI	Roswell park memorial institute
RT-PCR	Real time polymerase chain reaction
RTK	Receptor tyrosine kinase
S6K	S6 kinase
SAPK	Stress activated protein kinase

SB	SB431542 – Activin receptor-like kinase inhibitor
SD	Standard deviation
SDS	Sodium dodecyl sulphate
shRNA	Small hairpin RNA
SOC	Super optimal broth with catabolite repression
Sox	Sex determining region Y box
TE	Trophectoderm
TGFβ	Transforming growth factor-β
TSC	Tuberous sclerosis complex
v/v	Volume/volume
w/v	Weight/volume
Wort	Wortmannin
Wnt	Wingless-related integration site

Chapter One

Introduction

1.1 Preface

The initial emergence of multicellularity one billion years ago allowed for the evolution of complex organisms, resulting in the diversity of life we see around us today. However, the concept of being multicellular over unicellular presented a unique series of challenges for our ancestral eukaryotes. Principally, was the need to communicate and exchange information between cells in order to facilitate the specialisation of functions, as well as conveying the state of an ever-changing extracellular environment in order to coordinate adaptive responses. These challenges drove the evolution and diversification of early signal transduction pathways; multi-protein phosphorylation cascades which conveyed information from the cell surface to the nucleus from which different gene expression programs could be initiated depending on extrinsic cues.

Perhaps more importantly, an even greater obstacle for the evolution and persistence of multicellular life came upon reproduction, as multicellularity and cellular specialisation must once again arise anew from the zygote; the first cell of the new organism. It is this transitional process from a single cell to an entirely new organism, the development of new life from old that truly underscores the importance of signal transduction to the propagation of multicellular life. As the zygote proceeds through development, it undergoes cleavage and division, giving rise to new daughter cells that also proliferate and acquire the correct temporal and spatial information to form specialised tissues. During this transition, certain cells transitorily acquire the property of pluripotency; the unique ability to give rise to any cell type of the adult organism. The rapid conversion of a pluripotent to a specialised cell state is driven not only by signals received from the environment, but is also reinforced by mutual intercellular signalling cues which act to stringently consolidate the genetic programs needed to form functional tissues.

Whilst developmental studies using a variety of model multicellular organism from fruitfly to mouse have revealed the remarkable preservation of these signalling pathways across all species studied, there is nonetheless significant debate as to whether these pathways perform the same functions given that the reproductive systems across all organisms demonstrate significant variation. As such, although past studies have uncovered the inherent sophisticated molecular mechanisms controlling developmental progression, the regulative mechanisms coordinating their activities on a spatial and temporal level are likely to differ from species to species. For example, although the formation of morphogen gradients is a key mechanism that is conserved in fruitfly and mouse development, how different signalling gradients interact to drive formation of the body axes and the robust differentiation of certain tissues is very much different between both species.

Nevertheless, further studies of vertebrate development have helped shaped our understanding of the potential role signal crosstalk plays in human development, and has consequently allowed for the isolation and propagation of human embryonic stem cells (hESCs) from the pre-implantation blastocyst. These are cells resembling the zygotic daughter cells, which are able to be cultured indefinitely, and can differentiate to any cell type of the adult human *in vitro*. Thus, they are said to possess the dual properties of self-renewal and pluripotency. Isolation of hESCs has for the first time provided a platform from which to investigate the signalling processes that occur during human development, in that by simply changing the signalling molecules in the culture dish, one can directly manipulate the differentiation of the cells to a range of different lineages. Additionally, the advent of hESCs as well as induced pluripotent stem cells (iPSCs) has finally allowed the promise of regenerative therapies to be realised and has brought the allied fields of bioscience and medicine to the cusp of revolution.

The work described in this thesis utilises the hESC model to investigate the signalling crosstalk mechanisms driving the formation of the definitive endoderm; the precursory germ layer that gives rise to the gut, liver and pancreas. This chapter will firstly address the *in vivo* evidence garnered from developmental biology, which has contributed greatly to our understanding of how this germ layer is formed in mammalian systems and allowed the identification of the key signalling pathways involved. Next, this section will explore how this knowledge has been applied in the culture and directed differentiation of hESC to definitive endoderm followed by a detailed review of the signalling requirements facilitating the formation of definitive endoderm *in vitro*. Lastly, the current disparities of proposed crosstalk mechanisms between Activin/Smad and PI3K/Akt/mTOR in regulating the formation of this germ layer will be discussed, leading to the hypothesis of a direct role for mTORC2 in regulating this process.

1.2 The Definitive Endoderm

1.2.1 Emergence of the definitive endoderm in vertebrates

Amongst all vertebrates studied, germ layer differentiation and the specification of progenitor populations is one of the earliest events to occur upon fertilisation. In mammals, prior even to implantation, the zygote has already undergone several rounds of cleavage to form the first differentiated multicellular entity known as the blastocyst, consisting of two distinct populations of cells; the trophectoderm (TE) and inner cell mass (ICM), which further differentiate into the epiblast and hypoblast (also known as the primitive endoderm or PrE). After implantation, TE and PrE differentiate into the visceral (VE) and parietal (PE) endoderm, which contribute to the formation of yolk sac structures. Contrastingly, the epiblast cells undergo gastrulation to form the three initial germ layers of ectoderm, mesoderm and definitive endoderm (DE), which then give rise to all the tissues of the embryo (Figure 1.1). A clear distinction in terminology is required as PrE, VE and PE gives rise to mainly extraembryonic structures, with only the DE arising from the ICM giving rise to the embryo proper.

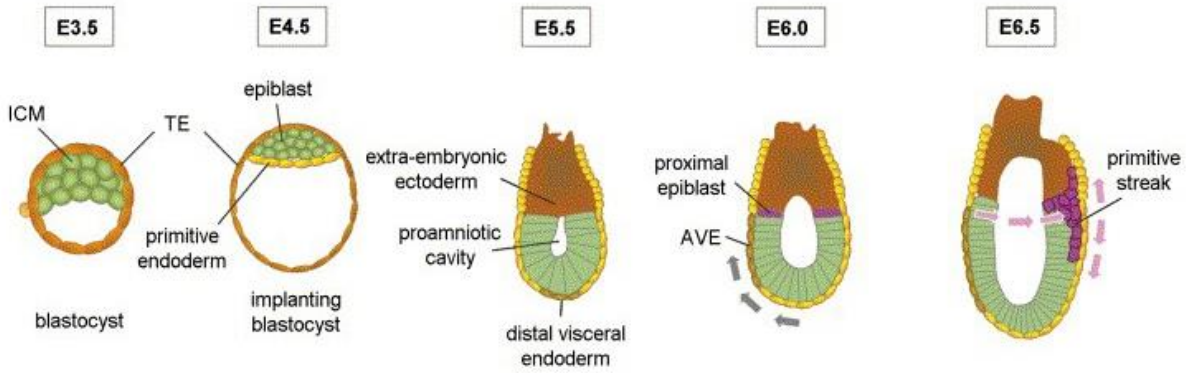

Figure 1.1: Emergence of definitive endoderm in the mouse

Diagram depicting early developmental progression in the mouse. Prior to implantation, cells of the ICM differentiate to form the epiblast and primitive endoderm (PrE) by E4.5. Gastrulation occurs post-implantation after E5.5. Cells of the TE form the extra-embryonic ectoderm, whilst cells of the PrE form visceral endoderm. Cells of the epiblast give rise to the primitive streak, which in turn will give rise to the mesoderm and definitive endoderm, with the residual cells making up the ectoderm. Image taken and adapted from Developmental Biology Interactive, 2013.

The process of gastrulation is a prime example where signalling plays a critical role in driving developmental progression. Specification of the DE begins with the ingression of mesendoderm progenitors into the anterior primitive streak, accompanied by epithelial to mesenchymal transition (EMT), which is necessary for the cells to gain mobility. During the latter stages of gastrulation, both mesoderm and endoderm progenitors are exposed to the node as it transits posteriorly, which confers positional and patterning instructions to the cells (Brennan et al., 2002). Whilst studies in *C. elegans*, sea urchin and zebrafish have suggested that both the mesoderm and endoderm derive from a common mesendoderm progenitor (Rodaway and Patient, 2001), this population of cells has never been formally demonstrated to exist in higher vertebrates. Nevertheless, it is clear that the initial separation of ectoderm progenitors from mesendoderm progenitors via internalisation through the primitive streak acts to spatially lay the foundations for further specification.

1.2.2 Induction of DE by signalling pathways

The molecular underpinnings governing the induction of both endoderm and mesoderm post-internalisation were elucidated mainly from studies made in *Xenopus* and mouse, which found that members of TGFβ signalling pathway are essential inducers of both germ layers. The introduction of a dominant negative Activin receptor which blocks the signalling activities of secreted TGFβ ligands such as Activin and Vg1 into *Xenopus* embryos induces the expression of ectoderm and mesoderm genes at the expense of endoderm markers (Henry et al., 1996), whilst ectopic expression of Xnr4; a *Xenopus* TGFβ ortholog, induced the formation of mesoderm (Joseph and Melton, 1997). In tandem with this finding, retroviral mutagenesis in the mouse allowed for the identification of the *Nodal* gene encoding for a mammalian TGFβ ligand, which had similar roles to Activin, Vg1 and Xnr4 in regulating mesendoderm formation (Zhou et al. 1993; Conlon et al., 1994;). Correspondingly, hypomorphic mutation of *Nodal* results in the selective loss of endoderm and mesoderm (Lowe et al., 2001), whilst inactivation of the natural Nodal antagonist Lefty2 leads to excessive endoderm formation (Meno et al., 1999). Further studies in zebrafish confirmed the importance of Nodal and its orthologs in specifying mesendoderm across multiple species, as in the absence of this signal, zebrafish embryos lacked all major mesendoderm derived structures such as the heart, kidney, liver and gut (Feldman et al., 1998; Gritsman et al., 1999). The mechanism by which Nodal and its orthologs acted to specify certain populations of cells as mesoderm whilst others are fated to become endoderm was deduced based on seminal work carried out on Activin and its *Xenopus* homologues, which alluded to the existence of morphogens; secreted proteins which act over a long-range to specify cell fates in a concentration-dependent manner (Green and Smith, 1990; Gurdon et al., 1994). The ability of Nodal to behave as a morphogen was first tested

and proved in zebrafish, in that high levels of Nodal signalling were required to induce the expression of *goosecoid* whilst lower levels maintained the expression of *brachyury,* markers of anterior and posterior mesoderm respectively (Chen and Schier, 2001). Concurrently, the specification of DE and mesoderm in mice was also found to be dependent on high and low levels of Nodal signalling respectively (Lowe et al., 2001; Vincent et al., 2003), which again emphasises the importance of TGFβ signalling to the development of both germ layers. However, it is important to note that although TGFβ signalling is required, it is not the sole regulator of DE formation. Studies in *Xenopus* have revealed that transcriptional integration of Wnt and Nodal pathways are required for the expression of *goosecoid,* hence cooperating to specify and consolidate the mesendoderm fate (Watabe et al., 1995). Furthermore, mice embryos lacking Nodal or β-catenin, a component of the canonical Wnt signalling pathway, fail to even form primitive streak (Conlon et al., 1994; Haegel et al., 1995) whilst Wnt3-null mutants demonstrate the need for Wnt3 in driving anterior-posterior definition as well as mesendoderm and primitive streak formation (Liu et al., 1999). Lessons learned from these developmental studies would later prove to be invaluable in the initial isolation and *in vitro* differentiation of hESCs to DE.

1.2.3 Intrinsic consolidation of the endoderm fate

The stimulation of both Nodal and Wnt pathways ultimately results in the upregulation of transcription factors that serve to reinforce the endoderm identity. In particular, Nodal signalling directly induces the expression of many of these factors which can act to both consolidate the definitive endoderm as well as endoderm-derived tissues:

i. Gata factors

The Gata factors constitute an ancient family of zinc finger transcription regulators whose role in consolidating mesendoderm-derived tissues can be traced right back to invertebrates. Loss of the drosophila Gata factor Serpent prevents endoderm and fat body formation, an organ analogous to the liver (Rehorn et al., 1996), whilst loss of Gata5 in zebrafish precludes the formation of heart and gut tissue (Reiter et al., 1999). In *Xenopus*, ectopic expression of Gata4, 5 or 6 converts ectomesoderm into endoderm, and are implicated in the proper formation of heart and intestinal tissues (Jiang and Evans, 1996; Gao et al., 1998; Afouda et al., 2005), whilst Gata4 and Gata6 knockout mice demonstrate defects in both visceral and endoderm development as well as improper differentiation of the gastric epithelium (Morrisey et al., 1998; Jacobsen et al., 2002). The observation of defects occurring in the liver and gut of organisms where Gata function is impaired

or absent therefore additionally suggests that these factors activate genes that are required to maintain endoderm-derived tissues in the adult organism.

ii. Forkhead factors

The Forkhead (Fox) family are another well-conserved group of transcription factors that are particularly important to the maintenance of endoderm-derived tissues. As a large and diverse family of proteins, many members have diversified in function and have gone on to regulate processes outside of development, yet certain members have been shown to play major roles in the development and maintenance of adult endodermal tissues. Loss of FoxA2 (HNF-3β) in mouse embryos results in severe developmental abnormalities, including the absence of node, notochord and foregut accompanied by the failure to progress beyond E8.5 (Ang and Rossant, 1994; Weinstein et al., 1994). Equally, loss of FoxH1 (FAST), a cofactor of the Nodal-activated transcription factor Smad2, produced a similar lethal phenotype in terms of complete node and mesendoderm loss (Chen et al., 1996; Hoodless et al., 2001; Yamamoto et al., 2001). More importantly, conditional and tissue specific inactivation have revealed further roles for Fox factors in both the organogenesis and homeostasis of the liver. FoxA1 deficient mutants fail to form the liver bud (Lee et al., 2005) whilst loss of FoxA3 results in decreased expression of hepatic-specific genes, such as the hepatic glucose transporter 2 protein (GLUT2), which results in fasting hypoglycaemia (Kaestner et al., 1998; Shen et al., 2001). Furthermore, conditional inactivation of FoxA2 in the pancreas also induces hypoglycaemia but due to excess insulin production (Sund et al., 2000). These findings therefore highlight the critical role Fox factors play in the consolidation of endoderm-derived tissues.

iii. Mixer factors and Sox17

The Mixer (Mix/Bix) family are a group of homeobox transcription factors that have been implicated in the specification of mesoderm and endoderm solely in vertebrates. Unlike the Gata and Fox factors, studies in *Xenopus* have shown that Mix factors possess the unique ability of being able to induce specifically endoderm fates in the absence of mesoderm and ectoderm (Henry and Melton, 1998), whilst being only able to induce mesoderm at lower expression levels (Tada et al., 1998; Latinkic and Smith, 1999). Mice embryos lacking MixL1 are characterised by a thickening of the primitive streak, accompanied by a reduction in DE recruitment and loss of hindgut (Hart et al., 2002; Tam et al., 2007), thus implicating its involvement in the consolidation of specifically endoderm fates.

The phenotype of MixL1 knockout mice closely resembles that of the high-mobility group (HMG) transcription factor Sox17-null mice, which is therefore yet another factor that has been implicated in the maintenance of specifically endoderm fates. Both mice and *Xenopus* embryos lacking Sox17 show a depletion in DE and despite still being able to form anterior endoderm, cannot form mid and hindgut structures (Kanai-Azuma et al., 2002; Clements et al., 2003). Further to its role in DE specification, Sox17 has also been implicated in the proper vascularisation of organs post-natal and hence may play a role in maintaining the proper function of highly vascularised tissues such as the liver and pancreas (Matsui et al., 2006). The similarity of the null phenotype of both MixL1 and Sox17 in the mouse and the ability of Mixer to induce Sox17 expression in *Xenopus* immediately suggest some form of coordination on the transcriptional level between these two factors.

iv. Eomesdermin

Although the T-box transcription factor Eomesdermin (Eomes) was originally identified as a mesoderm inducer in *Xenopus* (Ryan et al., 1996), more recent findings in zebrafish have highlighted the additional role it plays in consolidating the definitive endoderm. Specifically, ectopic expression of *Eomes* induces the increased expression of *goosecoid* and *chordin* accompanied by the formation of a secondary body axis (Bruce et al., 2003), whilst maternal Eomes coordinates with Gata5 in driving the expression of *Casanova*, the first endoderm specific factor expressed in zebrafish (Bjornson et al., 2005). Studies in mice have supported this argument, in that selective deletion of *Eomes* in epiblast derivatives blocks EMT and results in failed migration of the mesoderm away from the primitive streak concomitant with the loss of definitive endoderm (Arnold et al., 2008). However, given that the absence of Eomes does not affect mesoderm formation, it is likely that rather than being an endoderm-specifying factor, the mesoderm-specifying actions of Eomes also indirectly promote the consolidation of the endoderm identity in conjunction with Gata and Mix/Bix factors.

1.2.4 Epistatic regulation of endoderm identity

Cross-regulation and interaction amongst the endoderm-specifying factors serves as an important mechanism that acts to consolidate the specification of the germ layer. As summarised in Figure 1.2, auto-regulatory loops centred around Sox17 act to strengthen the endoderm identity in *Xenopus* (Sinner et al., 2006). The interlinking of these factors explains why ectopic expression of any one factor results in rapid endoderm induction, as feed-forward mechanisms ensures that all other required factors are expressed in conjunction with the first. As such, this consolidation is both self-sustaining long after the disappearance of Nodal ligand, whilst also being self-reinforcing, in

that Mixer and Sox17 can act to repress *Eomes* and *β-catenin* expression respectively to prevent mesoderm induction. However, although the endoderm specifying functions of the individual factors are generally well conserved across all species studied, whether or not these epistatic relationships also hold in higher vertebrates remains to be explored.

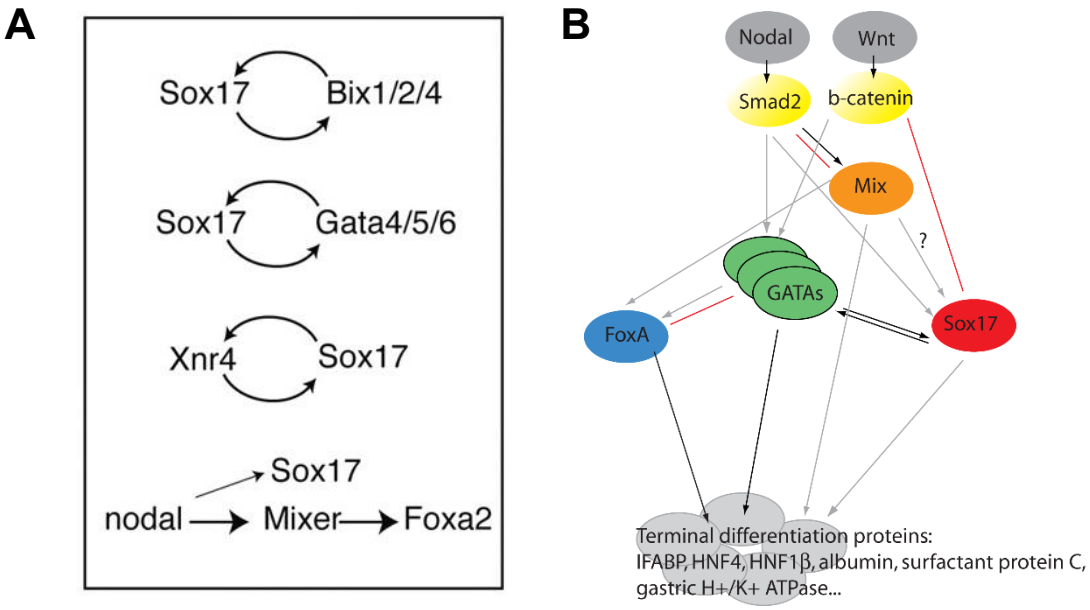

Figure 1.2: Epistatic consolidation of the definitive endoderm identity

Summary of the epistatic relationships uncovered in Xenopus and the proposed transcriptional network that exists to consolidate the definitive endoderm identity. Grey lines indicate induction, black lines indicate direct regulation and red lines indicate experimental evidence for direct interaction between factors. Integration of Nodal and Wnt signalling activities function to augment the transcriptional consolidation. Images taken and adapted from Sinner et al., 2006 (A) and Grapin-Botton, 2008 (B).

1.3 Signalling pathways that regulate DE differentiation

Although it has been formally demonstrated that Activin/Nodal and Wnt/β-catenin cooperatively act to specify the DE *in vivo*, recent evidence has shown that many other signal pathways act to regulate this process to ensure stringent specification. In particular, the PI3K/Akt pathway has been shown to regulate specification of foregut precursors by regionalising the surrounding extracellular matrix (Villegas et al., 2013), whilst *in vitro* differentiation of hESCs is impeded by the presence of serum containing stimulators of the PI3K/Akt pathway (D'Amour et al., 2005; McLean et al., 2007). As such, both *in vivo* and *in vitro* studies have increasingly shown the PI3K/Akt pathway to be a critical modulator of Activin/Nodal signalling activities that mediate DE formation.

1.3.1 Activin/Nodal

Activin/Nodal signalling plays a major role in both the maintenance of hESC pluripotency and *in vivo* specification of the DE (Vincent et al., 2003; Vallier et al., 2005), which is highly dependent on the level and duration of the signalling response. Taking a more molecular based overview, whether stimulation of this pathway induces differentiation or maintains pluripotency is dependent on the presence of determinants at both the signalling and gene level. Although the core components of the signalling cascade remain shared with other TGFβ family members, the presence or absence of these determinants drive the regulatory mechanisms that govern their functional competence.

1.3.1.1 Induction - Ligands and Receptors

TGFβ, Activin and Nodal are defining members of a TGFβ subfamily of 'Activin-like' ligands, which differ from the BMP subfamily in terms of their protein sequence and the mode by which they stimulate the receptor complex. These ligands operate as diffusible proteins, which are first synthesised as precursory proteins carrying a long N-terminal pro-peptide and short C-terminal polypeptide, which are separated upon cleavage by furin-like proteases prior to secretion from the cell (ten Djike and Arthur, 2007). The longer pro-peptide, termed latency associated peptide (LAP) remains associated with the shorter mature protein, and acts as a molecular chaperone, stabilising the mature protein whilst keeping it in a latent state. Emergence from this state is marked by the dimerization of ligand monomers stabilised by a network of intrachain disulphide bonds, hydrophobic interactions and a single disulphide bridge between them (Sun and Davis, 1995). Only dimerised ligands are conducive in binding receptor complexes consisting of type I and type II

receptor Ser/Thr protein kinases that cooperate to initiate the intracellular signal cascade. TGFβ receptors are the only Ser/Thr protein kinases receptors identified to date from which two distinct modes of induction are apparent, which serves to distinguish the Activin-like from the BMP subfamily (Figure 1.3).

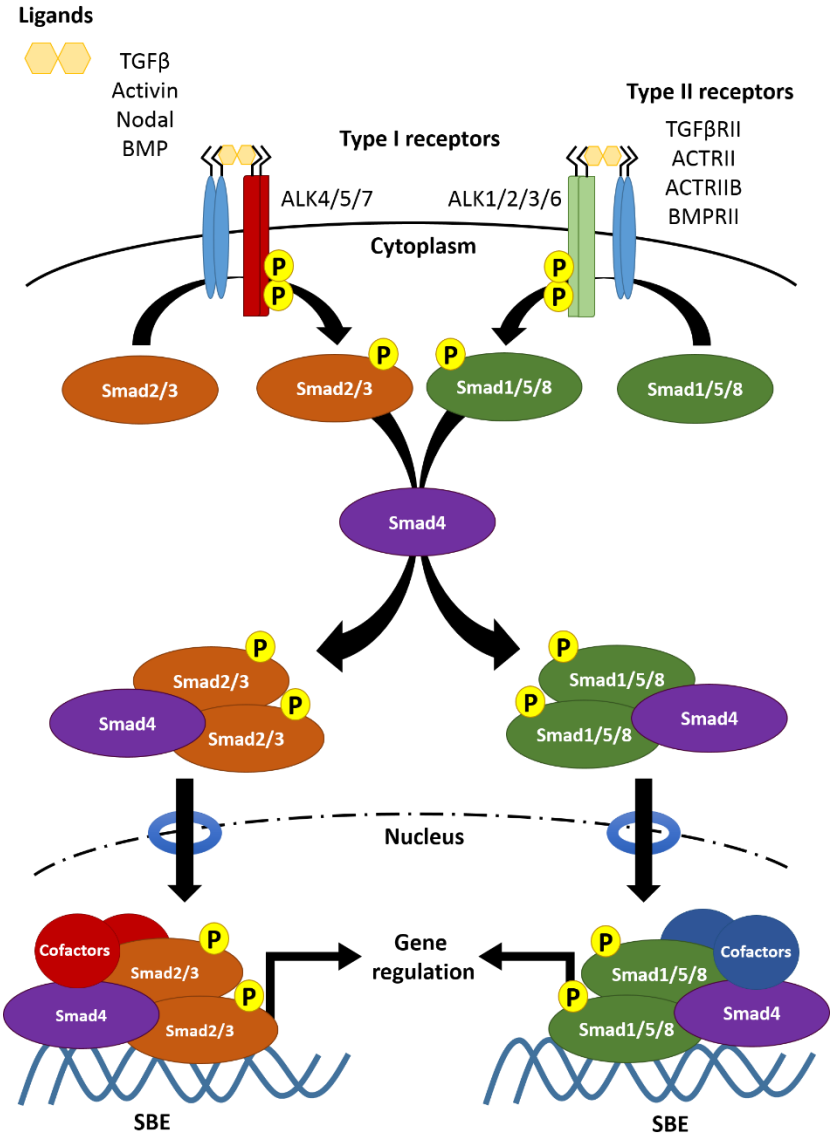

Figure 1.3: The TGFβ Signalling Pathway

Diagram illustrating the core components of the TGFβ signalling cascade. The TGFβ superfamily can be subdivided into two main subfamilies consisting of the 'Activin-like' ligands that stimulate the activation of Smad2 and 3 (in orange) and the BMP ligands that activate Smad1, 5 and 8 (in green). Smad4 (in purple) acts the Co-Smad common to both signalling branches. Trimeric Smad/Co-Smad complexes translocate into the nucleus to regulate gene expression. SBE indicates regions of DNA constituting Smad Binding Elements.

The Activin-like subfamily of ligands possess a high affinity for type II receptors, which upon binding, induces the phosphorylation of the type I receptor at multiple sites within the juxtamembrane Gly-Ser (GS) rich region, a highly conserved regulatory sequence which when phosphorylated permits the dissociation of the inhibitory 12 kDa FK506 binding protein (FKBP12) and recruitment of Smad substrate (Massagué, 1998; Huse et al., 2001). In the case of the BMP subfamily, given that BMP ligands have a greater affinity for type I receptors over type II and that formation of the BMP-type I receptor complex leads to improved affinity for type II receptors, ligand binding first occurs on the type I receptors before type II receptors are recruited to activate the GS region. However, the simplicity of the induction mechanism masks a range of regulatory mechanisms acting on both the ligand and receptor level that will ultimately affect the functional outcome of the signalling induction. For example, ligand-trapping proteins and antagonists such as Noggin and inhibin prevent the recruitment of BMPs and Activin to their receptors respectively (Lewis et al., 2000; Groppe et al., 2002), whilst other ligands such as Nodal requires cofactors such as Cripto to mediate receptor binding (Yeo and Whitman, 2001). Furthermore, given that there are over thirty TGFβ ligands, seven type I and five type II receptors that have been found to exist in humans, there is significant scope for mechanistically complex interplay that gives rise to the milieu of TGFβ-attributed functions observed in development, tissue homeostasis and tumourigenesis.

1.3.1.2 Transduction – Smad function and regulation

The translation of extrinsic cues into a meaningful gene response requires the transduction of the signal from the receptor down into the nucleus. In the TGFβ signalling cascade, Smad proteins (Figure 1.4) serve as the conduits through which the extrinsic signal is transmitted intracellularly. Eight Smad proteins have been identified and categorised into three groups: the receptor-regulated Smads termed R-Smads including Smad1, Smad2, Smad3, Smad5 and Smad8; the common mediator Smad, or Co-Smad, Smad4; and the inhibitory Smads or I-Smads which includes Smad6 and Smad7. Structurally, Smads consists of two globular MAD homology 1 (MH1) and 2 (MH2) domains linked by an unstructured, Pro-rich linker region. The N-terminal MH1 domain is responsible for the binding of Smad to the DNA and carries a nuclear localisation signal (NLS) motif, whilst the C-terminal MH2 domain facilitates Smad-receptor and Smad-Smad interactions, as well as the recruitment of transcriptional cofactors within the nucleus. The linker region carries multiple Ser/Thr residues, which are targeted by proline-directed Ser/Thr kinases that act to regulate Smad function and allow further recruitment of other modifying proteins such as ubiquitin

ligases. Phosphorylation of the type I receptor GS region allows for the recruitment and subsequent activation of R-Smads at the C-terminal Ser-X-Ser (SxS) motif facilitated by the Smad anchor for receptor activation or SARA protein (Tsukazaki et al., 1998; Xu et al., 2000). This results in conformational changes in the R-Smads, which permits the homo and heterologous dimerisation of R-Smads (Abdollah et al., 1997). Activated R-Smad dimers subsequently recruit the Co-Smad (Smad4), forming trimeric units that translocate into the nucleus and together with other factors, initiates the transcription of target genes (Chacko et al., 2001). Another key distinguishing feature between the Activin-like and BMP branches of TGFβ signalling is that Activin/Nodal stimulates the activation of Smad2 and Smad3, whilst BMP type I receptors phosphorylate Smad1, Smad5 and Smad8.

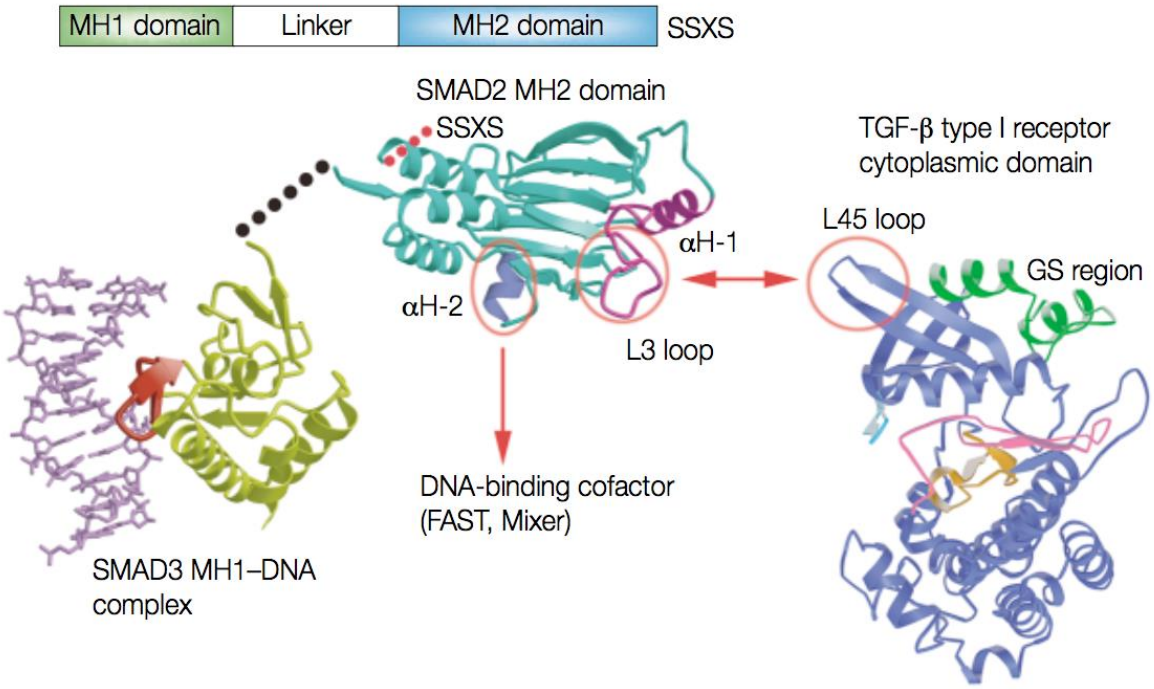

Figure 1.4: R-Smads – Structure and Function Relationships

X-ray crystallography has revealed the structural basis for Smad function. Phosphorylation of the GS region (in green) of the type I TGFβ receptor induces conformational changes that permit association with the R-Smad MH2 domain (in cyan) at the L3 loop (in purple) and phosphorylation of the SxS motif. DNA binding is mediated through the MH1 domain (in yellow) whilst cofactor recruitment is mainly facilitated by the αH-2 of the MH2 domain. No crystal structure is available for the linker region (dotted black line) due to the presence of crystal distorting proline residues. Adapted and presented with permission from Macmillan Publishers Ltd: Nature Reviews Molecular Cell Biology, Massagué, copyright 2000.

As with the induction of the signalling cascade, R-Smads are also regulated by a variety of mechanisms that affect their functional activities. In the absence of stimulation, Smads remain monomeric and constantly shuttle between the nucleus and cytoplasm to establish a basal state equilibrium (Shi and Massagué, 2003). The balance between the import and export activities results in the homogeneous distribution of Smad4 between both compartments, however R-Smads appear to be restricted to the cytoplasm (Pierreux et al., 2000; Watanabe et al., 2000). This is due to the occlusion of the NLS motif within the MH1 domain and binding by SARA, which is only diminished upon the receptor-mediated phosphorylation of the SxS motif (Xiao et al., 2000a; Kurisaki et al., 2001). However, the MH2 domain of R-Smads have also been shown to bind directly to nucleoporins themselves, indicating that shuttling of monomeric R-Smads may very well occur in a constant fashion (Xu et al., 2002). As such, the preferential nuclear exclusion of monomeric R-Smads in establishing the basal state may well be due to their inability to bind to stabilising factors within the nucleus that preferentially bind to trimeric complexes, resulting in a bias for export back out into the cytoplasm over nuclear import. The dynamic shuttling of R-Smads and preferential retention of transcriptionally active trimeric complexes allows for constant sensing of the receptor activation state, allowing for rapid signal termination once the exogenous ligand pool is exhausted and direct stoichiometric translation of receptor activation to levels of activated Smad (Inman et al., 2002).

1.3.1.3 Termination of Smad signalling

Since TGFβ signalling has been shown to be of great importance to development and tissue homeostasis, stringent mechanisms exist to regulate not only the stimulation, but also the termination of the signal to prevent aberrant functions. Given that receptor-mediated activation of Smads is essential for their nuclear retention and function, and that inhibition of the type I receptor results in the rapid dephosphorylation of Smads (Vogt et al., 2011), much attention has been focused on the identification of the phosphatase responsible. Protein phosphatases function to remove phosphate groups from phospho-Ser/Thr or Tyr residues and are subdivided based on their substrate preference. Since all reported phosphorylation sites on Smads are either Ser or Thr residues, the Ser/Thr subfamily of protein phosphatases have been the subject of intense scrutiny in this regard. The members within the subfamily can be further characterised into three groups based on the structure of their catalytic domains: the phospho-protein phosphatases (PPP), protein phosphatase Mg^{2+}/Mn^{2+}-dependent (PPM) and the transcription factor IIF-interacting CTD phosphatase 1 (FCP) families (Cohen, 2004). The utilisation of a functional genomic approach

resulted in the identification of PPM1A as the long sought nuclear R-Smad phosphatase, which was convincingly shown to impact TGFβ mediated responses through a series of gain and loss of function experiments in zebrafish (Lin et al., 2006). However, recent findings have cast doubt as to whether PPM1A is truly a *bona fide* nuclear phosphatase in that it has been reported to be exclusively cytoplasmic in greater than 10 different cell lines tested (Bruce et al., 2012), as well as functioning promiscuously to dephosphorylate targets such as phosphatidylinositide-3-kinases (PI3K) and axin which also reside in the cytoplasm (Strovel et al., 2000; Yoshizaki et al., 2004). Given that these targets are also key components in the PI3K/Akt and Wnt/β-catenin signalling pathways respectively, and that the same pathways have been shown to augment or antagonise TGFβ signalling activities, it is debatable whether the *in vivo* evidence truly reflects the direct function of PPM1A solely on TGFβ signalling. As such, although the major role phosphatases play in the termination of BMP-induced Smad activity has clearly been demonstrated (Duan et al., 2006; Knockaert et al., 2006), this has yet to be the case for the R-Smads and awaits further interrogation.

In addition to phosphatase-mediated dephosphorylation, activated R-Smads are also subject to degradation and turnover via the ubiquitin-proteasomal system (Lo and Massagué, 1999). Several E3 ubiquitin ligases have been reported to act upon activated R-Smads, including Smurf2, Arkadia and Nedd4L. Smurf2 has been shown to bind Smad1, Smad2 and Smad3, but not Smad4, whilst also having a preferential bias in binding activated Smads, particularly Smad2 (Lin et al., 2000). The notion of ubiquitin-mediated degradation as a valid mechanism by which TGFβ signalling can be terminated was further supported by the discovery of the RING-domain E3 ligase Arkadia, which was found to act upon activated Smad2 and Smad3 only upon entry into the nucleus (Mavrakis et al., 2007). More recently, characterisation of the Smad linker region has allowed for the identification of another homologous to the E6-AP carboxyl terminus (HECT) E3 ubiquitin ligase, neural precursor cell expressed developmentally downregulated gene 4-like (Nedd4L), which is recruited to Smad2/3 upon linker phosphorylation by cyclin-dependent kinases or CDKs (Alarcón et al., 2009; Gao et al., 2009). Thus ubiquitin-mediated turnover of R-Smads appears to be a stringently controlled mechanism that is regulated not only by the activation state of R-Smads, but also dependent on the phosphorylation status of the linker region. Furthermore, the fact that both Smurf2 and Arkadia have been demonstrated to act on active Smads alone strongly suggests that ubiquitin-mediated proteasomal degradation works in tandem with nuclear phosphatases to terminate Smad signalling, however whether this bias also applies to Nedd4L recruitment remains unknown.

1.3.1.4 Regulation of Activin/Nodal signalling

i. Role of the Smad linker region

The Smad linker region is an important site at which Smad activity is regulated on both branches of the TGFβ family, consisting of several Ser/Thr residues that are targeted by a plethora of kinases originating from many different signalling cascades (Figure 1.5).

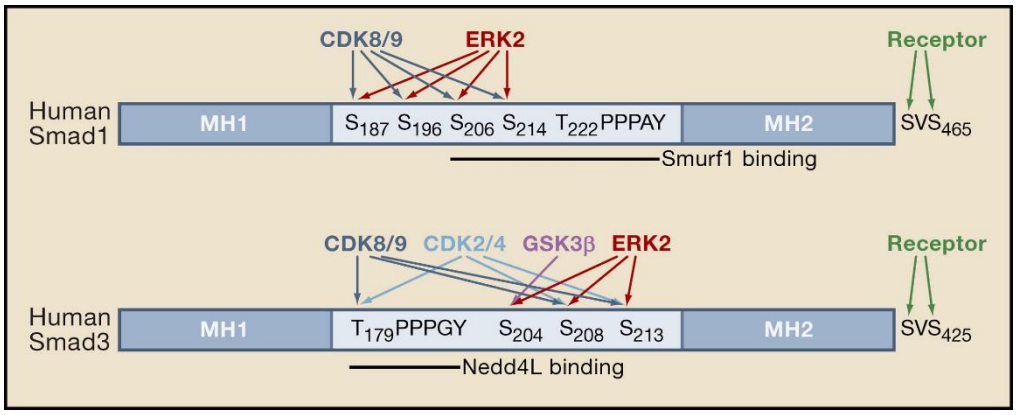

Figure 1.5: Smad linker region

Diagram depicting the linker region of human BMP-Smads and R-Smads. Linker regions are characterised by an abundance of Ser, Thr and Pro residues. Ser/Thr residues are targeted by kinases such as CDK, GSK3β and Erk2, which facilitate the recruitment of modifying factors including E3 ubiquitin ligases such as Smurf1 and Nedd4L. Image taken and adapted from Chen and Wang, 2009.

The identification of so many kinases acting upon the R-Smad underscores the importance of the linker region in modulating inter-pathway crosstalk. However, phosphorylation of the linker residues can act to both augment and antagonise R-Smad function in a context dependent manner. For example, although oncogenic induction of rat sarcoma (Ras) protein or stimulation of MEK/Erk signalling prevents the nuclear accumulation of R-Smads and preserves mesoderm competence in *Xenopus* during development (Kretzschmar et al., 1999; Grimm and Gurdon, 2002), phosphorylation of the same residues by p38 mitogen activated protein kinase (MAPK), Rho-associated protein kinase (ROCK) or c-Jun N-terminal kinase (JNK) enhances R-Smad transcriptional activity (Engel et al., 1999, Mori et al., 2004, Kamaraju et al., 2005). Furthermore, the phosphorylation of specific linker residues by one group of linker kinases can serve to augment the activities of another. The modulation of linker phosphorylation in BMP-Smads is an exemplary case, in that MAPK-mediated phosphorylation primes the site for further phosphorylation by

glycogen synthase 3 (GSK3), acting in a concerted fashion to inhibit Smad function by targeting nuclear localised active Smad for ubiquitin-proteasomal-mediated degradation (Kretzschmar et al., 1997; Fuentealba et al., 2007; Sapkota et al., 2007). This mechanism by which linker phosphorylation acts to direct the binding of E3 ubiquitin ligases which in turn earmarks Smad proteins for degradation, appears to be a key mechanism conserved between both BMP and Activin/Nodal pathways. Furthermore, an additional regulatory layer exists in that these linker residues are also targeted by linker phosphatases that act to promote Smad signalling activities (Sapkota et al., 2006; Wrighton et al., 2006). The pleiotropic activation of Activin/Nodal signalling by kinases belonging to other signalling streams such as the MAPKs, Akt and ROCK also function to regulate Smad and hence Activin/Nodal activity via the linker site, adding further layers of regulation on top of the canonical mechanisms.

ii. Function of I-Smads

Whilst the core regulatory process controlling the efficacy of Activin/Nodal signalling primarily occurs on the R-Smads, it is important to note that several other regulatory processes are in place to increase the stringency of regulation. Notably, Smad6 and Smad7 constitute members of the inhibitory Smad subgroup, and act to antagonise Smad signalling by blocking access to the active type I receptors (Hayashi et al., 1997). Smad7 binds and works cooperatively with Smurf1 and Smurf2 to block and terminate Activin/Nodal signalling via the degradation of the receptor complex (Ebisawa et al., 2001; Suzuki et al., 2002; Tajima et al., 2003). On the other hand, Smad6 mainly operates on the BMP branch in competing with Smad4 for Smad1 binding, sequestering and preventing access to active type I receptors (Hata et al., 1998). The existence of many different regulative mechanisms that control Smad activity acts to redundantly ensure stringent control over TGFβ signalling on a spatial and temporal level.

1.3.1.5 Regulation of gene expression by Smad – effects on development

Once inside the nucleus, Smad complexes are able to bind to specific regions of DNA to stimulate gene transcription, however it is notable that these complexes bind with relatively low affinity to Smad binding elements (SBE) which were initially minimally identified as 5'-GTCT-3' or its reverse complementary equivalent (Dennler et al., 1998; Shi et al., 1998). In fact, Smad2 itself has no inherent DNA binding ability due to an insertion within the MH1 domain that is missing in the Smad2-Δexon3 alternative splice variant (Yagi et al., 1999). Thus, all Smad complexes require the recruitment and binding to cofactors that possess higher affinity for DNA to cement the DNA to protein interaction (Feng and Derynck, 2005). Upon binding, Smad complexes and their

transcriptional partners recruit histone acetyl transferases (HATs) such as p300 and C/EBP-binding protein (CBP), acting to open the chromatin and stimulate targeted gene transcription (Massagué et al., 2005). Additionally, Smad complexes are able to recruit ubiquitin ligases such as Arkadia or Smurf2 to degrade SnoN, Ski and their associated co-repressors, thus facilitating the de-repression of Smad target genes (Bonni et al., 2001; Mavrakis et al., 2007; Le Scolan et al., 2008) (Table 1.1.). Conversely, Smad complexes can also act to repress gene expression, with the recruitment of transcriptional co-repressors such as 5'-TG-3'-interacting factors (TGIF) and chromatin modifiers such as histone deacetylases (HDACs) to silence Activin/Nodal gene targets. The repressive functions of Smad complexes are of equal importance to the stimulatory effects on gene transcription, as *Tgif* mutations in humans are associated with craniofacial defects, whilst complete loss of *Tgif* in the mouse results in persistent activation of Nodal responses that lead to holoprosencephaly and cyclopia (Taniguchi et al., 2012). Overall, these are but a few examples of the critical role Smad2/3 cofactors play in the regulation of both gene expression and cellular functions, acting to diversify the range of Smad2/3-dependent activities within the cell (Table 1.1).

Many Smad complex-cofactor interactions have been shown to have developmental relevance and are in most cases absolutely required for normal developmental progression. FoxH1 was the first cofactor reported to interact with Smads and mediates several developmental processes including formation of the endoderm and dorsal mesoderm (Zhou et al., 1998; Hoodless et al., 2001; Yamamoto et al., 2001). Interaction of Gata factors with Smad1 drives the expression of Smad7 and Nkk2.5, a key cardiac differentiation factor (Benchbane and Wrana, 2003; Brown et al., 2004), whilst Mixer factors interact with Smad2 and Smad4 to activate the expression of the mesoderm factor *goosecoid* (Germain et al., 2000). In addition, Smad complex-cofactor interactions have also been implicated in the maintenance of adult tissues, such as the skin and liver. For example, Smad3 has been shown to cooperate with FoxO in skin keratinocytes to inhibit Myc and hence proliferative gene responses (Chen et al., 2002), whilst Smad3 and Smad4 interact with hepatocyte nuclear factor-4a (HNF4a) to drive hepatic gene expression (Chou et al., 2003). Coordination of gene expression by Smad complex-cofactor interactions also extends to ES cells, in that bone morphogenetic protein (BMP)-induced Smad1, myeloid leukaemia inhibitory factor (LIF) and signal transducer and activator of transcription 3 (STAT3) were found to co-occupy sites of active gene transcription, including *Oct4*, *Sox2*, and *Nanog* in mouse embryonic stem cells or mESCs (Chen et al., 2008). As such, Smad complexes may initially function as pioneering factors, which act to recruit chromatin modifiers, and either pluripotency or lineage specific factors that cooperate to ultimately regulate lineage specific gene expression.

Table 1.1: List of experimentally verified Smad2/3 cofactors curated by BioGRID

Cofactor	Uniprot ID	Function
ACVR1B	P36896	Activin receptor
AKT1	P31749	Protein kinase
ANK3	Q12955	Membrane-cytoskeleton linker protein
ARKADIA	Q6ZNA4	E3 ubiquitin-protein ligase
CDK2	P24941	Cyclin dependent kinase
CDK4	P11802	Cyclin dependent kinase
CPSF7	Q8N684	mRNA processing factor
CREBP/CBP	Q92793	Histone acetylase
DAB2	P98082	Adaptor protein
DOCK9	Q9BZ29	Guanine nucleotide-exchange factor
EP300	Q09472	Histone acetyltransferase
EPAS1	Q99814	Transcriptional regulator of hypoxia response
FOXH1	P70056	Transcriptional activator
HDAC1	Q13547	Histone deacetylase
ITCH	Q96J02	E3 ubiquitin-protein ligase
JUN	P05412	Transcription factor
MAP2K3	P46734	Mitogen activated protein kinase
MTMR4	Q9NYA4	Ser/Thr/Tyr phosphatase
NEDD4	P46934	E3 ubiquitin-protein ligase
NEDD4L	Q96PU5	E3 ubiquitin-protein ligase
OLIG1	Q8TAK6	Oligodendrocyte maturation factor
OTUB1	Q96DC9	Deubiquitinase
PCK2	Q16822	Metabolic enzyme
PHC2	Q8IXK0	Polycomb group protein/transcriptional repressor
PPM1A	P35813	Broad specificity protein phosphatase
PPP2R1A	P30153	Protein phosphatase
RANBP3	Q9H6Z4	Nuclear export cofactor
RHOA	P61586	Plasma membrane signal transducer
ROCK1	Q13464	Rho associated protein kinase
SETD2	Q9BYW2	Histone methyltransferase
SKI	P12755	TGF-beta signalling repressor
SKIL/SnoN	P12757	TGF-beta signalling repressor
SMAD2	Q15796	TGF-beta signal transducer/transcription modulator
SMAD3	P84022	TGF-beta signal transducer/transcription modulator
SMAD4	Q13485	TGF-beta signal transducer/transcription modulator
SMAD7	O15105	TGF-beta signalling repressor
SMURF1	Q9HCE7	E3 ubiquitin-protein ligase
SMURF2	Q9HAU4	E3 ubiquitin-protein ligase
SP1	P08047	Transcription factor
SQSTM1	Q13501	Autophagy receptor
TGFBR1	P36897	TGF-beta receptor
TGIF1	Q15583	Homeobox protein
TP53	P04637	Tumour suppressor/cell cycle regulator
TRIM33	Q9UPN9	E3 ubiquitin-protein ligase
TSC2	P49815	GTPase-activating protein
USP7	Q93009	Deubiquitinase
WWP1	Q9H0M0	E3 ubiquitin-protein ligase
WWP2	O00308	E3 ubiquitin-protein ligase
ZFYVE9/SARA	O95405	Early endosome protein/transcriptional regulator

1.3.2 Wnt/β-catenin

Evident from developmental studies, the canonical Wnt/β-catenin signalling pathway plays a critical role in the regulation of embryonic development, cell proliferation and tissue homeostasis. The involvement of Wnt ligands in the regulation of developmental processes was first demonstrated in the fruitfly, whereby the Wnt1 homolog Wingless (Wg) was shown to control the segment polarity and hence the anterior-posterior patterning of the developing larvae (Nüsslein-Volhard and Wieschaus, 1980). Further studies performed in fruitfly, *Xenopus*, and mammalian models allowed for the elucidation of the intracellular components responsible for Wnt signal transduction, including GSK3 (Siegfried et al., 1992), adenomatous polyposis coli gene product or APC (Su et al., 1993), dishevelled (Noordermeer et al., 1994), lymphoid enhancer factor 1 or LEF-1 (Behrens et al., 1996), β-catenin (Molenaar et al., 1996), Frizzled (Bhanot et al., 1996) and casein kinase 1 or CK1 (Zeng et al., 2005). Each component forms a critical part of the transduction cascade that contribute directly to human diseases when mutated (Clevers and Nusse, 2012).

Key to the Wnt signal transduction cascade, the accumulation and translocation of β-catenin regulates the Wnt-activated genes, however the exact mechanisms by which Wnt induces this translocation remains unclear. Classically, in the absence of Wnt ligand (Figure 1.6), the axin degradation complex consisting of the scaffolding protein axin, APC, CK1 and GSK3 acts to downregulate cytoplasmic β-catenin via sequential phosphorylation first by CK1 and then by GSK3 at the N-terminal region. This phosphorylation recruits β-Trcp, an E3 ubiquitin ligase that acts to target β-catenin for proteasomal-mediated degradation (He et al., 2004). Loss of cytoplasmic β-catenin results in the binding of the transcriptional repressor Groucho (Cavallo et al., 1998) to LEF or T cell factor (TCF), resulting in the suppression of Wnt responsive gene activation. Conversely Wnt signalling is induced upon the binding of Wnt ligands to receptor complexes consisting of a 7-pass G-coupled transmembrane receptor Frizzled and its co-receptor LRP5/6 (Angers and Moon, 2009). This leads to the recruitment of the scaffolding protein dishevelled, which in conjunction with the lipoprotein receptor related protein 5/6 (LRP5/6) co-receptor and downstream G-proteins act to recruit axin to the plasma membrane. This sequestration of axin mitigates the formation of the degradation complex, resulting in the accumulation of β-catenin, which upon translocation into the nucleus, displaces Groucho transcriptional repressors and induces the upregulation of β-catenin target gene expression. Whilst the contribution of β-catenin as the main mediator of Wnt-induced gene expression is generally accepted, significant debate exists around the precise mechanism by which this is achieved. Notably, recent evidence proposes several non-canonical models to explain this effect. One study

proposes that the destruction of the degradation complex is an active process facilitated by co-endocytosis of the Wnt ligand and Frizzled receptor (Taelman et al., 2010), whilst another proposes that the degradation complex remains intact, albeit saturated with phosphorylated β-catenin, which blocks the degradation of newly synthesised unphosphorylated β-catenin (Li et al., 2012). Further studies will be required to fully establish the exact mechanisms by which β-catenin accumulation is promoted.

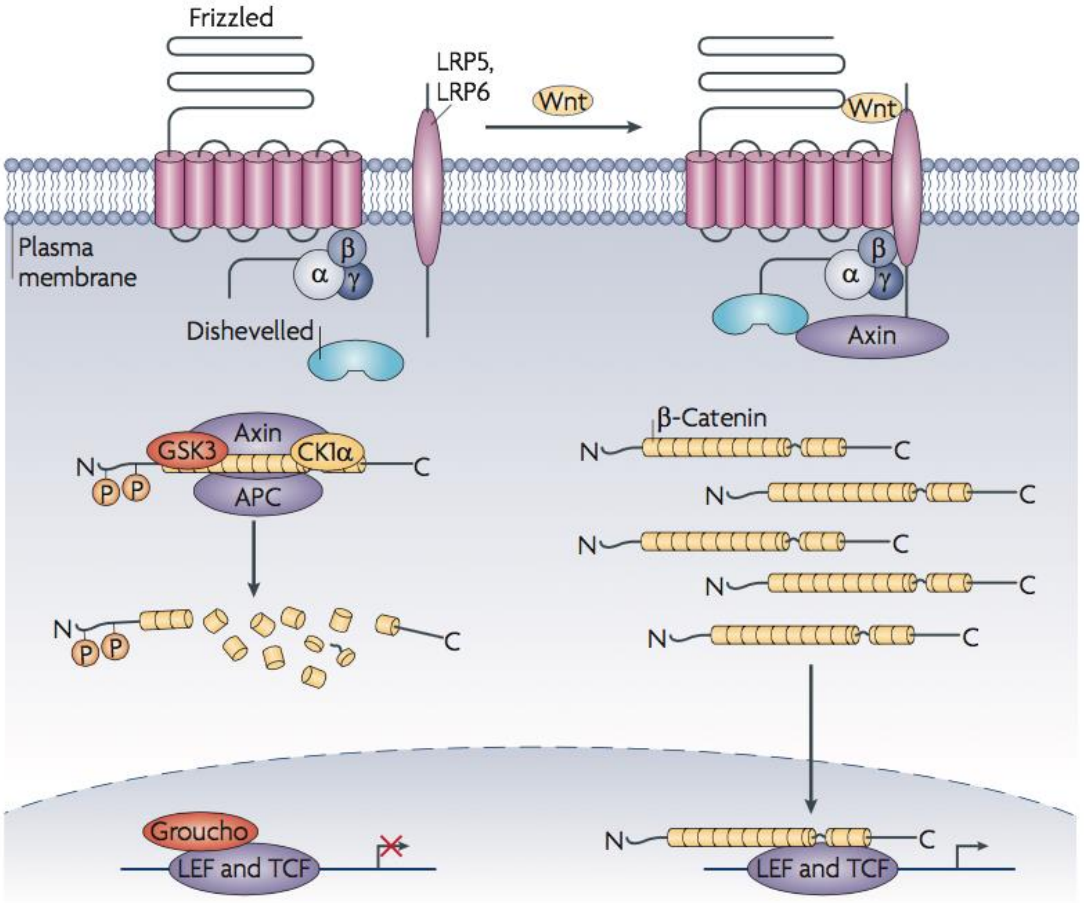

Figure 1.6: Canonical Wnt signalling

Diagram illustrating the canonical Wnt signalling cascade in the presence or absence of Wnt ligand. Alpha, beta and gamma indicate components of the G-protein coupled receptor Frizzled. N and C represent the N and C terminals of the β-catenin protein respectively. The axin degradation complex consists of axin, GSK3, APC and CK1 and acts to target β-catenin for degradation by the E3 ubiquitin ligase β-Trcp (not shown). The Groucho family of transcriptional repressors act to suppress LEF/TCF mediated gene expression, and are displaced upon the binding of β-catenin. Adapted and presented with permission from Macmillan Publishers Ltd: Nature Reviews Molecular Cell Biology, Angers and Moon, copyright 2009.

As outlined previously, Wnt/β-catenin signalling axis promotes the formation of DE by initially cooperating with Nodal to specify the primitive streak (Liu et al., 1999) followed by the augmentation of the DE gene transcriptional network. As such, supplementation of Wnt ligands together with Activin/Nodal in the early stages of *in vitro* differentiation may serve to accelerate the formation of DE by inducing the rapid formation and transition through the mesendoderm stage.

1.3.3 PI3K/Akt/mTOR

The PI3K/Akt/mTOR signalling axis constitutes an important pathway that regulates cellular growth and metabolism (Fig 1.7). However, the role this pathway plays in the regulation of cellular differentiation and development has only recently come to light. Studies refining the molecular details have revealed the complex nature of inter-pathway interactions occurring with other signalling pathways, defining the PI3K/Akt/mTOR pathway as a key component and modulator of the entire intrinsic signalling network.

1.3.3.1 PI3K and Phospho-inositol (PtdIns)

The original discovery of PI3K was initially brought about by the intriguing observation that hydrolysis of phospholipids resulted in the generation of secondary messengers that were capable of activating intracellular kinases such as protein kinase C or PKC (Kishimoto et al., 1980). This discovery firmly established the plasma membrane as a key signalling centre and phosphoinositide lipids as critical inducers of signalling events, spurring the search for modifiers that could create these secondary messengers. One such modifier was identified as a novel kinase with the unique ability to phosphorylate the 3-hydroxyl group of the phosphoinositide lipids, and hence named as phosphatidylinositol-3-kinase or PI3K (Whitman et al., 1988).

A range of growth factors activate PI3K, including insulin and insulin-like growth factors (IGFs), which suggests that induction of PI3K activity was likely to be an effect of receptor tyrosine kinase (RTK) activation and hence may function to regulate cell growth (Traynor-Kaplan et al., 1988; Ruderman et al., 1990). PI3K is structurally composed of two distinct proteins of ~110 kDa (p110) and ~85 kDa (p85) in size, of which p85 was frequently shown to be bound to activated RTKs (Kaplan et al., 1987). Although subsequent work revealed that the p85 protein possessed SRC homology 2 (SH2) domains, which facilitated binding to RTKs, it had no inherent kinase activity

(Escobedo et al., 1991). Thus, attention was swiftly focused on the p110 subunit, which was shown to carry the PI3K activity whilst additionally interacting with the p85 protein (Backer at al., 1992; Hiles et al., 1992). Therefore PI3K is a dimeric unit, with p85 serving as a regulatory factor in mediating RTK interaction whilst p110 fulfils the kinase function upon phosphoinositide substrate binding.

Further characterisation of PI3K has subsequently uncovered an entire family of kinases, which can be subdivided into distinct classes based on their structural and biochemical characteristics. Class IA enzymes represent the most studied, classically activated by RTK and consisting of five different p85 and three p110 isoforms (α, β, δ). Additionally, the class IB subgroup of enzymes utilise a larger regulatory subunit of which there are two isoforms coupled with p110γ and are mainly activated by G-coupled receptors. Class I enzymes mainly function to convert PtdIns(4,5)P_2 to PtdIns(3,4,5)P_3 by phosphorylating the 3'-hydroxyl of the PtdIns ring which leads to downstream signalling events. Class II and Class III enzymes dispense with the need for a regulatory subunit, however the stimulus required for the induction of their activity remains unknown, although they are functionally thought to catalyse the formation of PtdIns(3)P and possibly PtdIns(3,4)P_2. Additionally, the discovery of phosphatase and tensin homolog (PTEN) a phosphoinositide lipid phosphatase that opposes PI3K function (Maehama et al., 1998; Stambolic et al., 1998) provides a mechanism through which PI3K activity is regulated. The positioning of PTEN so far upstream of the PI3K/Akt/mTOR signal cascade defines its role as a master regulator and tumour suppressor, which is justified given that loss-of-function PTEN mutations lead to unrestricted activation of PI3K/Akt/mTOR signalling, resulting in aberrant proliferation and tumourigenesis. The need to investigate the functional properties of PI3K spurred the development of Wortmannin (Wort) and LY, cell-permeable, pan-PI3K specific inhibitors (Arcaro and Wymann, 1993; Vlahos et al., 1994) which facilitated the discovery of many PtdIns(3,4,5)P_3-activated effectors that contribute to the growth enhancing properties of PI3K activation.

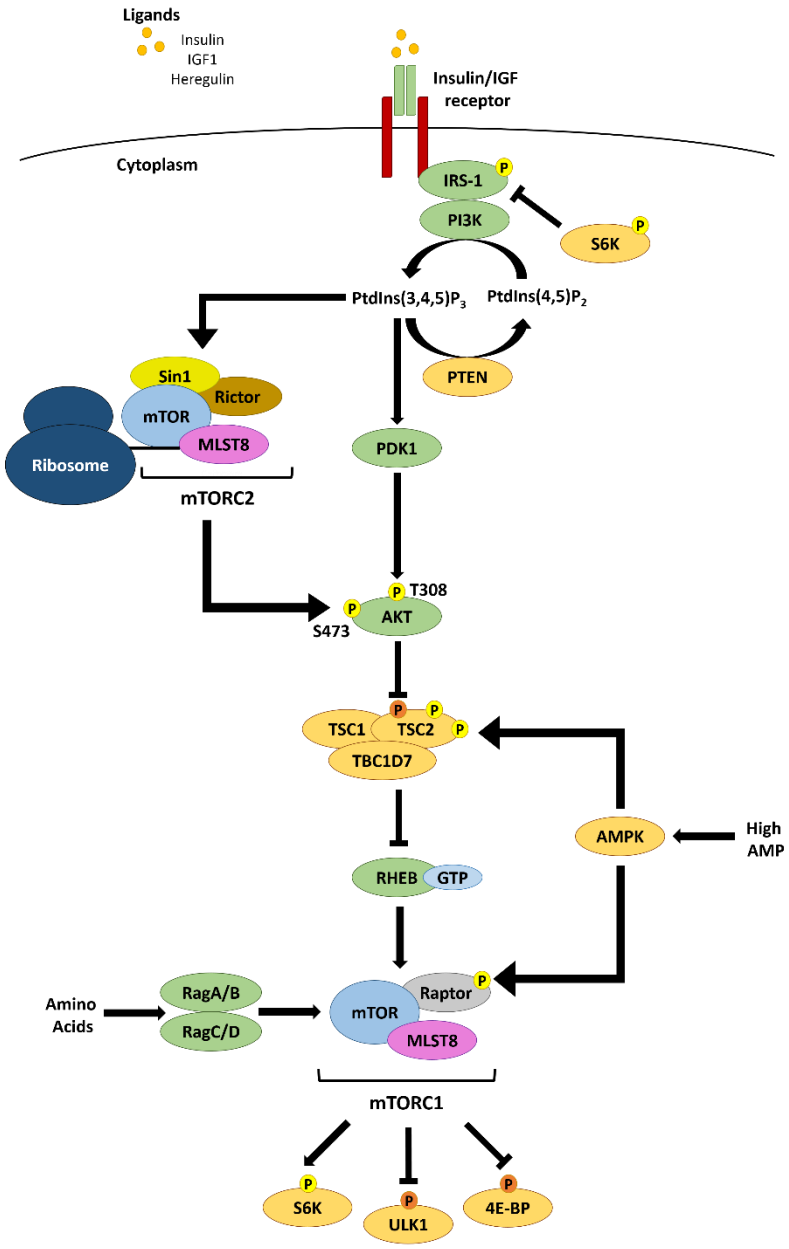

Figure 1.7: The PI3K/Akt/mTOR Signalling Pathway

Overview of the PI3K/Akt/mTOR signalling cascade. RTKs and G-coupled receptors act to stimulate the induction of PI3K activity, which in turn promotes the formation of the phosphoinositide mediator PtdIns(3,4,5)P_3 and the recruitment of PDK1, Akt and mTORC2 to the plasma membrane. Full activation of Akt is subsequently induced by the kinase activity of PDK1 and mTORC2, which phosphorylate Akt at T308 and S473 respectively. Active Akt acts to inhibit TSC1/TSC2 GTPase activity, which promotes the activation of the mTORC1 complex. Signalling inputs via AMPK also act to promote TSC1/TSC2 activity and inhibit mTORC1 activation. mTORC1 can also be activated by amino acids through Rag GTPases, which subsequently induces the growth stimulating activities of ULK1, S6K, and 4E-BP. PTEN acts to reduce PtdIns(3,4,5)P_3 levels which results in negative regulation of the pathway. Additionally, activated S6K negatively regulates PI3K/Akt/mTOR signalling by phosphorylating IRS-1.

1.3.3.2 Akt/PKB – The first effector

In identifying the product of PI3K activity as PtdIns(3,4,5)P_3, the search was on to find protein kinases that could be recruited and activated by this phosphoinositide lipid. Early bioinfomatic approaches identified a key domain shared amongst many signalling mediators that facilitates their association with membrane proteins, termed the pleckstrin homology (PH) domain (Haslam et al., 1993), which was subsequently shown to bind PtdIns(4,5)P_2 (Harlan et al., 1994). Akt or protein kinase B (PKB) was one of the kinases identified to possess a PH domain, and given its close relationship with PKC, was suspected to be a downstream effector stimulated by PtdIns(3,4,5)P_3. Subsequent studies revealed this to be the case, in that Akt binds PtdIns(4,5)P_2 and PtdIns(3,4,5)P_2 via its PH domain which localises Akt to the plasma membrane (Burgering and Coffer, 1995; Franke et al., 1995). Recruitment of Akt to the membrane alters its protein conformation and allows activation by phosphoinositide-dependent kinase 1 (PDK1), another kinase which was shown to have PtdIns(3,4,5)P_3 binding activity via a PH domain. PDK1 activity is absolutely dependent on the presence of either PtdIns(4,5)P_2 or PtdIns(3,4,5)P_3, and activates Akt by phosphorylating the Thr308 residue (Alessi et al., 1997; Stokoe et al., 1997). However, given that PDK1 is found to be mostly localised at the membrane prior to PI3K stimulation via binding to nascent PtdIns(4,5)P_2, and that Akt can also be recruited by PtdIns(4,5)P_2, mechanisms must exist to prevent constant Akt activation. This is thought to be due to the inherent differences in affinity, with PDK1 having a greater affinity for PtdIns(4,5)P_2 whilst Akt has a greater affinity for PtdIns(3,4,5)P_3. Furthermore, full activation of Akt is only achieved when both T308 and S473 sites are phosphorylated (Figure 1.7), with the latter being mediated by mammalian target of rapaymycin complex 2 or mTORC2 (Sarbarssov et al., 2005).

The physiological role of Akt within cells has been shown to be highly pleiotropic, affecting cell survival, proliferation and metabolism. This is demonstrated by the significant body of work implicating the hyperactivation of Akt and its downstream mediators in many human cancers. Overexpression or activation of Akt promotes anti-apoptotic activities within cells, such as by preventing the release of cytochrome C from the mitochondria (Kennedy et al., 1999), and by inactivating pro-apoptotic inducers such as pro-caspase 9 and Bad (Datta et al., 1997; Cardone et al., 1998), in addition to alleviating the pro-apoptotic and cell cycle suppressive effects of FoxO factors (Matsuzaki et al., 2003). Akt also actively promotes cell growth and proliferation by inactivating GSK3β by phosphorylation, which in turn prevents the degradation of cyclin D1 (Diehl et al., 1998), whilst also promoting the degradation of the cell cycle inhibitor $p27^{Kip1}$ and $p21^{cip1/Waf1}$ (Zhou et al., 2001; Liang et al., 2002). Furthermore, the effect of Akt on GSK3β also

extends to the control of glucose transport and metabolism, in that inactivation of GSK3β by Akt relieves GSK3β-mediated inhibition of glycogen synthase, promoting the conversion of glucose to glycogen (Cross et al., 1995). Additionally, microinjection of an antibody that binds to and disrupts Akt function inhibited the insulin-stimulated translocation of glucose transporter 4 (GLUT4) to the membrane, which therefore prevents uptake of extracellular glucose (Hill et al., 1999). Given that the above processes still only represents a small fraction of all Akt functions, its criticality to all cellular processes including development cannot be understated.

1.3.3.3 mTOR – New branches of PI3K signalling

The mammalian target of rapamycin (mTOR) is a protein kinase that exists within two structurally distinct complexes that perform different functions pertaining to the induction of PI3K signalling and are distinguishable in terms of their core components (Figure 1.7). mTORC1 is activated downstream of Akt and consists of the mTOR kinase along with the regulatory-associated protein of mTOR (Raptor), and mammalian lethal with SEC thirteen 8 (mLST8), whereas mTORC2 is activated upstream of Akt and consists of the mTOR kinase, rapamycin-insensitive companion of mTOR (Rictor), mammalian SAPK-interacting 1 (mSin1) and mLST8. Both complexes are also distinguishable in their response to rapamycin, an inhibitor that selectively binds to mTORC1 but not mTORC2 by forming an inhibitory complex with the FKBP12 immunophilin and hence prevent access to the catalytic cleft (Sabers et al., 1995; Benjamin et al., 2011; Yang et al., 2013). mTOR complexes serve as sensors of cellular energy and act to diversify the PI3K signalling response.

i. mTORC1

Activation of mTORC1 activity is conducive to many stimulants, which can be both of extracellular and intracellular origin. Canonically, Akt stimulates mTORC1 activation indirectly through phosphorylating a heterodimeric protein complex consisting of tuberous sclerosis 1 (TSC1) and 2 (TSC2). The TSC1/2 complex functions as a GTPase-activating protein for the Ras homolog enriched in brain (Rheb) GTPase. GTP-bound Rheb directly interacts with mTORC1 to stimulate its activity and as such, inactivation of TSC1/2 via phosphorylation by Akt promotes mTORC1 kinase activity (Inoki et al. 2002 and 2003a; Tee et al., 2003). Additionally, Akt can act in a TSC1/2 independent manner to activate mTORC1 activity by promoting the disassociation of the inhibitory PRAS40 from mTORC1 (Sancak et al., 2007; Vander Haar et al., 2007). The ability of TSC1/2 to transduce inputs to mTORC1 is not solely restricted to the PI3K pathway, or indeed solely to growth factor induced signalling. Activation of adenosine monophosphate

protein kinase (AMPK) in response to hypoxia or high levels of AMP results in the phosphorylation of TSC2 as well as Raptor, ultimately leading to the enhancement of TSC2 activity and inactivation of mTORC1 (Inoki et al., 2003b; Gwinn et al., 2008). In addition, mTORC1 plays a key role in the sensing of intracellular amino acid levels via a class of small G-proteins known as the Rag GTPases. RagA/B-RagC/D heterodimers associate directly with mTORC1, which is dependent upon the nucleotide-loading state of the Rag proteins, consisting of mainly GTP-bound RagA/B and GDP-bound RagC/D in amino acid rich conditions. Rag proteins possess the inherent ability to sense amino acid levels which is dependent on their nucleotide loading state, promoting the accumulation of GDP-bound RagA/D and GTP-bound RagC/D during starvation that cannot bind mTORC1 (Kim et al., 2008; Sancak et al., 2008). However, it appears that the Rag proteins do not function to directly stimulate mTORC1 activity, acting more to spatially control the localisation and exposure of mTORC1 to Rheb through other accessory proteins (Sancak et al., 2010; Bar-Peled et al., 2012).

In response to an abundance of nutrition, mTORC1 primarily serves to drive anabolic processes that result in cell growth and proliferation. Activation of mTORC1 directly regulates the eukaryotic translation machinery by phosphorylating the eukaryotic initiation factor 4E (eIF4E), which disassociates from the 5'-cap of mRNAs and allows translation to proceed (Gingras et al., 2001). Complementarily, activated mTORC1 also drives the phosphorylation and activation of S6 kinase (S6K), which activates downstream factors that stimulate ribosome biogenesis (Martin et al., 2002; Jastrzebski et al., 2007). S6K is also known to phosphorylate insulin receptor substrate 1 (IRS1), inhibiting its ability to activate PI3K and thus forming a negative feedback loop that acts to regulate further mTORC1 activation. In addition, mTORC1 also drives the biosynthesis of lipids and nucleotides, promoting the expression of several enzymes in the pentose phosphate pathway and activating Gln-dependent carbamoyl-phosphate synthase, Asp carbamoyltransferase, dihydroorotase (CAD), a key enzyme involved in *de novo* pyrimidine synthesis (Düvel et al., 2010; Ben-Sahra et al., 2013; Robitaille et al., 2013). Further to driving these anabolic processes, mTORC1 also positively enforces cell survival and proliferation by inhibiting autophagy via the phosphorylation and inhibition of UNC-51 like kinase 1 (ULK1), which is consequently unable to activate the vacuolar protein sorting 34 (VPS34)-Beclin 1-ATG14 complex that initiates autophagy (Kim et al., 2011).

ii. mTORC2

In contrast to mTORC1, the factors and regulative processes driving mTORC2 activation remain critically understudied. Unlike mTORC1, activation of mTORC2 appears to occur only upon PI3K

stimulation and is driven by association with the ribosome (Zinzalla et al. 2011), however the molecular details linking these two events remain unknown. Originally, mTORC2 was determined to be the long sought 'PDK2', phosphorylating Akt at the hydrophobic tail S473 residue, resulting in its full activation (Sarbassov et al., 2005), however further work has revealed other important functions for mTORC2. The ribosome-dependent activation immediately suggests that mTORC2 plays a critical role in the regulation of protein synthesis, and subsequent studies have shown this to be true. In addition to phosphorylating Akt at S473, mTORC2 also co-translationally phosphorylates Akt at the turn motif T450 residue, which has been demonstrated to promote Akt stabilisation and resistance to ubiquitination (Oh et al., 2010). More recently, mTORC2 has also been shown to promote stabilisation of the IGF2 mRNA-binding protein 1 (IMP1) via the same mechanism, which subsequently enhances the production of insulin-like growth factor 2 (IGF2) and cell proliferation (Dai et al., 2013). Thus, co-translational phosphorylation is a hallmark mechanism that is directly attributed to mTORC2, which is likely to apply to many other as of yet undiscovered substrates.

1.3.3.4 Relevance of mTOR signalling to development and differentiation

Given that the PI3K/Akt/mTOR signalling pathway plays a major role in promoting the growth and expansion of cells, it is perhaps unsurprising to find that this signalling axis also impinges upon many aspects of development and stem cell differentiation. With regards to development, loss of various components of the signalling cascade often results in embryonic lethality. Deletion of the p110 catalytic subunit in the mouse results in embryonic lethality at E9.5 due to cephalic and proliferative defects, (Bi et al., 1999) whilst Akt1/Akt3 double-null mice display embryonic lethality a little later at E10.5 due to cardiovascular defects and impaired brain development (Yang et al., 2005). Similar phenotypes are observed in TSC1 and TSC2 null embryos, which die around stage E10.5-11.5 due to a failure in neural tube closure and anencephaly (Onda et al., 1999; Kobayashi et al., 2001). More significantly, mTOR-null and rapamycin treated embryos display lethality at an even earlier stage at E5.5-6.5 not long after implantation due to defects in the proliferation of ICM and TE cells (Gangloff et al., 2004; Murakami et al., 2004). In taking this observation further, Raptor and Rictor knockout mice have also been generated in order to define the contributions of mTORC1 and mTORC2 respectively to these defects. *Raptor* knockout mice largely phenocopy that of mTOR-null embryos, in that blastocyst explants show proliferation defects in the ICM and trophoblast, whilst deletion of *Rictor* only results in lethality around E10.5 due to vascular defects (Guertin et al., 2006b; Shiota et al., 2006). Therefore, it appears that mTORC1 is required early on in development mainly to drive cell proliferation, whilst mTORC2

is required later during mid-gestation to coordinate tissue vascularisation and consolidate their response to growth factors. Furthermore, given that PTEN knockout mice possess more or less the same defective features and embryonic lethality observed in p110 knockouts (Suzuki et al., 1998), the role PI3K/Akt/mTOR signalling plays in modulating developmental processes may also depend on an optimal level of signalling, as well as interactions with other key developmental pathways.

Since developmental progression reaches the post-implantation stage in p110, Akt and mTORC-null mouse mutants, it appears that the PI3K/Akt/mTOR pathway is largely dispensable in germ layer specification. However, the fact that all of the above null phenotypes result in embryonic lethality suggests that rather than directly driving differentiation, components of the PI3K/Akt/mTOR cascade are likely to regulate the differentiation process and promote the expansion and homeostasis of differentiated progenitors. This is evident in that LY-mediated inhibition of PI3K in mESCs results in the loss of self-renewal and attenuated the expression of Nanog (Paling et al., 2004; Storm et al., 2007), whilst PI3K inhibition in hESCs downregulated the expression and activity of stage-specific embryonic-antigen 4 (SSEA4) and alkaline phosphatase respectively, which is indicative of pluripotency loss (Armstrong et al., 2006). Moreover, expression of constitutively active Akt is sufficient in preserving the pluripotency of mouse and primate ES cells (Watanabe et al., 2006), whilst treatment of hESCs with the mTORC1 inhibitor rapamycin induced the loss of pluripotency and the induction of definitive endoderm (Zhou et al., 2009). Furthermore, siRNA-mediated knockdown of PTEN in hESCs promoted self-renewal at the expense of differentiation potential, with a greater bias towards the formation of neuroectoderm over mesendoderm (Alva at al., 2011). This is in agreement with previous findings that demonstrated the need to inhibit PI3K/Akt/mTOR signalling in hESCs in order to achieve efficient differentiation towards the definitive endoderm, (McLean et al., 2007), as well as the ability of insulin to redirect endoderm and mesoderm progenitors during *in vitro* cardiogenesis towards the neuroectoderm (Freund et al., 2008). Therefore, efficient specification of the DE *in vitro* is likely to require a combinatorial approach that takes into consideration the regulatory contributions of PI3K/Akt/mTOR signalling.

1.4 Modelling DE development using hESCs

1.4.1 Derivation of hESC lines

Although developmental studies have undoubtedly been a success as an ideological springboard from which to investigate human development, there are both ethical and technological difficulties in performing similar experiments using human embryos. Furthermore, the complex environment cells reside in the embryo precludes any meaningful investigation of the molecular underpinnings, making a complete characterisation of the mechanisms responsible impossible. Once again in turning to the mouse model, seminal work performed by two independent groups demonstrated that cells from the ICM could be isolated and cultured from mouse blastocysts *in vitro* (Evans and Kaufman, 1981; Martin, 1981). These cells, termed mESCs were shown to possess a normal karyotype and could self-renew indefinitely in culture, whilst being able to be differentiated into cells derived from all three germ layers but not the placenta, much like the cells of the ICM. This powerful property of pluripotency is strikingly evident in that when these cells were injected into blastocysts, they were able to produce chimeras, contributing to the formation of all tissues, including germ cells and thus generating entire embryos via germline transmission. Furthermore when injected into developmentally compromised tetraploid blastocysts, some of these mESCs were able to generate the intact embryo by themselves; the most stringent definitive test of pluripotency (Nagy et al., 1990 and 1993). In addition to mESCs, another population of stem cells have been isolated from the post-implantation epiblast known as epiblast stem cells or EpiSCs (Brons et al., 2007; Tesar et al., 2007). These cells retain the self-renewing and pluripotent characteristics of mESCs in that they are able to be cultured indefinitely and form teratomas respectively, but critically, are unable to form chimeras unless directly reprogrammed to do so (Tesar et al., 2007; Guo et al., 2009). Although this suggests that EpiSCs may therefore represent a more primed stem cell population that are unable to completely recapitulate pluripotency to the same degree as the more naive mESCs, several findings contradict this argument. For example, EpiSCs retain the ability to give rise to TE, which is not observed in mESCs unless they are cultured under specific conditions (Schenke-Layland et al., 2007, Morgani et al., 2013). Therefore it can be argued that EpiSCs are in this respect more naive than mESCs in terms of their differentiation potential and that the pluripotent efficacy of all embryonic stem cells is likely to be heavily dependent on their culture conditions. Furthermore, the ability to form chimeras may be a species-dependent effect rather than a true reflection of stem cell naivety, since chimera formation from embryo-derived stem cells has only been demonstrated in the laboratory mouse and rat strains, but not in wild-type mouse, farm animals and primates (Nagy et al., 1993; Buehr et al.,

2008; Li et al., 2008; Tachibana et al., 2012). Thus, it is impossible to distinguish whether the failure of chimera formation in other species is truly due to a loss of naivety or simply due to immunological incompatibility with the host embryo. Nevertheless, the derivation of several embryonic stem cell populations allowed for the generation of transgenic organisms with relative ease, and thus offered a model through which the effect of genetic manipulation could be examined on an organism-wide scale, albeit with a significant caveat in place in terms of interspecies relevance (Robertson et al., 1986).

Several decades later, successful isolation of primate and human embryonic stem cells swiftly followed utilising refined techniques developed from their initial isolation in mice (Thomson et al., 1995 and 1998). These cells, much like their mouse counterparts, are karyotypically stable, and can give rise to cells originating from the three germ layers evidenced by teratoma formation in immunocompromised mice, whilst also being able to be propagated indefinitely in culture. However whether hESC could contribute to the formation of chimeras remains unknown due to ethical constraints, although recent success in forming chimeras by combining primate embryos at the 4-cell stage but not from primate ESCs provides compelling evidence to suggest that the same situation applies to human derived pluripotent cells (Tachibana et al., 2012). Although the inability of primate ESCs and likely hESCs to successfully form chimeras suggests that the isolated cells may represent a more primed population which has already lost some efficacy in terms of pluripotency, this again could equally be regarded as a consequence of species to species variation, as chimera generation has only been formally demonstrated in rodents. Furthermore, studies in atypical animal models such as cattle have begun to reveal species-dependent differences pertaining to the specification and maintenance of the TE (Berg et al., 2011), which is likely to also apply when translating findings from mouse and primate ESCs to human ESCs. As such, there remains ample scope for the use of hESCs in order to study human development, given that findings in mice and other vertebrate models may not necessarily correlate completely to that of humans.

1.4.2 Maintenance of pluripotency

The retention of pluripotency is a key hallmark demarcating embryonic and pluripotent stem cells from other cell types, and is governed by coordinated regulation of intrinsic and extrinsic factors. Intrinsic factors are transcription factors, represented by the key trio of Oct4, Sox2 and Nanog (OSN) that form a distinct core transcriptional circuitry to activate the expression of pluripotent genes, including themselves, whilst also acting to repress the expression of lineage-specific genes

and maintain the pluripotent state (Boyer et al., 2010). Expression of these core transcription factors is additionally subject to regulation by extrinsic signalling pathways (Figure 1.8).

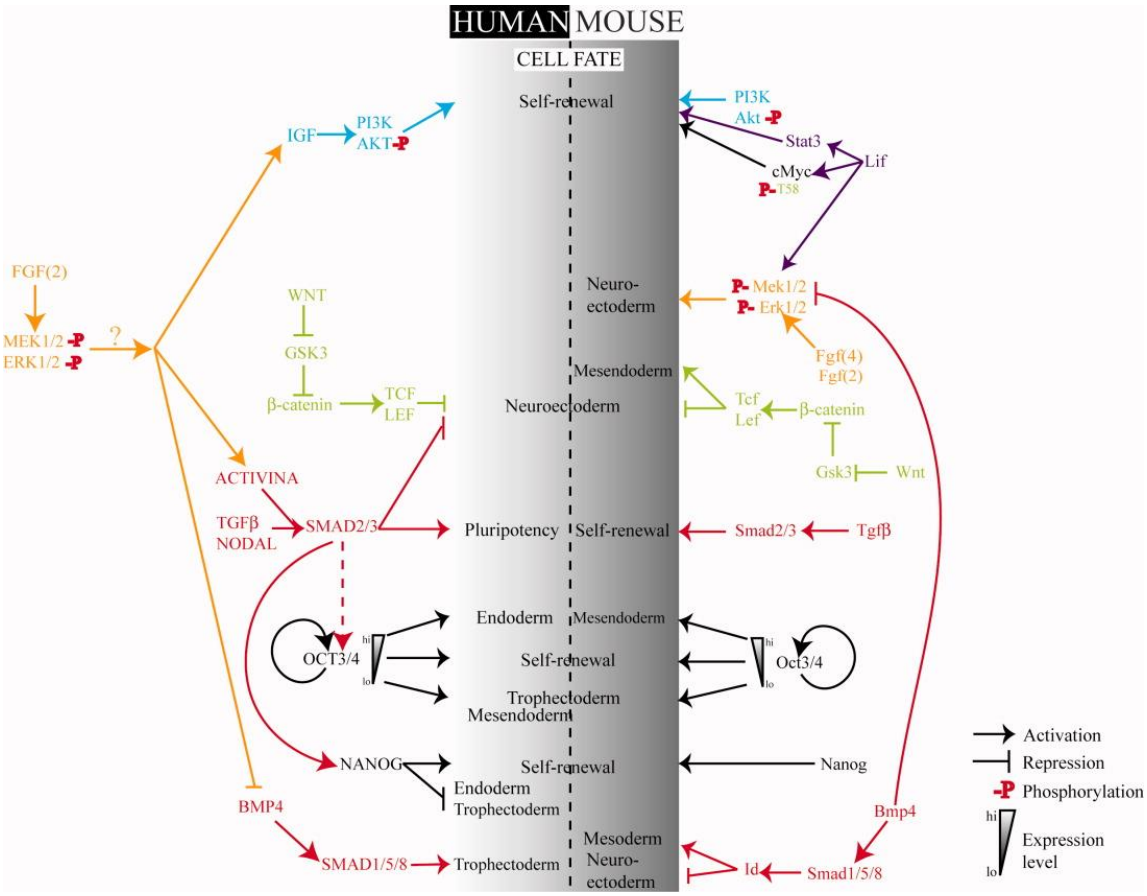

Figure 1.8: Differences in signalling requirements for human and mouse ESC maintenance and differentiation.

Summary of the shared and divergent actions of signalling pathways in mediating mouse and human ESC self-renewal, pluripotency and differentiation. In hESCs, FGF2 signalling is able to prevent differentiation by suppressing BMP4 and stimulating PI3K activity in combination with low amounts of Activin/Nodal and Wnt signalling. Conversely, mESCs depend upon LIF combined with BMP4 to suppress differentiation due to MEK1/2 and GSK3β activity. Adapted and presented with permission from John Wiley and Sons: Stem Cells, Schnerch, copyright 2010.

1.4.2.1 Intrinsic factors

i. Oct4

Oct4, encoded by the *Pou5f1* allele, is a member of the Pit-Oct-Unc (POU) family of homeodomain proteins whose expression is initially found in the blastomeres and later becomes restricted to the epiblast and primordial germ cells (Palmieri et al., 1994; Pesce et al., 1998). As such, hESCs isolated from the ICM also express Oct4 at high levels, which points to the involvement of this factor in the maintenance of the pluripotent state. Loss of Oct4 in mice embryos results in the complete absence of ICM, with only TE present (Nichols et al., 1998), whilst overexpression in ESCs triggers the formation of PrE and mesoderm (Niwa et al., 2000). Interestingly, the same study also noted that different levels of Oct4 expression resulted in different cell fates, ranging from TE to mesoderm at lower and higher than ESC levels of Oct4 respectively. More recent evidence suggests this lineage specifying property of Oct4 also applies to both mESC and hESC cultures, whilst also extending the same properties to Sox2 and Nanog (Hay et al., 2004; Wang et al., 2012). As such, Oct4 possesses multifaceted roles during the course of development, acting initially to preserve pluripotency by guarding against TE differentiation, whilst also playing a major role in the latter germ layer specification of endoderm and mesoderm before becoming restricted to the germ cells of the adult organism.

ii. Sox2

Sox2, a member of the HMG group of transcription factors is also implicitly involved in the preservation of the pluripotent state. Much like Oct4, Sox2 is initially detected at the morula stage, before being confined to the ICM of the pre-implantation epiblast, with the loss of Sox2 abolishing ICM formation (Avilion et al., 2003). As such, loss of Sox2 in ESCs results in the rapid loss of pluripotency markers and differentiation to primarily TE tissues (Ivanova et al., 2006; Masui et al., 2007). The remarkable similarity between Oct4-null and Sox2-null mutants led to the suspicion that both factors act to regulate a redundant set of genes necessary in preserving pluripotency. This is further evidenced by the fact that forced expression of Oct4 in Sox2-null mice is able to rescue the loss of pluripotency in these cells (Masui et al., 2007; Fong et al., 2008). Agreeably, both Sox2 and Oct4 have been shown to reciprocally occupy their respective enhancer regions, as well as co-occupying sites upstream of many genes that have been shown to be important for regulating pluripotency (Boyer et al., 2005; Loh et al., 2006; Chen et al., 2008), which further suggests mutual regulation of their expression and hence function. Furthermore, Sox2 has also been shown to suppress the expression of primitive streak markers (Wang et al., 2012), which implies that Sox2

acts to regulate the expression of Oct4, preventing both the formation of TE and mesendoderm, whilst also acting in conjunction with Oct4 to consolidate the pluripotent state. The powerful pluripotent inducing and consolidating properties of both Oct4 and Sox2 are strikingly evident in that transgenic overexpression in conjunction with Krüppel-like factor 4 (Klf4) and c-myc is capable of reprogramming fully differentiated fibroblasts back into an embryonic stem cell-like state (Takahashi and Yamanaka, 2006).

iii. Nanog

The third component of the pluripotency triad is Nanog, a homeobox protein that was originally discovered using a genetic screen for factors that could maintain mESC pluripotency in the absence of LIF, (Chambers et al., 2003; Mitsui et al., 2003). *In vivo*, Nanog expression is first detectable in the compacted morula, which like Oct4 and Sox2, becomes progressively restricted first to the ICM and latterly to the germ cells post-implantation (Mitsui et al., 2003). Subsequently, loss of Nanog results in the concurrent cessation of post-implantation development, however unlike the loss of Oct4 or Sox2, structures resembling the ICM is still evident in Nanog-null blastocysts. Although ESCs can be successfully isolated and propagated from these blastocysts, they are more prone to differentiate into primarily TE tissues (Mitsui el al., 2003). Concurrently, conditionally Nanog-null ESC lines are able to contribute to the formation of all somatic lineages with the exception of germ cells, which implies that Nanog is ultimately dispensable for ESC pluripotency (Chambers et al., 2007). Thus, it appears that Nanog plays a critical role in the establishment of the pluripotent state rather than strictly promoting its maintenance. However, given that *Nanog* itself is a Sox2/Oct4 target (Rodda et al., 2005), concurrent expression of all three factors acts to fully consolidate and maintain the pluripotent transcriptional program (Loh et al., 2006; Chen et al., 2008).

1.4.2.2 Extrinsic factors

The culture and maintenance of embryonic stem cells require specific combinations of signalling ligands that act to stimulate the transcriptional machinery necessary in preventing spontaneous differentiation, which appear to differ between human and mouse (Figure 1.3). In the case of mouse ESCs (mESCs), co-culture with mitotically inactivated embryonic fibroblasts in the presence of serum was sufficient in supplying the extrinsic cues needed to maintain the pluripotent state (Evans and Kaufman, 1981; Martin, 1981). This was further refined upon the discovery that LIF and BMP4 could replace both serum and feeders, allowing the development of more defined culture conditions (Smith et al., 1988; Williams et al., 1988; Ying et al., 2003). Recent evidence has

taken this even further, in that mESCs can be isolated and cultured in the absence of BMP4, but in the presence of GSK3 and MAPK inhibitors supplemented together with LIF (termed 2i/LIF), (Ying et al., 2008). The fact that ESCs can exist under different signalling environments posits the existence of a spectrum of cell states that reflect the differentiation capacity of the cells. This is evident in that mESCs when cultured under 2i/LIF conditions are able to form extraembryonic tissues (Morgani et al., 2013), which does not occur in feeder-dependent mESCs and is suggestive of a conversion to a more naive state, termed the ground-state. In contrast, EpiSCs whilst still retaining the pluripotent features of mESCs, fail to significantly contribute to chimeras and the germline, which is indicative of a loss in pluripotent efficacy (Brons et al., 2007; Tesar et al., 2007). However, isolation of a subpopulation within EpiSC cultures that resemble cells of the early epiblast is able to restore chimera formation (Han et al., 2010), which again highlights the inherent heterogeneity of ESC cultures in their propensity for differentiation and that culture conditions can act to determine the efficacy of differentiation.

The idea that embryonic stem cells can exist in varying states of differentiation efficacy becomes even more evident when considering the culture conditions that permit the propagation of hESCs. Whilst both mESCs and hESCs were originally isolated and propagated in similar ways, it quickly became evident that hESCs differed in many respects. Firstly, in terms of morphology, hESC colonies are flatter, opposed to the more domed appearance of mESCs and are more reminiscent of EpiSCs. Secondly, whilst mESCs can be propagated as single cells independent of feeder, hESCs undergo apoptosis when disassociated and rapidly differentiate in the absence of feeders. However, hESCs can be successfully cultured feeder-free if passaged onto Matrigel-coated plates supplemented with mouse embryonic fibroblast conditioned media (MEF-CM), and as single cells if the media is supplemented with Rho kinase inhibitor or ROCKi (Watanabe et al., 2007). Finally, and perhaps most importantly, hESCs differ in their response to extrinsic signalling cues. hESCs do not require LIF for propagation or maintenance, but instead requires fibroblast growth factor 2 (FGF2), (Dahéron et al., 2004; Dvorak et al., 2005). FGF2 is thought to exert both direct and indirect effects that positively enforce the pluripotent state. Provision of exogenous FGF2 to hESCs reduces spontaneous differentiation, promotes cell adhesion, survival and proliferation whilst also indirectly stimulating the secretion of AA from the feeder layer (Greber et al., 2007; Li et al., 2007; Eiselleova et al., 2009). Low levels of AA act to drive the expression of Nanog, a key pluripotency factor and hence act in tandem with the other pleiotropic effects of FGF2 to maintain hESC self-renewal and pluripotency (Vallier et al., 2005; Xu et al., 2008). Contrastingly, unlike in mESCs, the presence of BMPs in hESC cultures act to promote differentiation of hESCs, in that hESCs cultured in defined media containing the native BMP antagonist Noggin retain pluripotency

(Xu et al., 2005). The similarity in the signalling response between hESCs and EpiSCs rather than mESCs, coupled with the inability of primate derived ESCs to form chimeras suggests that hESCs are more equivalent to the primed EpiSCs than mESCs (Tesar et al., 2007). This has recently been supported by the successful derivation of naive hESCs by several groups, which retain molecular and functional properties that are more akin to mESCs but with different extrinsic culture conditions (Gafni et al., 2013; Takashima et al., 2014; Theunissen et al., 2014). However, hESCs do not express the EpiSC marker, FGF5, but retain expression of the mESC marker Rex1, indicating that the difference between hESCs and mESCs could also be attributed to distinct species to species differences. Nevertheless, the relative ease by which naive and primed hESCs can be propagated under increasingly more defined conditions makes them excellent cell models from which to interrogate molecular mechanisms governing directed differentiation.

1.4.3 Interaction of extrinsic and intrinsic factors in hESCs

Given that mouse and human ESCs differ significantly in their response to extrinsic cues necessary for the maintenance of self-renewal and pluripotency, the mechanism by which signalling pathways establish the OSN network must also differ. Although it is generally accepted that FGF2 and Activin/Nodal signalling are the two key pathways needed to maintain hESC pluripotency, unravelling the exact molecular mechanisms involved in this process have proved difficult and poorly characterised when compared to mESCs. This is due to the inherent pleiotropic effects attributed to FGF2 signalling and the multitude of culture conditions in which hESCs are propagated. Whilst it has been suggested that FGF2 may act via ERK to prevent differentiation to extra embryonic lineages (Li et al., 2007), it appears that this alone is insufficient in that both FGF2 and Activin/Nodal signalling are required to maintain hESCs in the absence of MEF-CM or feeders via the upregulation of Nanog (Vallier et al., 2005 and 2009). This has been supported by chromatin immunoprecipitation (CHIP) experiments which show the direct association of Smads with the *Nanog* proximal promoter (Xu et al., 2008) as well as with other pluripotency genes such as *Oct4,* Telomerase reverse transcriptase (*TERT*) and *myc* (Brown et al., 2011), thereby underscoring the critical importance of Smad2/3 and Nodal/Activin signalling to the maintenance of pluripotency.

The contentious issue of hESCs representing a more primed pluripotent population akin to that of EpiSCs has been recently reinforced by the successful derivation of naive hESCs, which may serve to account for the difference in extrinsic factors required for the propagation of mESCs and hESCs. The induction of naivety in conventional hESCs via the expression of *Klf2* and *Nanog*

transgenes results in global changes in DNA methylation, gene transcription and metabolic output that is more similar to mESCs (Takashima et al., 2014). This coupled with the ability of these cells to retain pluripotency under culture conditions which completely lack exogenous growth factors strongly suggests that the maintenance of pluripotency in conventional hESC cultures require FGF2 and Activin/Nodal signalling simply because the transcriptional circuitry requires greater reinforcement in order to be stably propagated. Moreover, the existence of this ground-state is evident in that transient transgene expression is sufficient to revert conventional hESCs into a more naive state albeit their propagation requires reinforcement via culture with 2i/LIF and the PKC inhibitor Gö6983. Together, these finding may reflect the transient nature of pluripotency *in vivo*, as well as the intrinsic propensity towards differentiation during development.

1.4.4 Differentiation of hESCs to definitive endoderm and hepatocytes

1.4.4.1 Combinatorial approaches to in vitro DE specification

As demonstrated in the mouse and ESCs, the induction of DE formation principally requires the presence of Activin/Nodal signalling. However, given that low levels of Activin/Nodal are conducive to preserving pluripotency *in vitro* (Vallier et al., 2005) and for specifying mesoderm *in vivo* (Vincent et al., 2003), the induction of DE should therefore require high or sustained levels of Activin/Nodal stimulus. AA serves as an effective surrogate for Nodal in the *in vitro* induction of DE as it is more stable in storage and in culture unlike Nodal whilst still inducing the same downstream signal cascade. Effective endoderm specification utilising high dose Activin was first demonstrated in mESCs, which when cultured under low attachment conditions in serum-free media containing AA readily forms embryoid bodies which contain brachyury-positive cells that formed endoderm structures when purified and transplanted into mouse kidney capsules (Kubo et al., 2004). This process was subsequently refined in the derivation of DE cells from hESCs, utilising monolayer cultures to maximise the exposure of the cells to the signalling ligand. Under these conditions, hESCs progressed through a primitive streak-like phase, recapitulating the *in vivo* developmental program and resulting in a greater number of Sox17-positive cells (D'Amour et al., 2005). Furthermore, the same study found that the presence of serum drastically reduced the efficiency of this specification, and a subsequent study would implicitly link the PI3K pathway to this inhibitive effect, in that dual treatment of hESCs with both Activin and the PI3K inhibitor LY promoted a more efficient Activin-induced DE differentiation (McLean et al., 2007). Thus, the conditions favouring efficient endoderm formation include high or sustained Activin coupled with low PI3K signalling, although the exact underlying mechanisms remain unknown.

Evidently from developmental studies, although Activin/Nodal signalling is critical in the formation of any mesendodermal tissue, the Wnt/β-catenin pathway also functions to cooperatively aid in the specification of the primitive streak and mesendoderm (Conlon et al., 1994; Liu et al., 1999). As such, modulation of the Wnt/β-catenin signalling in hESCs coupled with TGFβ signalling should also positively reinforce the formation of endoderm. Several studies have reported this effect, in that inducible expression of constitutively active β-catenin or supplementation with active Wnt3a ligand together with BMP or Activin in hESCs promoted the formation of mesoderm and endoderm respectively (Hay et al., 2008; Sumi et al., 2008). Furthermore, recent studies employing the use of GSK3β inhibitors that largely mimic the effects seen when Wnt/β-catenin signalling is activated also improved the derivation of Activin-induced DE to similar levels as that of directly supplying Wnt3a (Kunisada et al., 2012; Teo et al., 2014). In addition to signalling ligands, the application of epigenetic modifiers has also been shown to improve the derivation of DE when combined with high dose Activin. For example, use of sodium butyrate is known to improve the homogeneity of DE specification in hESCs by inhibiting the action of histone deacetylases (Jiang et al., 2007; Hay et al., 2008b). However this method also resulted in high levels of cell death and permanent modifications to the epigenetic landscape that impacted further differentiation from the DE stage. As such, the predominant method for deriving DE from hESCs is still very much a growth factor and small molecule inhibitor driven process, although the molecular mechanisms behind this process remains largely incomplete.

1.4.4.2 Derivation of hepatocytes from hESC-derived DE for therapeutic use

Liver disease represents a major health concern, given that over 1 million people die globally each year from acute or chronic liver failure (Gonzalez and Keeffe, 2011) and that the only effective therapeutic intervention in most cases is transplantation. Evidently, this has resulted in a significant number of patients dying whilst waiting for donor organs to become available, constituting a significant bottleneck in preventing liver disease associated mortality. Efforts to develop alternative therapeutic options using cells isolated from native sources such as foetal hepatocytes or using adult livers to derived hepatic cell lines have been largely unsuccessful due to their functional immaturity and limited capacity for expansion to levels required for therapeutic use respectively. As such, efforts made to circumvent these limitations have resulted in the use of pluripotent stem cells as a platform from which to derive functional hepatocytes, since stem cells are able to be cultured indefinitely while possessing the inherent ability to form any cell constituting the adult organism.

The efficient derivation of a highly homogenous population of DE from hESCs or iPSCs represents the first stage from which more specialised and therapeutically useful hepatocytes can be derived (Figure 1.8). As outlined in the previous section, several different methods exist by which to achieve this, mainly utilising high dose Activin in combination with inhibitors or growth factors that serve to improve the homogeneity of the final culture. However, the culture conditions driving the commitment of DE cells to hepatocyte progenitors are generally conserved in most protocols, in that BMP2/4 and FGF2 are either sequentially applied or given in combination to the culture (Cai et al., 2007; Song et al., 2009; Si-Tayeb et al., 2010; Touboul et al., 2010). The hepatic specifying activities of BMP2/4 and FGF2 are also well characterised in the mouse, and are consequently able to enforce the commitment of hESC and iPSC derived DE towards the hepatic lineage (Jung et al., 1999; Rossi et al., 2001). Following the formation of hepatocyte progenitors known as hepatoblasts, further culture is required to achieve functional maturation, involving treatment with hepatocyte growth factor (HGF), oncostatin M (OSM) and dexamethasone which have been shown to drive the maturation of foetal hepatocytes (Kamiya et al., 2001; Suzuki et al., 2003). The resultant cells are morphologically similar to that of primary hepatocytes, notably in being polygonal in shape, highly vacuolarised and possessing prominent nucleoli.

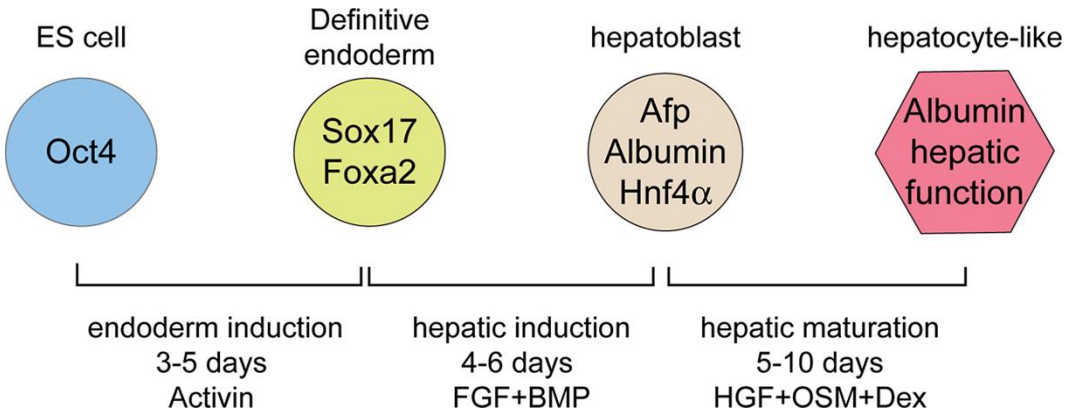

Figure 1.9: Hepatic differentiation from DE

Schematic depicting the most commonly used culture conditions in converting ESCs to hepatocyte-like cells. High dose Activin treatment converts ESCs to DE, which is accompanied by progressive downregulation of Oct4 coupled with the induction of Sox17 and FoxA2. DE cells are directed towards the hepatic lineage upon exposure to FGF and BMP signalling, resulting in the expression of AFP, albumin and HNF4α. Further maturation with HGF, OSM and Dex results in hepatocyte maturation, accompanied by increased albumin secretion and the gain of detoxification activities. Image taken and adapted from Zorn, 2008.

The progression from hESC/iPSC to mature hepatocyte-like cells is accompanied by distinctive changes in gene expression profiles that are characteristic of each stage of differentiation (Figure 1.9), which also largely mimics what is observed *in vivo*. Much like the cells of the ICM, hESCs/iPSCs express high levels of Oct4, Sox2 and Nanog, which become progressively downregulated upon DE conversion. This is accompanied by a transient upregulation of primitive streak markers such as Brachyury, which is rapidly downregulated upon continued culture as the cells adopt a more endoderm fate opposed to the mesoderm. The DE fate is consolidated by the increasing upregulation of factors such as MixL1, Eomes, Sox17 and FoxA2, which also serve as markers defining the successful formation of DE in culture. Sox17 expression is progressively lost during the maturation stages, whilst FoxA2 persists throughout (Si-Tayeb et al., 2010). However, in the early stages of DE specification, many of these profiles are shared with the extraembryonic endoderm. The DE identity is demarcated by the ability of DE to form cells of hepatic origin upon further culture, and serves as important test by which to verify the successful formation of DE over extraembryonic endoderm. Transition of DE to hepatoblast cells is marked by an increase in the expression of genes that are characteristic of the foetal liver such as alpha-fetoprotein (AFP), which is progressively downregulated as the hepatoblasts are matured into hepatocyte-like cells

concomitant with increased albumin secretion. Much like primary hepatocytes, these hepatocyte-like cells express several genes that strongly correlate with the acquisition of a functional hepatocyte phenotype, such as the expression of albumin and detoxification enzymes such as cytochrome P450 (CYP450), which can be further assessed on a functional level by specialised assays to determine the degree of maturation achieved by different protocols (Schwartz et al., 2005; Khetani and Bhatia, 2008; Chen et al., 2011).

Despite the relative ease by which hepatocyte-like cells can be derived from hESC/iPSCs, significant hurdles remain to be overcome before they can be used therapeutically. The main obstacles concern the inability of these cells to fully recapitulate all the functions associated with primary hepatocytes over long term and difficulties in scaling up the differentiation process to obtain a sufficient number of cells for therapeutic intervention. Furthermore, although the advent of iPSCs has made the prospect of autologous derivation and transplantation of hepatocytes possible, there are questions surrounding the genomic stability of these derived cells. Many of these problems stem from an inefficient derivation of DE, producing cells which although competent in converting to hepatic fates, are nonetheless already functionally compromised due to either partial conversion or exposure to toxic factors required to drive the initial exit from the stem cell state. As such there is an inherent need for a more complete molecular characterisation of this initial stage of differentiation, in an effort to improve the functional properties of resultant hepatocytes.

1.5 Aims and Hypothesis

Whilst Activin/Nodal signalling has been shown to be the critical pathway in driving DE formation, the importance of PI3K signalling in driving the proliferation and consolidation of differentiated tissues has firmly established this pathway as a key modulator of DE specification. Although previous studies have demonstrated the antagonistic effect of PI3K signalling upon DE differentiation, the use of undefined culture conditions precludes any attempt at defining the molecular basis for this effect (D'Amour et al., 2005; McLean et al., 2007). Although several groups have proposed a range of molecular mechanisms by which to explain why PI3K activity antagonises TGFβ-induced apoptosis and cell cycle arrest (Conery et al., 2004; Remy et al., 2004; Song et al., 2006), it is questionable whether these mechanisms apply to hESCs and their differentiation, given that all of these studies were performed in tumour lines that are known to possess abnormal signalling responses. Although one recent study attributed the antagonistic effect of PI3K/mTOR signalling on DE differentiation in hESCs to an indirect effect of Wnt/β-catenin inhibition (Singh et al., 2012), they could not explain the origin of the increase in Smad2/3 activation observed in their study, which hinted at a more direct mechanism through which PI3K/mTOR signalling impacts R-Smad activity (Chen et al., 2012).

As such, this study posits the existence of a direct mechanism through which components of the PI3K pathway interact to regulate the activity of Activin-induced R-Smads. Specifically this study aims to assess this hypothesis in the following manner:

1) Verify the relationship between PI3K mediators and R-Smad activity during DE differentiation in hESCs under chemically defined conditions.
2) Fully characterising and robustly testing the molecular mechanisms involved in mediating this crosstalk through inhibitor assays and gain or loss-of-function approaches.
3) Develop new methods by which to differentiate hESCs to DE utilising new insights gained from the molecular model in order to improve hepatocyte differentiation.

Completion of this study will hence contribute to a greater understanding of the crosstalk mechanisms governing DE formation, from which new methods can be developed to improve the efficiency of hESC to DE differentiation and ultimately improve the procurement of functionally competent hepatocytes.

Chapter Two

Materials and Methods

2.1 Cell Culture

2.1.1 Materials

2.1.1.1 Cell Lines

All cells were cultured at 37 °C with 5% CO_2.

Cells	Source
H1 hESC (WA-01)	Male human ES cell line isolated by Thomson et al., 1998, distributed by WiCell.
PC-3	Prostate adenocarcinoma cell line derived from a metastatic site in the bone, kind gift from Dr. Robert Krypta.
Hep3B	Liver cell line derived from hepatocellular carcinoma, obtained from the European Collection of Cell Cultures (ECACC).
HEK293T	Kidney cell line immortalised by T-antigen delivered by adenovirus, obtained from the ECACC.
Mouse Embryonic Fibroblasts (MEFs)	Wild-type MEFs isolated from E13.5 CD-1 mouse embryos.
Rictor-Control MEFs	Control MEFs for Rictor-null kind gift from Prof. Mark Magnuson (Shiota et al., 2006).
Rictor-Null MEFs	Immortalised MEFs with knockout of Rictor gene also from Prof. Mark Magnuson (Shiota et al., 2006).

2.1.1.2 Growth Factors and Inhibitors

All growth factors reconstituted in Dulbecco's Phosphate Buffered Saline (DPBS) supplemented with 0.2% BSA as carrier, all inhibitors reconstituted in DMSO with the exception of chloroquine, puromycin, ascorbic acid and ROCKi which were reconstituted in TC grade H_2O.

Reagent	Supplier	Working Concentration
Activin A (AA)	Peprotech	100 or 10 ng/ml
Ascorbic Acid	Sigma-Aldrich	50 μg/ml
Bone Morphogenetic Protein 2 (BMP2)	Peprotech	20 ng/ml
Chloroquine	Sigma-Aldrich	25 μM
Flavopiridol	Selleck Chemicals	1 μM
Hepatocyte Growth Factor (HGF)	Peprotech	10 ng/ml
Heregulin (H)	Peprotech	10 ng/ml
Basic Fibroblast Growth Factor (bFGF)	R&D	10 ng/ml
Hydrocortisone-21-hemisuccinate	Sigma-Aldrich	10 μM
Insulin	Sigma-Aldrich	1 μM
LR^3-IGF (I)	Sigma-Aldrich	100 ng/ml

LY294002 (LY)	NEB	20 μM
MG-132	Millipore	10 μM
Okadaic Acid	Millipore	5 nM
Oncostatin M (OSM)	R&D	20 ng/ml
Puromycin	Sigma-Aldrich	1-2.5 μg/ml
Rapamycin	Sigma-Aldrich	100 nM
Rho Kinase Inhibitor (ROCKi)	Sigma-Aldrich	10 μM
SB203580	R&D/Tocris	20 μM
SB431542	Sigma-Aldrich	10 μM
SP600125	Reagents Direct	500 nM
Torin-2 (Torin/Tor)	R&D/Tocris	10 nM
U0126	Reagents Direct	10 μM
Wortmannin (Wort)	Sigma-Aldrich	300 nM

2.1.1.3 Media Components

Component	Supplier
200 mM L-Glutamine	Sigma-Aldrich
100X Penicillin-Streptomycin	Sigma-Aldrich
20% Bovine Serum Albumin (BSA)	Sigma-Aldrich
50X B27 Supplement (-vitamin A)	Life Technologies
Dulbecco's Modified Eagle AQ Media (DMEM-AQ)	Sigma-Aldrich
Heat-inactivated Foetal Bovine Serum (FBS)	Sigma-Aldrich
Knockout DMEM	Life Technologies
Knockout Serum Replacement (KSR)	Sigma-Aldrich
Lebovitz's L-15 Media (L-15)	Sigma-Aldrich
Non-essential Amino Acids (NEAA)	Life Technologies
Opti-MEM® Reduced Serum Medium	Life Technologies
Roswell Park Memorial Institute AQ-Media 1640 (RPMI-AQ)	Sigma-Aldrich
Tryptose Phosphate Broth (TPB)	Sigma-Aldrich
50 mM β-mercaptoethanol	Life Technologies

2.1.1.4 Disassociation Enzymes

Enzyme	Supplier
Accutase	Sigma-Aldrich
Collagenase IV	Life Technologies
Trypsin-EDTA	Sigma-Aldrich

2.1.1.5 Chemicals, Kits and Coating Reagents

Reagent	Supplier
2% Gelatine in PBS	Sigma-Aldrich
Calcium Phosphate Transfection Kit	Sigma-Aldrich

Chondroitin Sulphate	Sigma-Aldrich
Dimethyl sulphoxide (DMSO)	Sigma-Aldrich
Dual-Glo® Luciferase Assay Kit	Promega
Dulbecco's Phosphate Buffered Saline (DPBS)	Sigma-Aldrich
Hexadimethrine bromide (Polybrene)	Sigma-Aldrich
Lipofectamine™ LTX with PLUS™ Reagent	Life Technologies
Matrigel® Matrix Growth Factor Reduced	BD Bioscience
Water Tissue Culture Grade (TC-H_2O)	Sigma-Aldrich

2.1.1.6 Media and Stock solutions

All media and stocks were filter sterilised and stored at 4 °C.

MEF/HEK293T/Hep3B medium (D10)	DMEM-AQ supplemented with: 10% FBS 1x NEAA 1x Penicillin-Streptomycin
PC-3 medium (R10)	RPMI-AQ supplemented with: 10% FBS 1x NEAA 1x Penicillin-Streptomycin
Knockout Serum Replacement Medium (KSR-M)	KO-DMEM supplemented with: 20% KSR 1 mM L-glutamine 1x NEAA 0.1 M β-mercaptoethanol for TC 1x Penicillin-Streptomycin
MEF-conditioned medium for H1 hESCs (MEF-CM)	MEF conditioned KSR-M supplemented with: 1 mM L-glutamine 10 ng/ml bFGF
RPMI/B27 medium (DE differentiation)	RPMI-AQ supplemented with: 1x B27 2 mM L-glutamine 1x Penicillin-Streptomycin
Hepatoblast Specification medium	KSR-M supplemented with: 20 ng/ml BMP2 10 ng/ml bFGF

Hepatocyte Maturation medium (L-15)	L-15 supplemented with: 8.3% TPB 8.3% FBS 2 mM L-Glutamine 10 μM Hydrocortisone-21-hemisuccinate 1 μM Insulin 50 μg/ml Ascorbic Acid 1x Penicillin-Streptomycin 20 ng/ml OSM 10 ng/ml HGF

2.1.2 Methods

2.1.2.1 Culture and propagation of hESCs

i. Isolation of wild-type MEFs from embryos

Uterine horns from terminated E13.5 pregnant CD-1 mice were washed three times with DPBS containing 2X Penicillin/Streptomycin. Embryos were then removed and individually dissected to remove the heart and liver, finely minced and disassociated into single cells with trypsin at 37°C in Bijou tubes with one embryo per tube. Tissues were periodically vortexed during this incubation period to break up any large clumps of cells. MEFs were then isolated following neutralisation with D10 medium by allowing any remaining clumps to settle and extracting the overlying cell suspension, which was transferred into T75 flasks with each tube contributing to one flask. Cells were allowed to plate down overnight and the medium was changed the following day after they were checked for contamination. After 2-3 more days of culture, all the flasks were trypsinised and combined and cells were frozen down at 1 x 10^7 cells per cryovial in D10 medium supplemented with 10% DMSO and labelled as P0 (passage 0).

ii. Generation of MEF-CM

Frozen MEFs were defrosted and passaged 3 to 4 times in order to obtain sufficient numbers to seed 5-7 T225 flasks with 2.5 x 10^7 cells per flask. After trypsinisation, cells were irradiated at 40 Gy using an IBL 637 Cell irradiator (CIS-Bio International) to abolish replicative potential. Irradiated MEFs were then counted and seeded into T225 flasks pre-coated with 0.5% gelatine at a density of 2.5 x 10^7 cells per flask. After 24 hours, cells were rinsed in DPBS and D10 medium was replaced with 150 ml KSR-M per flask. The following day, MEF-CM was collected and stored at -80 °C until needed. Fresh KSR-M was added back onto the MEFs and the entire collection process was repeated for up to 7 days. Upon use, defrosted MEF-CM was filtered to remove

cellular debris and additional 2 mM L-glutamine was added to replenish uptake by MEFs during the conditioning. MEF-CM was stored at 4 ºC following filtration and used for no longer than 1 week post-thaw.

iii. Preparation of Matrigel® coated plates

Stock Matrigel® was thawed overnight on ice at 4 ºC and diluted 1 in 2 with chilled KO-DMEM before being aliquoted into 15 ml tubes at 1 ml per tube. Aliquots were stored at -20 ºC until use, whereby they were again thawed overnight at 4 ºC before being further diluted 1 in 15 with chilled KO-DMEM. 6 well plates that were used for the routine culture of hESCs were coated with 1 ml per well of this new dilution. Plates were allowed to set at 4 ºC overnight and warmed to room temperature before use. Excess Matrigel® solution was aspirated off just prior to hESC passaging. In emergency circumstances, plates were made on the day of passaging and allowed to set for a minimum of 4 hours at room temperature before use.

iv. Routine culture and maintenance of hESCs

H1 hESCs grow as distinct colonies and were routinely passaged onto Matrigel® coated plates in MEF-CM which is supplemented with 10 ng/ml bFGF before use. Medium was changed daily and the cells were routinely passaged when confluent as smaller colonies every 5-7 days using 200U/ml collagenase IV to remove spontaneously differentiated cells followed by mechanical disassociation. Cells were routinely split at a 1:2-1:4 ratio depending on the confluency. For freezing hESCs, >80% confluent wells were treated with collagenase IV and mechanically dissociated in 1 ml cold KSR, after which 10% v/v DMSO was added in a dropwise fashion. Cells were then transferred as clumps into cryovials and stored overnight at -80 ºC before transfer into liquid nitrogen for long-term storage.

v. Accutase/ROCKi passaging of hESCs

hESCs which have been disassociated into single cells undergo rapid apoptosis and are prone to differentiate in MEF-CM. Thus, routine maintenance requires that these cells be passaged as small colonies to permit their expansion. However, cell clumps are not permissive for efficient DNA transfection and often form large compacted colonies during culture, which also impedes directed differentiation. As such, for these purposes, hESCs were subjected to an Accutase/ROCKi split, whereby confluent cultures were disassociated into single cells upon treatment with accutase and split at a ratio of 1:3-1:4. The activity of accutase was inhibited upon the addition of media, and the associated apoptosis was mitigated by the supplementation of 10 μM ROCKi (Watanabe et al., 2007) to the MEF-CM as the cells plate down overnight. The following day, ROCKi was removed

from the culture upon medium change to minimise chronic effects of Rho kinase inhibition. After one day of further culture, the resultant monolayer is hence conducive for efficient transfection and differentiation.

2.1.2.2 Differentiation of hESCs to DE and hepatocytes

i. AA-LY induced DE differentiation

High-quality hESC cultures were characterised based on their morphology to determine the feasibility of differentiation. Cultures contained less that 5% clearly differentiated or stromal cells, with a corresponding abundance of undifferentiated, non-compacted colonies making up at least 80% of the well. Alternatively, hESCs were passaged as single cells via Accutase/ROCKi split or re-split to provide a differentiation competent monolayer should the colonies become too compacted. In wells which fulfilled these criteria, MEF-CM was exchanged with RPMI/B27 supplemented with 100 ng/ml AA and 20 μM LY for 24 hours. Medium was refreshed for the following 2 days, however the concentration of LY was reduced by half to mitigate LY-induced cytotoxicity. Cells differentiated to the DE are morphologically distinguishable, being spiky and irregular in shape.

ii. Hepatic specification and maturation from DE

DE cultures were further specified to the hepatic lineage by exchanging the RPMI/B27 DE specifying medium with hepatoblast specification medium supplemented with 20 ng/ml BMP2 and 10 ng/ml bFGF for 3-5 days. Hepatoblasts were further matured into hepatocyte-like cells upon medium exchange with L-15 hepatocyte maturation medium supplemented with 20 ng/ml OSM and 10 ng/ml HGF for a further 3-5 days until the emergence of polygonal, binucleated cells that typify successful maturation and gain of hepatic functions.

2.1.2.3 Culture and propagation of HEK293T, Hep3B and PC-3 cells

Tumour cell lines were routinely cultured in either D10 (HEK293T and Hep3B) or R10 (PC-3) media and regularly passaged twice a week at a 1:3 to 1:10 splitting ratio using trypsin-EDTA. Cells were typically frozen at 1 x 10^6 cells per vial in fresh growth media supplemented with 10% DMSO.

2.1.2.4 Culture and propagation of Rictor-Control and Rictor-Null MEF

Both control and transgenic MEFs that had been spontaneously immortalised after their initial isolation from control and Rictor knockout mice were cultured in D10 and passaged regularly prior to confluence. Rictor-Control MEFs displayed growth rates that are not dissimilar to that of wild-

type MEFs and were consequently passaged at 1:3 to 1:10 splitting ratio. However, Rictor-Null MEFs had a markedly reduced proliferative rate and were therefore split at a ratio no greater than 1:3 to reduce senescence associated cell death. Both MEF lines were frozen at 3 x 10^6 cells per vial in enriched D10 media supplemented with 50% FBS and 10% DMSO.

2.1.2.5 Growth Factor and Inhibitor assays

Cells were treated with growth factors and/or inhibitors at the indicated working concentrations above typically for 1, 3 or 6 hours in the absence of serum unless otherwise indicated.

2.1.2.6 Genetic manipulation of cell lines

i. Lipofection

Transfection of hESCs and tumour cell lines with plasmid DNA was conducted via a modified lipofection protocol (Ma et al., 2012). For 1 x 10^6 cells, 1.6 μg of kit purified plasmid DNA was suspended in 50 μl of OptiMEM® supplemented with 1.6 μl of PLUS™ Reagent. In another tube, 4 μl of Lipofectamine™ LTX reagent was re-suspended in another 50 μl of OptiMEM®. Both tubes were incubated at room temperature for 5 min before being mixed together and incubated for a further 25 min. During this time, target cells were trypsinised, counted and pelleted before being directly resuspended in the transfection mix and incubated for 15 min. The transfection process was stopped upon the addition of growth media and cells were allowed to plate down overnight in the appropriate culture vessel. Cells were typically split 1:2-1:3 following transfection. Reagents were scaled up accordingly depending on the number of cells to be transfected. For MEFs, lipofection was conducted following the accompanying manufacturer's instructions with a DNA to Lipofectamine™ LTX ratio of 1:10.

ii. Lentiviral Transduction

Low passage HEK293T packaging cells were seeded at 1.5 x 10^7 cells per T225 flask and allowed to reach a confluency of 80-90% prior to transfection. On the morning of transfection, the media was refreshed and transfection was performed late afternoon by the calcium phosphate method with the following DNA ratios: 60 μg lentivector: 40 μg pCMVΔ8.91 helper: 40 μg VSV-G envelope according to the manufacturer's instructions. Cells were transfected overnight in the presence of 25 μM chloroquine in order to inhibit endosomal DNA degradation during endocytosis of the DNA. Medium was changed 18 hours post-transfection and supernatant containing viral particles was collected 48 and 72 hours post transfection and stored at -80 °C.

Viral particles within the harvested supernatant were concentrated prior to use in transduction. Supernatants were defrosted and filtered through a 0.45 μM unit into Ultra-Clear™ Beckman centrifuge tubes after which polybrene and chondroitin sulphate was added at 120 μg/ml each to precipitate the particles. Following a brief vortex, tubes were sealed with parafilm and incubated for 30 min at 37 °C. Tubes were then centrifuged at 10000 xg for 1.5 hours in a Beckman Coulter Avanti J-20 centrifuge at 4 °C to pellet the virus-chondroitin-polybrene complexes. Pellets were then dislodged from the tube wall in 200 μl cold DPBS by light tapping and the viral particles were allowed to dissolve into the solution at 4 °C for 2 hours. Concentrated virus solutions were then aliquoted into cryovials at 40 μl per vial and frozen at -80 °C. To create stable hESC and PC-3 lines, cells were dissociated with accutase or trypsin respectively and were infected overnight with concentrated viral particles as they were plating down. 48 hours post-infection, cells were selected with 2 μg/ml puromycin for stable transgene expression.

iii. hESC Luciferase Assay

High quality hESCs were accutase/ROCKi split 1:6 into 12 well plates and allowed to reach 70-80% confluence prior to transfection. hESCs were co-transfected with both firefly (pGL3-$CAGA_{12}$-MLP-luc) and renilla (pRL-T7-renilla) plasmids as an internal control at a ratio of 10:1 respectively using Lipofectamine 2000 (Life Technologies) following standard lipofection procedures with modifications. Both DNA and Lipofectamine™ were resuspended separately in equal volumes of OptiMEM® before being mixed together and incubated at room temperature for 20-30 min to allow transfection complexes to form. Transfection mixtures were applied to the cells in a dropwise fashion and media was changed 6 hours post-transfection to maintain hESC survival. 42 hours post transfection, cells were differentiated for 6 hours, harvested using accutase and each well dispensed equally into 3 corresponding wells of a 96-well luminometer plate. Luciferase assay was performed using Dual-Glo® luciferase assay kit, whereby cells were lysed using Dual-Glo® luciferase assay reagent for 10 minutes before luciferase luminescence was recorded using a Perkin Elmer Victor II luminometer. Following this, lysate was treated with Dual-Glo® Stop & Glo reagent to quench firefly luciferase activity and stimulate renilla luciferase-mediated luminescence recorded on the same luminometer. Firefly luminescence readings were normalised with corresponding renilla luminescence readings to give representative luciferase expression values that are independent of transfection efficiency and cell number.

2.2 Molecular Biology - DNA/RNA techniques

2.2.1 Materials

2.2.1.1 Reagents, Chemicals and Kits

Reagent	Supplier
1 kb Full Scale DNA ladder	Thermo Fisher
100 bp ladder	NEB
6X DNA loading buffer	NEB
Acetic Acid	Sigma-Aldrich
Agarose (molecular biology grade)	Sigma-Aldrich
Ampicillin	Sigma-Aldrich
Bacto-tryptone	Sigma-Aldrich
Boric Acid	Sigma-Aldrich
Chloroform:Isoamyl alcohol 24:1	Sigma-Aldrich
DH5α Competent *E. coli*	Active Motif
Deoxynucleotide mix (dNTP)	Sigma-Aldrich
Ethanol	VWR
Ethidium Bromide	Sigma-Aldrich
Ethylenediaminetetraacetic acid (EDTA)	Sigma-Aldrich
Glucose	Sigma-Aldrich
HiSpeed Maxiprep Kit	Qiagen
HiSpeed Midiprep Kit	Qiagen
Hydrochloric acid (37%)	Sigma-Aldrich
Isopropanol	VWR
Magnesium chloride ($MgCl_2$), anhydrous	Sigma-Aldrich
Molecular Grade Water	Sigma-Aldrich
Murine RNAse Inhibitor	NEB
$Oligo(dT)_{12-18}$	Thermo Fisher
Potassium chloride (KCl)	Sigma-Aldrich
Q5 Site Directed Mutagenesis Kit	NEB
QIAprep Gel Extraction Kit	Qiagen
Sodium chloride (NaCl)	Sigma-Aldrich
Sodium hydroxide	Sigma-Aldrich
SYBR® Green Jumpstart™ *Taq* Ready Mix	Sigma-Aldrich
Tri Reagent®	Sigma-Aldrich
Tris Base	Sigma-Aldrich
UltraClean™ Low Melting Sieve Agarose	Mobio
Yeast Extract	Sigma-Aldrich

2.2.1.2 Buffers and Solutions

10X Tris-Borate-EDTA Buffer (TBE)
108 g Tris Base
55 g Boric Acid
9.3 g EDTA
Autoclaved water to 1 L

50X Tris-Acetate-EDTA Buffer (TAE)
242 g Tris Base
57.1 ml Acetic Acid
18.6 g EDTA
Autoclaved water to 1 L

Tris-EDTA Buffer (TE)
1 ml Tris-HCL pH 8.0 (10 mM)
200 µl of 0.5M EDTA pH 8.0 (1 mM)
Autoclaved water to 100 ml

Lysogeny Broth (LB) Medium
10 g Bacto-tryptone
5 g Yeast extract
10 g NaCl
Autoclaved water to 1 L

LB Agar
5 g Bacto-tryptone
2.5 g Yeast extract
5 g NaCl
7.5 g Agar
Autoclaved water to 500 ml

SOC Media
20 g Bacto-tryptone
5 g Yeast extract
2 ml of 5 M NaCl
2.5 ml of 1 M KCl
10 ml of 1 M $MgCl_2$
20 ml of 1 M glucose
Autoclaved water to 1 L

P1 Resuspension Buffer (Qiagen)
50 mM Tris-HCl pH 8.0
10 mM EDTA
100 µg/ml RNAse A

P2 Lysis Buffer (Qiagen)
200 mM NaOH
1% Sodium Dodecyl Sulphate (SDS)

P3 Neutralisation Buffer (Qiagen)
3M Potassium acetate pH 5.5

Oligos annealing buffer	400 µl Tris-HCl pH 7.5 (10 mM) 80 µl of 0.5 M EDTA pH 8.0 (1 mM) 400 µl of 5 M NaCl (50 mM) Molecular grade water to 50 ml

2.2.1.3 Plasmids

All plasmids stored in TE buffer or molecular grade water and stored at -20 ºC. For subcloned plasmids, detailed cloning strategies are available in the Appendix section.

Plasmid	Source
pBluescript II KS	Stratagene (C4)
pcDNA3-Flag-mTOR-wt	Addgene 26603
pcDNA3-Myr-HA-Akt1	Addgene 9008
pcDNA3-Myr-HA-Akt1-S473A	Subcloned from Addgene 9031 and 9008
pcDNA3-T7-Akt1-K179M/T308A/S473A	Addgene 9031
pCMV-VSV-G	Gift from Dr. Anil Chandrashekran
pCMV-Δ8.91-helper	Gift from Dr. Anil Chandrashekran
pCS2-Flag-Smad2-T220V	Mutagenesis of Addgene 14042 (L57)
pCS2-Flag-Smad2-WT	Addgene 14042
pGEX-6P-2-GST	GE Healthcare (C45)
pGEX-6P-2-GST-Smad2-T220V	Subcloned from C45 and L57
pGEX-6P-2-GST-Smad2-WT	Subcloned from C45 and Addgene 14042
pHyg-Puro-2A-EGFP	Lab owned (L18)
pLKO.1-Puro-shGFP	shGFP insertion into Addgene 10878
pLKO.1-Puro-shNedd4L2	Subcloned from Addgene 10878
pLKO.1-Puro-shRictor1	Addgene 1853
pLKO.1-Puro-shRictor2	Addgene 1854
pLKO.1-Puro-TRC	Addgene 10878
pLVTHM-EGFP	Addgene 12247
pLVTHM-EGFP-shNedd4L1	shNedd4L insertion into Addgene 12247, (L54)
pLVTHM-Puro-2A-EGFP-shNedd4L1	Subcloned using L54 and L18
pLVTHM-Puro-2A-Smad2-T220V	Subcloned from L51 and L57
pLVTHM-Puro-2A-Smad2-WT	Subcloned from L51 and Addgene 14042
pLVTHM-Puro-2A-Sox2	Lab owned (L51)
pGL3-$CAGA_{12}$-MLP-luc	Gift from Dr. Vasso Episkopou
pRK-myc-Rictor	Addgene 11367
pRL-TK-Renilla	Promega, GenBank® no. AF025846

2.2.1.4 Primers and shRNA

All primers and shRNA reconstituted as 100 μM in molecular grade water and stored at -20 °C.

Primer	Forward strand	Reverse strand
Brachyury	TGCTTCCCTGAGACCCAGTT	GATCACTTCTTTCCTTTGCATCAAG
CLIC4	TGAAAGCATAGGAAACTGCCC	GGTCAACAGTCGTCACACTAAA
Eomes	AGGAATTCTTGCTTTGCTAATTCTG	CGAAGAAACAGCAAGAGCAGC
Flag-Smad2	GGACTACAAGGACGACGATGA	TCACTGCTTTCTCACACCACT
FoxA2	GGGAGCGGTGAAGATGGA	TCATGTTGCTCACGGAGGAGTA
Goosecoid	GAGGAGAAAGTGGAGGTCTGGTT	CTCTGATGAGGACCGCTTCTG
MixL1	CCGAGTCCAGGATCCAGGTA	CTCTGACGCCGAGACTTGG
Nanog	TGATTTGTGGGCCTGAAGAAAA	GAGGCATCTCAGCAGAAGACA
Nedd4L	TCCAATGGTCCTCAGCTGTTTA	ATTTTCCACGGCCATGAGA
Oct4	TCGAGAACCGAGTGAGAGGC	CACACTCGGACCACATCCTTC
Pax6	TCCGTTGGAACTGATGGAGT	GTTGGTATCCGGGGACTTC
PPM1A	AGGGGCAGGGTAATGGGTT	GATCACAGCCGTATGTGCATC
RPL22	TCGCTCACCTCCCTTTCTAA	TCACGGTGATCTTGCTCTTG
Smad2	ATTCCAGAAACGCCACCTCC	GCTATTGAACACCAAAATGCAGG
Sox17	ACGCCGAGCTCAGCAAGAT	TCCACGTACGGCCTCTTCTG
Sox2	GCCGAGTGGAAACTTTTGTCG	GCAGCGTGTACTTATCCTTCTT
β-actin	TGTCTGGCGGCACCACCATG	AGGATGGAGCCGCCGATCCA

shRNA	Sense strand	Anti-sense strand
Nedd4L1	GCTAGACTGTGGATTGAGT	ACTCAATCCACAGTCTAGC
Nedd4L2	AGAGTCCTATCGGAGAATTAT	ATAATTCTCCGATAGGACTCT
Rictor1	ACTTGTGAAGAATCGTATCTT	AAGATACGATTCTTCACAAGT
Rictor2	CAGCCTTGAACTGTTTAA	TTAAACAGTTCAAGGCTG
shGFP	CTACGTCCAGGAGCGCACC	GGTGCGCTCCTGGACGTAG

2.2.1.5 DNA Modifying Enzymes

Enzyme	Source
Antarctic Phosphatase	NEB
DNAse I	Sigma
Jumpstart™ *Taq* Polymerase	Sigma
ProtoScript II Reverse Transcriptase	NEB
Q5® High Fidelity Polymerase	NEB
Restriction endonucleases	NEB
T4 ligase	NEB
T4 polynucleotide kinase (PNK)	NEB

2.2.2 Methods

2.2.2.1 Plasmid manipulation and cloning

i. Bacterial Transformation

Competent DH5α *E.coli* cells were thawed on ice to which plasmid DNA was added to no greater than 10% of the total volume and mixed gently with tapping. Transformation reactions were incubated on ice for 30 min after which the cells were subjected to heat shock upon immersion in a 42 °C water bath for 40 sec. Cells were allowed to recover on ice for 2 minutes before the aseptic addition of 250 µl of SOC media per reaction. Tubes were incubated for 1 hour at 37 °C with shaking at 225-250 rpm to allow the outgrowth of transformants. Bacteria were then pelleted by centrifugation at 3000 rpm for 5 min, before being resuspended in 50 µl of the SOC supernatant and plated onto LB agar plates supplemented with 100 µg/ml ampicillin. Plates were inverted and incubated overnight at 37 °C to allow outgrowth and selection of transformants. Plates were inspected the following day for transformed colonies.

ii. Plasmid Amplification and Purification

For small scale DNA amplification for use in subcloning, transformed colonies were picked from LB agar plates and cultured in 5 ml of LB broth supplemented with 100 µg/ml ampicillin overnight at 37 °C with 230 rpm shaking. The following day, cultures were centrifuged for 15 min at 6000 xg to pellet the bacteria cells. The supernatant was then discarded and the tubes were inverted to remove all traces of LB broth, after which the pellets were resuspended in 300 µl of P1 resuspension buffer. An equal volume of P2 lysis buffer was added to initiate alkaline lysis of the cells for no longer than 5 min before the addition of 300 µl of P3 neutralisation buffer to neutralise and precipitate out the bacterial debris. The debris was removed via centrifugation for 5 min at 14000 rpm, and the supernatant containing solubilised plasmid DNA was transferred into fresh tubes. 600 µl of isopropanol was added to the extract, which was in turn immediately centrifuged to pellet and precipitate out the DNA. Pellets were washed with 1 ml of 70% ethanol before undergoing a final centrifugation. After removal of the ethanol, pellets were allowed to air-dry for 5 min before resuspension in 50 µl of molecular grade water. The concentration of plasmid DNA was measured by nanodrop spectrometer 1000 (Thermo Fisher) at A_{260} and is of sufficient purity for use in subcloning and sequencing procedures.

For large scale DNA amplification required for transfection and lentiviral production, transformed colonies were picked from LB agar plates and cultured in 2 ml of LB broth supplemented with 100 µg/ml of ampicillin and incubated for 6-8 hours at 37 °C with shaking. This starter culture was

used to inoculate 50 ml (Midiprep), 150 ml (Maxiprep, high copy no.) or 250 ml (Maxiprep, low copy no.) LB broth supplemented with 100 μg/ml of ampicillin and incubated overnight at 37 °C at 230 rpm shaking. Typically, lentiviral vectors and plasmids over 10 kb in size were treated as low copy number given that more time is required to replicate large plasmids. The following day, plasmid DNA was isolated using the HiSpeed Midiprep or Maxiprep kits, with the final elution of the DNA in 500 μl of sterile TE buffer. DNA was quantified via nanodrop and stored at -20 °C until use.

iii. Restriction digests and gel extraction

Plasmid DNA was subjected to restriction endonuclease digests either for sequence verification or for subcloning purposes utilising the NEB restriction enzyme system. In brief, reactions were typically set up in a 10-20 μl total volume containing 500 to 1000 ng of plasmid DNA and no more than 10% v/v restriction enzyme, which typically equates to 10-20 U enzyme/reaction together with the appropriate buffer. For verification purposes, plasmids were digested for a minimum of 30 min while digestion is allowed to proceed for 2 hours or more for subcloning. Reactions were terminated upon the addition of 6X loading buffer and are analysed via agarose gel electrophoresis. Samples are typically run along with the appropriate DNA ladder at 100V for 30 min through a 0.8-1.5% agarose gel dissolved in either 1X TAE or TBE buffer, containing 0.5 μg/ml ethidium bromide depending on the size of the fragments to be resolved. Fragments for use in subcloning were typically run through a 1% w/v low melt TAE agarose gel after which they were excised using a sharp scalpel and purified using the QIAprep Gel Extraction Kit. DNA fragments are typically eluted in 30 μl to maximise the concentration for ligation.

iv. DNA dephosphorylation

After purification, digested vectors were typically dephosphorylated by Antarctic phosphatase to eliminate any chance of religation of singly digested plasmids. Typically $1/10^{th}$ volume of 10X Antarctic phosphatase buffer and 5 U Antarctic Phosphatase was added to 1-5 μg of digested vector and incubated for 30 to 60 min to dephosphorylate 5' or 3' extensions respectively. Enzyme was heat inactivated for 5 min at 70 °C before use in ligation reactions.

v. Oligo annealing and phosphorylation

Equal volumes of both sense and antisense strands for were mixed at an equimolar ratio to achieve annealing reaction volume of 100 μl of annealing buffer containing 10 μM of each oligo. Reactions were placed onto a heating block set at 95 °C for 5 min after which the entire block was removed from the heating plate and allowed to slowly cool to room temperature to allow the strands to

anneal. The concentration of the now double-stranded fragments was determined by nanodrop after which up to 300 pM 5' ends were phosphorylated with 10 U of T4 PNK in 1X T4 ligase buffer with ATP according to the conversion equation: 1 μg of 20 bp oligo = 150 pM 5' ends. Reactions were incubated for 30 min at 37 °C and heat inactivated at 65 °C for 20 min before use in ligation reactions.

vi. Ligation

Ligations were performed with T4 ligase according to manufacturer's guidelines. Typically, a vector to insert molar ratio of 1:3 was incubated in a 10 to 20 μl total volume containing 20 U of T4 ligase in 1X T4 ligase buffer supplemented with ATP and incubated for 1 hour at 22 °C. Care was taken to ensure that total DNA concentration in the reactions did not exceed 10 ng/μl and more difficult ligation reactions that required blunt ended or triple fragment ligations were incubated overnight at 16 °C. After ligation, 5 to 10 μl of the reaction was used to transform bacteria as indicated in above in order to select for positive transformants.

vii. Site-directed mutagenesis

Using pCS2-Flag-Smad2 (Addgene 14042) as a template, non-overlapping primers were first designed with 5' ends annealing back-to-back, through which a substitution was created by designing a mismatch in the centre of the forward primer, with 19 complementary base pairs before and after the mismatch. The 5' end of the anti-sense primer begins at the base adjacent to the 5' end of the sense primer and continues in the opposite direction on the complementary strand. The anti-sense primer is fully complementary to the plasmid sequence. Primers sequences were designed using the NEBaseChanger™ online too and are as follows:

Sense: 5'-GAGTAATTATATTCCAGAAGTGCCACCTCCTGGATATATC-3'

Anti-sense: 5' TGTGGCTCAATTCCTGCTGG 3'

Mutagenesis was carried out essentially as outlined in the procedures accompanying the Q5 Site Directed Mutagenesis Kit. Briefly, 1.25 μl of each 10 μM primer stock was added to a thin walled PCR tube containing 12.5 μl of Q5 Hot Start High Fidelity 2X Master mix and 25 ng of template DNA. Reaction was performed in a Bio-Rad Dyad DNA Engine thermocycler with the following cycling conditions:

1: 98 °C	30 sec	Initial denaturation
2: 98 °C	10 sec	Cycling denaturation
69 °C	30 sec	Primer annealing (T_a)
72 °C	3 min	Extension
Repeat from step 2 for 25 cycles.		
3: 72 °C	2 min	Final extension
4: 4 °C	Forever	Hold

The amplified PCR product was added directly to the Kinase-Ligase-DpnI (KLD) enzyme mix to digest the template and circularise the new plasmid. Reactions were incubated at room temperature for 5 min after which 5 to 10 µl was directly used for bacterial transformation to amplify the new plasmid. Clones were confirmed via sequencing using a CMV universal primer supplied by Beckman Coulter Genomics. Primer designs and generation of this plasmid was performed by Mr. Nick Murphy, a master student under my supervision.

2.2.2.2 Gene expression analysis

i. RNA Isolation and extraction

For gene expression analysis, typically 1 x 10^6 cells or one fully confluent well of hESCs or their derivatives were lysed in 1 ml of TRI Reagent® and stored at -80 °C until further processing. To isolate the RNA, samples were defrosted at room temperature and allowed to stand for 5 min to equilibrate. For each 1 ml of TRI Reagent® used, 200 µl of chloroform:isoamyl alcohol was added and the tube vigorously shaken and allowed to stand at room temperature for 15 min to extract the RNA via phase separation. Following centrifugation at 12000 xg for 15 min at 4 °C, the aqueous top layer containing the RNA was transferred into a new tube. 500 µl of isopropanol was added and the tubes allowed to stand at room temperature for 10 min to precipitate the RNA. Precipitated RNA was pelleted upon centrifugation at 12000 xg for 10 min at 4 °C before the supernatant was removed and the pellet washed in 1 ml of 75% ethanol. A final centrifugation was perform at 7500 xg for 5 min to pellet the washed RNA pellet and upon the removal of the ethanol, tubes were allowed air-dry for 10 to 15 min before being resuspended in 20 µl of molecular grade water to re-dissolve in RNA. Samples were further subjected to DNAse I treatment in order to remove any residual genomic DNA contamination. 2 µl of 10X reaction buffer along with 2 U of DNAse I was added to each sample, which was incubated at room temperature for 15 min before the addition of 2 µl of stop solution and heating at 70 °C to fully inactivate the DNAse I. The final

RNA concentration was measured via nanodrop after which 500 ng to 1 μg of total RNA was used for cDNA synthesis.

ii. cDNA Synthesis

Typically 1 μg of total RNA was used as template to generate cDNA for use in gene expression analysis. RNA was initially incubated with 2 μl of 50 μM Oligo(dT)$_{12-18}$ and 1 μl of 10 mM dNTP in a total volume of 12 μl and incubated in a thermocycler at 65 °C for 5 min to fully denature the RNA and anneal the Oligo(dT)$_{12-18}$ primers to the template. After the initial annealing reaction, tubes were placed promptly back on ice to which 4 μl of 5X ProtoScript II RT reaction buffer, 2 μl 0.1 M DTT, 40 U of murine RNAse inhibitor and 200 U of ProtoScript II reverse transcriptase was added to each reaction to a final volume of 20 μl. Additionally, samples also had a 'minus RT' counterpart reaction in which no reverse transcriptase was added to ensure that all genomic contamination has been removed. Reactions were incubated at 42 °C for 1 hour followed by 5 min at 80 °C to inactivate the enzyme. The newly generated cDNA solutions were diluted 1 in 10 with the addition of 180 μl of molecular grade water and stored at -20 °C until use.

iii. Semi-quantitative Polymerase Chain Reaction (PCR)

Prior to quantitative real-time analysis, cDNA samples were subjected to standard PCR reactions with known housekeeping markers such as RPL22 and β-actin to ensure that cDNA synthesis was successful. Furthermore, newly designed primers were also subjected to the same test to ensure their specificity and effectiveness for use in quantitative reactions. Typically, 2 to 3 μl of diluted cDNA solution was used as template, to which 1X Jumpstart™ *Taq* reaction buffer, 200 μM dNTP, 200 nM of forward and reverse primer, and 1.25 U of Jumpstart™ *Taq* polymerase was added to a total volume of 25 μl. Assembled reactions were incubated in the thermocycler with the following cycling conditions:

1: 94 °C	2 min	Initial denaturation
2: 94 °C	30 sec	Cycling denaturation
58 °C	30 sec	Primer annealing (T_a)
72 °C	45 sec	Extension
Repeat from step 2 for 25-35 cycles depending on primer used.		
3: 72 °C	5 min	Final extension
4: 4 °C	Forever	Hold

Primers are typically designed with a melting temperature (T_m) of between 60 to 65 °C with the T_a of the annealing step adjusted accordingly to around 3 to 5 °C lower than the primer with the

higher T_m value. Reactions were stopped following the addition of 6X loading buffer and half the reaction was typically loaded and run through a 1.5% TBE gel to resolve the PCR fragments in the same manner as outlined above. PCR products are typically 100 to 200 bp in size.

iv. Quantitative Real-Time PCR (qRT-PCR)

Once efficacy has been verified by standard PCR, cDNA samples are subjected to quantitative real-time assessment to measure gene expression. 2 µl of cDNA template was used per reaction to which 15 µl of SYBR® Green Jumpstart™ *Taq* Ready Mix, 300 nM of forward and reverse primer was added to a final volume of 30 µl per reaction. Each reaction was setup up in triplicate for each gene, with each cDNA sample analysed twice on two different occasions to generate n=6 Ct values for each sample and for each gene analysed. Reactions were run on a Bio-Rad Opticon2™ DNA Engine Real-time fluorescence thermocycler with the following conditions:

1: 94 °C	2 min	Initial denaturation
2: 94 °C	15 sec	Cycling denaturation
60 °C	30 sec	Primer annealing (T_a)
72 °C	30 sec	Extension
75 – 84 °C	+3 °C/sec	Real-time fluorescence read/sec
Repeat from step 2 for 40 cycles depending on primer used.		
3: 67 – 91 °C	+0.3 °C/sec	Melting curve read/sec

Production of double stranded product was tracked in real-time by measuring the SYBR® green fluorescence. Melting curve was performed at least once for each primer set to ensure the formation of a single PCR product. Analysis was performed using accompanying software and using the $2^{\Delta\Delta Ct}$ method as outlined by Livak and Schmittgen, 2001. In brief, raw Ct values were normalised to either RPL22 and β-actin values for each sample by subtraction giving the ΔCt value. ΔΔCt values were obtained via normalisation with control samples, after which the relative gene expression was obtained by taking the ΔΔCt value as the exponential function of 2. Students *t* test was used to assess significance in changes observed in gene expression.

2.3 Molecular Biology – Protein techniques

2.3.1 Materials

2.3.1.1 Reagents, Chemicals and Kits

Reagent	Supplier
30% Acrylamide/Bis	Sigma
4-(2-hydroxyethyl)-1-piperazineethanesulfonic acid (HEPES)	Sigma
4',6 diamidino-2-phenylindole (DAPI)	Sigma
Adenosine triphosphate (ATP)	Sigma
Ammonium persulphate (APS)	Sigma
Bicinchoninic Acid Assay (BCA) Protein Quantification Kit	Thermo Fisher
BL-21 strain *E.coli* for recombinant protein synthesis	GE Healthcare
Bromophenol blue	Sigma
Bovine Serum Albumin (BSA)	Sigma
CL-Xposure film	Scientific Labs
Dithiothreitol (DTT)	Sigma
Enhanced chemiluminescence substrate (ECL)	Thermo Fisher
Ethylene glycol tetraacetic acid (EGTA)	Sigma
Glutathione magnetic beads	Thermo Fisher
Glycerol	Sigma
Glycine	Sigma
Goat serum	Sigma
Guanidine hydrochloride (GnHCl)	Sigma
Immobilon® polyvinylidene fluoride (PVDF) membrane	Millipore
Isopropyl β-D-1-thiogalactopyranoside (IPTG)	Sigma
Lambda phosphatase	NEB
Luminate Forte Enhanced ECL substrate	Millipore
Methanol	VWR
Mowiol 4-88	Sigma
Nonidet P-40 (NP-40)	Anachem
PageRuler Plus Protein Ladder	Thermo Fisher
Paraformaldehyde	NEB
Phenylmethanesulfonylfluoride (PMSF)	Sigma
Phosphatase Inhibitor Cocktail 2	Sigma
Potassium acetate	Sigma
Protease Inhibitor Cocktail	Sigma
Protein G Dynabeads®	Life Technologies
Recombinant active Erk2 kinase	NEB
Recombinant GST-GSK3 fusion protein	NEB
Recombinant His-6-tagged Akt1	Millipore
Reduced L-glutathione	Sigma
Skim milk powder	Sigma
Sodium azide (NaN_3)	Sigma
Sodium deoxycholate	Sigma

Sodium dodecyl sulphate (SDS)	Sigma
Sodium fluoride (NaF)	Sigma
Sodium orthovanadate (Na_3VO_4)	Sigma
Tetramethylethylenediamine (TEMED)	Sigma
Tetrasodium pyrophosphate ($Na_4O_7P_2$)	Sigma
Triton X-100	Sigma
Tween-20	Sigma
Ubiquitin aldehyde	R&D/Boston Biochem
β-glycerophosphate	Sigma
β-mercaptoethanol	Sigma

2.3.1.2 Buffers and Solutions

Immunoblotting

Radio Immunoprecipitation Assay Buffer (RIPA)	25 ml 1 M Tris-HCl pH 8.0 (50 mM) 15 ml 5 M NaCl (150 mM) 5 ml NP-40 (1% v/v) 2.5 g Sodium deoxycholate (0.5% w/v) 0.5 g SDS (0.1% w/v) Autoclaved water to 500 ml
2X Sample buffer	2.5 ml 0.5 M Tris-HCl pH 6.8 (125 mM) 2 ml glvcerol (20% v/v) 4 ml 10 % SDS (4% w/v) 160 µl 1.25% bromophenol blue (0.02 % w/v) 500 µl β-mercaptoethanol (715 mM) Autoclaved water to 10 ml
Sodium Orthovanadate stock	183.9 mg Na_3VO_4 (200 mM) Adjust pH to 10.0 Boil solution until colourless Cool and readjust pH back to 10 Repeat boil/cool cycles until solution remains colourless at pH 10.0
5X Sample buffer	1.25 ml 0.5 M Tris-HCl pH 6.8 (50 mM) 2.5 ml glycerol (25 % v/v) 2 ml 10% SDS (2% w/v) 400 µl 0.5% bromophenol blue (0.02 % w/v) 500 µl β-mercaptoethanol (715 mM) Autoclaved water to 10 ml

4% Polyacrylamide Stacking Gel	2.5 ml 0.5 M Tris-HCl pH 6.8 (125 mM) 1.3 ml 30% Acrylamide/Bis (4% v/v) 100 µl 10% SDS (0.1 % w/v) 50 µl 12% APS (0.06 % w/v) 12 µl TEMED (0.12 % v/v) Autoclaved water to 10 ml
8% Polyacrylamide Running Gel	2.5 ml 0.5 M Tris-HCl pH 6.8 (125 mM) 2.7 ml 30% Acrylamide/Bis (6% v/v) 100 µl 10% SDS (0.1 % w/v) 75 µl 12% APS (0.075 % w/v) 18 µl TEMED (0.18 % v/v) Autoclaved water to 10 ml
10X SDS Running Buffer	30.3 g Tris base (250 mM) 144.2 g Glycine (1.9 M) 50 ml 20% SDS (1%) Autoclaved water to 1 L
Transfer Buffer	5.82 g Tris base (48 mM) 2.93 g Glycine (39 mM) 3.75 ml 10% SDS (0.04% w/v) 200 ml methanol (20% v/v) Autoclaved water to 1 L
Tris Buffered Saline with Tween-20 (TBS-T)	20 ml Tris-HCl pH 7.6 (20 mM) 26 ml NaCl (130 mM) 1 ml Tween-20 (0.1 % v/v) Autoclaved water to 1 L
Blocking buffer	5 g BSA or Skim milk (5% w/v) 1 L 1X TBS-T
Stripping buffer	10 ml Tris-HCl pH 7.5 (20 mM) 286.6 g GnHCl (6 M) 1 ml NP-40 (0.2% v/v) 3.5 ml β-mercaptoethanol (0.1 M) Autoclaved water to 500 ml

Cytoplasmic/Nuclear Fractionation

Cytoplasmic extraction buffer

5 ml 0.5 M HEPES-NaOH pH 7.5 (10 mM)
50 µl 0.5 M EDTA pH 8.0 (0.1 mM)
200 µl 0.125 EGTA pH 8.0 (0.1 mM)
2.5 ml 1 M KCl (10 mM)
125 µl 1 M DTT (0.5 mM)
Autoclaved water to 250 ml
Adjust pH to 7.9 with 10 M NaOH

Nuclear extraction buffer

10 ml 0.5 M HEPES-NaOH pH 7.5 (20 mM)
500 µl 0.5 M EDTA pH 8.0 (1 mM)
2 ml 0.125 EGTA pH 8.0 (1 mM)
250 µl 1 M DTT (1 mM)
20 ml NaCl (400 mM)
Autoclaved water to 250 ml
Adjust pH to 7.9 with 10 M NaOH

Immunoprecipitation

HEPES lysis buffer

476.6 mg HEPES (40 mM)
1 ml 0.5 M EDTA pH 8.0 (10 mM)
5 ml glycerol (10% v/v)
Autoclaved water to 50 ml
Adjust pH to 7.4 with 10 M NaOH

2X Non-denaturing CS lysis buffer

1 ml 1 M Tris-HCl pH 7.5 (20 mM)
1.5 ml 5 M NaCl (150 mM)
100 µl 0.5 M EDTA ph 8.0 (1 mM)
400 µl 0.125 EGTA pH 8.0 (1 mM)
500 µl NP-40 (1% v/v)
Autoclaved water to 25 ml

mTORC Co-IP lysis buffer

8 ml 0.5 M HEPES-NaOH pH 7.5 (40 mM)
2.4 ml 5 M NaCl (120 mM)
200 µl 0.5 M EDTA pH 8.0 (1 mM)
4 ml 0.25 M $Na_4P_2O_7$ (10 mM)
10 ml 0.5 M NaF (50 mM)
10 ml 3% NP-50 (0.3% v/v)
Autoclaved water to 100 ml

6% Stacking Gel (High MW proteins)	2.5 ml 0.5 M Tris-HCl pH 6.8 (125 mM) 2.0 ml 30% Acrylamide/Bis (6% v/v) 100 µl 10% SDS (0.1 % w/v) 75 µl 12% APS (0.075 % w/v) 18 µl TEMED (0.18 % v/v) Autoclaved water to 10 ml
Protein elution buffer	750 mg glycine 100 ml autoclaved water Adjust pH to 2.5 with 9.61 M HCl acid

Kinase Assay

10X Akt kinase assay buffer	1.25 ml 1 M Tris-HCl pH 7.5 (250 mM) 500 µl 0.5 M β-glycerophosphate (50 mM) 100 µl 1 M DTT (20 mM) 500 µl 1 M $MgCl_2$ (100 mM) Autoclaved water to 10 ml
10X mTORC kinase assay buffer	2.5 ml 0.5 M HEPES-NaOH pH7.5 (250 mM) 2.5 ml 2 M Potassium acetate (1 M) 200 µl $MgCl_2$ (10 mM) Autoclaved water to 10 ml
10X Erk2 kinase assay buffer (NEB)	500 mM Tris-HCl pH 7.5 100 mM $MgCl_2$ 1 mM EDTA 20 mM DTT 0.1% Brij 35
10X NEBuffer for PMP (NEB)	500 mM HEPES pH 7.5 1 M NaCl 20 mM DTT 0.1% Brij 25

Immunocytochemistry

Fixation buffer	4 g paraformaldehyde dissolved in 90 ml autoclaved water at 60 °C 10 M NaOH added dropwise till solution clears 10 ml 10X DPBS Adjust pH to 7.2 with 9.61 M HCl acid Adjust volume to 100 ml with autoclaved water

Blocking/permeablising buffer	1 ml goat serum (10% v/v) 0.25 g BSA (2.5% w/v) 30 µl Triton X-100 (0.3% v/v) DPBS to 10 ml
Mowiol mounting solution	12 ml 200 mM Tris-HCl pH 8.5 (135 mM) 6 g glycerol 2.4 g Mowiol 4-88 6 ml autoclaved water Heat tubes at 60 ºC to dissolve Mowiol

2.3.1.3 Antibodies

All antibodies stored according to manufacturer's instructions and reconstituted in blocking buffer supplemented with 0.01% NaN_3 for long term storage and use.

Antigen	Supplier	Application and dilution
Akt	NEB/Cell Signaling: 9727	IB: 1:1000
Akt-pS473	NEB/Cell Signaling: 4060	IB: 1:2000
Akt-pT308	NEB/Cell Signaling: 9275	IB: 1:1000
Brachyury	R&D: AF2085	IB: 1:500
CLIC4	Santa Cruz: 130723	IB: 1:500
Erk1/2	NEB/Cell Signaling: 9102	IB: 1:1000
Erk1/2-pT202/Y204	NEB/Cell Signaling: 9106	IB: 1:1000
Flag	Sigma: F1804	IB: 1:1000, IP: 1:100
FoxA2	Abcam: ab60721	IB: 1:200
Goat IgG-HRP	Santa Cruz: 2020	IB: 1:5000
GSK3α/β-pS21/9	NEB/Cell Signaling: 9331	IB: 1:1000
GST	Sigma: G7781	IB: 1:2000
Lamin B	Santa Cruz: 365962	IB: 1:500
Mouse IgG-HRP	Santa Cruz: 2005	IB: 1:5000
Mouse IgG-HRP light chain specific	Stratech: 211-032-174	IB: 1:10000
mTOR	NEB/Cell Signaling: 2972	IB: 1:1000
Nedd4L	Abcam: ab131167	IB: 1:5000
Normal mouse IgG2a	Santa Cruz: 2025	IP: µg equivalent to Flag
Normal rabbit IgG	Santa Cruz: 2027	IP: µg equivalent to Smad
P70S6K	NEB/Cell Signaling: 2972	IB: 1:1000
P70S6K-pT421/S424	NEB/Cell Signaling: 9204	IB: 1:1000
PPM1A	Santa Cruz: 56956	IB: 1:500
Rabbit IgG-Alexa Fluor® 488	Life Technologies: A11055	IF: 1:400
Rabbit IgG-HRP	Santa Cruz: 2004	IB: 1:2000
Rabbit IgG-HRP light chain specific	Stratech: 211-032-171	IB: 1:10000
Rb-pS780	NEB/Cell Signaling: 9307	IB: 1:1000

Rictor	Bethyl Labs: A300-459A	IB: 1:5000, IP: 1:100
JNK-pT183/Y185	NEB/Cell Signaling: 4668	IB: 1:1000
Smad2	NEB/Cell Signaling: 3122	IB: 1:1000, IP: 1:100
Smad2/3	NEB/Cell Signaling: 3102	IB: 1:1000
Smad2/3-pT220/179	Abgent: AP3675a	IB: 1:500
Smad2-pS245/250/255	NEB/Cell Signaling: 3104	IB: 1:1000
Smad2-pS465/467	NEB/Cell Signaling: 3108	IB: 1:1000, IF: 1:100
Smad3-pS423/425	Millipore: EP823Y	IB: 1:1000
Smad4	NEB/Cell Signaling: 9515	IB: 1:1000
Sox17	R&D: MAB1924	IB: 1:500
Ubiquitin	NEB/Cell Signaling: 3936	IB: 1:1000
β-actin	Sigma: A5316	IB: 1:5000
β-tubulin	Abcam: ab6046	IB: 1:200

2.3.2 Methods

2.3.2.1 Immunoblotting

For standard immunoblotting, cells were lysed using RIPA buffer supplemented with phosphatase (Na_3VO_4, 1:100 or phosphatase inhibitor cocktail 2) and protease inhibitors (PMSF in ethanol or protease inhibitor cocktail, 1:100). Protein was purified from cell debris via centrifugation at 14000 rpm for 20 min at 4 °C. Total protein content in cell lysates was quantified using the BCA Assay Protein Quantification Kit following manufacturer's instructions, with the protein absorbance read at a wavelength of 562 nm on an Optimax Tuneable microplate reader (Bio-Rad). Typically, 5 to 25 μg of protein was loaded per lane, with lysates being diluted in either 2X or 5X sample buffer and resolved at 180 V for 1 hour through 6-8% Tris-Bis acrylamide gels immersed in SDS running buffer before being transferred onto PVDF membranes via electroblotting. Proteins were typically transferred using the semi-dry method at 20 V for 75 min, with the classical wet method being employed for the transfer of proteins greater than 150 kDa in size at 120 V for 90 min at 4 °C. Both methods utilised the same transfer buffer. Blots were blocked for 20 min with the appropriate blocking buffer before being probed with primary antibody overnight. Blots were washed 3x with 1X TBS-T the following day followed by a 1 hour incubation with the appropriate horse radish peroxidase (HRP)-conjugated secondary antibody diluted in blocking buffer. Membranes were washed a further 3x with TBS-T after incubation with secondary antibody before the addition of ECL substrate and exposure onto CL-Xposure film. Films were developed using an Optimax X-ray film processor (Thermo Fisher).

2.3.2.2 Cytoplasmic/nuclear fractionation

Cells were harvested in cytoplasmic buffer supplemented with protease and phosphatase inhibitors as per immunoblotting and allowed to swell on ice for 20 min, after which NP-40 was added to a final concentration of 0.5%, Samples were immediately vortexed for 10 sec and centrifuged at 13000 rpm for 30 sec to pellet the cell nuclei. The supernatant was extracted and retained as the cytoplasmic fraction. The nuclear pellet was washed 3X with cytoplasmic buffer without NP-40 to remove residual cytoplasmic contamination before being resuspended in nuclear buffer and vigorously shaken for 15 min at 4 °C. Nuclear lysates were then centrifuged for 5 min at 13000 rpm to remove nuclear debris and the supernatant extracted as the nuclear fraction. Samples were quantified and analysed as per immunoblotting.

2.3.2.3 Co-immunoprecipitation (Co-IP)

Cells were harvested in HEPES lysis buffer supplemented with protease and phosphatase inhibitors as per immunoblotting. Due to the absence of salt and detergents, cell lysis was induced mechanically by repeated passaging of lysate through a 25G needle on ice. Proteins within the lysate were purified and extracted via centrifugation at 12000 rpm for 10 min to preserve the integrity of protein complexes. Total protein was quantified as per immunoblotting with 1-2 mg of protein being used in the subsequent immunoprecipitation (IP) step. Smad2 antibody was incubated with 1-2 mg total protein in a 200 µl total volume for 90 min at 4 °C with rotation, after which 100 µl of protein-G conjugated Dynabeads® was added per IP reaction and incubated for a further hour under the same conditions. Precipitated immunocomplexes were separated from the lysate using a magnetic stand, and washed 3 times with cold HEPES lysis buffer to remove non-specific binding prior to elution with 2X sample buffer. Elutes were subjected to immunoblotting and the co-IP assessed with the relevant antibodies. Light chain specific HRP-conjugated secondary antibodies were used to eliminate the background signal associated with the heavy chain contamination from the use of 2X sample buffer as the elution buffer.

2.3.2.4 Smad2 ubiquitination assay

Cells were harvested in 1X non-denaturing CS lysis buffer supplemented with protease and phosphatase inhibitors as per immunoblotting. Lysates were additionally supplemented with 2 µM ubiquitin aldehyde to prevent the action of deubiqutinating enzymes. Proteins within lysates were purified and quantified as per immunoblotting, with 1-2 mg being used in the subsequent IP with Smad2 antibody as per co-IP. Immunocomplexes were washed 3x with cold CS lysis buffer to remove non-specific binding and eluted with 2X Sample buffer. Elutes were subjected to immunoblotting and the degree of ubiquitination assessed using anti-ubiquitin antibody.

2.3.2.5 Generation/purification of recombinant GST-Flag-Smad2/Smad2-T220V

Wild-type and mutant T220V Flag-Smad2 sequences were cloned into pGEX-6p2 plasmids containing the GST sequence and transformed as per bacterial transformation protocol. Single colonies were picked and expanded as per miniprep bacteria culture protocol, with 5 ml used to inoculate a 50 ml LB supplemented with 100 μg/ml ampicillin the following day. This larger culture was allowed to grow until mid-log phase ($OD_{550-600}$ ~0.6-1.0) before the addition of isopropyl β-D-1-thiogalactopyranoside (IPTG) to a final concentration of 0.1 mM. Growth was continued for a further 6 hours at 37 °C, after which the bacteria were pelleted by centrifugation at 2500 xg for 15 min at 4 °C. Bacterial pellets were resuspended in 2.5 ml PBS ($1/20^{th}$ original volume) and sonicated on a Diagenode Bioruptor sonicator on medium setting for 2X 15 sec cycles. Triton X-100 was added to a final concentration of 1% and incubated for 30 min at room temperature to release and solubilise the recombinant protein from inclusion bodies. Crude extracts were subjected to a final centrifugation at 10000 xg for 5 min at 4 °C before being aliquoted and stored at -80 °C. A fraction of the purified extract was subjected to immunoblotting with anti-GST antibody to verify successful expression of the recombinant protein. Recombinant proteins were further purified and concentrated via IP with glutathione-imbued magnetic beads. Beads were washed thrice with 3X volume of 50 mM Tris-HCl pH8.0 wash buffer before the addition of purified bacterial extract. Immunoprecipitation was conducted at 4 °C for 2 hours with rotation. Beads were separated from the bacterial lysates using a magnetic stand and washed 3x with wash buffer before recombinant proteins were eluted in 200 μl wash buffer containing 10 mM reduced glutathione. Elution was performed at 4 °C for 10 min with rotation after which protein solutions were aliquoted and stored at -80 °C. Typically, 3 to 6 μl of the final elution was used in subsequent kinase assays.

2.3.2.6 Production/purification and dephosphorylation of recombinant Smad2

PC-3 cells were transfected with either pCS2-Flag-Smad2-WT or pCS2-Flag-Smad2-T220V using lipofection according to the previously outlined protocol and harvested 48 hours post-transfection using non-denaturing CS lysis buffer supplemented with protease and phosphatase inhibitors as per immunoblotting. Lysates were subjected to IP with anti-Flag antibody in the same manner as outlined previously to precipitate Flag-Smad2-WT/Flag-Smad2-T220V. Immunocomplexes were washed 4X with lysis buffer to remove non-specific binding and subjected to dephosphorylation on bead by resuspending in 50 µl of 1x NEBuffer for PMP provided by NEB supplemented with 1000 U of lambda phosphatase and 1 mM $MnCl_2$. Samples were incubated for 90 min at 30 °C with agitation, after which the phosphatase was washed off the beads with 2X washes with non-denaturing CS lysis buffer followed by 2X washes with 1X Akt kinase buffer. Finally, dephosphorylated recombinant proteins were eluted off the beads via incubation with elution buffer for 10 min at 4 °C with rotation and immediately neutralised with $1/10^{th}$ volume of 1 M Tris-HCl pH 8.2 to prevent hydrolysis of the proteins. Solutions containing the recombinant protein were aliquoted at -80 °C. Typically 6 to 12 µl of the final elution was used in subsequent kinase assays.

2.3.2.7 Akt/Erk2 kinase assay

HEK293T or PC-3 cells were grown in in serum containing cultures after which they were harvested in non-denaturing lysis buffer supplemented with protease and phosphatase inhibitors as per immunoblotting. Active Akt was immunoprecipitated as previously using anti-Akt-pS473 antibody and washed 3X with non-denaturing CS lysis buffer followed by 1X wash with 1X Akt kinase buffer. Preservation of kinase activity was tested via incubation with 1 µg recombinant GST-GSK3 fusion protein and phosphorylation assessed via immunoblotting with anti-GSK3α/β-pS9/21 antibody. 25 µl beads carrying active Akt was used per kinase reaction, to which 1X kinase assay buffer, substrate, 200 mM ATP and molecular grade water were added to a final volume of 30 µl. Reactions were incubated at 30 °C for an hour with agitation after which an equal volume of 2X sample buffer was added to stop the reaction. Phosphorylation was then assessed by immunoblotting with the appropriate phospho-specific antibodies. As a positive control, GST-Flag-Smad2-WT/Smad2-T220V proteins were incubated with Erk2 kinase in 1X Erk kinase buffer supplemented with 200 mM ATP and assessed for phosphorylation via immunoblotting with anti-Smad2-pT220/T179 and anti-Smad2-pS245/S250/S255 antibodies after the reaction is terminated.

2.3.2.8 mTORC2 kinase assay

HEK293T cells were grown in serum containing cultures after which they were harvested in mTORC lysis buffer supplemented with protease and phosphatase inhibitors as per immunoblotting. Cells were gently lysed with rotation for 20 min at 4 °C, after which 1.2 mg of total protein was used in the subsequent IP with 3 µg of anti-Rictor antibody to selectively isolate mTORC2 over mTORC1. Immunoprecipitation was performed in the same manner as outlined previously. Immunocomplexes were washed 3X with mTORC lysis buffer with a gradually decreasing NP-40 series from the initial 0.3% to 0.15% and finally 0% to preserve mTOR kinase activity. Complexes were subjected to a further wash in 1x mTORC kinase assay buffer to completely remove all traces of detergents and incubated with 250 ng phosphatase treated his-6-tagged Akt1 to verify the preservation of kinase activity using anti-Akt-pS473 antibody. 25 µl beads carrying mTORC2 was used per kinase reaction, to which 1X mTORC kinase assay buffer, substrate, 400 nM ATP and molecular grade water were added to a final volume of 30 µl. Reactions were incubated at 37 °C for an hour with agitation after which an equal volume of 2X sample buffer was added to stop the reaction. Phosphorylation was then assessed by immunoblotting with the appropriate phospho-specific antibodies.

2.3.2.9 Immunostaining of hESCs

hESCs were split and cultured on Matrigel® coated coverslips until the desired confluency was reached. Cells were then washed with DPBS and fixed for 10-20 min with 4% fresh paraformaldehyde solution. Excess paraformaldehyde was removed via 3X wash with DPBS and the coverslips were the incubated with blocking/permeablisation buffer for 1 hour followed by an overnight incubation with primary antibody at the appropriate dilution at 4°C with tilting. The following day, coverslips were subjected to 3X 10 min washes with DPBS followed by 40 min incubation with the appropriate fluorophore-conjugated secondary antibody in the dark. Coverslips were then subjected to a further 2X 10 min DPBS wash followed by 1X 10 min DPBS+DAPI wash with DAPI at a final concentration of 1 µg/ml to counterstain the nuclei also in the dark. Slides were mounted onto microscope slides using Mowiol 4-88 solution and allowed to dry overnight. Slides were visualised using a Leica SP5 II confocal fluorescent microscope typically at 64X magnification.

2.4 Software and Online Tools

Computer Software
A Plasmid Editor (ApE)
Adobe Photoshop CS5
Leica LAS AF Lite
Microsoft Office 2013 (Word, Excel, Powerpoint)
Opticon Monitor 3
Quantity One 1D Gel Analysis Software
Serial Cloner 2.6

Online Tools	**Website**
Addgene Plasmid Repository	https://www.addgene.org/
Basic Local Alignment Search Tool (BLAST)	http://blast.ncbi.nlm.nih.gov/Blast.cgi
BioGRID[3,4] Protein Interaction Repository	http://thebiogrid.org
Clustal OMEGA Protein Alignment Tool	http://www.ebi.ac.uk/Tools/msa/clustalo/
Endnote Web	https://www.myendnoteweb.com/EndNoteWeb.html
Genebank® DNA Sequence Database	http://www.ncbi.nlm.nih.gov/genbank/
Molarity Calculator	http://www.graphpad.com/quickcalcs/Molarityform.cfm
NEB Double Digest Finder	https://www.neb.com/tools-and-resources/interactive-tools/double-digest-finder
NEBaseChanger™ for Site-directed mutagenesis	http://nebasechanger.neb.com/
Pubmed	http://www.ncbi.nlm.nih.gov/pubmed
REBASE® Restriction Enzyme database	https://www.neb.com/external-links/rebase
UniProt Protein Database	http://www.uniprot.org/

Chapter Three

Results

Inhibition of PI3K signalling improves DE specification by prolonging the Activin-induced activation of Smad2/3

3.1 Introduction

It has been well established that the specification of DE both *in vivo* and *in vitro* requires high levels of TGFβ signalling, either through endogenously secreted Nodal or by exogenous supplementation of Activin ligands respectively (Lowe et al., 2001; Vincent et al., 2003; Kubo et al., 2004). However, model systems used by these studies are not conducive for the interrogation of the underlying molecular mechanisms. In the case of *in vivo* studies, the tissue complexity and inherent redundancy of development preclude investigations at the molecular level, whilst early *in vitro* hESC to DE differentiation protocols were conducted in the presence of serum, an undefined media component containing milieu of signalling ligands whose effects overwhelm those supplied exogenously. The chance discovery that serum components actually interfere with Activin-induced DE differentiation in feeder-free hESCs cultures (D'Amour et al., 2005) partially resolved this issue, in that advantageously, efficient hESC to DE conversion could be and should be performed in the absence of serum, which together with the use of defined media, is conducive for molecular interrogation. A following study into the inhibitive action of serum on DE also uncovered for the first time the involvement of PI3K signalling in modulating this process, in that supplementation of hESC cultures with the PI3K inhibitor LY promoted efficient DE formation much like the removal of serum (McLean et al., 2007). Although it has recently been proposed that the negative effects of PI3K signaling upon DE differentiation are an indirect effect attributed to the inhibition of Wnt-β-catenin pathway (Singh et al., 2012), a more direct mechanism in which PI3K signaling impacts R-Smad activity itself cannot be completely dismissed (Chen et al., 2012), and provides further scope for fuller molecular interrogation of this process.

Although efforts to develop a completely defined hESC culture condition have been successful in terms of eliminating the need for the majority of serum components (Ludwig et al., 2006; Vallier et al., 2005; Singh et al., 2012), such media often contains high amounts PI3K/mTOR stimulators such as insulin, which have been shown to promote the maintenance of hESC self-renewal and pluripotency (Armstrong et al., 2006; Watanabe et al., 2006). As such, there is currently no culture media that has been shown to support the expansion of hESCs in the absence of PI3K stimulators. In order to interrogate the effect of PI3K signalling upon Activin-induced DE differentiation, our laboratory has developed a defined protocol in which to perform this differentiation. Given that hESCs cannot be propagated in the absence of PI3K stimulators, there was no obvious advantage in utilising defined media in hESC cultures and as such, I maintained our lines in undefined MEF-CM. However, since the focus of the study is to interrogate the molecular events surrounding DE conversion from hESCs, I ensured that the DE differentiation conditions were fully defined

(Figure 3.1A). Although the original B27 formulation does contain insulin (Brewer and Cotman, 1989, 4 μg/ml), this is less when compared to other types of defined media (Thomson's mTeSR1: 10 μg/ml, Vallier's CDM: 7 μg/ml) and is required to maintain the survival of differentiated DE cells (Hay et al., 2008b). Our protocol also encompassed further differentiation to hepatocyte-like cells, which can only be derived from the DE and hence offer verification of DE identity and effectiveness of differentiation (Figure 3.1E). Each stage of differentiation in marked by distinct morphological changes accompanied by the expression of stage specific proteins (Figure 3.1B, C). With the defined protocol established, I utilised LY inhibitor in combination with AA (AA-LY) to drive the DE differentiation and compared these cells to ones that have been differentiated with AA alone in order to dissect the contribution of PI3K signalling. As expected, AA-LY treatment promoted a more effective DE formation as evidenced by increased Sox17 expression and hepatocyte formation (Figure 3.1C, D and E)

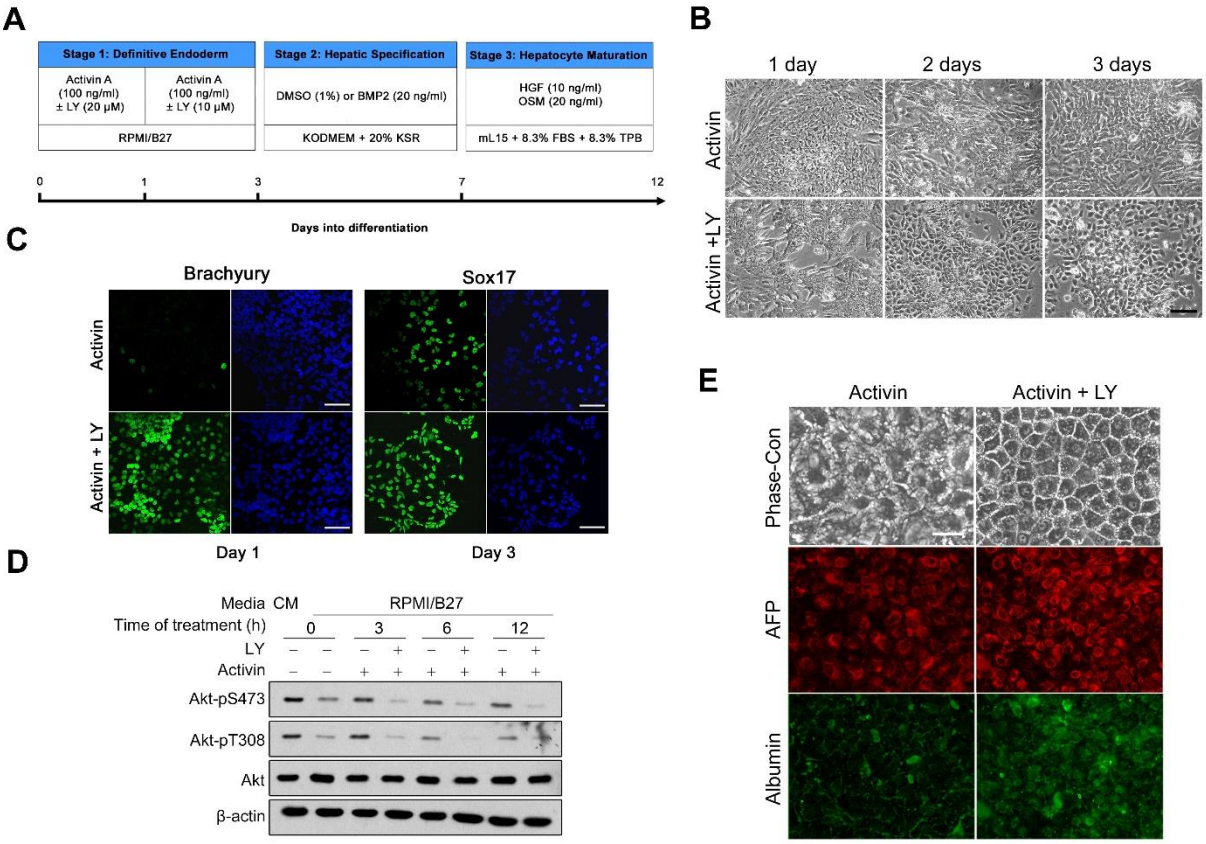

Figure 3.1: Defined DE and hepatic differentiation protocols from hESC

(A) Overview of differentiation protocol, full details available in section 2.1.2.2. (B) Phase contrast microscopy depicting morphological changes associated with DE differentiation over 3 days. (C) Immunostaining depicting increased expression of mesendoderm (Brachyury) and DE (Sox17) markers upon AA-LY treatment. (D) Verification of 20 μM LY efficacy over time as indicated by decrease Akt-pS473/pT308 phosphorylation. (E) Morphological changes associated the formation of hepatocyte-like cells following the end of the protocol marked by increased alpha-fetoprotein (AFP) and albumin expression (B, C and E by Ramasamy 2012).

3.2 Results

3.2.1 PI3K signalling antagonises the duration of Smad2/3 activation

With the establishment of a defined system by which we can investigate the molecular underpinning governing the inhibitory effects of PI3K on AA-induced DE specification, I next asked whether PI3K signalling interferes with the activation of the downstream mediators of the TGFβ pathway. Modulation of the PI3K signalling using both LY inhibitor and stimulators such as heregulin (Her) and IGF-1 (IGF) under serum-free conditions in the absence of AA stimulation in hESCs revealed that activation of endogenous Smad2-pS465/S467 (Smad2-pTail) is largely inversely reciprocal to that of PI3K activity as indicated by Akt-pS473 activation and by densitometric measurements (Figure 3.2A). Furthermore, replacement of undefined MEF-CM with defined RPMI/B27 medium induced an increase in Smad2 activation, which is likely a consequence of the removal of serum components and transfer into a pro-differentiation medium. Consistent with this, time-course analysis revealed that although LY had no effect on the initial activation of Smad2/3 by AA, cells treated with LY exhibited a slower decline of activated Smad2/3, which became more apparent 6 hours post-treatment (Figure 3.2B). The experiment was repeated several times in which a greater abundance of active Smad2/3 (>1.5 folds) in the AA-LY treated cells compared with those treated with Activin alone was observed in all cases at 6 hours post-treatment, despite there being no effect on total Smad2/3 and Smad4 expression (Figure 3.2C).

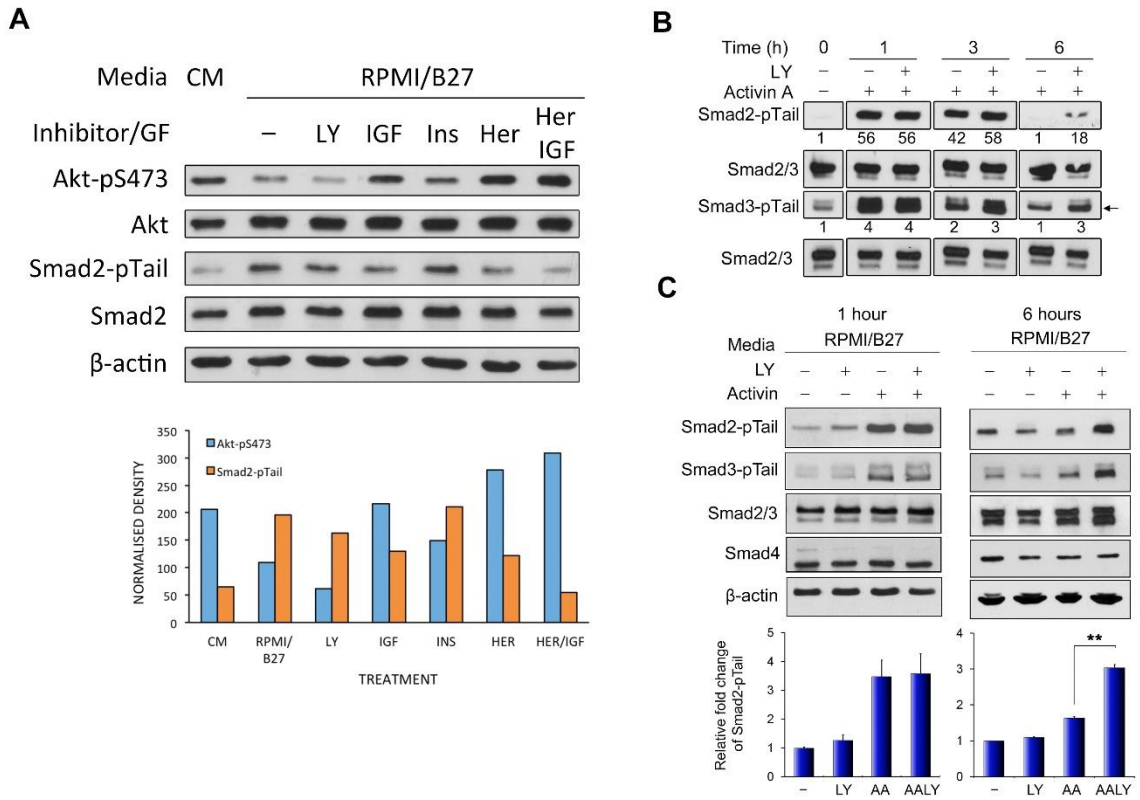

Figure 3.2: Effect of PI3K/mTOR signalling on Smad2/3 activation

*(A) hESCs were treated with activators or inhibitors of the PI3K/mTOR pathway for 1 hour and analysed by immunoblot. Densitometry of bands is shown below blot in which densities of phosphoproteins was normalised to total protein. (B) Time-course analysis of hESCs treated with AA or AA-LY for 1, 3, and 6 hours depicting the levels of Smad2-p465/467 and Smad3-p423/S425 (Smad2/3-pTail) phosphorylation. Arrow indicates Smad3. Numbers indicate quantification of activated Smad2 and Smad3. Experiment was repeated twice and representative image shown.(C) Treatment of hESCs with RPMI/B27 or with RPMI/B27 supplemented with LY/AA/AA-LY for 1 and 6 hours as indicated. Proteins were analysed by immunoblot and densitometry of three independent experiments are represented below as relative fold change in Smad2-pTail compared to RPMI/B27 treated cells. Error bars represent standard deviation (SD) of three independent experiments and ** indicates $p<0.001$ by Student's t test.*

3.2.2 Prolonged activated Smad2/3 accumulate primarily in the nucleus and drives mesendoderm and DE gene expression

In observing that inhibition of PI3K with LY prolongs or sustains the Activin-induced activation of Smad2/3 in hESCs, I next explored whether this population of activated Smad2/3 persists long enough to contribute to the improved DE specification associated with AA-LY treatment. Cytoplasmic-nuclear fractionation and immunostaining of hESCs treated for 3 or 6 hours revealed the predominant localisation of activated Smad2/3 within the nuclear compartment, particularly in hESCs treated with AA-LY (Figure 3.3A, B). This accumulation is also suggestive of an increase in transcriptional function, and a luciferase assay was performed to assess this. hESCs transfected with a luciferase expression vector controlled by twelve repeated CAGA Smad binding elements revealed that AA-LY treated hESCs had a significant increase in luciferase activity when compared to LY and AA treated cells (Figure 3.3C, D). Remarkably, gene expression analysis revealed that even at this early stage into the differentiation process, mesendoderm markers such as Brachyury, Eomes, and Goosecoid were already increased in AA-LY treated cells when compared with AA treated, whilst the DE marker also showed an increase albeit to a lesser extent than the mesendoderm markers (Figure 3.3E). Although the pluripotency markers Oct4 and Nanog showed little difference between AA and AA-LY treated cells, the expression of Sox2 was already reduced in cells of both treatments, further suggesting that there is preferential bias towards the formation of mesendoderm fated cells opposed to the neuroectoderm.

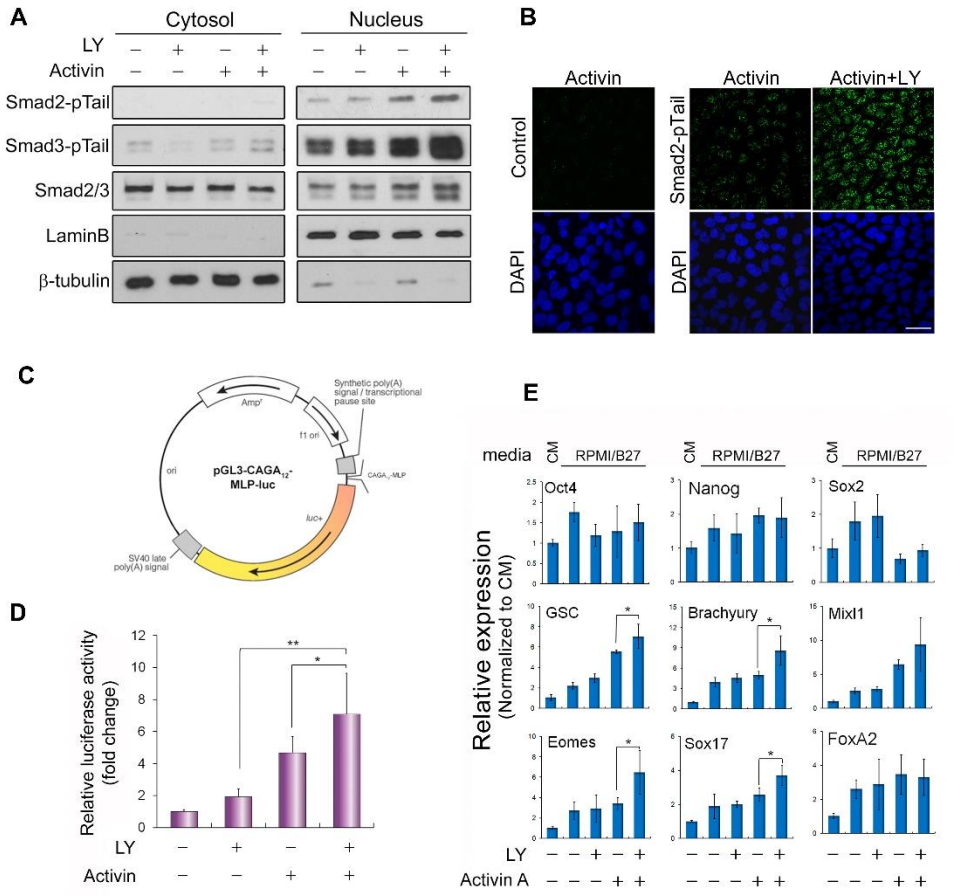

Figure 3.3: Localisation and transcriptional efficacy of Smad2/3 in treated hESCs

*(A) hESCs were treated with either RPMI/B27 alone or supplemented with LY/AA/AA-LY for 6 hours after which lysates were subjected to cytoplasmic-nuclear fractionation and analysed by immunoblot. Lamin B and β-tubulin were used to assess levels of nuclear and cytoplasmic contamination respectively in opposing fractions. (B) Immunostaining of activated Smad2 in hESCs treated for 3 hours with either AA or AA-LY. Control coverslip was incubated with secondary antibody alone to distinguish background from true staining. Scale bar represents 30 μm. (C) Schematic of the luciferase construct used showing the placement of the $CAGA_{12}$ Smad binding elements upstream of the major late promoter (MLP) which drives Smad-dependent expression of luciferase. (D) Luciferase assay performed on hESCs co-transfected with luciferase and renilla constructs treated as in (A) for 6 hours. Data obtained from three independent experiments, error bars represent SD. * and ** indicates $p<0.05$ and $p<0.001$ by Student's t test respectively. (E) Gene expression analysis by qRT-PCR in hESCs treated as in (A) from two independent experiments with the qRT-PCR reaction performed in triplicate (n=6). Graphs indicate relative fold change with respect to day 0 hESCs maintained in MEF-CM. Error bars represent SD. * indicates $p<0.05$ by Student's t test. All experiments repeated at least twice with representative image depicted unless otherwise stated.*

3.2.3 DE differentiation induced by AA-Wort mimics AA-LY treatment

To ensure that the enhance of DE differentiation by LY was solely due to its inhibitive effects on PI3K rather than any off target effects, I utilised Wort, an alternative PI3K inhibitor, in combination with AA to induce DE differentiation for 3 days to replicate the normal differentiation procedure with AA-LY. Effects upon signalling were assessed at 6 hours into the differentiation, which revealed an identical prolonged Smad2/3 activation in AA-Wort treated cells compared to cells treated with AA alone as previously seen in AA-LY treated cells (Figure 3.4A vs. Figure 3.2C). Furthermore, gene expression analysis of hESCs differentiated for 2 days under these conditions showed that AA-Wort derived DE cells exhibited substantial increases in all mesendoderm and DE markers with the exception of Brachyury, which is however known to be drastically downregulated 2 days into the differentiation and routinely signifies a conversion to a more endoderm fate over mesoderm (Hay et al., 2008b; Teo et al., 2011).

Figure 3.4: Induction of DE differentiation with AA-Wort

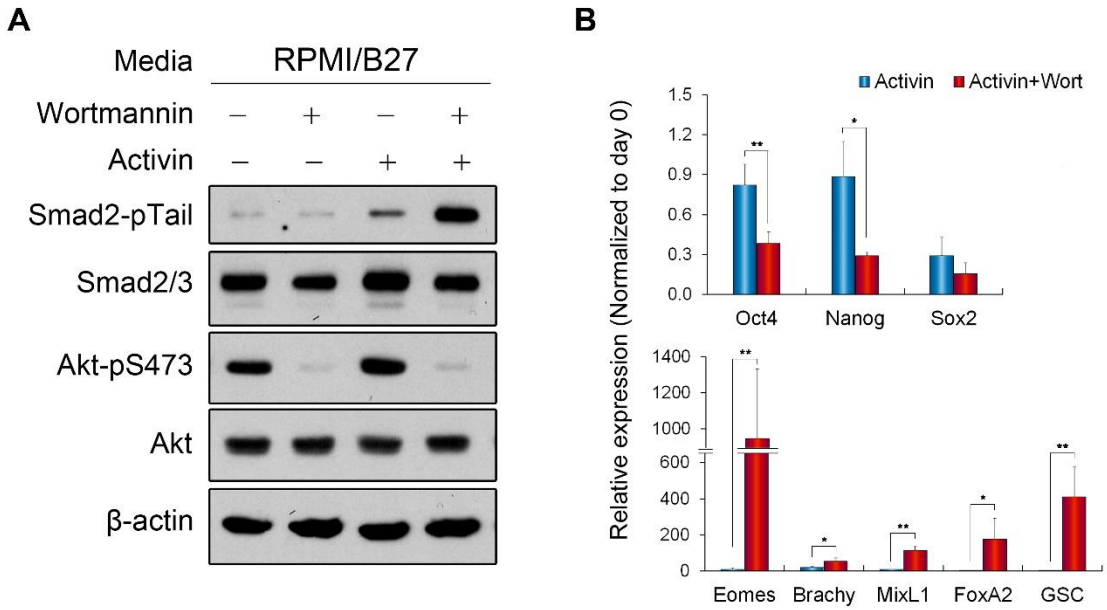

*(A) hESCs were treated with either RPMI/B27 alone or supplemented with Wort/AA/AA-Wort for 6 hours after which lysates were analysed by immunoblot. Like LY, Akt-pS473 was used to assess inhibitive efficacy of Wort. Experiment repeated twice with representative image depicted.(B) Gene expression analysis of AA/AA-Wort differentiated cells by qRT-PCR. Graphs indicate relative fold change as per Figure 3.3E. Error bars indicate SD from two independent experiments with qRT-PCR reaction conducted in triplicate for each (n=6). * and ** indicates $p<0.05$ and $p<0.001$ by Student's t test respectively.*

3.3 Discussion and Conclusions

A full description of the molecular underpinnings in how PI3K signalling negatively impacts Activin-induced DE differentiation of hESCs has been hampered by the inability to interrogate the cross-interaction of both pathways without interference from serum. Here, we have established a defined culture condition that facilitates the efficient conversion of hESC to DE in the absence of serum, which additionally allows for a fuller interrogation of the process on a molecular level. Initial experiments revealed that the basal level of Smad2 activation appears to be quite low in the MEF-CM condition, supporting previous findings which indicate that low levels of TGFβ stimulation is beneficial in maintaining pluripotency by driving the expression of Nanog (Paling et al., 2004; Storm et al., 2007; Vallier et al., 2009). However, low levels of Smad2 activation may not necessarily be due to the lack of Activin/Nodal ligand present in the MEF-CM. As evidenced by the amount of Akt activation, MEF-CM contains potent stimulators of PI3K signalling, which in turn acts to reduce the activation of Smad2. This supports the findings of previous studies in which PI3K signalling was shown to promote the maintenance of pluripotency and self-renewal (Armstrong et al., 2006), and acts to keep Activin/Nodal signalling low to prevent aberrant differentiation. This negative influence of PI3K upon Smad2 activation becomes more apparent upon medium exchange with defined RPMI/B27, in that reduction in the stimulation of PI3K promotes increased Smad2 activation even in the absence of exogenous Activin/Nodal stimulation. Furthermore, the negative effects of PI3K activation can be further enhanced when stimulators such as IGF-1 and Heregulin are supplemented into the RPMI/B27 base media, which when applied together, act to suppresses Smad2 activation to a similar extent as with MEF-CM. Therefore, PI3K signalling negatively affects the activation of Smad2/3 in a reciprocal manner, with a higher PI3K activation resulting in a greater reduction of Smad2/3-pTail phosphorylation and hence a reduction in their functional output. Full manifestation of this effect is evident when DE differentiation conditions are applied to the hESCs. When PI3K is inhibited by LY in the presence of high AA supplementation, a prolonged accumulation or increased activation of Smad2/3 was observable between 3 and 6 hours into the process that is entirely independent of total Smad2/3 and Smad4 levels. Given that Smad2/3 activation is similar at 1 hour into the differentiation, two explanations can be offered; either Smad2/3 activation by the receptors is being sustained or that the pool of activated Smad2/3 persists for longer following maximal activation at 1 hour and are somehow resistant to PI3K-induced deactivation. In order to distinguish which explanation is true, further experimentation was performed which will be described in subsequent chapters.

The prolonged activation of Smad2/3 upon PI3K inhibition by LY immediately suggests an explanation as to why AA-LY treated hESCs ultimately differentiate better in terms DE and hepatocyte formation efficacy when compared to AA treated hESCs. Given that activated Smad2/3 together with Smad4 function as transcription factors upon entry into the nucleus, I next asked whether this prolonged population of activated Smad2/3 are able to drive a more robust transcriptional response when compared to the levels observed in AA treated cells. In this regard, I found that not only was this prolonged population of activated Smad2/3 present mainly in the nucleus, but that they were also transcriptionally active as indicated by the luciferase reporter assay. Furthermore, as several mesendoderm genes are known to be direct Smad2/3 targets (Teo et al., 2011), I also found that these genes were upregulated in AA-LY treated cells albeit may not necessarily be statistically relevant at this early stage of differentiation. Notably, as the same enhancement in Smad2/3 activation was observed in both cytoplasmic and nuclear fractions upon AA-LY treatment, this suggests that the underpinning molecular events leading to this effect are likely to take place in the cytoplasm prior to the nuclear translocation of activated Smad2/3. As a whole, this data reflects two intriguing findings from which to move forward with; firstly in that PI3K signalling appears to directly influence Smad2/3 activation, and secondly, in that this effect may explain why DE conversion from hESC is enhanced upon the inhibition of PI3K by LY. However, whether this is truly an effect of PI3K signalling alone, or via an indirect mechanism as outlined previously (Singh et al. 2012), will be explored further into this study, although experiments with Wort encouragingly indicate the involvement of at least PI3K in mitigating this effect.

Chapter Four

Results

PI3K modulates Nedd4L-mediated proteasomal degradation of activated Smad2/3

4.1 Introduction

Evidence acquired from the experiments performed in the previous chapter suggests that the negative impact of PI3K signalling on AA-induced DE differentiation is primarily due to a PI3K-mediated downregulation of Smad2/3 activation, which is also independent of total Smad2/3 turnover. This represents the first line of evidence linking PI3K activity with the regulation of Smad2/3 activity, which is well supported given that inhibition of PI3K with either LY or Wort enhances Smad2/3 activation in the presence of AA (Figure 3.2C and 3.4A). This could be as a result of either prolonged receptor kinase activity or sustained stabilisation of the activated Smad2/3 pool. However, given that levels of activated Smad2/3 are stoichiometrically related to levels of receptor activation (Inman et al., 2002), and that supplementation of the culture with 100 ng/ml AA ensures that activating ligands are initially available in abundance, if LY did affect receptor activation, a difference in the activation of Smad2/3 by AA would have been observed at an earlier point before 1 hour of treatment. The fact that the difference was observed 3 hours into the treatment and peaked at 6 hours indicates that it is less likely that effect of PI3K inhibition is due to an effect upon the receptor activity. Thus it is more likely that the second scenario, whereby the activated Smad2/3 pool is sustained for longer periods of time in the presence of LY is true.

In considering how to experimentally verify this scenario, one must first understand the mechanisms by which active Smad2/3 is regulated. Upon the cessation of transcriptional activity within the nucleus, activated Smad2/3 are subjected to dephosphorylation by phosphatases such as PPM1A and protein phosphatase 5 (PP5), which in turn triggers their export back into the cytoplasm (Lin et al., 2006; Bruce et al., 2012). Alternatively, activated Smad2/3 may also to bind proteins such as chloride intracellular channel 4 (CLIC4), which function to preserve their activation and prevent phosphatase-mediated deactivation (Shukla et al., 2009). As such, LY-mediated inhibition of PI3K could also in turn inhibit or promote the action of nuclear phosphatase or activated Smad2/3 stabilisation proteins respectively.

Equally, another mechanism by which activated Smad2/3 can be subjected to deactivation is via the ubiquitin-mediated proteasomal degradation pathway. Several E3-ubiquitin ligases such as Smurf2, Nedd4L and Arkadia have been shown to bind and target Smad2/3 for degradation (Lin et al., 2000; Alarcón et al., 2009; Gao et al., 2009; Mavrakis et al., 2007) and represents a critical mechanism by which Smad2/3 activity is regulated. Given that most of these ubiquitin ligases are rather appropriately, expressed ubiquitously, regulation of their activity upon Smad2/3 is mediated through the substrate such as phosphorylation of the Smad linker region (Gao et al., 2009) or

Smad2/3 interaction with Smad7 (Hayashi et al., 1997). As such, it can be envisaged that PI3K signalling could act to mediate ubiquitin ligase recruitment simply by modulating the Smad linker region, and thus directly control their turnover via degradation.

4.2 Results

4.2.1 LY-mediated stabilisation of activated Smad2/3 is not through affecting PPM1A and CLIC4 expression nor PPP activity

Since phosphatase-mediated deactivation is thought to represent the most effective mechanism by which Smad2/3 signalling activity is terminated, I questioned whether LY-mediated inhibition of PI3K affects the expression or activity of any Smad2/3-specific phosphatases or active Smad2/3 binding proteins. I first examined the expression of PPM1A, which was up until recently the only Smad2/3 phosphatase reported to exist along with its modulator CLIC4 by qRT-PCR and immunoblotting, which revealed no obvious changes on both mRNA and protein levels in relation to the presence or absence of LY (Figure 4.1A, B). More importantly, PPM1A was detected exclusively in the cytoplasmic fraction, which is incompatible with its role as a nuclear localised Smad2/3 phosphatase (Lin et al., 2006). I further extended my investigations to other phosphatase families including phosphoprotein phosphatases (PPP) of which one family member; PP5 has been recently shown to be a Smad2/3 phosphatase (Bruce et al., 2012). In order to track the degradation kinetics of activated Smad2, I designed an experimental protocol whereby cells were pulse treated with high dose AA before subsequent incubation with SB431542 (SB), a potent ALK receptor inhibitor that prevents further activation of Smad2 (Figure 4.1C). Co-treatment of the cells with SB and Okadaic acid (OA), a pan-specific inhibitor of PPPs, revealed no significant differences in terms of the decay kinetics of activated Smad2 when compared to SB treated cells (Figure 4.2B), which suggests that phosphatase-mediated deactivation of Smad2/3 is not the mechanism by which PI3K antagonises Smad2 activity.

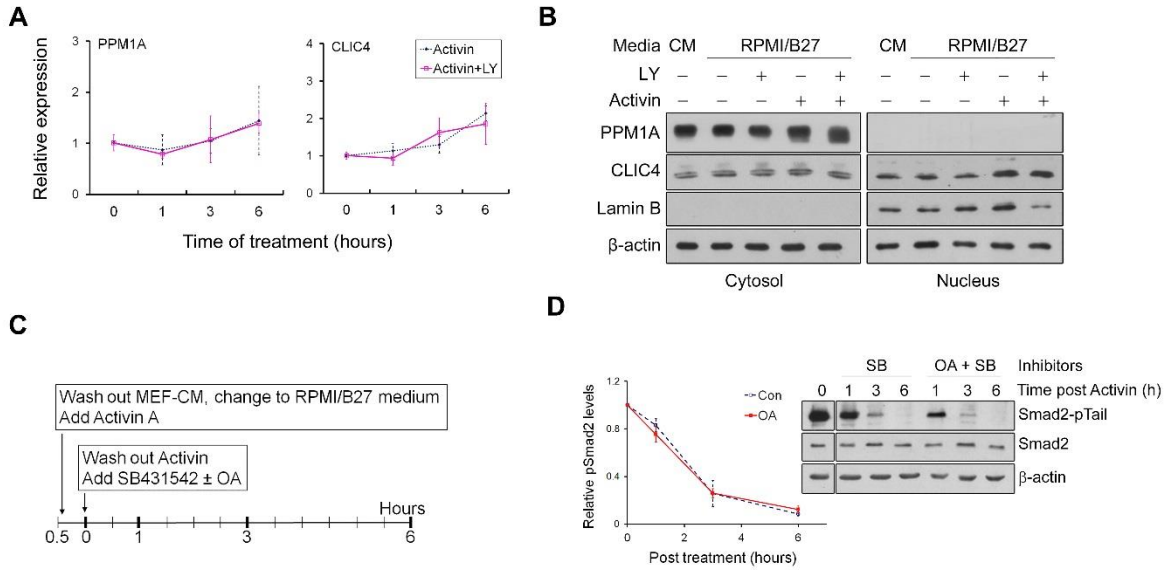

Figure 4.1: Effect of PPM1A, PPP family and CLIC4 in the regulation of Smad2/3 activity

(A) hESCs were treated with either AA or AA-LY for 1, 3 and 6 hours after which gene expression was analysed by qRT-PCR. Graphs indicate relative fold change in relation to hESCs in MEF-CM. Error bars indicate SD from two independent biological replicates with qRT-PCR reaction conducted in triplicate for each (n=6). (B) Cytoplasmic/nuclear fractionation of lysates treated as indicated, with Lamin B and β-actin used contamination and loading control respectively. (C) Schematic depicting setup of experiments used to track the degradation of activated Smad2 over 6 hours in the presence of SB ± OA. (D) Immunoblot of cells treated according to schematic in C. Zero time-point indicates levels of Activin-induced Smad2-pTail following 20 min of incubation. Graphs indicate relative activated Smad2/3 levels normalised to total Smad2 and β-actin. Error bars indicate SD from three independent biological replicates. All experiments repeated twice with representative image depicted.

4.2.2 LY inhibits the ubiquitin-mediated proteasomal degradation of activated Smad2 by preventing the recruitment of Nedd4L

As the antagonistic effect of PI3K upon Smad2/3 activation appears to be independent of phosphatase activity, and given that ubiquitin-mediated proteasomal degradation has also been reported to regulate active Smad2/3 signal termination, I next asked whether LY-mediated inhibition of PI3K acts to prevent the degradation of activated Smad2. By replicating the experiment outlined in Figure 4.1C but substituting OA with LY or the proteasome inhibitor MG132, I found that LY reduced the active Smad2 degradation much like MG132 albeit not with the same efficacy (Figure 4.2A, B). Additionally, SB treatment did not appear to affect the rate of active Smad2 degradation, although the LY-mediated resistance of Smad2 against degradation was

now observable earlier at 1 hour into the treatment (Figure 4.2A). This again suggests that the inhibition of PI3K activity affects Smad2 activity independent of receptor activity and that it may act to suppress ubiquitin-mediated proteasomal degradation of active Smad2/3. Although Nedd4L has been previously identified as a Smad2/3 ubiquitin ligase (Gao et al., 2009), the presence of LY had no discernable effect on Nedd4L expression (Figure 4.2C). However, LY treatment substantially reduced the binding of Nedd4L to Smad2 (Figure 4.2D), which consequently resulted in the decreased ubiquitination of Smad2 (Figure 4.2E). Notably, LY treatment also appeared to reduce the phosphorylation of the Smad2 T220 linker residue, which has been shown to be required for Nedd4L recruitment (Gao et al., 2009). Therefore, downregulation of this phosphorylation by LY treatment could account for the reduction of Nedd4L recruitment, which in turn prevents Smad2 ubiquitination and prolongs its activation.

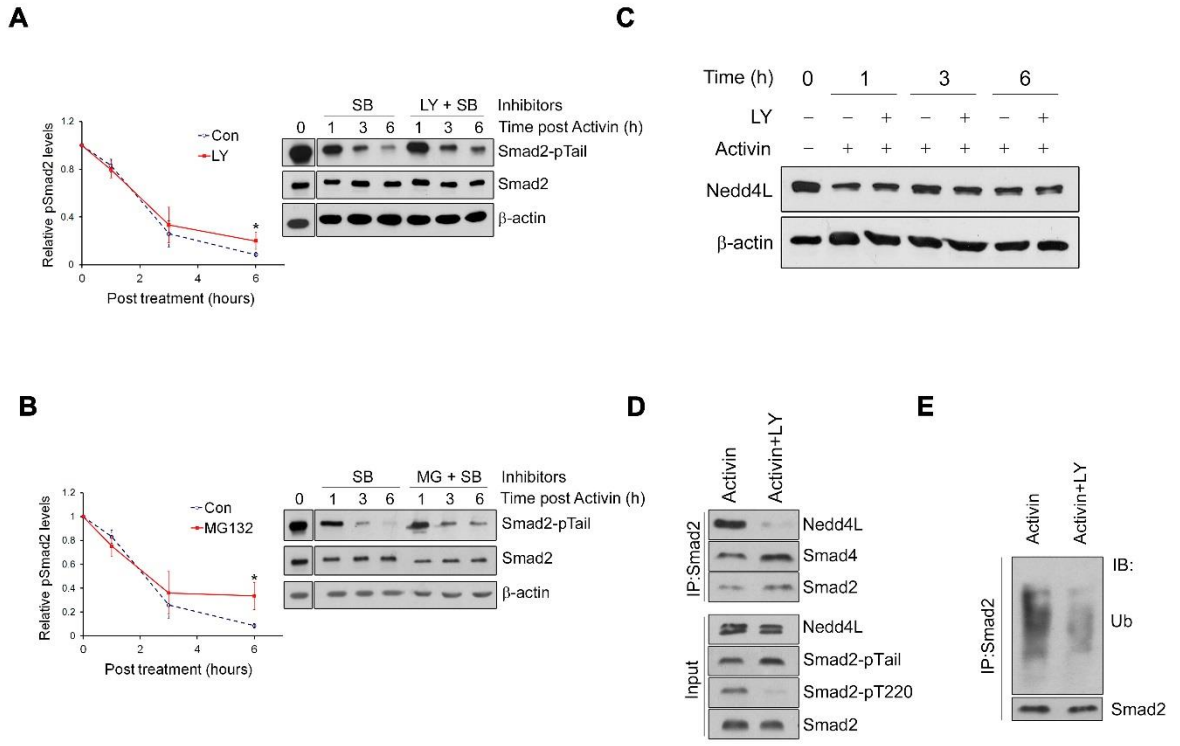

Figure 4.2: Effect of ubiquitin-mediated proteasomal degradation in the regulation of Smad2/3 activity

(A) and (B) Immunoblot of hESCs treated according to schematic in Figure 4.1C, but with OA substituted with either LY or MG132 (MG). Zero time-point indicates levels of Activin-induced Smad2-pTail following 20 min of incubation. Graphs indicate relative activated Smad2/3 levels normalised to total Smad2 and β-actin. Error bars indicate SD from three independent biological replicates. (C) hESCs were treated as indicated for 1, 3, and 6 hours as indicated and analysed by immunoblot. (D) Co-IP of Smad2 with Nedd4L and Smad4 in hESCs treated for 1 hour as indicated. (E) Ubiquitination assay of immunoprecipitated Smad2 from hESCs treated for 1 hour as indicated. All experiments repeated at least twice with representative image depicted.

4.2.3 shRNA-mediated knockdown of Nedd4L enhances the stabilisation of activated Smad2 and promotes DE induction in the absence of LY

It has been shown in the previous sections that inhibition of PI3K promotes Activin-induced DE differentiation of hESCs by reducing the recruitment of Nedd4L to activated Smad2/3, which enhances their activity. Thus, I next sought to verify this mechanism by diminishing Nedd4L in cells via genetic means. If the hypothesised mechanism is correct, the reduction of Nedd4L levels will increase Activin-induced Smad2/3 activity and promote the DE differentiation of hESCs.

Furthermore, as PI3K signalling promotes Nedd4L binding, loss of Nedd4L itself will lead to the stabilisation of activated Smad2/3 regardless of LY treatment. In utilising lentiviral delivery of shRNA-containing constructs, I was able to obtain both PC-3 and hESC knockdown lines (shNedd4L-PC-3/hESCs) possessing over ~50% knockdown as assessed by qRT-PCR and immunoblotting (Figure 4.3C)

A). PC-3 cells were chosen as a surrogate cell line to initially perform this experiment due to its hESC-like responsiveness to Activin stimulation. Indeed, decreased Nedd4L expression mitigates the antagonistic effect of PI3K upon Smad2/3 activation, resulting in their enhanced resistance to ubiquitin-mediated proteasomal degradation with LY treatment having no effect upon Smad2/3 activation. This is clearly demonstrated in shNedd4L-PC-3 cells whereby Smad2 activity was enhanced regardless of the presence or absence of LY unlike that observed in control cells (Figure 4.3B). Notably, the same downregulation of Smad-T220 linker phosphorylation was also observed in the presence of LY, indicating that this effect is attributed to the presence of LY. Since Nedd4L knockdown serves to enhance Smad2 activity, I next assessed whether it enhances the induction of DE in hESCs. In complete agreement with the effects observed in PC-3 cells, shNedd4L-hESCs when treated with AA alone showed higher levels of mesendoderm and endoderm gene expression when compared to control cells (Figure 4.3C). Therefore, regulation of the ubiquitination activity of Nedd4L by PI3K signalling has a direct impact upon the differentiation of hESCs to DE.

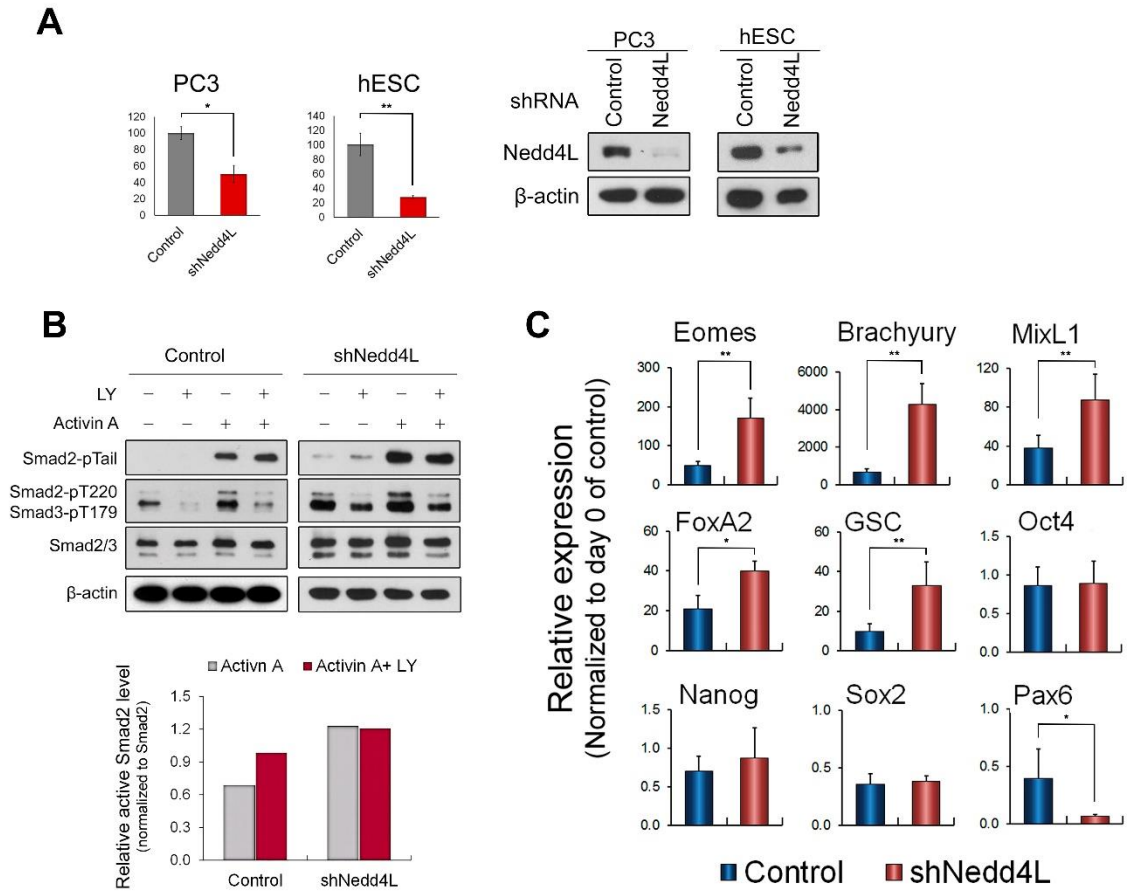

Figure 4.3: Effect of Nedd4L knockdown on Smad2 activity and DE induction

*(A) Verification of shRNA-mediated Nedd4L knockdown in PC-3 and hESCs by qRT-PCR and immunoblot. Graphs indicated percentage of knockdown when compared to controls infected with shGFP-containing virus. Error bars indicate SD from two independent experiments from which PCR reaction was performed in triplicate (n=6). * and ** indicates p<0.05 and p<0.001 by Student's t test respectively. (B) shGFP control and shNedd4L-PC-3 cells treated for 1 hour as indicated before lysis and assessment by immunoblot. AA dosage was reduced to 10 ng/ml. Graphs depict densitometry measurements of activated Smad2 normalised to total Smad2 and β-actin in AA and AA-LY treated cells. Experiment repeated twice with representative image depicted. (C) Gene expression analysis of shGFP control and shNedd4L-hESCs differentiated for three days with AA alone. Graphs indicate relative fold change when normalised with day 0 shGFP/shNedd4L-hESCs in MEF-CM. Error bars indicate SD from two independent experiments from which PCR reaction was performed in triplicate (n=6). * and ** indicates p<0.05 and p<0.001 by Student's t test respectively.*

4.3 Discussion and Conclusions

In establishing that PI3K signalling negatively affects the duration of Smad2/3 activity, two different mechanisms were posited to induce this effect. Given that the duration of the Smad2/3 response is directly related to its activation (Inman et al., 2002), I reasoned that PI3K may act to modulate the activity of Smad2/3-specific phosphatases or proteins that stabilise activated Smad2/3. Subsequent experimentation served to discount this mechanism, in that LY treatment did not result in any significant changes in PPM1A or CLIC4 expression on both mRNA and protein levels. Furthermore, my study has found PPM1A expression to be largely restricted to the cytoplasmic fraction, whilst the majority of Smad2/3 are shown to rapidly translocate into the nucleus post-activation (Chacko et al., 2001). These results were initially very surprising as PPM1A had been the only phosphatase identified to be responsible to dephosphorylate C-terminal Smad2/3 serine residues (Lin et al., 2006). However, a recent report (Bruce et al., 2012) has demonstrated a similar pattern of PPM1A expression in HaCaT cells, utilising the same cell type as in the original paper (Lin et al., 2006), which is additionally in line with my results and indicates the cell line independency of this effect. Furthermore, PPM1A does not appear to be in the right cellular compartment to perform its phosphatase function, and given that it has also been shown to promiscuously act upon cytoplasmic targets such as PI3K and axin (Yoshizaki et al., 2004; Strovel et al., 2000), it is hence questionable whether PPM1A truly is a *bona fide* nuclear phosphatase.

Although Bruce et al. provided convincing evidence to suggest that PP5 rather than PPM1A is the Smad2/3 phosphatase, treatment of hESCs with the pan-PPP inhibitor OA had no effect on the decay kinetics of activated Smad2, which together with the previous lines of evidence, discounts the involvement of phosphatases in mediating the LY-dependent stabilisation activated Smad2/3. However, despite the characterisation of OA as a pan-PPP inhibitor, it is known that certain phosphatases are inhibited to a greater degree than others, even amongst the same family. Notably, PP2A is preferentially inhibited to a greater extent than PP1, although both at the nanomolar range, whilst PP2B requires much higher concentrations for effective inhibition (Bialojan and Takai, 1988). Therefore OA treatment alone cannot comprehensively rule out the involvement of all PPP family members, although these results almost certainly rule out the involvement of PP5 due to its inherent sensitivity to OA inhibition to the same extent as that of PP2A (Chen et al., 1994). The use of improved pan-phosphatase inhibitors such as calyculin A that potently inhibits both PP1 and PP2A should allow future studies to address this issue with greater confidence (Resjö et al., 1999).

In comparing the decay kinetics of LY-treated with MG-treated cells, I observed that although the pattern of decay was similar to each other, in that both prolonged the activation of Smad2, the effect was more pronounced in MG-treated cells. This is perhaps unsurprising given that MG acts to prevent the degradation of both total and activated Smad2 regardless of the identity of the E3 ligase, whilst LY only acts specifically to prevent Nedd4L-mediated Smad2 degradation. However, it is notable that the total Smad2 levels did not show a great deal of increase even in the presence of MG for extended periods of time, which suggests that the rate at which total Smad2 undergoes ubiquitin-mediated turnover is rather slow, although whether MG treatment affects global protein synthesis is debatable. Nonetheless, this data indicates that the effect of LY treatment in the stabilisation of activated Smad2 might be manifested via the inhibition of their ubiquitin-mediated proteasomal degradation. In pursuing this line of enquiry, I identified Nedd4L as a likely candidate for investigation, as it was reported to be the most effective E3 ubiquitin ligase acting upon activated Smad2/3 (Gao et al., 2009). Experimentation along these lines revealed that as characteristic of most E3 ubiquitin ligases, Nedd4L is ubiquitously expressed in hESCs and unaffected by either AA or AA-LY treatment. However, I reasoned that although LY may not affect Nedd4L expression, it could still interfere with Nedd4L recruitment to Smad2/3. Enticingly, this was proven to be the case, in that less Nedd4L was bound to Smad2 in cells that were treated with LY to suppress PI3K activity, which was corroborated with a reduction in their overall ubiquitination. Therefore, the experiments have demonstrated that PI3K signalling antagonising Activin-Smad signalling could be through regulation of the recruitment of Nedd4L to Smad2/3.

In establishing the involvement of Nedd4L in the regulation of Smad2 activity by PI3K, I then sought to verify whether this mechanism accounts for the inhibitive effects of PI3K signalling on DE induction using a loss of function approach to target Nedd4L using shRNA. As predicted, reduction in Nedd4L expression resulted in prolonged Smad2 activation, dispensing with the need for LY, which additionally resulted in a more effective DE differentiation in hESCs when supplied with AA alone. As a whole, this body of evidence suggests that PI3K/Akt signalling acts to promote the phosphorylation the Nedd4L-mediated degradation of activated Smad2/3 and curtails the AA-induced DE differentiation of hESC.

Chapter Five

Results

PI3K modulates Smad2/3 degradation via phosphorylating Smad2/3 linker T220/T179 residue

5.1 Introduction

Emerging evidence has lent weight to the idea that the linker region of Smad2/3 serves as an important site at which their activity is regulated. This region contains multiple phosphorylation sites that are targeted by various proline-directed kinases stemming from other signaling pathways and thus can additionally be considered as a key site for inter-pathway crosstalk. Phosphorylation of this region controls the interactions between Smad2/3 and other proteins, which consequently affects active Smad2/3 stability, nuclear translocation and transcriptional activity (Guo et al., 2009; Wrighton et al., 2006). In particular, it has been demonstrated that recruitment of Nedd4L to the Smad2/3 linker PPxY motif requires the phosphorylation of the upstream linker threonine residue lying adjacent to the PPxY sequence, Smad2-T220 and Smad3-T179 (Figure 5.1A and Figure 1.5). In previously observing that LY-treatment acts to reduce the phosphorylation of these residues (Figure 4.2D and 4.3B), it remains however unknown whether this effect is contributory in promoting Smad2/3 activation or DE differentiation. Nonetheless, if this is indeed the case, genetic manipulation of the T220/T179 residue should be able to replicate the positive effects of LY-mediated PI3K inhibition in terms of promoting Smad2/3 activation and consequently DE differentiation in the absence of LY, not too dissimilar to the effects observed with Nedd4L knockdown.

It is also unclear as to whether this effect is a direct or indirect consequence of PI3K signalling, since several kinases have been definitively shown to act upon the Smad2/3 linker residue such as Erk1/2 (Kretzschmar et al., 1999) and CDK (Alarcón et al., 2009). Conceptually, should targeted inhibition of such kinases recapitulate the effects seen with LY or Wort treatment, one could at least partially resolve this issue. Whilst it might be evidently more likely that PI3K may exert its influence upon Smad2/3 activity via the modulation of linker region kinases, the direct involvement of kinases along the PI3K signalling axis itself cannot be completely discounted. The following experiments in this chapter aimed to address these issues, firstly in verifying whether LY-mediated regulation of the T220/T179 residue is sufficient in driving improved DE, and secondly, whether this modulation is a direct or indirect effect of PI3K signalling.

5.2 Results

5.2.1 LY treatment specifically inhibits the phosphorylation of the T220 residue and promotes the prolonged activation of Smad2

The linker region of Smad2 is characterised by Ser and Thr residues adjacent to Pro residues that are the target of various proline-directed Ser/Thr kinases. Nedd4L recruitment is mediated by the phosphorylation state of the T220/T179 residue lying adjacent to the PPxY binding site (Figure 5.1A and Figure 1.5), (Gao et al., 2009). In observing the downregulation of the T2220 phosphorylation in LY treated hESCs and the possibility that this could account for the reduced association of Smad2 with Nedd4L, it is conceivable that PI3K may affect Smad2/3 activation through regulating the phosphorylation of the Smad2/3 linker threonine residue that subsequently affects Smad2/3 interaction with Nedd4L. In addition to T220/T179, the Smad2/3 linker region also contains three other Ser residues that can also be phosphorylated. These residues are denoted as S245/S250/S255 in Smad2 (Smad2-LS, Figure 5.1A) and S204/S208/S213 in Smad3 (Smad3-LS, Figure 1.5). Therefore it was important to ascertain whether PI3K signalling specifically regulates the threonine residue of the Smad2/3 linker region, or whether it affects the linker region more generally by regulating the phosphorylation of the other Ser residues. Furthermore, given that phosphorylation of these linker sites have been shown to alter the efficacy of endoderm specification in *Xenopus* (Grimm and Gurdon, 2002), it was also important to assess how their phosphorylation status changes during the course of *in vitro* DE differentiation in response to AA or AA-LY treatment.

A time course experiment in hESCs analysing the dynamics of Smad2-T220 and Smad-LS revealed that T220 phosphorylation was increased upon AA treatment, which was downregulated in the presence of LY, most evidently at 6 hours post-treatment (Figure 5.1B, C). In contrast, phosphorylation of the LS residues showed no changes in response to either AA or LY treatment, indicating that the phosphorylation of the T220/T179 and LS residues are regulated by different mechanisms. Interestingly, hESCs that were transferred to RPMI/B27 medium supplemented with SB to block TGFβ/Activin signalling also exhibited high levels of Smad2/3-T220/T179 phosphorylation, which could be inhibited by LY treatment, thereby demonstrating that PI3K-mediated T220/T179 phosphorylation is independent of TGFβ/Activin signalling (Figure 5.1D). The effect of LY in downregulating the phosphorylation of Smad2-T220 also corresponds exactly with the time point at which Smad2 activation is also increased (Figure 5.1E, F), suggesting that these two events are related each other. Furthermore, when subjecting PC-3 cells to similar

treatment, albeit with a lower dosage of AA, similar effects were observed at 1 hour post-treatment (Figure 5.1G). Independent observation of the same effect in two different cell lines suggests that PI3K is involved in the regulation of the Smad2/3 linker Thr residue and that this occurs solely upon the T220 residue in Smad2. Moreover, it is probable that this is a more general effect that is not dependent on the cell line used. This data causatively links the downregulation of T220 phosphorylation with the prolonged activation of Smad2 and offers a mechanism by which PI3K activity can influence Smad2/3 function.

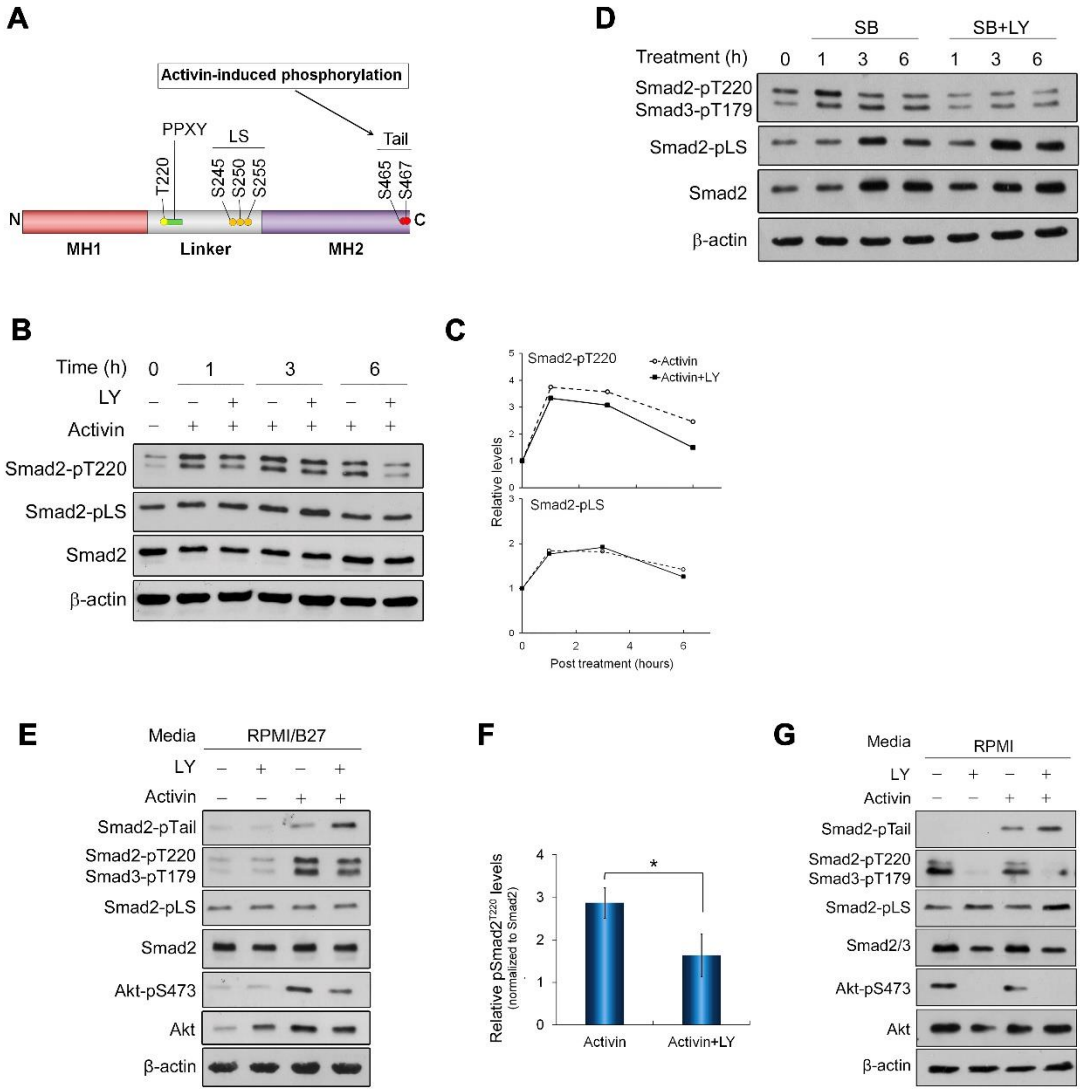

Figure 5.1: LY-mediated downregulation of T220 phosphorylation prolongs Smad2 activation

*(A) Schematic illustrating the structure of the Smad2 linker region. (B) hESCs were treated with either AA or AA-LY for 1, 3 and 6 hours after which cell lysates were analysed by immunoblotting. (C) Densitometric measurements of linker T220 and LS phosphorylated Smad2 normalised to total Smad2 and β-actin levels depicting LY-dependent downregulation in AA-LY treated cells as per B. (D) hESCs pre-treated with AA followed by incubation with RPMI/B27+SB as indicated (E) hESCs treated for 6 hours with the indicated treatments and analysed by immunoblotting. (F) Densitometric measurements of T220 phosphorylated Smad2 normalised to total Smad2 and β-actin levels from repeated experiments of E. Graph represents data from three independent experiments, error bars indicate SD. Statistical analysis was performed via Student's t test where * indicates P<0.05. (G) PC-3 cells treated as in B but with reduced AA dosage (10 ng/ml) and duration (1 hour) and analysed by immunoblotting. All experiments repeated twice with representative image depicted.*

5.2.2 Ectopic expression of mutant Smad2-T220V promotes LY-independent prolonged activation of Smad2 and induces DE differentiation in hESCs

Previously, I have found that Nedd4L knockdown serves to enhance the resistance of activated Smad2 to degradation and thereby promote DE induction irrespective of the T220 phosphorylation status. This provided corroborating evidence to support the notion of PI3K affecting Smad2/3 activity and DE differentiation through the proposed mechanism in which Nedd4L-mediates Smad2/3 degradation. Similarly, I anticipated that if this mechanism is indeed regulated by PI3K via the modulation of the Smad2/3 linker Thr, mutation of this residue to a non-phosphorylatable Val residue by genetic manipulation could serve to further corroborate this data in producing a similar effect.

To these means, a construct was generated via site-directed mutagenesis in which the T220 residue in the Flag-tagged wild-type Smad2 (Smad2-WT) coding sequence was mutated to V220 (Smad2-T220V). Substitution of the Thr residue with Val generates a mutant form of Smad2 that is effectively permanently dephosphorylated and hence incapable of recruiting Nedd4L. This mutant sequence along with the wild-type were further subcloned into lentiviral expression vectors downstream of a PuroR-2A sequence in order to generate puromycin-resistant cell lines that also express Smad2-WT/T220V protein (Figure 5.2A). A lentiviral vector encoding for PuroR alone was used as an empty vector control. Transgenic cells were generated from both PC-3 and H1 hESC lines via lentiviral transduction, which express either Smad2-WT or Smad2-T220V. Treatment of transgenic PC-3 cells with AA or AA-LY revealed that Smad2-T220V cells treated with AA exhibited similar levels of activated Smad2 as that of the AA-LY treated, indicating that the activation of these cells is independent of the presence of LY (Figure 5.2B), whilst both control and Smad2-WT cells showed a much higher Smad2 activation only in the presence of AA-LY as observed in experiments previously. In addition to the differential activation of Smad2 between Smad2-WT and Smad2-T220V transgenic lines, AA-induced DE differentiation over 2 days in transgenic hESCs also revealed an upregulation of mesendoderm and DE markers in Smad2-T220V expressing cells when compared to WT (Figure 5.2C). These effects in both PC-3 cells and hESCs were not due to the differential expression of Smad2 as both total and transgenic Smad2 levels in the two transgenic lines were shown to be largely equal as indicated by Smad2 and Flag levels assessed via immunoblot and qRT-PCR. These results have demonstrated the effect of Smad2/3 activity and DE differentiation by PI3K signalling is regulated through the phosphorylation of Smad2/3 linker Thr phosphorylation.

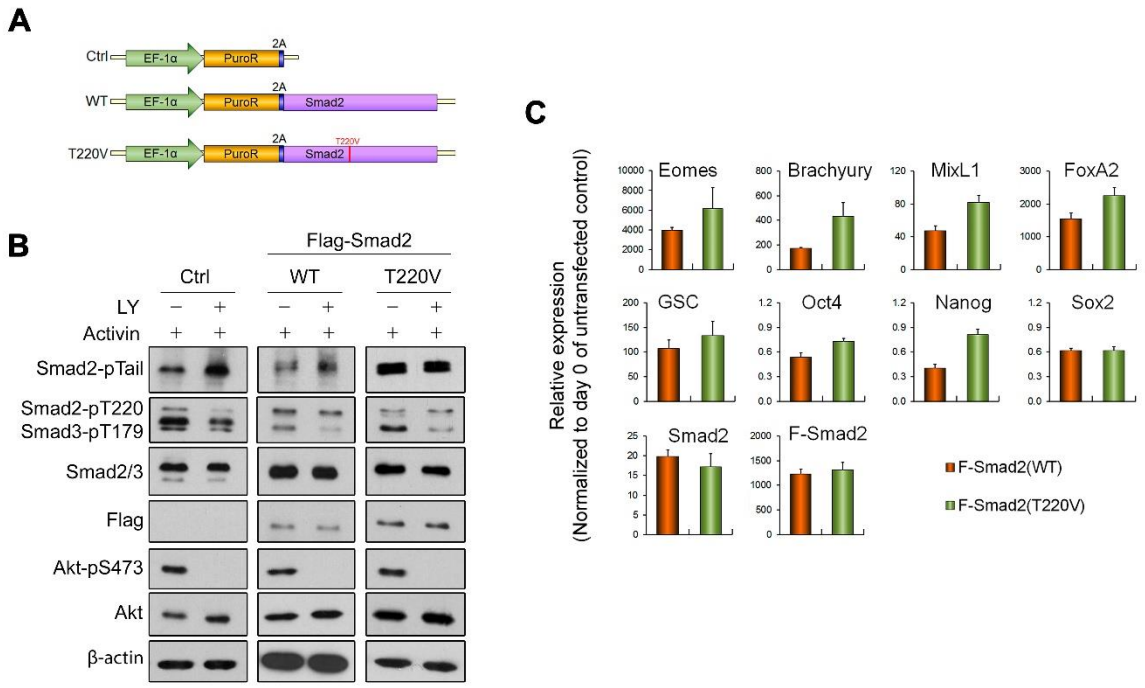

Figure 5.2: Ectopic expression of mutant Flag-Smad2-T220V into PC-3 and hESCs

(A) Schematic illustrating three lentiviral constructs used ectopically express Puro, Puro-2A-Flag-Smad2(WT) and Puro-2A-Flag-Smad2(T220V). Infected cells were selected with puromycin and propagated as stable cell lines. (B) Transgenic PC-3 cells were treated with either AA or AA-LY for 1 hour after which cell lysates were analysed by immunoblotting. Experiment repeated twice with representative image depicted. (C) Gene expression analysis of transgenic Smad2-WT and Smad2-T220V expressing hESCs differentiated for 2 days in the presence of AA alone. Graphs represent data from 2 independent experiments from which RT-PCR was performed in triplicate for each (n=6). Error bars indicate SD. F-Smad2 refers to expression of Flag-tagged Smad2 expressed via transgene.

5.2.3 Known linker kinases do not contribute to the PI3K-mediated downregulation of T220 phosphorylation

In verifying that T220 phosphorylation regulates the activity of Smad2/3 via recruitment of Nedd4L, I next sought to uncover the kinase responsible for this phosphorylation. Specifically, I questioned whether the regulation of this phosphorylation by PI3K occurs indirectly through affecting the activity of known linker kinases such as Erk1/2, CDK and other MAPKs. Given that LY and Wort treatments are shown to be effective in downregulating the PI3K-dependent T220 phosphorylation, inhibition of the target kinase should equally be able to recapitulate the effects of LY treatment upon the T220 residue. To these means, I applied various inhibitors that are

known to specifically act against these linker kinases (Figure 5.3A) to hESCs and assessed their efficacy by analysing their canonical downstream targets (Figure 5.3B). MEK1/2, PI3K and CDK were effectively inhibited as indicated by the downregulation of Erk1/2-pT202/Y204, Akt-p473 and Rb-pS780 phosphorylation respectively, whilst the effectiveness of the JNK inhibitor was demonstrated by the downregulation of its own pT183/Y185 phosphorylation due its ability for autophosphorylation. I was unfortunately unable to assess the effectiveness of the p38 inhibitor, owing to the lack of a working MAPKAPK-2 antibody. However, of the currently reported linker kinases, Erk1/2 and CDK appear to be the best characterised (Kretzschmar et al., 1999; Grimm and Gurdon, 2002; Alarcón et al., 2009; Gao et al., 2009) and therefore became the main focus of my investigations. hESCs pulse treated with high-dose Activin were subjected to a further 1 hour treatment with the various inhibitors in combination with SB to prevent further activation of Smad2/3 via Activin. Analysis via immunoblot following treatment revealed that although all the inhibitors did reduce T220 phosphorylation to some degree, none was as effective as LY treatment (Figure 5.3C). Notably, T220 phosphorylation persisted even in the presence of the Activin receptor inhibitor SB, supporting the previous notion of T220 phosphorylation being independent of Activin stimulation. Furthermore, extending the treatment time to 6 hours also revealed that only LY treatment was able to maintain the suppression of T220 phosphorylation (Figure 5.3D). Surprisingly, treatment with the CDK inhibitor flavopiridol enhanced T220 phosphorylation, whilst simultaneously reducing Smad2-pLS and total Smad2 levels, which was particularly evident in the prolonged treatment. These results suggest that CDK may affect Smad2/3 signalling by a mechanism that is completely different from that mediated by PI3K.

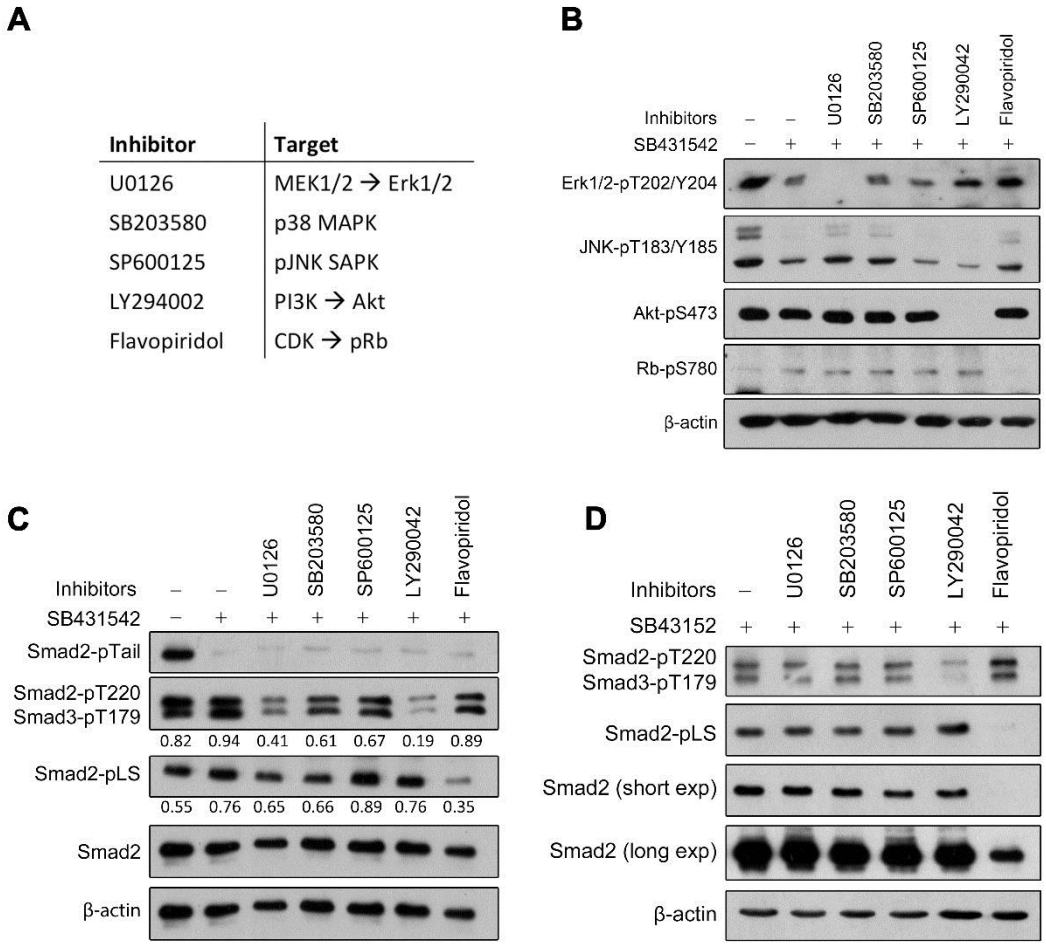

Figure 5.3: Effect of various linker kinase inhibitors on T220 phosphorylation

(A) Table outlining the inhibitors used, direct targets and affected downstream targets. (B) hESCs were pulse treated 100 ng/ml Activin after which they were further incubated with inhibitors for 1 hour as indicated and assessed by immunoblotting. (C) hESCs treated as in B and assessed by immunoblotting. Numbers indicate densitometric measurements of Smad2-pT220 and Smad2-pLS normalised to total Smad2 and β-actin levels. (D) hESCs treated as in C but for 6 hours, total Smad2 levels were assessed by both short and long exposure as indicated. All experiments repeated twice with representative image depicted.

5.2.4 Erk1/2 kinase does not contribute to the LY-mediated downregulation of T220 phosphorylation

As Erk1/2 has been previously demonstrated to be a key linker kinase implicated in the regulation of Smad2/3 activity (Grimm and Gurdon, 2002) and more recently, induction of DE differentiation (Singh et al., 2012), I performed further experiments to further verify the hypothesis

of PI3K-mediated inhibition of Smad2 activity being both a CDK and Erk-independent effect. Analysis of Erk in hESCs treated with AA or AA-LY for 1, 3 and 6 hours revealed no significant LY-dependent changes in Erk activation (Figure 5.4A). Since heregulin and IGF-1 (HI) could potentially activate Erk via non-canonical activation of PI3K signalling, I treated hESCs in RPMI/B27 supplemented with both factors and compared the Erk activity levels from cells supplemented with RPMI/B27 alone or in combination with LY (Figure 5.4B). Notably, under these conditions, both LY and HI treatment actually enhanced Erk activity, with LY treatment being the more effective. Importantly, despite the LY-dependent increase in Erk activation, no substantial increase in Smad2-T220 or Smad2-LS phosphorylation was observed, indicating that Erk1/2 does not function as the PI3K-induced linker kinase responsible for the inhibition of Smad2 activity. In fact, PI3K acts to inhibit Erk activity under these culture conditions, which is similar to findings in previous studies (Singh et al., 2012). Although HI treatment enhanced PI3K signalling as evidenced by Akt activation and P70S6K-pT389 phosphorylation, no difference in T220 phosphorylation was observed between untreated and HI treated samples, which was surprising. However, it is worth noting that even though Smad2-T220 phosphorylation did not increase upon HI treatment, it was dramatically reduced when PI3K activity was inhibited by LY treatment as assessed by Akt-p473 levels. This suggests that a low level of PI3K activity is sufficient to maximally phosphorylate Smad2/3 at the T220/T179 residue, meaning that increasing PI3K activity via HI would have no further effect as phosphorylation of this residue was already saturated. It is plausible that this low level PI3K activity is due to the insulin component of the B27 supplement. This hypothesis was subsequently confirmed upon the treatment of hESC with HI in the absence of B27, which evidently increased the phosphorylation of the T220 residue when compared to untreated cells (Figure 5.4C), additionally demonstrating the inherent sensitivity of this residue to PI3K-induced phosphorylation. Therefore, this data shows that none of the reported linker kinases appear to be responsible for mediating the PI3K-dependent inhibition of Smad2 activity via the T220 residue, which strongly suggests that this function is solely restricted to a kinase with the PI3K signalling pathway itself or is directly regulated by PI3K activation. Nevertheless, the involvement of these linker kinases in regulating Smad2/3 activity through mechanisms beyond the one examined cannot be fully discounted based on these experimental observations.

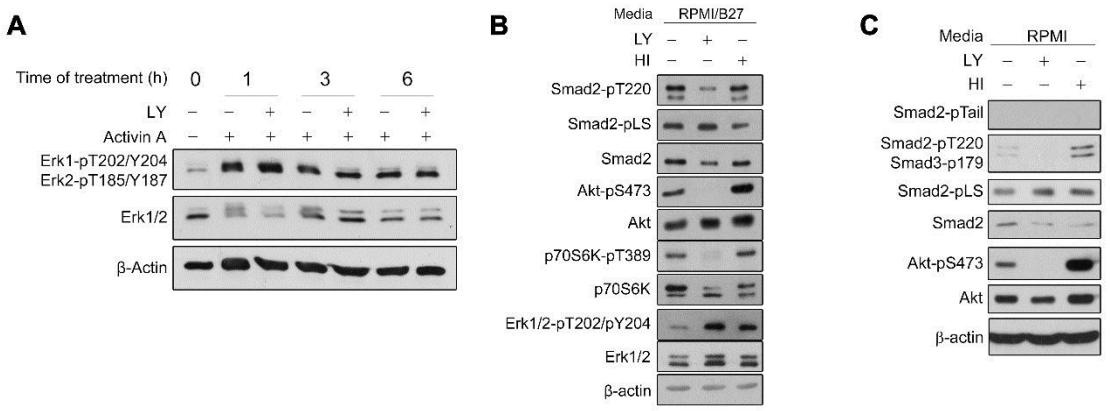

Figure 5.4: Effect of Erk1/2 to the PI3K-mediated downregulation of T220 phosphorylation

(A) hESC treated with AA/AA-LY for 1, 3, and 6 hours after which Erk activity was assessed by immunoblotting. (B) hESCs treated with RPMI/B27 alone or supplemented with LY or HI for 1 hour and assessed by immunoblotting. (C) hESCs treated as in B, but in the absence of B27 supplement and assessed by immunoblotting. All experiments repeated twice with representative image depicted.

5.2.5 Nedd4L recruitment requires both receptor-mediated activation and phosphorylation of Smad2 at the linker region

I have thus far shown that LY treatment acts to prevent the recruitment of Nedd4L to Smad2/3 via the downregulation of the T220/T179 phosphorylation and that this PI3K-mediated phosphorylation does not require the activation of Smad2/3 nor their nuclear translocation. However, given that Nedd4L is an E3 ubiquitin ligase that is primarily localised in the cytoplasm (Gao et al., 2009), immediate questions arise as to whether Nedd4L only targets active Smad2/3 for degradation and if so, how it distinguishes activated Smad2/3 from the inactive form. It is plausible that Nedd4L either possesses some inherent mechanisms to detect the activation state of Smad2/3 or that access to the binding site differs between active and inactive Smad2/3. To resolve these issues, I performed a co-IP experiment to assess the degree of Nedd4L recruitment to populations of Smad2 with different phosphorylation states on their SxS and T220 residues (Figure 5.5). PC-3 cells were chosen as the model to perform this particular experiment due to their intrinsic hyperactivation of the PI3K pathway even after starvation due to a PTEN mutation that enhances the duration of PI3K signalling via prolonging the half-life of the phosphatidylinositide mediator PtdIns(3,4,5)P_3. Thus, upon overnight starvation in base medium, the majority of the signalling pathways in PC-3 cells are repressed with the exception of PI3K,

which would result in the phosphorylation of Smad2/3 at the linker T220/T179 residue but not at the SxS motif. In these cells, AA treatment would thus result in both sites becoming phosphorylated, whereas AA-LY treatment would result in phosphorylation mainly at the SxS site alone. In comparing the three treatments in terms of their ability to recruit Nedd4L, it is notable that both maximal Nedd4L binding and ubiquitination is present only when both the linker T220/T179 and SxS residues are phosphorylated (AA treated), which is substantially reduced in cells where Smad2 phosphorylation at the T220 is reduced and SxS activation is sustained (AA-LY treated) or in cells with high T220 phosphorylation alone (starved). This suggests that T220 phosphorylation is insufficient in inducing maximal Nedd4L recruitment, merely serving to prime Smad2 for Nedd4L binding upon activation via SxS phosphorylation.

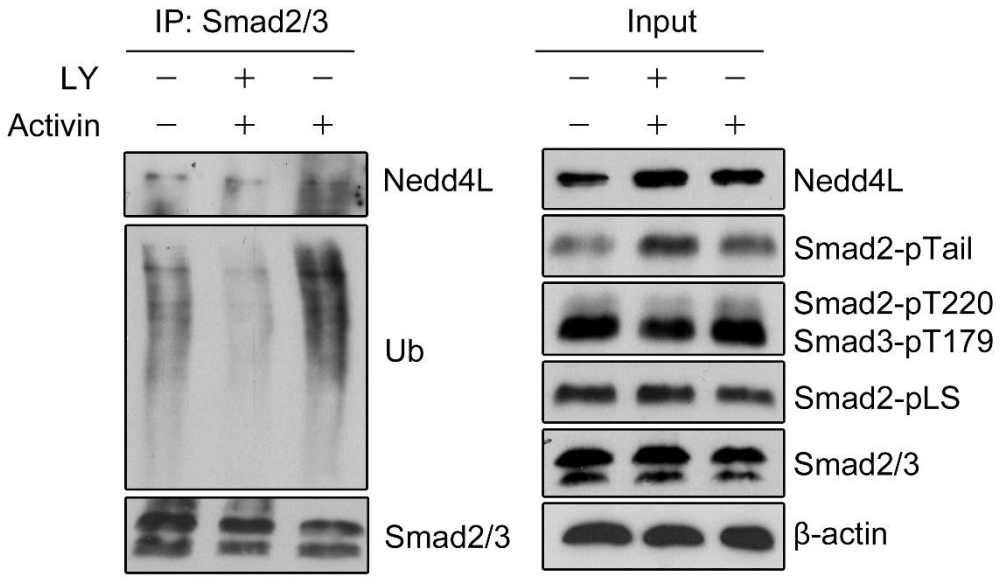

Figure 5.5: Effect of different Smad2 phosphorylation states on Nedd4L recruitment

Co-IP experiment whereby starved PC-3 cells were pre-treated for 1 hour with MG132 followed RPMI base medium alone or supplemented with AA/AA-LY for a further hour as indicated before lysates were subjected to IP with Smad2 antibody. Immunoprecipitates were assessed for Nedd4L binding and also degree of ubiquitination. Input samples were assessed by immunoblot to determine the effectiveness of the treatments in modulating the T220 and SxS phosphorylation states. Experiment was repeated twice with representative image depicted.

5.3 Discussion and Conclusions

In finding that the prolonged activation of Smad2 is attributed to a reduction in Nedd4L recruitment which is mediated by a downregulation of linker T220 phosphorylation, experiments in this chapter has comprehensively established the importance of this residue in controlling the Smad-dependent induction of DE from hESCs and has stringently corroborated the phosphorylation of this residue as a direct result of PI3K signalling. The intriguing finding that downregulation of T220 phosphorylation coincided with prolonged activation of Smad2 immediately suggested that these two events are linked and related to each other. Correspondingly, and complementary to the Nedd4L knockdown experiments in the previous chapter, ectopic expression of degradation-resistant Smad2-T220V prolonged the activation of Smad2 independent of LY, which in turn bolstered the DE induction in transgenic hESCs. Therefore, much like the downregulation of Nedd4L, reduction of T220 phosphorylation is itself sufficient in driving effective DE formation regardless of the presence of PI3K signalling. This experiment served as the acid test by which the phenotypic outcome of the proposed mechanism is verified, in that modulation of T220 phosphorylation by PI3K affects Smad2 turnover and activity, resulting in the inhibitive effects of PI3K upon AA-induced DE differentiation. This therefore concretely establishes ubiquitin-mediated proteasomal degradation as a critical mechanism in the control and termination of Smad2 activity.

Another missing link in the derivation of a complete mechanism characterising the inhibitive effects of PI3K signalling upon TGFβ activities concerns the relationship between PI3K activity and T220 phosphorylation. Given the pleiotropic properties of PI3K, I envisaged that this could be mediated via PI3K-mediated activation of various linker kinases that have been shown to regulate the phosphorylation of this residue. However, inhibition of these known linker kinases failed to recapitulate the downregulation of T220 phosphorylation to the same degree as LY treatment, implying that although they do act to regulate the phosphorylation state of this residue, none are involved in regulating Smad2 activity via the proposed mechanism. This is particularly true of CDK. Several members of the CDK family have been reported to be capable of modulating the phosphorylation of the Smad2/3 linker residues and subsequently inhibiting tis transcriptional activity (Matsuura et al., 2004; Gao et al., 2009). CDK2 and CDK4 were found to regulate the phosphorylation of the Smad3 linker at all four residues without specifically distinguishing them individually (Matsuura et al., 2004). More recently, CDK8 and CDK9 were identified as linker kinases in mediating Nedd4L recruitment via T220 phosphorylation (Gao et al., 2009). However, in my study, although flavopiridol treatment reduced the Smad2-LS phosphorylation as observed

in the original study, T220/T179 phosphorylation demonstrated either no obvious change or notably increased with prolonged treatment accompanied by a decrease in total Smad2 levels. It is unclear whether the upregulation of the T220/T179 phosphorylation is attributed to the inhibition of CDK or an effect of flavopiridol itself, however, flavopiridol treatment has been reported to upregulate the phosphorylation of Akt-S473, which is in line with my own findings detailing the involvement of the PI3K signalling pathway in mediating T220/T179 phosphorylation (Caracciolo et al., 2012). The decrease in total Smad2 is likely a result of the unforeseen inhibition of RNA polymerase II activity, which requires CDK activity for its own activation and hence induces a global downregulation of gene expression (Chao et al., 2001). Although inhibition of Erk did not fully recapitulate the effect of LY, I nonetheless persevered to assess its effects upon hESC differentiation given that PI3K has been shown to stimulate Erk activity and hence drive DE specification (Singh et al., 2012). In finding that both LY and HI treatments stimulated Erk activity without any effect on the linker phosphorylation, I comprehensively ruled out the role of PI3K-induced Erk activity in the mechanism. This was further evidenced by subsequent experiments in hESCs, in that T220 phosphorylation could only be increased by PI3K stimulation alone and further corroborated in that although the study by Singh et al. identified a LY-dependent increase in both Erk and Smad2 activation, no mechanism was proposed to explain this effect, which is likely to be in actuality a consequence of the mechanism I have currently outlined.

The role of the E3 ubiquitin ligase-mediated degradation of activated Smad2/3 in regulating TGFβ signalling has been a contentious issue with differing opinions as to whether this mechanism plays a key role in mediating TGFβ activities. Whilst there is evidence to suggest that Smad2/3-SxS dephosphorylation is a critical mechanism by which TGFβ signalling is terminated (Inman et al., 2002; Xu et al., 2002; Lin et al., 2006), a wealth of studies support the notion of E3 ubiquitin ligase-mediated Smad2/3 degradation as the primary means by which this is achieved (Lo and Massagué, 1999; Lin et al., 2000; Mavrakis et al., 2007; Gao et al., 2009). In the previous chapters, I have provided evidence to support this idea, in that LY-mediated enhancement of the duration and intensity of Smad2/3 activity is not dependent on C-terminal phosphatases, but rather dependent on Nedd4L-mediated Smad2/3 degradation, which was associated with and regulated by the phosphorylation of the Smad2/3-T220/T179 residue. In originally uncovering the role of Nedd4L in mediating Smad2/3 degradation via the T220/T179 residue, Massagué and colleagues have proposed a mechanism by which Smad2/3 activity is terminated. Upon ligand-induced activation, Smad2/3 translocates into the nucleus whereupon it becomes phosphorylated at the T220/T170 site by CDK8/9, which in turn induces the export of activated Smad2/3 back into the cytoplasm by an as of yet uncharacterised mechanism. Once in the cytoplasm, Nedd4L is recruited to

Smad2/3 by virtue of the CDK8/9-mediated phosphorylation of T220/T179, which induces the ubiquitination and subsequent proteasome-mediated degradation of Smad2/3 (Gao et al., 2009). However, in exploring the mechanisms that regulate Smad2/3 linker phosphorylation, I found that AA-induced activation of Smad2/3 was not required in sustaining their T220/T179 phosphorylation, and that CDK-mediated linker phosphorylation plays no part in regulating the LY-induced prolonging of Smad2/3 activation. This presented a new problem in that Nedd4L must therefore be able to recognise activated Smad2/3 in order to selectively degrade it over inactive forms to produce the resultant effect, given that T220/T179 phosphorylation can occur independent of AA-induced Smad2/3 activation. In finding that Nedd4L recruitment is maximal only when both T220 and SxS residues are phosphorylated, I propose a new mechanism by which Nedd4L acts to selectively distinguish activated Smad2 for degradation, which is likely to occur even prior to the nuclear translocation of activated Smad2/3. Although PI3K-dependent phosphorylation of the linker T220/T179 residue primes Smad2/3 for degradation even prior to their activation, Nedd4L binding to the PPXY motif is prevented by steric hindrance, which is resolved upon Smad2 activation via SxS phosphorylation. However, as the rate of Smad2/3 activation is likely to outpace that of its degradation, the effect is negligible under conditions whereby the total pool of Smad2/3 is maximally activated, yet this effect becomes gradually more evident with time or under low Activin conditions as an increasing proportion of activated Smad2/3 undergoes degradation (Figure 4.2B verses Figure 4.4B). In this way, Nedd4L-mediated degradation serves as an ever more potent mechanism by which activated Smad2/3 signalling activities are downregulated upon ligand exhaustion, allowing for stringent and rapid termination of Activin/Nodal signalling. This results in clear phenotypic changes with regards to DE specification in that interference with the mechanism via Nedd4L knockdown or ectopic expression of Smad2-T220V serves to enhance the AA-induced DE differentiation of hESCs, which is due to attenuated Smad2/3 signal termination.

Chapter Six

Results

PI3K-mediated mTORC2 signalling regulates the phosphorylation of Smad2/3 linker threonine

6.1 Introduction

In considering the results obtained from the previous chapter, the modulation of Smad2/3-T220/T179 linker phosphorylation appears to be more specifically associated with the PI3K pathway. This pathway contains several Ser/Thr-directed kinases of which the most characterised are the Akt and mTOR. Previous studies have shown that Smad3 activity can be modulated by Akt, a highly pleiotropic kinase downstream of PI3K that has been shown to be responsible for mediating cell growth, survival and resistance against apoptosis. More relevant to this study, Akt has also been shown to bind to and sequester Smad3 away from receptor-mediated activation and hence directly impact Smad3 activity (Conery et al., 2004; Remy et al., 2004). However, there is still significant debate as to whether this process requires Akt kinase activity, or indeed whether this binding event is even regulated by linker phosphorylation (Song et al., 2006). Furthermore, less characterised branches of the PI3K pathway such as the mTOR could also contribute to the regulation of Smad2/3 activity, particularly as inhibition of mTOR activity by rapamycin has been shown to drive DE differentiation of hESCs (Zhou et al., 2009).

The mTOR branch of PI3K signalling appeared to be a promising direction of investigation, given that in tandem with the PI3K/Akt signalling cascade, PI3K-induced activation of the mTOR activity has been shown to antagonise Smad3 activity (Song et al., 2006), whilst another study exploring the role mTOR signalling plays in hESCs has also hinted its role in regulating the maintenance of pluripotency (Zhou et al., 2009). Furthermore, the physiological roles of mTOR in controlling cell growth and survival counters many of the anti-proliferative properties attributed TGFβ signalling, which therefore suggest a role for mTOR in modulating TGFβ activities, although the molecular underpinnings remain undefined. mTOR also fulfils two distinct properties that make it a likely candidate. Firstly, mTOR kinase activity, be it as part of mTORC1 or mTORC2, has been shown to be dependent on PI3K activation (Vander Haar et al., 2007; Gan et al., 2011; Zinzalla et al., 2011), and secondly, mTOR is inherently a proline-directed Ser/Thr kinase which confers upon it the ability to possibly phosphorylate residues such as the Smad2/3-T220/T179.

To bring more clarity to these issues, experiments in this chapter attempted to identify the PI3K-dependent kinase responsible for phosphorylation of the T220 linker residue, which serves as the defining link mediating PI3K and TGFβ crosstalk. Since the activity of Akt is primarily controlled by three critical residues serving to both activate (phosphorylation of T308 and S473) and confer kinase activity (K179) to the enzyme, I decided to mutate Akt by targeting these residues individually or in combination to investigate their effects on Smad2/3-T220/T179

phosphorylation. In relation to mTOR, given that its kinase activity is dependent upon association with either of two different protein complexes, I utilised specific inhibitors to explore their involvement in regulating this phosphorylation. As with the previous linker kinase screening experiments, inhibition of mTOR should replicate the effects observed when LY or Wort treatment is applied to the cells in terms of both prolonged Smad2/3 activity and downregulation of the linker T220 phosphorylation should it be involved in this mechanism.

6.2 Results

6.2.1 PI3K-mediated phosphorylation of the T220 residue is unaffected by Akt activity

Since PI3K-mediated T220/T179 phosphorylation was shown to be independent of both Erk and CDK activity, and occurs only in the presence of HI treatment, I concluded that the identity of the linker kinase must lie within the PI3K pathway itself. Given that Akt has been shown by other studies to affect Smad3 activity (Conery et al., 2004; Remy et al., 2004; Song et al., 2006), I explored whether Akt functions to either directly regulate this phosphorylation or indirectly via a downstream kinase. To experimentally investigate this idea, I obtained constructs (Section 2.2.1.3) encoding for a constitutively active (WT), dominant negative (Tri-mut whereby K179M, T308A and S473A), and partially active (S473A) forms of Akt, which were ectopically expressed in Hep3B cells that retain a largely normal PI3K and TGFβ signalling response. Control cells that were transfected with an expression construct for GFP responded in the same manner in terms of their Smad2-T220 phosphorylation status as PC-3 and hESCs when treated with LY or HI after overnight starvation as expected. Contrastingly, expression of Akt of various activation states had no impact on the phosphorylation of this residue (Figure 6.1A). This implies that Akt activity does not affect T220 phosphorylation, which therefore also suggests that Akt does not function as a linker kinase. This was proven by an *in vitro* kinase assay in that no increase in T220 phosphorylation was detected when de-phosphorylated Smad2-WT substrate was incubated with fully active Akt as opposed to with active Erk2 (Figure 6.1B). Hence Akt does not act to regulate Smad2 activity via this mechanism.

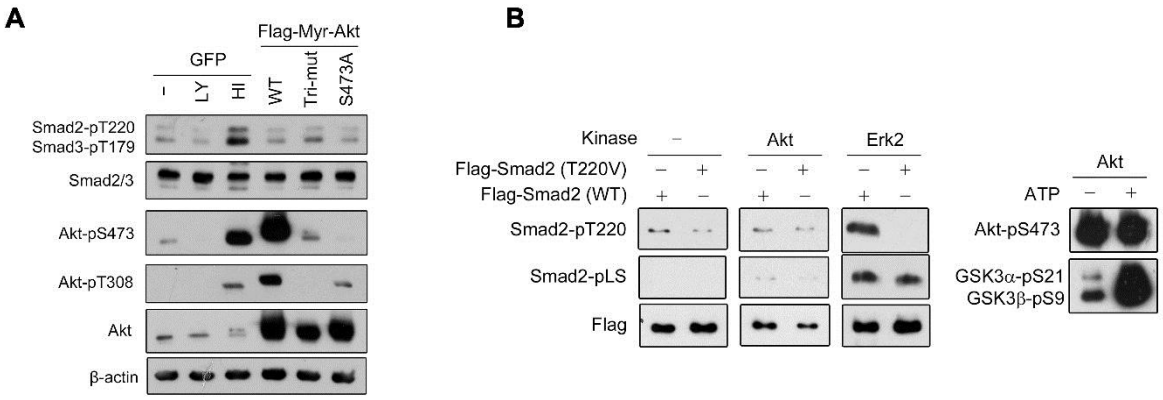

Figure 6.1: Effect of Akt to the PI3K-mediated downregulation of T220 phosphorylation

(A) Hep3B cells transfected with control GFP or Flag-Myr-Akt constructs encoding for various forms of Akt as indicated. Cells were starved overnight 24 hours post-transfection and control cells were treated for 1 hour with indicated factors. Expression and mutations were verified via immunoblotting with phospho-specific and total Akt antibodies as indicated. (B) In vitro Akt and Erk2 kinase assay. Active Akt was obtained via IP from HEK293T cells and assessed for activity via incubation with GST-GSK3 fusion protein. Reactions were supplemented with 200 μM ATP and dephosphorylated Flag-Smad2 or recombinant GST-Flag-Smad2 as substrate. Phosphorylation of T220 residue was analysed via immunoblotting. All experiments repeated twice with representative image depicted.

6.2.2 Inhibition of mTOR prolongs Smad2/3 activation and downregulation of the linker T220 phosphorylation

In order to explore the impact of mTOR activation upon Smad2/3 activity, I utilised specific inhibitors to inhibit its kinase activity. As mTOR is found within two distinct complexes I also sought to distinguish the effect of inhibiting either complex. Although specific inhibition of mTORC1 is readily accomplished by the use of rapamycin, inhibitors targeting specifically mTORC2 have yet to be developed. Therefore, to indirectly distinguish the effects of mTORC2 from mTORC1, I compared cells treated with rapamycin against Torin-2, an inhibitor that inhibits mTOR activity irrespective of which complex they reside in. PC-3 cells treated with rapamycin for 1 hour in the presence or absence of AA demonstrated no significant difference in terms of Smad2 activation or T220 phosphorylation (Figure 6.2A). Rapamycin treatment was shown to be specific in inhibiting mTORC1 alone as characterised by a reduction in the downstream P70S6K-pT421/S424 in the absence of any change to Akt-p473 phosphorylation, which is induced by mTORC2 activity. However, cells treated with Torin-2 in the presence of AA fully replicated the

effects of AA-LY treatment, exhibiting higher levels of Smad2 activation accompanied by a downregulation in T220 phosphorylation (Figure 6.2B). Both complexes were be inhibited by Torin-2 as demonstrated by the downregulation of both P70S6K-pT421/S424 and Akt-p473 phosphorylation. Given that rapamycin-mediated inhibition of mTORC1 had no significant impact upon Smad2 phosphorylation, I therefore concluded that the effect of Torin-2 upon Smad2 activity was likely to be as a consequence of interfering with mTORC2 activity.

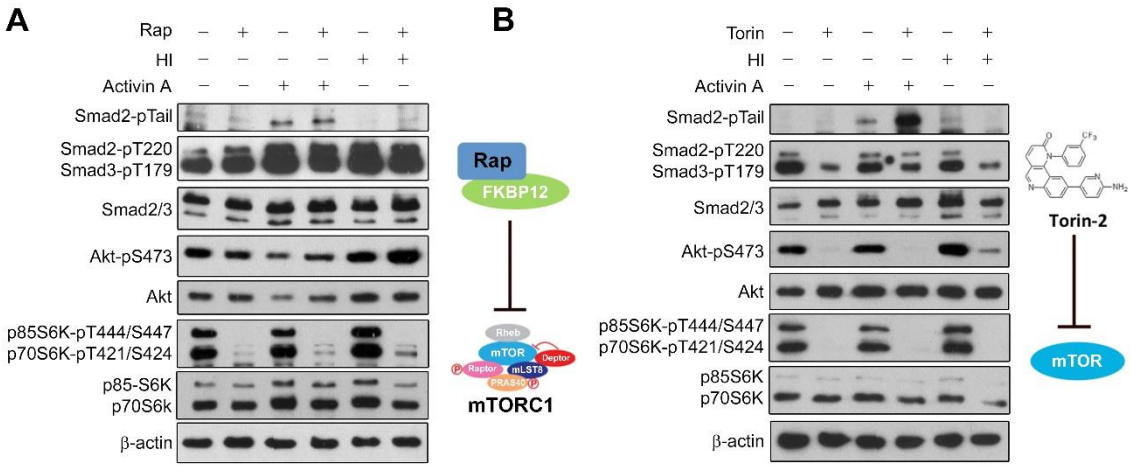

Figure 6.2: Effect of rapamycin and Torin-2 treatment on AA-induced Smad2 activation

(A) PC-3 cells were starved overnight and treated with factors as indicated for 1 hour before lysis and analysis by immunoblotting. Schematic illustrates mechanism of rapamycin-mediated inhibition of the mTORC1 complex in cooperation with the FKBP-12 immunophilin. (B) PC-3 cells were treated as in A with Torin-2 in the place of rapamycin. Schematic illustrates the Torin-2 mode of inhibition as an ATP-competitive inhibitor upon the mTOR kinase directly irrespective of which complex it is associated with. Experiments were repeated twice with representative image depicted.

6.2.3 Genetic manipulation of Rictor recapitulates the effects of Torin-2 treatment

In finding that Torin-2-mediated downregulation of mTORC2 activity appears to replicate the effects of LY-mediated inhibition of PI3K, I next asked whether this effect truly is specific to mTORC2 rather than any potential side effects upon PI3K activity, particularly due to the fact that inhibition of mTORC1 is known to induce the upregulation of PI3K due to reduced S6K activity (Trembley and Marette, 2001). Given that Rictor is an essential and specific component of the mTORC2 complex and is required for its kinase activity, I thought to address this question using spontaneously immortalised MEF cell lines derived from knockout mice in which the *Rictor* gene

was ablated, therefore solely inhibiting the mTORC2 complex by genetic means (Shiota et al., 2006). Analysis of Rictor protein expression confirmed the presence of the knockout, which did not affect the expression of mTOR and hence mTORC1 activity (Figure 6.3). Remarkably, Rictor-null MEFs also displayed a reduction in Smad2/3-T220/T179 phosphorylation much like that of Torin-2 treated cells, which therefore implicates the involvement of mTORC2 in regulating Smad2/3 activity via T220/T179 phosphorylation that is independent of mTORC1 activity. This was further supported in that transfection of a construct encoding for human Rictor rescued this phenotype by restoring the T220/T179 phosphorylation (Figure 6.3). Together, this data strongly suggests that mTORC2 may serve as the linker kinase responsible for regulating Smad2 activity via my proposed mechanism.

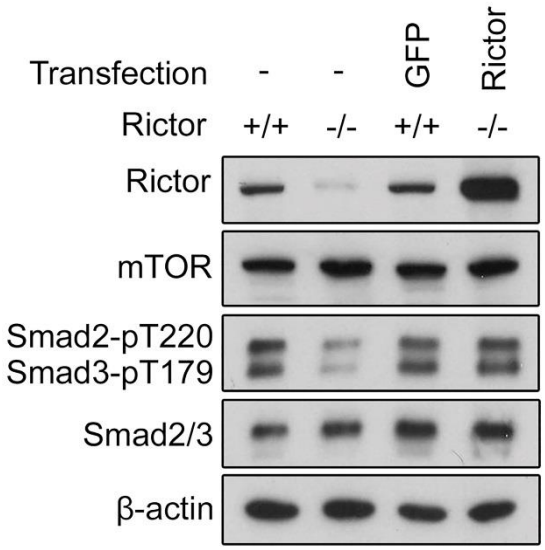

Figure 6.3: Germline knockout of *Rictor* mimics effect of Torin-2 treatment on Smad2-T220

Control and Rictor-null MEFs were cultured in D10 media. First two columns indicate comparison between control Rictor$^{+/+}$ and Rictor$^{-/-}$ MEFs as assessed by immunoblotting. Last two columns represent rescue experiment, whereby Rictor expression was restored in null cells via transfection of construct encoding for human Rictor. Control MEFs were transfected with PINCO-CMV-EGFP-PURO construct as transfection control. Experiment was repeated twice with representative image depicted.

6.2.4 mTORC2 does not function as the direct kinase acting upon the Smad2-T220 residue

Since both Torin-2 treatment and germline knockout of Rictor implicated mTORC2 in regulating the activity and degradation of Smad2, I assessed whether mTORC2 served as the direct kinase regulating T220 phosphorylation. To achieve this, I performed an *in vitro* kinase assay utilising Rictor-immunoprecipitated active mTORC2 isolated from HEK293T cells and incubated with dephosphorylated Flag-Smad2 substrate as per the Akt/Erk2 kinase assay. However, mTORC2 was unable to phosphorylate the T220 residue despite being able to phosphorylate the S473 residue of Akt (Figure 6.4). Thus, it appears that mTORC2 does not serve to directly phosphorylate Smad2 at the T220 residue, and may function to regulate another novel linker kinase that performs this function.

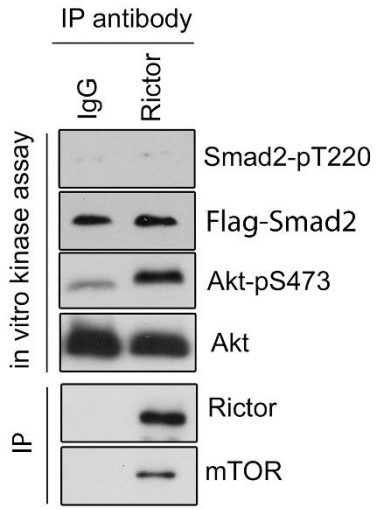

Figure 6.4: mTORC2 *in vitro* kinase assay with Flag-Smad2 substrate

Active mTORC2 was immunoprecipitated using Rictor antibody and assessed for activity using dephosphorylated His-Akt substrate, which was assessed for S473 phosphorylation upon incubation with immunoprecipitates. Non-specific rabbit IgG was used as control for both IP and kinase assay. 400 μM ATP was used to overcome the low affinity of mTOR for ATP. Experiment was repeated twice with representative image depicted.

6.2.5 shRNA-mediated Rictor knockdown enhances DE induction in hESCs

Although mTORC2 does not function as the direct kinase responsible for modulating Smad2-T220 phosphorylation, germline deficiency and Torin-2 treatment nonetheless showed that mTORC2 activity is at the very least, required in inducing the PI3K/mTOR-dependent inhibition of Smad2/3 activation via T220/T179 phosphorylation. Therefore, I conducted experiments to verify whether deficiency of Rictor can directly affect the differentiation of hESCs to DE and thereby recapitulate the phenotypic effects of AA-LY treatment. Efficiency of shRNA-mediated knockdown of Rictor was verified in PC-3 cells, characterised by the reduction in Rictor protein in addition to the downregulation of Akt-pS473 phosphorylation (Figure 6.5A). Notably, Smad2/3-T220/T179 was also observed to be downregulated, albeit not to the same extent as with LY or Torin treatment. Nevertheless, utilising the same lentivirus to infect and knockdown Rictor in hESCs, I was able to obtain transgenic hESC line deficient in mTORC2 activity. Morphologically, these cells resemble parental hESCs albeit the rate of proliferation was reduced, which is similar to that observed in Rictor-null MEFs. Subsequent differentiation of these shRictor-hESCs with AA produced morphological changes that are reminiscent of both AA-LY and AA-Torin treatment when compared to control cells (Figure 6.5B). Improved differentiation of shRictor-hESCs towards the DE was subsequently confirmed via gene expression analysis, which revealed an increased expression of the majority of mesendoderm and endoderm markers, not too dissimilar what was observed in the differentiation of shNedd4L-hESCs (Figure 6.5C). Overall, these results demonstrate that genetic ablation of mTORC2 activity via Rictor knockdown sufficiently recapitulated all the phenotypic changes associated with improved DE specification that was observed in previous treatments.

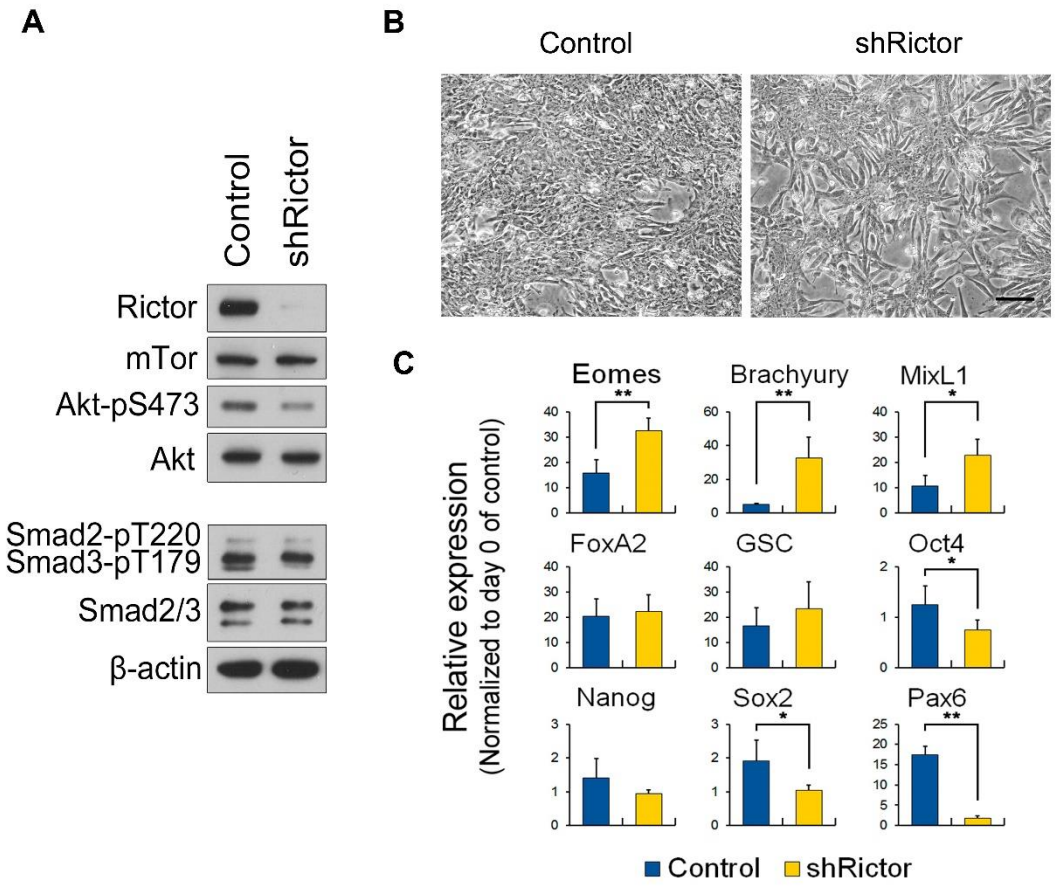

Figure 6.5: Effect of shRNA-mediated Rictor knockdown on DE specification

*(A) PC-3 cells were infected with lentivirus harbouring two different shRNA sequences that target the Rictor mRNA. After selection and establishment of stable lines, cells were lysed and subjected to immunoblotting to verify Rictor knockdown, mTORC2 activity and Smad2/3-T220/T179 phosphorylation. (B) Phase contrast images of transgenic hESCs infected with the same virus as in A, before being subjected to AA-induced DE differentiation for 1 day. Control indicates cells which have been transduced with non-targeting shRNA against GFP. Experiment was repeated twice with representative image depicted. (C) Gene expression analysis was performed on cells from B which have been differentiated for 2 days in order to assess the efficacy of DE induction. Graphs illustrate relative expression normalised to transgenic hESCs cultured in MEF-CM. Data represents average of two independent experiment in which PCR reactions were performed in triplicate (n=6). Error bars indicate SD. * and ** indicates $p<0.05$ and $p<0.001$ by Student's t test respectively.*

6.2.6 AA-induced DE and hepatocyte differentiation occurs more effectively in the presence of Torin-2 when compared with LY

Given that Torin-2 treatment was able to recapitulate the effects of LY in promoting Smad2/3 activation via the downregulation of T220/T179 phosphorylation, and that shRictor-hESCs appeared to differentiate towards the DE with greater robustness than control hESCs, I next investigated whether Torin-mediated inhibition of mTORC2 activity induces a better overall differentiation when compared to LY treatment. As with AA-LY treatment, AA-Torin treatment resulted in increased expression of both mesendoderm and endoderm markers when compared with AA alone (Figure 6.6A). Additionally, AA-Torin induced DE cells expressed Sox17 and FoxA2 to a greater extent when compared to AA-LY cells, which therefore further indicates a more robust differentiation as evidence by Rictor knockdown (Figure 6.6B). Notably, the DE induction process additionally benefitted from a reduction in cytotoxic-induced cell death, increasing the yield of DE cells from the original hESC culture. Furthermore, AA-Torin differentiated DE were fully competent in forming both hepatoblast and hepatocyte-like cells upon further differentiation and maturation (Figure 6.6C). Overall, this indicates that direct inhibition of mTORC2 with Torin-2 mitigates the cytotoxic effects of PI3K inhibition, which consequently results in a more robust and effective DE specification.

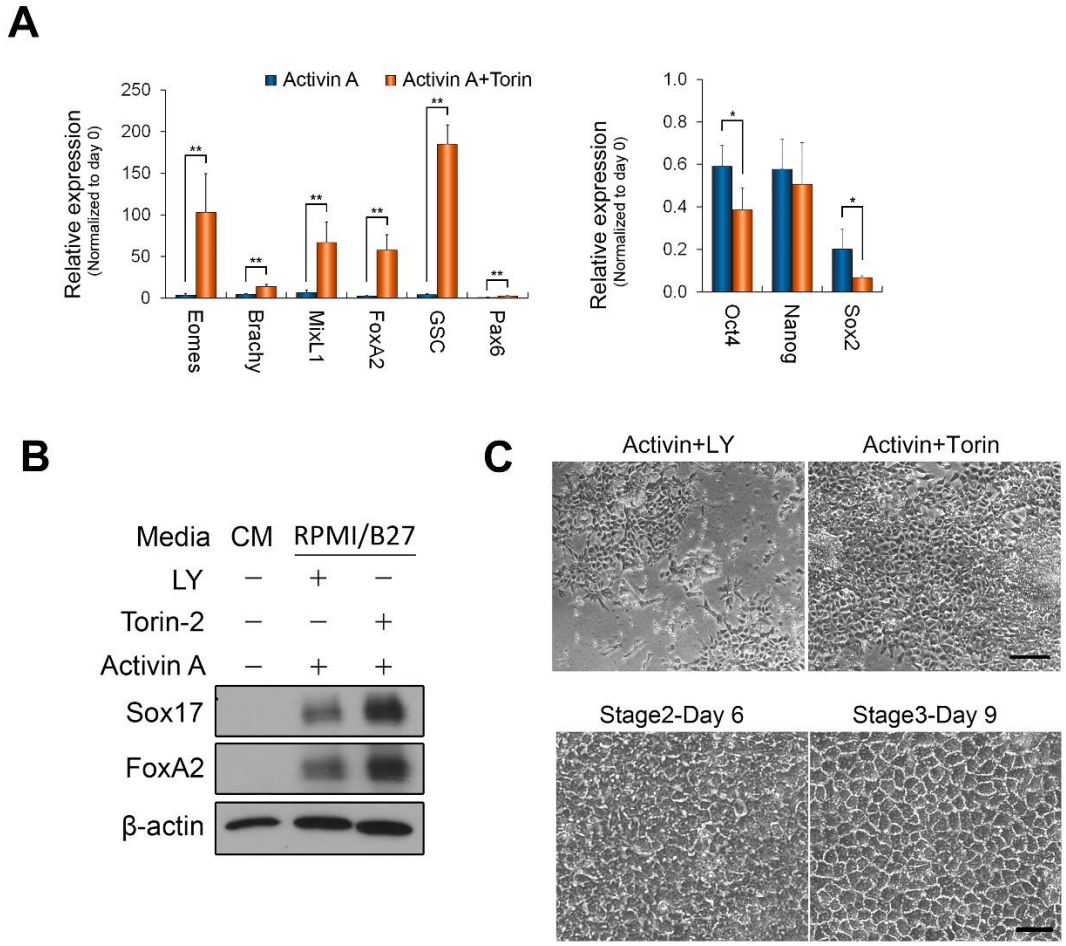

Figure 6.6: Effect of AA-Torin treatment on DE and hepatic induction

*(A) hESCs were subjected to AA or AA-Torin induced DE differentiation for 2 days. Gene expression analysis was performed to assess the efficacy of DE induction. Graphs illustrate relative expression normalised to transgenic hESCs cultured in MEF-CM. Data represents average of two independent experiment in which PCR reactions were performed in triplicate (n=6). Error bars indicate SD. * and ** indicates $p<0.05$ and $p<0.001$ by Student's t test respectively. (B) Expression of DE markers Sox17 and FoxA2 in hESCs differentiated with either AA-LY or AA-Torin was assessed by immunoblotting. Experiment was repeated twice with representative image depicted. (C) Phase contrast depicting the difference in cytotoxic-induced cell death between AA-LY and AA-Torin treated cells (top panels). AA-Torin treated cells were subsequently able to progress through Stage II and III of hepatocyte specification (bottom panels). Scale bar indicates 50 μm.*

6.3 Discussion and Conclusions

Given that both CDK and Erk activity was previously discounted to be involved in modulating Smad2/3-T220/T179 phosphorylation, and that the PI3K pathway appeared to play a more direct role in regulating this phosphorylation, my attention next turned to Akt, the principal kinase functioning downstream of PI3K that has been shown to mediate Smad3 activity via a sequestration mechanism via its phosphorylated form (Conery et al., 2004; Remy et al., 2004) or through its kinase activity (Song et al., 2006). However, my experiments using various forms of Akt indicate that neither phosphorylated Akt nor its kinase activity has any impact on Smad2/3-T220/T179 phosphorylation and hence does not serve as a linker kinase targeting Smad2/3. Additionally, as indicated by mutagenesis studies, regulation of Smad2/3 activity via the proposed mechanism does not appear to be dependent on Akt activity at any level, which therefore implies that PI3K-mediated phosphorylation of Smad2/3-T220/T179 does not occur via Akt, or via any downstream kinase whose activity is regulated by Akt. However, it is likely that the Smad2/3 sequestration by Akt functions as a distinct mechanism which Smad regulates activity although it does not appear to play a role in regualting Smad2/3 activity in this instance.

Whilst previous studies have hinted at the involvement of mTOR activity in regulating TGFβ-induced functions via the regulation of Smad activity, no study has thus far been able to propose a mechanism that fully accounts for this effect (Song et al., 2006; Zhou et al., 2009). In treating PC-3 cells with AA in the presence of rapamycin or Torin-2, I have shown that this effect is likely to be mediated via an mTORC2 dependent mechanism. Although the study by Zhou et al. showed that rapamycin treatment does induce the loss of pluripotency and the induction of DE, prolonged exposure to rapamycin has been shown to ultimately inhibit mTORC2 via the sequestration of mTOR by rapamycin-inactivated mTORC1 complexes (Lamming et al., 2012). Therefore, the phenotypic changes observed upon long term rapamycin treatment is likely due to the inhibition of mTORC2 rather than the acute inhibition of mTORC1. Involvement of mTORC2 in my proposed mechanism is also supported genetic manipulation in that both germline knockout and shRNA-mediated knockdown of Rictor, a critical component of the active mTORC2, reduced the phosphorylation of Smad2 at the T220 residue, as previously observed with LY, Wort and Torin-2 treatment. This effect was fully rescued upon the re-introduction of human Rictor into Rictor-null MEFs, which additionally suggests that this mechanism is likely to also exist in other mammalian models. These experiments also additionally corroborated the indirect evidence from Torin-2 treated cells which suggested that mTORC2 was the principle culprit responsible for this effect. Although shRNA-mediated knockdown of Rictor did not reduce the Smad2/3-T220/T179

phosphorylation to the same degree as germline knockout or Torin treatment, residual mTORC2 activity may well be sufficient in maintaining the phosphorylation of this residue given its inherent sensitivity to PI3K stimulation (Figure 5.4B vs 5.4C). However, in spite of mTORC2 fulfilling most of the criteria necessary for a Smad2/3 linker kinase, the subsequent kinase assay showed that immunoprecipitated mTORC2 did not phosphorylate Smad2 at the T220 residue. Nonetheless, the mechanism by which mTORC2 acts as a kinase has been shown to be quite diverse, and may rely on other components or conditions that are not necessarily present in our reactions. For example, one study have reported that the ribosome is required for full activation of mTORC2 activity (Zinzalla et al., 2011), whilst two other studies demonstrate a mechanism by which mTORC2 phosphorylates its target substrate in a co-translational manner as the protein is still being synthesised at the ribosome (Oh et al., 2010; Dai et al., 2013).

Although mTORC2 does not appear to be the linker kinase responsible for T220/T179 phosphorylation, mTORC2 activity is nonetheless required for this phosphorylation to occur. As indicated in my experiments, absence of Rictor results in the downregulation of T220/T179 phosphorylation even in the presence of serum and high PI3K activity. Therefore, the original effect of PI3K-dependent inhibition of Smad2/3 activity is highly likely to be as a result of PI3K-dependent activation of mTORC2. This is particularly evident when comparing AA-LY treatment to that of AA-Torin, in that AA-Torin can fully replicate the DE inducing effects of AA-LY. In many respects, the effect of AA-Torin is superior to that of AA-LY in terms of reducing the cytotoxic-associated cells death and increasing the expression of *bona fide* DE markers such as Sox17 and FoxA2. The added effect of these enhancements culminates in the increased yield of hepatocyte-like cells from the initial DE population, which are likely to be improved on a functional level. Thus, I have uncovered a distinct and direct mechanism by which mTORC2 activity directly acts to inhibit the duration of Smad2 activation via modulating the T220/T179 linker phosphorylation. This in turn regulates the recruitment of Nedd4L, which serves to selectively target activated Smad2 for degradation. Through this proposed model, PI3K/mTOR signalling thereby directly impacts the DE specifying activities of AA, and hence offers a convincing explanation as to why high levels of PI3K/mTOR stimulation can act to antagonise the derivation of DE from hESCs.

Chapter Seven

General Discussion

7.1 Direct impact of PI3K signalling on Smad2/3 activity via regulation of Smad2/3 degradation

Ever since the discovery of the antagonistic action of PI3K signalling upon the induction of DE from hESCs, many studies have tried to uncover and propose a molecular overview for this relationship. However, this work has proven challenging, confounded by the unique difficulties associated with hESC culture including interference from other signalling inputs and reciprocal regulative mechanisms between branches within the PI3K pathway. The work presented here marks the culmination of these effort, and represents the most complete molecular description of the critical interplay occurring between these two signalling pathways in the derivation of DE. In exploring the relationship between PI3K and Smad2/3 activation utilising our fully defined differentiation protocol, I initially found that PI3K signalling directly impacts the duration of Smad2/3 activation, in that the higher the level of PI3K activation, the greater the suppression of endogenous Smad2/3 phosphorylation at the SxS motif. This result correlated well with studies that previously identified the negative impact of PI3K signalling upon DE differentiation (D'Amour et al., 2005; McLean et al., 2007) and offered the first molecular insights into how this antagonism occurs. Specifically, the duration of Smad2/3 activation is attenuated in the presence of PI3K signalling, which is mitigated during AA-LY or AA-Wort-mediated DE derivation where PI3K activity is robustly suppressed. As demonstrated by luciferase assay, this prolonged activation of Smad2/3 results in the upregulation of their transcriptional efficacy, ultimately leading to the increased expression of known Smad2/3 target genes such as MixL1, Eomes and GSC that drive the differentiation of hESCs to DE (Teo et al., 2011).

In demonstrating the direct involvement of PI3K in regulating TGFβ activities, the next question was how this enhanced activation of Smad2/3 occurs on the molecular level. Although other studies have also observed that AA-LY induction of DE is accompanied by increased Smad2/3 activation (Singh et al., 2012), no mechanism was proposed to explain this effect. Given the dynamism of phosphorylation and the fact that Smad2/3 activity is stoichiometrically dependent on the degree of Smad2/3-SxS phosphorylation (Inman et al., 2002), it was anticipated that the LY-mediated inhibition of PI3K served to affect the regulation of Smad2 at this site. However, the fact that LY-treated and untreated cells exhibited similar levels of Smad2/3 activation and that inhibition of Activin type I receptors did not alter the outcome of LY treatment suggests that the effect of PI3K on TGFβ is likely to be attributed to its role in sustaining Smad2/3 activation rather than increasing levels of initial stimulation. Further experiments exploring the regulation of Smad2/3-SxS phosphorylation served to discount the involvement of PPM1A, CLIC4 and PP5,

which have all been previously reported to regulate Smad2 SxS phosphorylation or TGFβ activity (Lin et al., 2006; Shukla et al., 2009; Bruce et al., 2012). The case of PPM1A is especially notable, given that despite being shown to be a *bona fide* Smad2/3 phosphatase, its preferentially cytoplasmic localisation along with promiscuity in targeting cytoplasmic targets counters this argument (Yoshizaki et al., 2004; Strovel et al., 2000; Bruce et al., 2012). Contrastingly, in finding that the decay kinetics of Smad2 in LY treated cells strongly mimicked that of MG132 treated cells, this suggested that the effect of LY in prolonging Smad2 activation was likely due to the inhibition of its ubiquitin-mediated proteasomal degradation. Indeed, Activin-induced activated Smad2/3 exhibited a considerably reduced ubiquitination in the presence of LY.

In the last decade, several studies have attempted to explore the mechanisms underpinning the negative effects of PI3K signalling on TGFβ induced apoptosis in cancer cells (Conery et al., 2004; Remy et al., 2004; Song et al., 2006), although the vast majority of mechanisms proposed rely heavily on the direct interaction between Akt and Smad2/3. Despite there being ample evidence for this interaction, the regulative mechanisms mediating Smad2/3 to Akt recruitment are still currently ill-defined, casting doubt as to the general applicability of this model, particularly in the context of normal cell homeostasis and development. Furthermore, this passive mechanism does not explain the other facet of TGFβ signalling in promoting tumourigenic responses at the later stages of cancer progression, and given the fact that both pathways are often simultaneously activated in certain cancers (Hanahan and Weinberg, 2013), lends further weight to the idea of active crosstalk mechanisms modulating the tumourigenic effects of both pathways. Thus, in finding that PI3K signalling can act to directly modulate the degradation of activated Smad2/3, and therefore, is implicitly involved in the regulation of TGFβ activities, this study has opened new avenues for exploring whether such a mechanism influences tumourigenesis and cancer progression.

7.2 PI3K-mediated regulation of Nedd4L recruitment

It has been long proposed that the proteasomal degradation of the active Smad complexes serves as an important mechanism that facilitates the termination of Smad2/3 activities (Lo and Massagué, 1999). However, the identity of these E3 ubiquitin ligases acting upon Smad2/3 has only recently come to light. Notably, several different classes of ubiquitin ligases have been shown to mark Smad2/3 for degradation, including the HECT class Smurf2 and Nedd4L as well as the RING class Arkadia (Lin et al, 2000; Mavrakis et al., 2007; Gao at al 2009). However, given that

these ligases are ubiquitously expressed, questions were raised as to how these ligases identify and specifically target activated Smad2/3 for turnover. Furthermore, what role does PI3K signalling play in mediating this process, especially with regards to the most characterised Smad E3 ligase, Nedd4L in this context?

The HECT class Nedd4L E3 ubiquitin ligase served as an attractive proposition in mediating the PI3K-mediated turnover of activated Smad2/3. In comparison to other reported ligases, its mode of action is well defined in that Nedd4L recruitment is modulated by the phosphorylation status of the linker T220/T179 residue (Gao et al., 2009). Given that the linker region serves as an important site for inter-pathway crosstalk, this immediately suggested a mechanism by which PI3K activity can directly influence Smad2/3 activity. Remarkably, PI3K/mTOR signalling is capable of modulating the phosphorylation of T220/T179 independent of Smad2/3 activation. Given that T220/T179 is necessary for the recruitment of Nedd4L to Smad2/3 and that Nedd4L is a cytoplasmic localised E3 ubiquitin ligase, this raised a new question as to how Nedd4L selectively targets active Smad2/3 for degradation. In addressing these issues, I found that the recruitment of Nedd4L to Smad2 is not solely dependent on T220 phosphorylation, but also dependent on its activation state. Additionally, even upon the slightest activation of PI3K/mTOR signalling, the Smad2-T220 residue is rapidly phosphorylated regardless presence or absence of AA ligand. This, coupled with the previous notion, suggests that inactive Smad2/3 is already poised for Nedd4L recruitment, which occurs immediately following activation. It is likely that the conformational changes associated with activation increases the accessibility of Nedd4L to the Smad2/3 linker region, hence promoting its degradation. However, it is difficult to reconcile this notion with a certain discrepancy in that if active Smad2 is immediately subject to turnover even before reaching the nucleus, how does any Smad2/3 related upregulation of genes occur? It has been previously well documented that the conformational changes of Smad2/3 associated with its activation enables the formation of trimeric complexes with themselves as well as with Smad4, and that only a small proportion of active Smad2/3 actually are degraded by the ubiquitin-proteasomal system (Section 1.3.1.3). Therefore, it remains to be further elucidated whether the interactions between the Smad2/3 and Smad4 or other factors act to impede the recruitment of Nedd4L to activated Smad2/3, which results in the majority of activated Smad2/3 forming trimeric complexes and translocating into the nucleus. It is probable that in the presence of abundant ligand and persistent receptor activation, the rate of Smad2/3 activation outpaces that of its Nedd4L-mediated degradation. Thus, LY treatment does not result any obvious effect on Smad2/3 activation at 1 hour post 100 ng/ml AA treatment. The biological significance of this mechanism is only evident when activation of the receptor complexes becomes reduced due to ligand scarcity. As receptor

activation decreases, the proportion of the activated Smad2/3 becomes targeted for Nedd4L-mediated degradation becomes relatively high, which in turn promotes the rapid downregulation of all Smad2/3 related activities. This is also the likely reason why AA-LY mediated preservation of Smad2/3 activation is only observed 3-6 hours into the differentiation process, or when receptor complexes are inhibited. Experiments demonstrating that mutation of Smad2-T220 to a non-phosphorylatable residue abolished the binding of Nedd4L to Smad2 coupled with the fact that this mutation and Nedd4L knockdown both served to diminish the effect of LY on Activin-Smad2/3 signalling and DE differentiation provides further evidence in support of the proposed mechanism. Therefore, Nedd4L-mediated turnover of activated Smad2/3 is a self-propelling mechanism that promotes the rapid termination of TGFβ activities upon the reduction of ligand availability, which in the context of development, is likely to enhance the stringency of differentiation.

7.3 mTORC2: A new player in PI3K/mTOR and TGFβ crosstalk

One important finding in my study is the identification of mTORC2 signalling as a modulator for TGFβ signalling, specifically by regulating the phosphorylation of Smad2/3 linker threonine residue. In assessing the contribution of the most prominent of the previously identified linker kinases, Erk1/2 and CDK, I found that inhibition of either kinase could not replicate the effects observed when PI3K was inhibited by LY. Furthermore, LY-mediated inhibition of PI3K under certain conditions served to enhance the activation of Erk1/2, although no significant effects were observed in terms of Smad2/3-T220/T179 phosphorylation. As such, enhancement of DE differentiation via downregulation of the phosphorylation of this residue and degradation of activated Smad2/3 does not appear to be through an Erk/Wnt/β-catenin-mediated mechanism as outlined in a recent study (Singh et al., 2012), and is therefore a more distinct and direct mechanism.

The finding that none of the prominent linker kinases appeared to play any part in the LY-mediated enhancement of DE differentiation suggests that the presence of a linker kinase along the PI3K signalling axis itself. Subsequent experimentation revealed that although Akt has been reported to bind to and prevent the activation of Smad3 (Conery et al., 2004; Remy et al 2004), ectopic expression of constitutively active Akt does not appear to affect T220/T179 phosphorylation. Furthermore, Akt activity itself appears to be dispensable in mediating the PI3K-dependent downregulation of Smad2/3-T220/T179 phosphorylation via the proposed mechanism, as shown

via mutagenesis studies and also by *in vitro* kinase assay. The inability of Akt to inhibit the activation of Smad2/3 via downregulation of T220/T179 phosphorylation alluded to the presence of a kinase whose function is independent of Akt, yet dependent on PI3K.

Of the numerous kinases forming the core of the PI3K pathway, the two mTOR complexes served as prime candidates in fulfilling this role. Moreover, since mTORC1 and mTORC2 are regulated down and upstream of Akt respectively, mTORC2 served as the more promising candidate given that modulation of Akt activity was previously shown to have no effect on T220/T179 phosphorylation. Although several studies have alluded to the role of mTORC1 in inhibiting Smad2 activation (Song et al., 2006; Zhou et al., 2009), these studies were highly dependent on the use of rapamycin, an mTORC1 inhibitor that has also been recently shown to inhibit the activity of mTORC2 upon chronic exposure (Lamming et al., 2012). Therefore, in comparing the effects of rapamycin-mediated inhibition of mTORC1 with the Torin-2-mediated inhibition of both complexes, I was able to also assess the effect of mTORC2 inhibition upon Smad2/3 activity albeit indirectly. The ability of Torin-2 rather than rapamycin in completely recapitulating the effects of LY treatment strongly hinted to the involvement of mTORC2 in my mechanism, which was ultimately confirmed via the gain and loss-of-function of Rictor, a key component of the mTORC2 complex. Taken together, this clearly demonstrates an important role for mTORC2 in the modulation of Smad2/3 linker threonine phosphorylation. Although, mTORC2 does not appear to function as the direct kinase responsible for modulating the phosphorylation of the T220 residue as per *in vitro* kinase assay, the probability of this occurring through novel mechanisms that cannot be detected via the standard assay cannot be fully discounted, (Oh et al., 2010; Zinzalla et al., 2011; Dai et al., 2013). Nevertheless, my experiments have established a previously unreported role for mTORC2 in the regulation of Smad2 activity, and additionally, outlines a detailed mechanistic description of the molecular events responsible for the antagonistic effects of PI3K/mTOR signalling upon TGFβ activities as summarised in Figure 7.1.

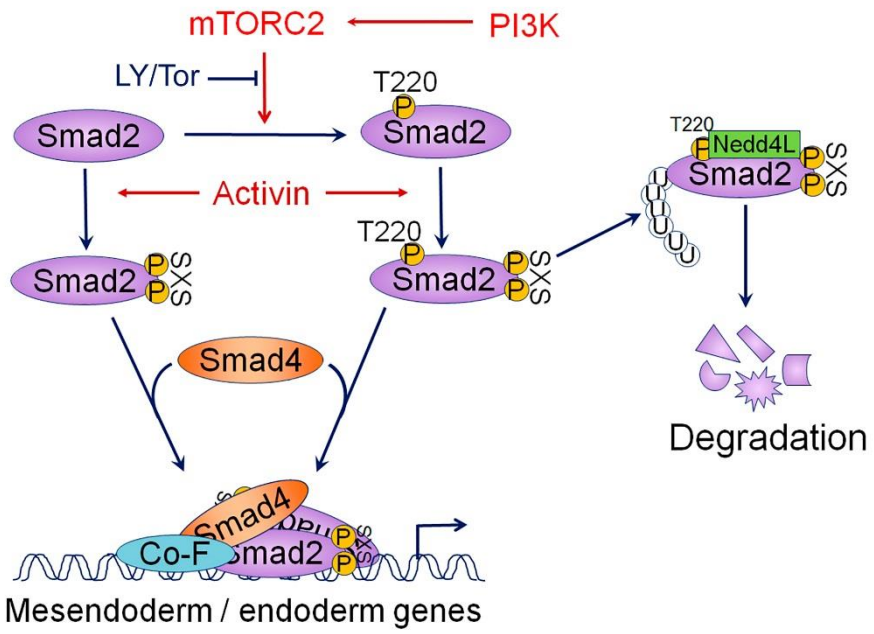

Figure 7.1: Molecular mechanisms governing the inhibition of Smad2 activity via PI3K/mTORC2

PI3K induces the activation of mTORC2 kinase that in turn promotes the phosphorylation of Smad2 at the T220 residue. This is mitigated in the presence of LY or Torin-2 (Tor). T220 phosphorylation primes Smad2 for Nedd4L binding upon activation by Activin, initiating the polyubiquitination and degradation of Smad2. Regardless of whether the T220 is phosphorylated, activated Smad2 translocates into the nucleus upon Smad4 binding, inducing the expression of mesendoderm and endoderm genes.

7.4 Future work

Whilst my current work describes a previously unknown mechanism through which mTORC2 regulates Smad2/3 activity, several questions remain open for further interrogation. Firstly, an immediate question is raised as to how activated Smad2/3 successfully evades degradation in spite of enhanced Nedd4L mediated degradation. In keeping with the fact that cofactor recruitment can drastically alter the protein conformation and thereby accessibility of activated Smad2/3 to Nedd4L, I postulate that homo- and heterodimerisation of activated Smad2/3 as well as the recruitment of Smad4 may establish a complex that is resistant to Nedd4L binding and hence degradation. Equally, Nedd4L itself may also be subject to regulative mechanisms via the PI3K pathway that may additionally influence its binding affinity to activated Smad2/3 (Gao et al., 2009). Therefore, the degree to which PI3K/mTOR signalling concurrently influences Smad2/3 and Nedd4L activity serves as a notable aveneue for further study. Indeed, both of these hypotheses

can be addressed through the ectopic expression of Smad2/3 or Nedd4L truncation mutants, which will provide the first experimental evidence to establish a definitive answer.

Another interesting question which arose from this study relates to the importance of the linker residues in mediating Smad2/3 activity in a more general sense. Whilst this study has clearly demonstrated the impact of mTORC2 activity upon Smad2/3 linker phosphorylation at the T220/T179 residue, it remains whether mTOR activity also influences the phosphorylation status of the other linker residues. This is particularly important given that phosphorylation of the other linker residues plays a critical role in regulating the timing and competency of Smad2/3 activity during the *Xenopus* development (Grimm and Gurdon, 2002), which thusfar has yet to be demonstrated in a mammalian model. Equally, owing to the difficulties in performing Smad2/3 knockout experiments without compromising hESC pluripotency, experiments conducted in this study has always utilised the ectopic expression of Smad2 mutants amongst a background of endogenous Smad2 to investigate the effects of linker mutation, which may mask more subtle phenotypic effects. With the recent emergence of genome editing technologies such as transcription activator-like effector nucleases (TALENs) and clustered regularly interspaced short palindromic repeat (CRISPR)-Cas (CRISPR-associated nucleases), the technology is now in place to generate mutations directly on endogenous Smad2/3 genes without the need for ectopic expression. Utilising such methods to generate endogenous phospho-deficient or phospho-mimetic linker mutants of Smad2/3 represent the definitive method by which to establish their importance in regulating Smad2/3 activities, allowing interrogation in the absence of endogenous wild-type intereference. In addition, such powerful editing methods also provides a relatively easy method to generate mice that harbour Smad2/3 linker mutations, hence allowing the interrogation of their phenotypic effects throughout the course of development. This can be further utilised to investigate tissue-specific effects aside from endoderm derived lineages.

7.5 Implications on development and disease

Inter-pathway crosstalk represents an important mechanism by which the downstream activities of each pathway are regulated. In considering these two pathways, the differentiation promoting and apoptotic inducing properties of TGFβ/Smad signalling are directly countered by the pluripotency promoting and pro-survival activities of PI3K. As outlined above, I propose a mechanism by which PI3K/mTOR acts to directly modulate the activity of Smad2/3 via regulation of the linker T220/T179 phosphorylation, which in turn regulates the resistance of activated Smad2/3 to Nedd4L-mediated degradation. Utilising genetic manipulation, I have verified several aspects of the mechanism that lends weight to its existence in an *in vivo* setting. Specifically, Nedd4L

knockdown, ectopic Smad2-T220V expression and Rictor knockdown serve to enhance the formation of DE from hESCs, whilst the rescue of Rictor-null MEFs with ectopic expression of human Rictor was sufficient in restoring the phosphorylation of the T220 residue and by extension, the antagonistic properties of PI3K/mTOR upon Smad2 activation. Equally, these experiments can be cross-referenced with inhibitor and growth factor supplementation studies. Treatment of hESCs with AA in the presence of PI3K (LY/Wort) and mTORC2 (Torin-2) inhibitors markedly increased the efficiency of DE formation, whilst treatment with activators of PI3K (serum/Her/IGF-1) increased T220 phosphorylation, which in turn promoted Smad2 degradation and decreased the effectiveness of AA-induced DE specification. In fact, AA-Torin appears to be far superior in promoting the formation of DE over AA-LY treatment, further testament to the improved understanding of the mechanisms behind PI3K-mediated inhibition of AA-induced DE differentiation gained during this study.

The fact that these findings appear to be applicable to PC-3, Hep3B, MEFs and hESCs lends further weight to the general applicability of this mechanism, functioning to regulate TGFβ activities in tumour, mouse and human cell lines. In relation to tumourigenesis, since stimulation of mTORC2 activity intrinsically acts to antagonise the activities of Smad2/3, drugs that specifically target to inhibit mTORC2 activity could effectively enhance the pro-apoptotic properties of TGFβ signalling without drastically affecting the pro-survival properties of the rest of the PI3K cascade. However, it is important to note that any drug developed must not illicit any inhibition upon the mTORC1 complex, which has been shown to induce hyperactivation of the PI3K/Akt signalling cascade via a S6K-mediated feedback loop (Section 1.3.3.3). This becomes evidently more important when considering the biphasic action of TGFβ in initially suppressing tumour growth at early stage, yet enhancing tumour metastasis at the latter stages. Whilst downregulation of mTORC2 activity at an early stage could serve to mitigate tumour progression by reinforcing the pro-apoptotic activities of TGFβ signalling, induction of mTORC2 activity could equally serve to inhibit the pro-tumourigenic properties of TGFβ induction. For example, in the case of bulk tumours, poor vascularisation and hypoxic nature of the tumour core is thought to enhance the emergence of metastatic tumour cells via EMT, which is a TGFβ-induced process. Therefore, the delivery of drugs or factors which enhance mTORC2 activity in this situation may serve to be beneficial by stimulating the downregulation of Smad2/3 activation, and the hence inhibition of EMT. However, given that both mTOR complexes share the same kinase component, development of mTORC2-specific inhibitors is currently a rather daunting yet challenging prospect. Nonetheless, this work outlines and proposes an elegant crosstalk mechanism that occurs between PI3K/mTOR and TGFβ/Activin pathways, which has a direct

impact on Activin-induced DE differentiation and possibly other TGFβ functions such as TGFβ-induced tumourigenesis. The identification of mTORC2 as a key player in the regulation of this differentiation provides new avenues through which hESC differentiation protocols can be improved for both regenerative and biomedical applications, adding yet another novel function to the growing mTORC2 repertoire. Furthermore, in clarifying the involvement of mTORC2 in mediating PI3K and TGFβ crosstalk, this work will hopefully spur the development of mTORC2 specific drug and treatment regimes that will serve to mitigate the disease inducing aspects of TGFβ signalling.

References

Abdollah, S., Macías-Silva, M., Tsukazaki, T., Hayashi, H., Attisano, L. and Wrana, J.L. (1997). TβRI phosphorylation of Smad2 on Ser465 and Ser467 is required for Smad2-Smad4 complex formation and signaling. *The Journal of Biological Chemistry*. 272 (44), 27678–27685.

Afouda, B.A., Ciau-Uitz, A. and Patient, R. (2005). GATA4, 5 and 6 mediate TGFβ maintenance of endodermal gene expression in *Xenopus* embryos. *Development*. 132 (4), 763–774.

Alarcón, C., Zaromytidou, A.-I., Xi, Q., Gao, S., Yu, J., Fujisawa, S., Barlas, A., Miller, A.N., Manova-Todorova, K., Macias, M.J., et al. (2009). Nuclear CDKs drive Smad transcriptional activation and turnover in BMP and TGF-β pathways. *Cell*. 139 (4), 757–769.

Alessi, D.R., James, S.R., Downes, C.P., Holmes, A.B., Gaffney, P.R., Reese, C.B., and Cohen, P. (1997). Characterization of a 3-phosphoinositide-dependent protein kinase which phosphorylates and activates protein kinase Balpha. *Current Biology*. 7 (4), 261–269.

Alva, J.A., Lee, G.E., Escobar, E.E. and Pyle, A.D. (2011). Phosphatase and tensin homolog regulates the pluripotent state and lineage fate choice in human embryonic stem cells. *Stem Cells*. 29 (12), 1952–1962.

Ang, S.L. and Rossant, J. (1994). HNF-3β is essential for node and notochord formation in mouse development. *Cell*. 78 (4), 561–574.

Angers, S. and Moon, R.T. (2009) Proximal events in Wnt signal transduction. *Nature reviews. Molecular Cell Biology*. 10 (7), 468–477.

Arcaro, A. and Wymann, M.P. (1993). Wortmannin is a potent phosphatidylinositol 3-kinase inhibitor: the role of phosphatidylinositol 3,4,5-trisphosphate in neutrophil responses. *The Biochemical Journal*. 296 (Pt 2)297–301.

Armstrong, L., Hughes, O., Yung, S., Hyslop, L., Stewart, R., Wappler, I., Peters, H., Walter, T., Stojkovic, P., Evans, J., et al. (2006). The role of PI3K/AKT, MAPK/ERK and NFκB signalling in the maintenance of human embryonic stem cell pluripotency and viability highlighted by transcriptional profiling and functional analysis. *Human Molecular Genetics*. 15 (11), 1894–1913.

Arnold, S.J., Hofmann, U.K., Bikoff, E.K. and Robertson, E.J. (2008). Pivotal roles for eomesodermin during axis formation, epithelium-to-mesenchyme transition and endoderm specification in the mouse. *Development*. 135 (3), 501–511.

Avilion, A.A., Nicolis, S.K., Pevny, L.H., Perez, L., Vivian, N. and Lovell-Badge, R. (2003). Multipotent cell lineages in early mouse development depend on SOX2 function. *Genes & Development*. 17 (1), 126–140.

Backer, J.M., Myers, M.G., Shoelson, S.E., Chin, D.J., Sun, X.J., Miralpeix, M., Hu, P., Margolis, B., Skolnik, E.Y., Schlessinger, J., et al. (1992). Phosphatidylinositol 3'-Kinase Is Activated by Association with IRS-1 During Insulin Stimulation. *EMBO J*. 11 (9), 3469–3479.

Bar-Peled, L., Schweitzer, L.D., Zoncu, R. and Sabatini, D.M. (2012). Ragulator Is a GEF for the Rag GTPases that Signal Amino Acid Levels to mTORC1. *Cell*. 150 (6), 1196–1208.

Behrens, J., von Kries, J.P., Kuhl, M., Bruhn, L., Wedlich, D., Grosschedl, R. and Birchmeier, W. (1996) Functional interaction of beta-catenin with the transcription factor LEF-1. *Nature*. 382 (6592), 638–642.

Ben-Sahra, I., Howell, J.J., Asara, J.M. and Manning, B.D. (2013). Stimulation of de Novo Pyrimidine Synthesis by Growth Signaling Through mTOR and S6K1. *Science*. 339 (6125), 1323–1328.

Benchabane, H. and Wrana, J.L. (2003). GATA- and Smad1-dependent enhancers in the Smad7 gene differentially interpret bone morphogenetic protein concentrations. *Molecular and Cellular Biology*. 23 (18), 6646–6661.

Benjamin, D., Colombi, M., Moroni, C. and Hall, M.N. (2011). Rapamycin passes the torch: a new generation of mTOR inhibitors. *Nature Reviews Drug Discovery*. 10 (11), 868–880.

Berg, D.K., Smith, C.S., Pearton, D.J., Wells, D.N., Broadhurst, R., Donnison, M. and Pfeffer, P.L. (2011). Trophectoderm Lineage Determination in Cattle. *Developmental Cell*. 20 (2), 244–255.

Bhanot, P., Brink, M., Samos, C.H., Hsieh, J.C., Wang, Y., Macke, J.P., Andrew, D., Nathans, J. and Nusse, R. (1996) A new member of the frizzled family from Drosophila functions as a Wingless receptor. *Nature*. 382 (6588), 225–230.

Bi, L., Okabe, I., Bernard, D.J., Wynshaw-Boris, A. and Nussbaum, R.L. (1999). Proliferative defect and embryonic lethality in mice homozygous for a deletion in the p110α subunit of phosphoinositide 3-kinase. *The Journal of Biological Chemistry*. 274 (16), 10963–10968.

Bialojan, C. and Takai, A. (1988) Inhibitory effect of a marine-sponge toxin, okadaic acid, on protein phosphatases. Specificity and kinetics. *The Biochemical Journal*. 256 (1), 283–290.

Bjornson, C., Griffin, K., Farr, G.H., Terashima, A., Himeda, C., Kikuchi, Y., and Kimelman, D. (2005). Eomesodermin is a localized maternal determinant required for endoderm induction in zebrafish. *Developmental Cell*. 9 (4), 523–533.

Bonni, S., Wang, H.R., Causing, C.G., Kavsak, P., Stroschein, S.L., Luo, K.X., and Wrana, J.L. (2001). TGF-β induces assembly of a Smad2-Smurf2 ubiquitin ligase complex that targets SnoN for degradation. *Nature Cell Biology*. 3 (6), 587–595.

Boyer, L.A., Lee, T.I., Cole, M.F., Johnstone, S.E., Levine, S.S., Zucker, J.R., Guenther, M.G., Kumar, R.M., Murray, H.L., Jenner, R.G., et al. (2005). Core transcriptional regulatory circuitry in human embryonic stem cells. *Cell*. 122 (6), 947–956.

Brennan, J., Norris, D.P. and Robertson, E.J. (2002). Nodal activity in the node governs left-right asymmetry. *Genes & Development*. 16 (18), 2339–2344.

Brewer, G.J. and Cotman, C.W. (1989). Survival and Growth of Hippocampal-Neurons in Defined Medium at Low-Density - Advantages of a Sandwich Culture Technique or Low Oxygen. *Brain Research*. 494 (1), 65–74.

Brons, I.G.M., Smithers, L.E., Trotter, M.W.B., Rugg-Gunn, P., Sun, B., de Sousa Lopes, S.M.C., Howlett, S.K., Clarkson, A., Ahrlund-Richter, L., Pedersen, R.A., et al. (2007). Derivation of pluripotent epiblast stem cells from mammalian embryos. *Nature*. 448 (7150), 191–197.

Brown, C.O., Chi, X., Garcia-Gras, E., Shirai, M., Feng, X.H., and Schwartz, R.J. (2004). The cardiac determination factor, Nkx2-5, is activated by mutual cofactors GATA-4 and Smad1/4 via a novel upstream enhancer. *The Journal of Biological Chemistry*. 279 (11), 10659–10669.

Brown, S., Teo, A., Pauklin, S., Hannan, N., Cho, C.H.-H., Lim, B., Vardy, L., Dunn, N.R., Trotter, M., Pedersen, R., et al. (2011). Activin/Nodal Signaling Controls Divergent Transcriptional Networks in Human Embryonic Stem Cells and in Endoderm Progenitors. *Stem Cells*. 29 (8), 1176–1185.

Bruce, A., Howley, C., Zhou, Y., Vickers, S.L., Silver, L.M., King, M.L. and Ho, R.K. (2003). The maternally expressed zebrafish T-box gene eomesodermin regulates organizer formation. *Development*. 130 (22), 5503–5517.

Bruce, D.L., Macartney, T., Yong, W., Shou, W. and Sapkota, G.P. (2012). Protein phosphatase 5 modulates SMAD3 function in the transforming growth factor-beta pathway. *Cellular Signalling*. 24 (11), 1999–2006.

Buehr, M., Meek, S., Blair, K., Yang, J., Ure, J., Silva, J., McLay, R., Hall, J., Ying, Q.-L. and Smith, A. (2008). Capture of Authentic Embryonic Stem Cells from Rat Blastocysts. *Cell*. 135 (7), 1287–1298.

Burgering, B. and Coffer, P.J. (1995). Protein-Kinase-B (C-Akt) in Phosphatidylinositol-3-OH Kinase Signal Transduction. *Nature*. 376 (6541), 599–602.

Cai, J., Zhao, Y., Liu, Y., Ye, F., Song, Z., Qin, H., Meng, S., Chen, Y., Zhou, R., Song, X., et al. (2007). Directed differentiation of human embryonic stem cells into functional hepatic cells. *Hepatology*. 45 (5), 1229–1239.

Caracciolo, V., Laurenti, G., Romano, G., Carnevale, V., Cimini, A.M., Crozier-Fitzgerald, C., Warschauer, E.M., Russo, G. and Giordano, A. (2012) Flavopiridol induces phosphorylation of AKT in a human glioblastoma cell line, in contrast to siRNA-mediated silencing of Cdk9: Implications for drug design and development. *Cell Cycle*. 11 (6), 1202–1216.

Cardone, M.H., Roy, N., Stennicke, H.R., Salvesen, G.S., Franke, T.F., Stanbridge, E., Frisch, S. and Reed, J.C. (1998). Regulation of cell death protease caspase-9 by phosphorylation. *Science*. 282 (5392), 1318–1321.

Cavallo, R.A., Cox, R.T., Moline, M.M., Roose, J., Polevoy, G.A., Clevers, H., Peifer, M. and Bejsovec, A. (1998) Drosophila Tcf and Groucho interact to repress Wingless signalling activity. *Nature*. 395 (6702), 604–608.

Chacko, B.M., Qin, B., Correia, J.J., Lam, S.S., de Caestecker, M.P. and Lin, K. (2001). The L3 loop and C-terminal phosphorylation jointly define Smad protein trimerization. *Nature Structural Biology*. 8 (3), 248–253.

Chambers, I., Colby, D., Robertson, M., Nichols, J., Lee, S., Tweedie, S. and Smith, A. (2003). Functional expression cloning of Nanog, a pluripotency sustaining factor in embryonic stem cells. *Cell*. 113 (5), 643–655.

Chambers, I., Silva, J., Colby, D., Nichols, J., Nijmeijer, B., Robertson, M., Vrana, J., Jones, K., Grotewold, L. and Smith, A. (2007). Nanog safeguards pluripotency and mediates germline development. *Nature*. 450 (7173), 1230–1238.

Chao, S.H. and Price, D.H. (2001). Flavopiridol inactivates P-TEFb and blocks most RNA polymerase II transcription in vivo. *The Journal of Biological Chemistry*. 276 (34), 31793–31799.

Chen, A.A., Thomas, D.K., Ong, L.L., Schwartz, R.E., Golub, T.R. and Bhatia, S.N. (2011). Humanized mice with ectopic artificial liver tissues. *Proceedings of the National Academy of Sciences of the United States of America*. 108 (29), 11842–11847.

Chen, C.R., Kang, Y.B., Siegel, P.M. and Massague, J. (2002). E2F4/5 and p107 as Smad cofactors linking the TGFβ receptor to c-myc repression. *Cell*. 110 (1), 19–32.

Chen, M.X., McPartlin, A.E., Brown, L., Chen, Y.H., Barker, M. and Cohen P.T. (1994) A novel human protein serine/threonine phosphatase, which possesses four tetratricopeptide repeat motifs and localizes to the nucleus. *EMBO J*. 13 (18), 4278–4290.

Chen, X., Rubock, M.J. and Whitman, M. (1996). A transcriptional partner for MAD proteins in TGF-β signalling. *Nature*. 383 (6602), 691–696.

Chen, X., Xu, H., Yuan, P., Fang, F., Huss, M., Vega, V.B., Wong, E., Orlov, Y.L., Zhang, W., Jiang, J., et al. (2008). Integration of external signaling pathways with the core transcriptional network in embryonic stem cells. *Cell*. 133 (6), 1106–1117.

Chen, Y. and Schier, A.F. (2001). The zebrafish Nodal signal Squint functions as a morphogen. *Nature*. 411 (6837), 607–610.

Chen, Y.-G. and Wang, X.-F. (2009). Finale: The Last Minutes of Smads. *Cell*. 139 (4), 658–660.

Chen, Y.-G., Li, Z. and Wang, X.-F. (2012). Where PI3K/Akt Meets Smads: The Crosstalk Determines Human Embryonic Stem Cell Fate. *Stem Cell*. 10 (3), 231–232.

Choi, J. (2013). Mammalian Development. *Developmental Biology Interactive*. [Online] Available from http://www.devbio.biology.gatech.edu/?page_id=8796 [Accessed: 16th January 2015].

Chou, W.C., Prokova, V., Shiraishi, K., Valcourt, U., Moustakas, A., Hadzopoulou-Cladaras, M., Zannis, V.I. and Kardassis, D. (2003). Mechanism of a transcriptional cross talk between transforming growth factor-beta-regulated Smad3 and Smad4 proteins and orphan nuclear receptor hepatocyte nuclear factor-4. *Molecular Biology of the Cell*. 14 (3), 1279–1294.

Clements, D., Cameleyre, I. and Woodland, H.R. (2003). Redundant early and overlapping larval roles of Xsox17 subgroup genes in Xenopus endoderm development. *Mechanisms of Development*. 120 (3), 337–348.

Clevers, H. and Nusse, R. (2012) Wnt/β-Catenin Signaling and Disease. *Cell*. 149 (6), 1192-1205.

Cohen, P.T.W. (2003) Overview of protein serine/threonine phosphatases. In: *Topics in Current Genetics*. Topics in Current Genetics. Berlin, Heidelberg, Springer Berlin Heidelberg. pp. 1–20.

Conery, A.R., Cao, Y., Thompson, E.A., Townsend, C.M., Ko, T.C. and Luo, K. (2004). Akt interacts directly with Smad3 to regulate the sensitivity to TGF-β induced apoptosis. *Nature Cell Biology*. 6 (4), 366–372.

Conlon, F.L., Lyons, K.M., Takaesu, N., Barth, K.S., Kispert, A., Herrmann, B. and Robertson, E.J. (1994). A Primary Requirement for Nodal in the Formation and Maintenance of the Primitive Streak in the Mouse. *Development*. 120 (7), 1919–1928.

Cross, D., Alessi, D.R., Cohen, P., Andjelkovich, M. and Hemmings, B.A. (1995). Inhibition of Glycogen-Synthase Kinase-3 by Insulin-Mediated by Protein-Kinase-B. *Nature*. 378 (6559), 785–789.

D'Amour, K.A., Agulnick, A.D., Eliazer, S., Kelly, O.G., Kroon, E. and Baetge, E.E. (2005). Efficient differentiation of human embryonic stem cells to definitive endoderm. *Nat Biotech*. 23 (12), 1534–1541.

Daheron, L., Opitz, S.L., Zaehres, H., Lensch, W.M., Andrews, P.W., Itskovitz-Eldor, J. and Daley, G.Q. (2004). LIF/STAT3 signaling fails to maintain self-renewal of human embryonic stem cells. *Stem Cells*. 22 (5), 770–778.

Dai, N., Christiansen, J., Nielsen, F.C. and Avruch, J. (2013). mTOR complex 2 phosphorylates IMP1 cotranslationally to promote IGF2 production and the proliferation of mouse embryonic fibroblasts. *Genes & Development*. 27 (3), 301–312.

Datta, S.R., Dudek, H., Tao, X., Masters, S., Fu, H.A., Gotoh, Y. and Greenberg, M.E. (1997). Akt phosphorylation of BAD couples survival signals to the cell-intrinsic death machinery. *Cell*. 91 (2), 231–241.

Dennler, S., Itoh, S., Vivien, D., Dijke, ten, P., Huet, S. and Gauthier, J.M. (1998). Direct binding of Smad3 and Smad4 to critical TGFβ-inducible elements in the promoter of human plasminogen activator inhibitor-type 1 gene. *EMBO J*. 17 (11), 3091–3100.

Diehl, J.A., Cheng, M., Roussel, M.F. and Sherr, C.J. (1998). Glycogen synthase kinase-3β regulates cyclin D1 proteolysis and subcellular localization. *Genes & Development*. 12 (22), 3499–3511.

Dijke, ten, P. and Arthur, H.M. (2007). Extracellular control of TGFβ signalling in vascular development and disease. *Nature reviews. Molecular cell biology*. 8 (11), 857–869.

Duan, X., Liang, Y.-Y., Feng, X.-H. and Lin, X. (2006). Protein serine/threonine phosphatase PPM1A dephosphorylates Smad1 in the bone morphogenetic protein signaling pathway. *The Journal of Biological Chemistry*. 281 (48), 36526–36532.

Düvel, K., Yecies, J.L., Menon, S., Raman, P., Lipovsky, A.I., Souza, A.L., Triantafellow, E., Ma, Q., Gorski, R., Cleaver, S., et al. (2010). Activation of a Metabolic Gene Regulatory Network Downstream of mTOR Complex 1. *Molecular Cell*. 39 (2), 171–183.

Dvorak, P., Dvorakova, D., Koskova, S., Vodinska, M., Najvirtova, M., Krekac, D. and Hampl, A. (2005). Expression and potential role of fibroblast growth factor 2 and its receptors in human embryonic stem cells. *Stem Cells*. 23 (8), 1200–1211.

Ebisawa, T., Fukuchi, M., Murakami, G., Chiba, T., Tanaka, K., Imamura, T. and Miyazono, K. (2001). Smurf1 interacts with transforming growth factor-β type I receptor through Smad7 and induces receptor degradation. *The Journal of Biological Chemistry*. 276 (16), 12477–12480.

Eiselleova, L., Matulka, K., Kriz, V., Kunova, M., Schmidtova, Z., Neradil, J., Tichy, B., Dvorakova, D., Pospisilova, S., Hampl, A., et al. (2009). A Complex Role for FGF-2 in Self-Renewal, Survival, and Adhesion of Human Embryonic Stem Cells. *Stem Cells*. 27 (8), 1847–1857.

Engel, M.E., McDonnell, M.A., Law, B.K. and Moses, H.L. (1999). Interdependent SMAD and JNK signaling in transforming growth factor-beta-mediated transcription. *The Journal of Biological Chemistry*. 274 (52), 37413–37420.

Escobedo, J.A., Navankasattusas, S., Kavanaugh, W.M., Milfay, D., Fried, V.A. and Williams, L.T. (1991). cDNA Cloning of a Novel 85kd Protein That Has Sh2 Domains and Regulates Binding of PI3-Kinase to the PDGFβ-Receptor. *Cell*. 65 (1), 75–82.

Evans, M.J. and Kaufman, M.H. (1981). Establishment in Culture of Pluripotential Cells From Mouse Embryos. *Nature*. 292 (5819), 154–156.

Feldman, B., Gates, M.A., Egan, E.S., Dougan, S.T., Rennebeck, G., Sirotkin, H.I., Schier, A.F. and Talbot, W.S. (1998). Zebrafish organizer development and germ-layer formation require nodal-related signals. *Nature*. 395 (6698), 181–185.

Feng, X.H. and Derynck, R. (2005). Specificity and versatility in TGF-β signaling through Smads. *Annual Review of Cell and Developmental Biology*. 21659–693.

Fong, H., Hohenstein, K.A. and Donovan, P.J. (2008). Regulation of self-renewal and pluripotency by Sox2 in human embryonic stem cells. *Stem Cells*. 26 (8), 1931–1938.

Franke, T.F., Yang, S.I., Chan, T.O., Datta, K., Kazlauskas, A., Morrison, D.K., Kaplan, D.R. and Tsichlis, P.N. (1995). The Protein-Kinase Encoded by the Akt Protooncogene Is a Target of the PDGF-Activated Phosphatidylinositol 3-Kinase. *Cell*. 81 (5), 727–736.

Freund, C., Oostwaard, D.W.-V., Monshouwer-Kloots, J., van den Brink, S., van Rooijen, M., Xu, X., Zweigerdt, R., Mummery, C. and Passier, R. (2008). Insulin redirects differentiation from cardiogenic mesoderm and endoderm to neuroectoderm in differentiating human embryonic stem cells. *Stem Cells*. 26 (3), 724–733.

Fuentealba, L.C., Eivers, E., Ikeda, A., Hurtado, C., Kuroda, H., Pera, E.M. and De Robertis, E.M. (2007). Integrating Patterning Signals: Wnt/GSK3 Regulates the Duration of the BMP/Smad1 Signal. *Cell*. 131 (5), 980–993.

Gafni, O., Weinberger, L., Mansour, A.A., Manor, Y.S., Chomsky, E., Ben-Yosef, D., Kalma, Y., Viukov, S., Maza, I., Zviran, A., et al. (2013). Derivation of novel human ground state naive pluripotent stem cells. *Nature*. 504 (7479), 282–286.

Gan, X., Wang, J., Su, B. and Wu, D. (2011) Evidence for Direct Activation of mTORC2 Kinase Activity by Phosphatidylinositol 3,4,5-Trisphosphate. *The Journal of Biological Chemistry*. 286 (13), 10998–11002.

Gangloff, Y.G., Mueller, M., Dann, S.G., Svoboda, P., Sticker, M., Spetz, J.F., Um, S.H., Brown, E.J., Cereghini, S., Thomas, G., et al. (2004). Disruption of the mouse mTOR gene leads to early postimplantation lethality and prohibits embryonic stem cell development. *Molecular and Cellular Biology*. 24 (21), 9508–9516.

Gao, S., Alarcón, C., Sapkota, G., Rahman, S., Chen, P.-Y., Goerner, N., Macias, M.J., Erdjument-Bromage, H., Tempst, P. and Massagué, J. (2009). Ubiquitin Ligase Nedd4L Targets Activated Smad2/3 to Limit TGF-β Signaling. *Molecular Cell*. 36 (3), 457–468.

Gao, X.P., Sedgwick, T., Shi, Y.B. and Evans, T. (1998). Distinct functions are implicated for the GATA-4, -5, and -6 transcription factors in the regulation of intestine epithelial cell differentiation. *Molecular and Cellular Biology*. 18 (5), 2901–2911.

Germain, S., Howell, M., Esslemont, G.M. and Hill, C.S. (2000). Homeodomain and winged-helix transcription factors recruit activated Smads to distinct promoter elements via a common Smad interaction motif. *Genes & Development*. 14 (4), 435–451.

Gingras, A.C., Raught, B., Gygi, S.P., Niedzwiecka, A., Miron, M., Burley, S.K., Polakiewicz, R.D., Wyslouch-Cieszynska, A., Aebersold, R. and Sonenberg, N. (2001). Hierarchical phosphorylation of the translation inhibitor 4E-BP1. *Genes & Development*. 15 (21), 2852–2864.

Gonzalez, S.A. and Keeffe, E.B. (2011). Chronic viral hepatitis: epidemiology, molecular biology, and antiviral therapy. *Frontiers in Bioscience-Landmark*. 16225–250.

Grapin-Botton, A. (2008). *Endoderm specification - StemBook - NCBI Bookshelf*.

Greber, B., Lehrach, H. and Adjaye, J. (2007). Fibroblast growth factor 2 modulates transforming growth factor beta signaling in mouse embryonic fibroblasts and human ESCs (hESCs) to support hESC self-renewal. *Stem Cells*. 25 (2), 455–464.

Green, J. and Smith, J.C. (1990). Graded Changes in Dose of a *Xenopus* Activin-A Homolog Elicit Stepwise Transitions in Embryonic Cell Fate. *Nature*. 347 (6291), 391–394.

Grimm, O.H. and Gurdon, J.B. (2002). Nuclear exclusion of Smad2 is a mechanism leading to loss of competence. *Nature Cell Biology*. 4 (7), 519–522.

Gritsman, K., Zhang, J.J., Cheng, S., Heckscher, E., Talbot, W.S. and Schier, A.F. (1999). The EGF-CFC protein one-eyed pinhead is essential for nodal signaling. *Cell*. 97 (1), 121–132.

Groppe, J., Greenwald, J., Wiater, E., Rodriguez-Leon, J., Economides, A.N., Kwiatkowski, W., Affolter, M., Vale, W.W., Belmonte, J. and Choe, S. (2002). Structural basis of BMP signalling inhibition by the cystine knot protein Noggin. *Nature*. 420 (6916), 636–642.

Guertin, D.A., Stevens, D.M., Thoreen, C.C., Burds, A.A., Kalaany, N.Y., Moffat, J., Brown, M., Fitzgerald, K.J. and Sabatini, D.M. (2006). Ablation in mice of the mTORC components raptor, rictor, or mLST8 reveals that mTORC2 is required for signaling to Akt-FOXO and PKC alpha but not S6K1. *Developmental Cell*. 11 (6), 859–871.

Guo, G., Yang, J., Nichols, J., Hall, J.S., Eyres, I., Mansfield, W. and Smith, A. (2009). Klf4 reverts developmentally programmed restriction of ground state pluripotency. *Development*. 136 (7), 1063–1069.

Gurdon, J.B., Harger, P., Mitchell, A. and Lemaire, P. (1994). Activin signalling and response to a morphogen gradient. *Nature*. 371 (6497), 487–492.

Gwinn, D.M., Shackelford, D.B., Egan, D.F., Mihaylova, M.M., Mery, A., Vasquez, D.S., Turk, B.E. and Shaw, R.J. (2008). AMPK phosphorylation of raptor mediates a metabolic checkpoint. *Molecular Cell*. 30 (2), 214–226.

Haegel, H., Larue, L., Ohsugi, M., Fedorov, L., Herrenknecht, K. and Kemler, R. (1995). Lack of β-catenin affects mouse development at gastrulation. *Development*. 121 (11), 3529–3537.

Han, D.W., Tapia, N., Joo, J.Y., Greber, B., Arauzo-Bravo, M.J., Bernemann, C., Ko, K., Wu, G., Stehling, M., Do, J.T., et al. (2010). Epiblast Stem Cell Subpopulations Represent Mouse Embryos of Distinct Pregastrulation Stages. *Cell*. 143 (4), 617–627.

Hanahan, D. and Weinberg, R.A. (2011) Hallmarks of Cancer: The Next Generation. *Cell*. 144 (5), 646–674.

Harlan, J.E., Hajduk, P.J., Yoon, H.S. and Fesik, S.W. (1994). Pleckstrin Homology Domains Bind to Phosphatidylinositol-4,5-Bisphosphate. *Nature*. 371 (6493), 168–170.

Hart, A.H., Hartley, L., Sourris, K., Stadler, E.S., Li, R., Stanley, E.G., Tam, P.P.L., Elefanty, A.G. and Robb, L. (2002). Mixl1 is required for axial mesendoderm morphogenesis and patterning in the murine embryo. *Development*. 129 (15), 3597–3608.

Haslam, R.J., Koide, H.B. and Hemmings, B.A. (1993). Pleckstrin Domain Homology. *Nature*. 363 (6427), 309–310.

Hata, A., Lagna, G., Massague, J. and Hemmati-Brivanlou, A. (1998). Smad6 inhibits BMP/Smad1 signaling by specifically competing with the Smad4 tumor suppressor. *Genes & Development*. 12 (2), 186–197.

Hay, D.C., Fletcher, J., Payne, C., Terrace, J.D., Gallagher, R.C.J., Snoeys, J., Black, J.R., Wojtacha, D., Samuel, K., Hannoun, Z., et al. (2008a). Highly efficient differentiation of hESCs to functional hepatic endoderm requires ActivinA and Wnt3a signaling. *Proceedings of the National Academy of Sciences of the United States of America*. 105 (34), 12301–12306.

Hay, D.C., Sutherland, L., Clark, J. and Burdon, T. (2004). Oct-4 knockdown induces similar patterns of endoderm and trophoblast differentiation markers in human and mouse embryonic stem cells. *Stem Cells*. 22 (2), 225–235.

Hay, D.C., Zhao, D., Fletcher, J., Hewitt, Z.A., McLean, D., Urruticoechea-Uriguen, A., Black, J.R., Elcombe, C., Ross, J.A., Wolf, R., et al. (2008b). Efficient differentiation of hepatocytes from human embryonic stem cells exhibiting markers recapitulating liver development in vivo. *Stem Cells*. 26 (4), 894–902.

Hayashi, H., Abdollah, S., Qiu, Y., Cai, J., Xu, Y.-Y., Grinnell, B.W., Richardson, M.A., Topper, J.N., Gimbrone, M.A., Jr., Wrana, J.L., et al. (1997). The MAD-Related Protein Smad7 Associates with the TGFβ Receptor and Functions as an Antagonist of TGFβ Signaling. *Cell*. 89 (7), 1165–1173.

He, X., Semenov, M., Tamai, K. and Zeng, X. (2004) LDL receptor-related proteins 5 and 6 in Wnt/beta-catenin signaling: Arrows point the way. *Development*. 131 (8), 1663–1677.

Henry, G.L. and Melton, D.A. (1998). Mixer, a homeobox gene required for endoderm development. *Science*. 281 (5373), 91–96.

Henry, G.L., Brivanlou, I.H., Kessler, D.S., HemmatiBrivanlou, A., and Melton, D.A. (1996). TGF-β signals and a pre-pattern in *Xenopus laevis* endodermal development. *Development*. 122 (3), 1007–1015.

Hiles, I.D., Otsu, M., Volinia, S., Fry, M.J., Gout, I., Dhand, R., Panayotou, G., Ruizlarrea, F., Thompson, A., Totty, N.F., et al. (1992). Phosphatidylinositol 3-Kinase - Structure and Expression of the 110kd Catalytic Subunit. *Cell*. 70 (3), 419–429.

Hill, M.M., Clark, S.F., Tucker, D.F., Birnbaum, M.J., James, D.E. and Macaulay, S.L. (1999). A role for protein kinase B beta/Akt2 in insulin-stimulated GLUT4 translocation in adipocytes. *Molecular and Cellular Biology*. 19 (11), 7771–7781.

Hoodless, P.A., Pye, M., Chazaud, C., Labbe, E., Attisano, L., Rossant, J. and Wrana, J.L. (2001). FoxH1 (Fast) functions to specify the anterior primitive streak in the mouse. *Genes & Development*. 15 (10), 1257–1271.

Huse, M., Muir, T.W., Xu, L., Chen, Y.G., Kuriyan, J. and Massague, J. (2001). The TGFβ receptor activation process: An inhibitor- to substrate-binding switch. *Molecular Cell*. 8 (3), 671–682.

Inman, G.J. and Hill, C.S. (2002). Stoichiometry of active Smad-transcription factor complexes on DNA. *The Journal of Biological Chemistry*. 277 (52), 51008–51016.

Inoki, K., Li, Y., Xu, T. and Guan, K.L. (2003a). Rheb GTPase is a direct target of TSC2 GAP activity and regulates mTOR signaling. *Genes & Development*. 17 (15), 1829–1834.

Inoki, K., Li, Y., Zhu, T.Q., Wu, J. and Guan, K.L. (2002). TSC2 is phosphorylated and inhibited by Akt and suppresses mTOR signalling. *Nature Cell Biology*. 4 (9), 648–657.

Inoki, K., Zhu, T.Q. and Guan, K.L. (2003b). TSC2 mediates cellular energy response to control cell growth and survival. *Cell*. 115 (5), 577–590.

Ivanova, N., Dobrin, R., Lu, R., Kotenko, I., Levorse, J., DeCoste, C., Schafer, X., Lun, Y. and Lemischka, I.R. (2006). Dissecting self-renewal in stem cells with RNA interference. *Nature*. 442 (7102), 533–538.

Jacobsen, C.M., Narita, N., Bielinska, M., Syder, A.J., Gordon, J.I. and Wilson, D.B. (2002). Genetic mosaic analysis reveals that GATA-4 is required for proper differentiation of mouse gastric epithelium. *Developmental Biology*. 241 (1), 34–46.

Jastrzebski, K., Hannan, K.M., Tchoubrieva, E.B., Hannan, R.D. and Pearson, R.B. (2007). Coordinate regulation of ribosome biogenesis and function by the ribosomal protein S6 kinase, a key mediator of mTOR function. *Growth Factors*. 25 (4), 209–226.

Jiang, J., Au, M., Lu, K., Eshpeter, A., Korbutt, G., Fisk, G. and Majumdar, A.S. (2007). Generation of insulin-producing islet-like clusters from human embryonic stem cells. *Stem Cells*. 25 (8), 1940–1953.

Jiang, Y.M. and Evans, T. (1996). The *Xenopus* GATA-4/5/6 genes are associated with cardiac specification and can regulate cardiac-specific transcription during embryogenesis. *Developmental Biology*. 174 (2), 258–270.

Joseph, E.M. and Melton, D.A. (1997). XNR4: A *Xenopus* nodal-related gene expressed in the Spemann organizer. *Developmental Biology*. 184 (2), 367–372.

Jung, J.N., Zheng, M.H., Goldfarb, M. and Zaret, K.S. (1999). Initiation of mammalian liver development from endoderm by fibroblast growth factors. *Science*. 284 (5422), 1998–2003.

Kaestner, K.H., Hiemisch, H. and Schütz, G. (1998). Targeted disruption of the gene encoding hepatocyte nuclear factor 3gamma results in reduced transcription of hepatocyte-specific genes. *Molecular and Cellular Biology*. 18 (7), 4245–4251.

Kamaraju, S.K.Roberts, AB (2005). Role of Rho/ROCK and p38 MAP kinase pathways in transforming growth factor-beta-mediated Smad-dependent growth inhibition of human breast carcinoma cells in vivo. *The Journal of Biological Chemistry*. 280 (2), 1024–1036.

Kamiya, A., Inoue, Y. and Gonzalez, F.J. (2003). Role of the hepatocyte nuclear factor 4 alpha in control of the pregnane X receptor during fetal liver development. *Hepatology (Baltimore, Md.)*. 37 (6), 1375–1384.

Kanai-Azuma, M., Kanai, Y., Gad, J.M., Tajima, Y., Taya, C., Kurohmaru, M., Sanai, Y., Yonekawa, H., Yazaki, K., Tam, P., et al. (2002). Depletion of definitive gut endoderm in Sox17-null mutant mice. *Development*. 129 (10), 2367–2379.

Kaplan, D.R., Whitman, M., Schaffhausen, B., Pallas, D.C., White, M., Cantley, L. and Roberts, T.M. (1987). Common Elements in Growth-Factor Stimulation and Oncogenic Transformation - 85-Kd Phosphoprotein and Phosphatidylinositol Kinase-Activity. *Cell*. 50 (7), 1021–1029.

Kennedy, S.G., Kandel, E.S., Cross, T.K. and Hay, N. (1999). Akt protein kinase B inhibits cell death by preventing the release of cytochrome c from mitochondria. *Molecular and Cellular Biology*. 19 (8), 5800–5810.

Khetani, S.R. and Bhatia, S.N. (2008). Microscale culture of human liver cells for drug development. *Nat Biotech*. 26 (1), 120–126.

Kim, E., Goraksha-Hicks, P., Li, L., Neufeld, T.P. and Guan, K.-L. (2008). Regulation of TORC1 by Rag GTPases in nutrient response. *Nature Cell Biology*. 10 (8), 935–945.

Kim, J., Kundu, M., Viollet, B. and Guan, K.-L. (2011). AMPK and mTOR regulate autophagy through direct phosphorylation of Ulk1. *Nature Cell Biology*. 13 (2), 132–171.

Kishimoto, A., Takai, Y., Mori, T., Kikkawa, U. and Nishizuka, Y. (1980). Activation of Calcium and Phospholipid-Dependent Protein-Kinase by Diacylglycerol, Its Possible Relation to Phosphatidylinositol Turnover. *The Journal of Biological Chemistry*. 255 (6), 2273–2276.

Knockaert, M., Sapkota, G., Alarcón, C., Massagué, J. and Brivanlou, A.H. (2006). Unique players in the BMP pathway: Small C-terminal domain phosphatases dephosphorylate Smad1 to attenuate BMP signaling. *Proceedings of the National Academy of Sciences of the United States of America*. 103 (32), 11940–11945.

Kobayashi, T., Minowa, O., Sugitani, Y., Takai, S., Mitani, H., Kobayashi, E., Noda, T. and Hino, O. (2001). A germ-line Tsc1 mutation causes tumor development and embryonic lethality that are similar, but not identical to, those caused by Tsc2 mutation in mice. *Proceedings of the National Academy of Sciences of the United States of America*. 98 (15), 8762–8767.

Kretzschmar, M., Doody, J. and Massague, J. (1997). Opposing BMP and EGF signalling pathways converge on the TGF-β family mediator Smad1. *Nature*. 389 (6651), 618–622.

Kretzschmar, M., Doody, J., Timokhina, I. and Massague, J. (1999). A mechanism of repression of TGFβ / Smad signaling by oncogenic Ras. *Genes & Development*. 13 (7), 804–816.

Kubo, A., Shinozaki, K., Shannon, J.M., Kouskoff, V., Kennedy, M., Woo, S., Fehling, H.J. and Keller, G. (2004). Development of definitive endoderm from embryonic stem cells in culture. *Development*. 131 (7), 1651–1662.

Kunisada, Y., Tsubooka-Yamazoe, N., Shoji, M. and Hosoya, M. (2012). Small molecules induce efficient differentiation into insulin-producing cells from human induced pluripotent stem cells. *Stem Cell Research*. 8 (2), 274–284.

Kurisaki, A., Kose, S., Yoneda, Y., Heldin, C.H. and Moustakas, A. (2001). Transforming growth factor-beta induces nuclear import of Smad3 in an importin-beta 1 and Ran-dependent manner. *Molecular Biology of the Cell*. 12 (4), 1079–1091.

Lamming, D.W., Ye, L., Katajisto, P., Goncalves, M.D., Saitoh, M., Stevens, D.M., Davis, J.G., Salmon, A.B., Richardson, A., Ahima, R.S., et al. (2012). Rapamycin-induced insulin resistance is mediated by mTORC2 loss and uncoupled from longevity. *Science*. 335 (6076), 1638–1643.

Latinkic, BV and Smith, J.C. (1999). Goosecoid and Mix.1 repress Brachyury expression and are required for head formation in *Xenopus*. *Development*. 126 (8), 1769–1779.

Le Scolan, E., Zhu, Q., Wang, L., Bandyopadhyay, A., Javelaud, D., Mauviel, M., Sun, L. and Luo, K. (2008). Transforming growth factor-beta suppresses the ability of ski to inhibit tumor metastasis by inducing its degradation. *Cancer Research*. 68 (9), 3277–3285.

Lee, C.S., Friedman, J.R., Fulmer, J.T. and Kaestner, K.H. (2005). The initiation of liver development is dependent on Foxa transcription factors. *Nature*. 435 (7044), 944–947.

Lewis, K.A., Gray, P.C., Blount, A.L., MacConnell, L.A., Wiater, E., Bilezikjian, L.M. and Vale, W. (2000). Betaglycan binds inhibin and can mediate functional antagonism of activin signalling. *Nature*. 404 (6776), 411–414.

Li, J., Wang, G., Wang, C., Zhao, Y., Zhang, H., Tan, Z., Song, Z., Ding, M. and Deng, H. (2007). MEK/ERK signaling contributes to the maintenance of human embryonic stem cell self-renewal. *Differentiation*. 75 (4), 299–307.

Li, P., Tong, C., Mehrian-Shai, R., Jia, L., Wu, N., Yan, Y., Maxson, R.E., Schulze, E.N., Song, H., Hsieh, C.-L., et al. (2008). Germline Competent Embryonic Stem Cells Derived from Rat Blastocysts. *Cell*. 135 (7), 1299–1310.

Li, V.S.W., Ng, S.S., Boersema, P.J., Low, T.Y., Karthaus, W.R., Gerlach, J.P., Mohammed, S., Heck, A.J.R., Maurice, M.M., Mahmoudi T., et al. (2012) Wnt signaling through inhibition of β-catenin degradation in an intact Axin1 complex. *Cell*. 149 (6), 1245–1256.

Liang, J., Zubovitz, J., Petrocelli, T., Kotchetkov, R., Connor, M.K., Han, K., Lee, J.H., Ciarallo, S., Catzavelos, C., Beniston, R., et al. (2002). PKB/Akt phosphorylates p27, impairs nuclear import of p27 and opposes p27-mediated G1 arrest. *Nature Medicine*. 8 (10), 1153–1160.

Lin, X., Duan, X., Liang, Y.-Y., Su, Y., Wrighton, K.H., Long, J., Hu, M., Davis, C.M., Wang, J., Brunicardi, F.C., et al. (2006). PPM1A Functions as a Smad Phosphatase to Terminate TGFβ Signaling. *Cell*. 125 (5), 915–928.

Lin, X., Liang, M. and Feng, X.H. (2000). Smurf2 is a ubiquitin E3 ligase mediating proteasome-dependent degradation of Smad2 in transforming growth factor-beta signaling. *The Journal of Biological Chemistry*. 275 (47), 36818–36822.

Liu, P.T., Wakamiya, M., Shea, M.J., Albrecht, U., Behringer, R.R. and Bradley, A. (1999). Requirement for Wnt3 in vertebrate axis formation. *Nature Genetics*. 22 (4), 361–365.

Lo, R.S. and Massague, J. (1999) Ubiquitin-dependent degradation of TGF-beta-activated Smad2. *Nature Cell Biology*. 1 (8), 472–478.

Loh, Y.H., Wu, Q., Chew, J.L., Vega, V.B., Zhang, W.W., Chen, X., Bourque, G., George, J., Leong, B., Liu, J., et al. (2006). The Oct4 and Nanog transcription network regulates pluripotency in mouse embryonic stem cells. *Nature Genetics*. 38 (4), 431–440.

Lowe, L.A., Yamada, S. and Kuehn, M.R. (2001). Genetic dissection of nodal function in patterning the mouse embryo. *Development*. 128 (10), 1831–1843.

Ludwig, T.E., Bergendahl, V., Levenstein, M.E., Yu, J., Probasco, M.D. and Thomson, J.A. (2006). Feeder-independent culture of human embryonic stem cells (vol 3, pg 637, 2006). *Nature Methods*. 3 (10), 867–867.

Ma, Y., Lin, H. and Qiu, C. (2012) High-efficiency transfection and siRNA-mediated gene knockdown in human pluripotent stem cells. *Current Protocols in Stem Cell Biology*. Chapter 2, Unit5C.2.

Maehama, T. and Dixon, J.E. (1998). The tumor suppressor, PTEN/MMAC1, dephosphorylates the lipid second messenger, phosphatidylinositol 3,4,5-trisphosphate. *The Journal of Biological Chemistry*. 273 (22), 13375–13378.

Martin, G.R. (1981). Isolation of a Pluripotent Cell-Line From Early Mouse Embryos Cultured in Medium Conditioned by Teratocarcinoma Stem-Cells. *Proceedings of the National Academy of Sciences of the United States of America*. 78 (12), 7634–7638.

Martin, K.A. and Blenis, J. (2002). Coordinate regulation of translation by the PI 3-kinase and mTOR pathways. *Advances in Cancer Research, Vol 86*. 861–39.

Massague, J. (1998). TGF-β Signal Transduction. *Annual Review of Biochemistry*, 67(1):753.

Massagué, J. (2000) How cells read TGF-β signals. *Nature Reviews. Molecular Cell Biology*. 1 (3), 169–178.

Massagué, J. (2012) TGFβ signalling in context. *Nature Reviews. Molecular Cell Biology*. 13 (10), 616–630.

Massague, J., Seoane, J. and Wotton, D. (2005). Smad transcription factors. *Genes & Development*. 19 (23), 2783–2810.

Masui, S., Nakatake, Y., Toyooka, Y., Shimosato, D., Yagi, R., Takahashi, K., Okochi, H., Okuda, A., Matoba, R., Sharov, A.A., et al. (2007). Pluripotency governed by Sox2 via regulation of Oct3/4 expression in mouse embryonic stem cells. *Nature Cell Biology*. 9 (6), 625–U626.

Matsui, T., Kanai-Azuma, M., Hara, K., Matoba, S., Hiramatsu, R., Kawakami, H., Kurohmaru, M., Koopman, P. and Kanai, Y. (2006). Redundant roles of Sox17 and Sox18 in postnatal angiogenesis in mice. *Journal of Cell Science*. 119 (17), 3513–3526.

Matsuura, I., Denissova, N.G., Wang, G., He, D., Long, J. and Liu F. (2004) Cyclin-dependent kinases regulate the antiproliferative function of Smads. *Nature*. 430 (6996), 226–231.

Matsuzaki, H., Daitoku, H., Hatta, M., Tanaka, K. and Fukamizu, A. (2003). Insulin-induced phosphorylation of FKHR (Foxo1) targets to proteasomal degradation. *Proceedings of the National Academy of Sciences of the United States of America*. 100 (20), 11285–11290.

Mavrakis, K.J., Andrew, R.L., Lee, K.L., Petropoulou, C., Dixon, J.E., Navaratnam, N., Norris, D.P. and Episkopou, V. (2007). Arkadia enhances nodal/TGF-β signaling by coupling phospho-Smad2/3 activity and turnover. *PLoS Biology*. 5 (3), 586–603.

McLean, A.B., D'Amour, K.A., Jones, K.L., Krishnamoorthy, M., Kulik, M.J., Reynolds, D.M., Sheppard, A.M., Liu, H., Xu, Y., Baetge, E.E., et al. (2007). Activin A Efficiently Specifies Definitive Endoderm from Human Embryonic Stem Cells Only When Phosphatidylinositol 3-Kinase Signaling Is Suppressed. *Stem Cells*. 25 (1), 29–38.

Meno, C., Gritsman, K., Ohishi, S., Ohfuji, Y., Heckscher, E., Mochida, K., Shimono, A., Kondoh, H., Talbot, W.S., Robertson, E.J., et al. (1999). Mouse lefty2 and zebrafish antivin are feedback inhibitors of nodal signaling during vertebrate gastrulation. *Molecular Cell*. 4 (3), 287–298.

Mitsui, K., Tokuzawa, Y., Itoh, H., Segawa, K., Murakami, M., Takahashi, K., Maruyama, M., Maeda, M. and Yamanaka, S. (2003). The homeoprotein Nanog is required for maintenance of pluripotency in mouse epiblast and ES cells. *Cell*. 113 (5), 631–642.

Molenaar, M., van de Wetering, M., Oosterwegel, M., Peterson-Maduro, J., Godsave, S., Korinek, V., Roose, J., Destrée, O, and Clevers, H. (1996) XTcf-3 transcription factor mediates beta-catenin-induced axis formation in Xenopus embryos. *Cell*. 86 (3), 391–399.

Morgani, S.M., Canham, M.A., Nichols, J., Sharov, A.A., Migueles, R.P., Ko, M.S.H. and Brickman, J.M. (2013). Totipotent Embryonic Stem Cells Arise in Ground-State Culture Conditions. *Cell Reports*. 3 (6), 1945–1957.

Mori, S., Matsuzaki, K., Yoshida, K., Furukawa, F., Tahashi, Y., Yamagata, H., Sekimoto, G., Seki, T., Matsui, H., Nishizawa, M., et al. (2004). TGF-β and HGF transmit the signals through JNK-dependent Smad2/3 phosphorylation at the linker regions. *Oncogene*. 23 (44), 7416–7429.

Morrisey, E.E., Tang, Z.H., Sigrist, K., Lu, M.M., Jiang, F., Ip, H.S. and Parmacek, M.S. (1998). GATA6 regulates HNF4 and is required for differentiation of visceral endoderm in the mouse embryo. *Genes & Development*. 12 (22), 3579–3590.

Murakami, M., Ichisaka, T., Maeda, M., Oshiro, N., Hara, K., Edenhofer, F., Kiyama, H., Yonezawa, K. and Yamanaka, S. (2004). mTOR is essential for growth and proliferation in early mouse embryos and embryonic stem cells. *Molecular and Cellular Biology*. 24 (15), 6710–6718.

Nagy, A., Gocza, E., Diaz, E.M., Prideaux, V.R., Ivanyi, E., Markkula, M. and Rossant, J. (1990). Embryonic Stem-Cells Alone Are Able to Support Fetal Development in the Mouse. *Development*. 110 (3), 815–821.

Nagy, A., Rossant, J., Nagy, R., Abramownewerly, W. and Roder, J.C. (1993). Derivation of Completely Cell Culture-Derived Mice From Early-Passage Embryonic Stem-Cells. *Proceedings of the National Academy of Sciences of the United States of America*. 90 (18), 8424–8428.

Nichols, J., Zevnik, B., Anastassiadis, K., Niwa, H., Klewe-Nebenius, D., Chambers, I., Scholer, H. and Smith, A. (1998). Formation of pluripotent stem cells in the mammalian embryo depends on the POU transcription factor Oct4. *Cell*. 95 (3), 379–391.

Niwa, H., Masui, S., Chambers, I., Smith, A.G. and Miyazaki, J. (2002). Phenotypic complementation establishes requirements for specific POU domain and generic transactivation function of Oct-3/4 in embryonic stem cells. *Molecular and Cellular Biology*. 22 (5), 1526–1536.

Noordermeer, J., Klingensmith, J., Perrimon, N. and Nusse, R. (1994) Dishevelled and Armadillo Act in the Wingless Signaling Pathway in Drosophila. *Nature*. 367 (6458), 80–83.

Nüsslein-Volhard, C. and Wieschaus, E. (1980) Mutations affecting segment number and polarity in Drosophila. *Nature*

Oh, W.J., Wu, C.-C., Kim, S.J., Facchinetti, V., Julien, L.-A., Finlan, M., Roux, P.P., Su, B. and Jacinto, E. (2010). mTORC2 can associate with ribosomes to promote cotranslational phosphorylation and stability of nascent Akt polypeptide. *EMBO J*. 29 (23), 3939–3951.

Onda, H., Lueck, A., Marks, P.W., Warren, H.B. and Kwiatkowski, D.J. (1999). Tsc2(+/-) mice develop tumors in multiple sites that express gelsolin and are influenced by genetic background. *Journal of Clinical Investigation*. 104 (6), 687–695.

Paling, N., Wheadon, H., Bone, H.K. and Welham, M.J. (2004). Regulation of embryonic stem cell self-renewal by phosphoinositide 3-kinase-dependent signaling. *The Journal of Biological Chemistry*. 279 (46), 48063–48070.

Palmieri, S.L., Peter, W., Hess, H. and Schöler, H.R. (1994). Oct-4 transcription factor is differentially expressed in the mouse embryo during establishment of the first two extraembryonic cell lineages involved in implantation. *Developmental Biology*. 166 (1), 259–267.

Pesce, M., Wang, X.Y., Wolgemuth, D.J. and Scholer, H. (1998). Differential expression of the Oct-4 transcription factor during mouse germ cell differentiation. *Mechanisms of Development*. 71 (1-2), 89–98.

Pierreux, C.E., Nicolas, F.J. and Hill, C.S. (2000). Transforming growth factor beta-independent shuttling of Smad4 between the cytoplasm and nucleus. *Molecular and Cellular Biology*. 20 (23), 9041–9054.

Rehorn, K.P., Thelen, H., Michelson, A.M. and Reuter, R. (1996). A molecular aspect of hematopoiesis and endoderm development common to vertebrates and Drosophila. *Development*. 122 (12), 4023–4031.

Reiter, J.F., Alexander, J., Rodaway, A., Yelon, D., Patient, R., Holder, N. and Stainier, D. (1999). Gata5 is required for the development of the heart and endoderm in zebrafish. *Genes & Development*. 13 (22), 2983–2995.

Remy, I., Montmarquette, A. and Michnick, S.W. (2004). PKB/Akt modulates TGF-β signalling through a direct interaction with Smad3. *Nature Cell Biology*. 6 (4), 358–365.

Resjö, S., Oknianska, A., Zolnierowicz, S., Manganiello, V., and Degerman E. (1999) Phosphorylation and activation of phosphodiesterase type 3B (PDE3B) in adipocytes in response to serine/threonine phosphatase inhibitors: deactivation of PDE3B in vitro by protein phosphatase type 2A. *The Biochemical Journal*. 341 (Pt 3) 839–845.

Robertson, E., Bradley, A., Kuehn, M. and Evans, M. (1986). Germ-Line Transmission of Genes Introduced Into Cultured Pluripotential Cells by Retroviral Vector. *Nature*. 323 (6087), 445–448.

Robitaille, A.M., Christen, S., Shimobayashi, M., Cornu, M., Fava, L.L., Moes, S., Prescianotto-Baschong, C., Sauer, U., Jenoe, P. and Hall, M.N. (2013). Quantitative Phosphoproteomics Reveal mTORC1 Activates de Novo Pyrimidine Synthesis. *Science*. 339 (6125), 1320–1323.

Rodaway, A. and Patient, R. (2001). Mesendoderm: An ancient germ layer? *Cell*. 105 (2), 169–172.

Rodda, D.J., Chew, J.L., Lim, L.H., Loh, Y.H., Wang, B., Ng, H.H. and Robson, P. (2005). Transcriptional regulation of Nanog by Oct4 and Sox2. *The Journal of Biological Chemistry*. 280 (26), 24731–24737.

Rossi, J.M., Dunn, N.R., Hogan, B. and Zaret, K.S. (2001). Distinct mesodermal signals, including BMPs from the septum transversum mesenchyme, are required in combination for hepatogenesis from the endoderm. *Genes & Development*. 15 (15), 1998–2009.

Ruderman, N.B., Kapeller, R., White, M.F. and Cantley, L.C. (1990). Activation of phosphatidylinositol 3-kinase by insulin. *Proceedings of the National Academy of Sciences of the United States of America*. 87 (4), 1411–1415.

Ryan, K., Garrett, N., Mitchell, A. and Gurdon, J.B. (1996). Eomesodermin, a key early gene in *Xenopus* mesoderm differentiation. *Cell*. 87 (6), 989–1000.

Sabers, C.J., Martin, M.M., Brunn, G.J., Williams, J.M., Dumont, F.J., Wiederrecht, G. and Abraham, R.T. (1995). Isolation of a Protein Target of the FKBP12-Rapamycin Complex in Mammalian Cells. *The Journal of Biological Chemistry*. 270 (2), 815–822.

Sancak, Y., Bar-Peled, L., Zoncu, R., Markhard, A.L., Nada, S., and Sabatini, D.M. (2010). Ragulator-Rag Complex Targets mTORC1 to the Lysosomal Surface and Is Necessary for Its Activation by Amino Acids. *Cell*. 141, 290–303.

Sancak, Y., Peterson, T.R., Shaul, Y.D., Lindquist, R.A., Thoreen, C.C., Bar-Peled, L. and Sabatini, D.M. (2008). The Rag GTPases bind raptor and mediate amino acid signaling to mTORC1. *Science*. 320 (5882), 1496–1501.

Sancak, Y., Thoreen, C.C., Peterson, T.R., Lindquist, R.A., Kang, S.A., Spooner, E., Carr, S.A. and Sabatini, D.M. (2007). PRAS40 is an insulin-regulated inhibitor of the mTORC1 protein kinase. *Molecular Cell*. 25 (6), 903–915.

Sapkota, G., Alarcón, C., Spagnoli, F.M., Brivanlou, A.H. and Massagué, J. (2007). Balancing BMP signaling through integrated inputs into the Smad1 linker. *Molecular Cell*. 25 (3), 441–454.

Sapkota, G., Knockaert, M., Alarcón, C., Montalvo, E., Brivanlou, A.H. and Massagué, J. (2006). Dephosphorylation of the linker regions of Smad1 and Smad2/3 by small C-terminal domain phosphatases has distinct outcomes for bone morphogenetic protein and transforming growth factor-beta pathways. *The Journal of Biological Chemistry*. 281 (52), 40412–40419.

Sarbassov, D.D., Guertin, D.A., Ali, S.M. and Sabatini, D.M. (2005). Phosphorylation and regulation of Akt/PKB by the rictor-mTOR complex. *Science*. 307 (5712), 1098–1101.

Schenke-Layland, K., Angelis, E., Rhodes, K.E., Heydarkhan-Hagvall, S., Mikkola, H.K. and Maclellan, W.R. (2007). Collagen IV induces trophoectoderm differentiation of mouse embryonic stem cells. *Stem Cells*. 25 (6), 1529–1538.

Schnerch, A., Cerdan, C. and Bhatia, M. (2010). Distinguishing between mouse and human pluripotent stem cell regulation: the best laid plans of mice and men. *Stem Cells*. 28 (3), 419–430.

Schwartz, R.E., Linehan, J.L., Painschab, M.S., Hu, W.-S., Verfaillie, C.M. and Kaufman, D.S. (2005). Defined conditions for development of functional hepatic cells from human embryonic stem cells. *Stem Cells and Development*. 14 (6), 643–655.

Shen, W., Scearce, L.M., Brestelli, J.E., Sund, N.J. and Kaestner, K.H. (2001). Foxa3 (hepatocyte nuclear factor 3γ) is required for the regulation of hepatic GLUT2 expression and the maintenance of glucose homeostasis during a prolonged fast. *The Journal of Biological Chemistry*. 276 (46), 42812–42817.

Shi, Y.G. and Massague, J. (2003). Mechanisms of TGF-β signaling from cell membrane to the nucleus. *Cell*. 113 (6), 685–700.

Shi, Y.G., Wang, Y.F., Jayaraman, L., Yang, H.J., Massague, J. and Pavletich, N.P. (1998). Crystal structure of a Smad MH1 domain bound to DNA: Insights on DNA binding in TGF-β signaling. *Cell*. 94 (5), 585–594.

Shimobayashi, M. and Hall, M.N. (2014). Making new contacts: the mTOR network in metabolism and signalling crosstalk. *Nature reviews. Molecular cell biology*. 15 (3), 155–162.

Shiota, C., Woo, J.-T., Lindner, J., Shelton, K.D. and Magnuson, M.A. (2006). Multiallelic disruption of the rictor gene in mice reveals that mTOR complex 2 is essential for fetal growth and viability. *Developmental Cell*. 11 (4), 583–589.

Shukla, A., Malik, M., Cataisson, C., Ho, Y., Friesen, T., Suh, K.S. and Yuspa, S.H. (2009). TGF-β signalling is regulated by Schnurri-2-dependent nuclear translocation of CLIC4 and consequent stabilization of phospho-Smad2 and 3. *Nature Cell Biology*. 11 (6), 777–784.

Siegfried, E., Chou, T.B. and Perrimon, N. (1992) wingless signaling acts through zeste-white 3, the Drosophila homolog of glycogen synthase kinase-3, to regulate engrailed and establish cell fate. *Cell*. 71 (7), 1167–1179.

Si-Tayeb, K., Noto, F.K., Nagaoka, M., Li, J., Battle, M.A., Duris, C., North, P.E., Dalton, S. and Duncan, S.A. (2010). Highly Efficient Generation of Human Hepatocyte-Like Cells from Induced Pluripotent Stem Cells. *Hepatology (Baltimore, Md.)*. 51 (1), 297–305.

Singh, A.M., Reynolds, D., Cliff, T., Ohtsuka, S., Mattheyses, A.L., Sun, Y., Menendez, L., Kulik, M. and Dalton, S. (2012). Signaling Network Crosstalk in Human Pluripotent Cells: A Smad2/3-Regulated Switch that Controls the Balance between Self-Renewal and Differentiation. *Stem Cell*. 10 (3), 312–326.

Sinner, D., Kirilenko, P., Rankin, S., Wei, E., Howard, L., Kofron, M., Heasman, J., Woodland, H.R. and Zorn, A.M. (2006). Global analysis of the transcriptional network controlling *Xenopus* endoderm formation. *Development*. 133 (10), 1955–1966.

Smith, A.G., Heath, J.K., Donaldson, D.D., Wong, G.G., Moreau, J., Stahl, M. and Rogers, D. (1988). Inhibition of Pluripotential Embryonic Stem-Cell Differentiation by Purified Polypeptides. *Nature*. 336 (6200), 688–690.

Song, K.Y., Wang, H., Krebs, T.L. and Danielpour, D. (2006). Novel roles of Akt and mTOR in suppressing TGF-β/ALK5-mediated Smad3 activation. *EMBO J*. 25 (1), 58–69.

Song, Z., Cai, J., Liu, Y., Zhao, D., Yong, J., Duo, S., Song, X., Guo, Y., Zhao, Y., Qin, H., et al. (2009). Efficient generation of hepatocyte-like cells from human induced pluripotent stem cells. *Cell Research*. 19 (11), 1233–1242.

Stambolic, V., Suzuki, A., la Pompa, de, J.L., Brothers, G.M., Mirtsos, C., Sasaki, T., Ruland, J., Penninger, J.M., Siderovski, D.P. and Mak, T.W. (1998). Negative regulation of PKB/Akt-dependent cell survival by the tumor suppressor PTEN. *Cell*. 95 (1), 29–39.

Stokoe, D., Stephens, L.R., Copeland, T., Gaffney, P., Reese, C.B., Painter, G.F., Holmes, AB, McCormick, F. and Hawkins, P.T. (1997). Dual role of phosphatidylinositol-3,4,5-trisphosphate in the activation of protein kinase B. *Science*. 277 (5325), 567–570.

Storm, M.P., Bone, H.K., Beck, C.G., Bourillot, P.-Y., Schreiber, V., Damiano, T., Nelson, A., Savatier, P. and Welham, M.J. (2007). Regulation of nanog expression by phosphoinositide 3-kinase-dependent signaling in murine embryonic stem cells. *The Journal of Biological Chemistry*. 282 (9), 6265–6273.

Strovel, E.T., Wu, D.Q. and Sussman, D.J. (2000). Protein phosphatase 2C alpha dephosphorylates axin and activates LEF-1-dependent transcription. *The Journal of Biological Chemistry*. 275 (4), 2399–2403.

Su, L.K., Vogelstein, B. and Kinzler, K.W. (1993) Association of the Apc Tumor-Suppressor Protein with Catenins. *Science*. 262 (5140), 1734–1737.

Sumi, T., Tsuneyoshi, N., Nakatsuji, N. and Suemori, H. (2008). Defining early lineage specification of human embryonic stem cells by the orchestrated balance of canonical Wnt/β-catenin, Activin/Nodal and BMP signaling. *Development*. 135 (17), 2969–2979.

Sun, P.D. and Davies, D.R. (1995). The Cystine-Knot Growth-Factor Superfamily. *Annual Review of Biophysics and Biomolecular Structure*. 24269–291.

Sund, N.J., Ang, S.L., Sackett, S.D., Shen, W., Daigle, N., Magnuson, M.A. and Kaestner, K.H. (2000). Hepatocyte nuclear factor 3β (Foxa2) is dispensable for maintaining the differentiated state of the adult hepatocyte. *Molecular and Cellular Biology*. 20 (14), 5175–5183.

Suzuki, A., Iwama, A., Miyashita, H., Nakauchi, H. and Taniguchi, H. (2003). Role for growth factors and extracellular matrix in controlling differentiation of prospectively isolated hepatic stem cells. *Development*. 130 (11), 2513–2524.

Suzuki, A., la Pompa, de, J.L., Stambolic, V., Elia, A.J., Sasaki, T., Barrantes, I.D., Ho, A., Wakeham, A., Itie, A., Khoo, W., et al. (1998). High cancer susceptibility and embryonic lethality associated with mutation of the PTEN tumor suppressor gene in mice. *Current Biology*. 8 (21), 1169–1178.

Suzuki, C., Murakami, G., Fukuchi, M., Shimanuki, T., Shikauchi, Y., Imamura, T. and Miyazono, K. (2002). Smurf1 regulates the inhibitory activity of Smad7 by targeting Smad7 to the plasma membrane. *The Journal of Biological Chemistry*. 277 (42), 39919–39925.

Tachibana, M., Sparman, M., Ramsey, C., Ma, H., Lee, H.-S., Penedo, M.C.T. and Mitalipov, S. (2012). Generation of Chimeric Rhesus Monkeys. *Cell*. 148 (1-2), 285–295.

Tada, M., Casey, E.S., Fairclough, L. and Smith, J.C. (1998). Bix1, a direct target of *Xenopus* T-box genes, causes formation of ventral mesoderm and endoderm. *Development*. 125 (20), 3997–4006.

Taelman, V.F., Dobrowolski, R., Plouhinec, J.-L., Fuentealba, L.C., Vorwald, P.P., Gumper, I., Sabatini D.D., de Robertis, E. M. (2010) Wnt signaling requires sequestration of glycogen synthase kinase 3 inside multivesicular endosomes. *Cell*. 143 (7), 1136–1148.

Tajima, Y., Goto, K., Yoshida, M., Shinomiya, K., Sekimoto, T., Yoneda, Y., Miyazono, K. and Imamura, T. (2003). Chromosomal region maintenance 1 (CRM1)-dependent nuclear export of Smad ubiquitin regulatory factor 1 (Smurf1) is essential for negative regulation of transforming growth factor-beta signaling by Smad7. *The Journal of Biological Chemistry*. 278 (12), 10716–10721.

Takahashi, K. and Yamanaka, S. (2006). Induction of pluripotent stem cells from mouse embryonic and adult fibroblast cultures by defined factors. *Cell*. 126 (4), 663–676.

Takashima, Y., Guo, G., Loos, R., Nichols, J., Ficz, G., Krueger, F., Oxley, D., Santos, F., Clarke, J., Mansfield, W., et al. (2014). Resetting Transcription Factor Control Circuitry toward Ground-State Pluripotency in Human. *Cell*. 158 (6), 1254–1269.

Tam, P.P.L., Khoo, P.-L., Lewis, S.L., Bildsoe, H., Wong, N., Tsang, T.E., Gad, J.M. and Robb, L. (2007). Sequential allocation and global pattern of movement of the definitive endoderm in the mouse embryo during gastrulation. *Development*. 134 (2), 251–260.

Taniguchi, K., Anderson, A.E., Sutherland, A.E. and Wotton, D. (2012). Loss of Tgif Function Causes Holoprosencephaly by Disrupting the Shh Signaling Pathway. *Plos Genetics*. 8 (2).

Tee, A.R., Manning, B.D., Roux, P.P., Cantley, L.C. and Blenis, J. (2003). Tuberous sclerosis complex gene products, tuberin and hamartin, control mTOR signaling by acting as a GTPase-activating protein complex toward Rheb. *Current Biology* 13 (15), 1259–1268.

Teo, A.K.K., Valdez, I.A., Dirice, E. and Kulkarni, R.N. (2014). Comparable Generation of Activin-Induced Definitive Endoderm via Additive Wnt or BMP Signaling in Absence of Serum. *Stem Cell Reports*. 3 (1).

Tesar, P.J., Chenoweth, J.G., Brook, F.A., Davies, T.J., Evans, E.P., Mack, D.L., Gardner, R.L. and McKay, R.D.G. (2007). New cell lines from mouse epiblast share defining features with human embryonic stem cells. *Nature*. 448 (7150), 196–U10.

Theunissen, T.W., Powell, B.E., Wang, H., Mitalipova, M., Faddah, D.A., Reddy, J., Fan, Z.P., Maetzel, D., Ganz, K., Shi, L., et al. (2014). Systematic Identification of Culture Conditions for Induction and Maintenance of Naive Human Pluripotency. *Stem Cell*. 15 (4), 471–487.

Thomson, J.A., Itskovitz-Eldor, J., Shapiro, S.S., Waknitz, M.A., Swiergiel, J.J., Marshall, V.S. and Jones, J.M. (1998). Embryonic stem cell lines derived from human blastocysts. *Science*. 282 (5391), 1145–1147.

Thomson, J.A., Kalishman, J., Golos, T.G., Durning, M., Harris, C.P., Becker, R.A. and Hearn, J.P. (1995). Isolation of a Primate Embryonic Stem-Cell Line. *Proceedings of the National Academy of Sciences of the United States of America*. 92 (17), 7844–7848.

Touboul, T., Hannan, N.R.F., Corbineau, S., Martinez, A., Martinet, C., Branchereau, S., Mainot, S., Strick-Marchand, H., Pedersen, R., Di Santo, J., et al. (2010). Generation of Functional Hepatocytes from Human Embryonic Stem Cells Under Chemically Defined Conditions that Recapitulate Liver Development. *Hepatology (Baltimore, Md.)*. 51 (5), 1754–1765.

Traynorkaplan, A.E., Harris, A.L., Thompson, B.L., Taylor, P., and Sklar, L.A. (1988). An Inositol Tetrakisphosphate-Containing Phospholipid in Activated Neutrophils. *Nature*. 334 (6180), 353–356.

Tremblay, F. and Marette, A. (2001). Amino acid and insulin signaling via the mTOR/p70 S6 kinase pathway. A negative feedback mechanism leading to insulin resistance in skeletal muscle cells. *The Journal of Biological Chemistry*. 276 (41), 38052–38060.

Tsukazaki, T., Chiang, T.A., Davison, A.F., Attisano, L. and Wrana, J.L. (1998). SARA, a FYVE domain protein that recruits Smad2 to the TGFβ receptor. *Cell*. 95 (6), 779–791.

Vallier, L., Alexander, M. and Pedersen, R.A. (2005) Activin/Nodal and FGF pathways cooperate to maintain pluripotency of human embryonic stem cells. *Journal of Cell Science*. 118 (19), 4495–4509.

Vallier, L., Mendjan, S., Brown, S., Chng, Z., Teo, A., Smithers, L.E., Trotter, M.W.B., Cho, C.H.-H., Martinez, A., Rugg-Gunn, P., et al. (2009). Activin/Nodal signalling maintains pluripotency by controlling Nanog expression. *Development*. 136 (8), 1339–1349.

Vander Haar, E., Lee, S.-I., Bandhakavi, S., Griffin, T.J., and Kim, D.-H. (2007). Insulin signalling to mTOR mediated by the Akt/PKB substrate PRAS40. *Nature Cell Biology*. 9 (3), 316–U126.

Villegas, S.N., Rothova, M., Barrios-Llerena, M.E., Pulina, M., Hadjantonakis, A.-K., Le Bihan, T., Astrof, S. and Brickman, J.M. (2013). PI3K/Akt1 signalling specifies foregut precursors by generating regionalized extra-cellular matrix. *Elife*. 2.

Vincent, S.D., Dunn, N.R., Hayashi, S., Norris, D.P. and Robertson, E.J. (2003). Cell fate decisions within the mouse organizer are governed by graded Nodal signals. *Genes & Development*. 17 (13), 1646–1662.

Vlahos, C.J., Matter, W.F., Hui, K.Y. and Brown, R.F. (1994). A Specific Inhibitor of Phosphatidylnositol 3-Kinase, 2-(4-Morpholinyl)-8-Phenyl-4h-1-Benzopyran-4-One (LY294002). *The Journal of Biological Chemistry*. 269 (7), 5241–5248.

Vogt, J., Traynor, R. and Sapkota, G.P. (2011). The specificities of small molecule inhibitors of the TGFß and BMP pathways. *Cellular Signalling*. 23 (11), 1831–1842.

Wang, Z., Oron, E., Nelson, B., Razis, S. and Ivanova, N. (2012). Distinct Lineage Specification Roles for NANOG, OCT4, and SOX2 in Human Embryonic Stem Cells. *Stem Cell*. 10 (4), 440–454.

Watabe, T., Kim, S., Candia, A., Rothbächer, U., Hashimoto, C., Inoue, K. and Cho, K.W. (1995). Molecular mechanisms of Spemann's organizer formation: conserved growth factor synergy between *Xenopus* and mouse. *Genes & Development*. 9 (24), 3038–3050.

Watanabe, K., Ueno, M., Kamiya, D., Nishiyama, A., Matsumura, M., Wataya, T., Takahashi, J.B., Nishikawa, S., Nishikawa, S.-I., Muguruma, K., et al. (2007). A ROCK inhibitor permits survival of dissociated human embryonic stem cells. *Nat Biotech*. 25 (6), 681–686.

Watanabe, M., Masuyama, N., Fukuda, M. and Nishida, E. (2000). Regulation of intracellular dynamics of Smad4 by its leucine-rich nuclear export signal. *Embo Reports*. 1 (2), 176–182.

Watanabe, S., Umehara, H., Murayama, K., Okabe, M., Kimura, T. and Nakano, T. (2006). Activation of Akt signaling is sufficient to maintain pluripotency in mouse and primate embryonic stem cells. *Oncogene*. 25 (19), 2697–2707.

Weinstein, D.C., Altaba, A., Chen, W.S., Hoodless, P., Prezioso, V.R., Jessell, T.M. and Darnell, J.E. (1994). The Winged-Helix Transcription Factor Hnf-3-β Is Required for Notochord Development in the Mouse Embryo. *Cell*. 78 (4), 575–588.

Whitman, M., Downes, C.P., Keeler, M., Keller, T., and Cantley, L. (1988). Type-I Phosphatidylinositol Kinase Makes a Novel Inositol Phospholipid, Phosphatidylinositol-3-Phosphate. *Nature*. 332 (6165), 644–646.

Williams, R.L., Hilton, D.J., Pease, S., Willson, T.A., Stewart, C.L., Gearing, D.P., Wagner, E.F., Metcalf, D., Nicola, N.A. and Gough, N.M. (1988). Myeloid-Leukemia Inhibitory Factor Maintains the Developmental Potential of Embryonic Stem-Cells. *Nature*. 336 (6200), 684–687.

Wrighton, K.H., Willis, D., Long, J., Liu, F., Lin, X. and Feng, X.-H. (2006). Small C-terminal domain phosphatases dephosphorylate the regulatory linker regions of Smad2 and Smad3 to enhance transforming growth factor-beta signaling. *The Journal of Biological Chemistry*. 281 (50), 38365–38375.

Xiao, Z., Liu, X.D., Henis, Y.I. and Lodish, H.F. (2000). A distinct nuclear localization signal in the N terminus of Smad 3 determines its ligand-induced nuclear translocation. *Proceedings of the National Academy of Sciences of the United States of America*. 97 (14), 7853–7858.

Xu, L., Chen, Y.G. and Massague, J. (2000). The nuclear import function of Smad2 is masked by SARA and unmasked by TGFβ dependent phosphorylation. *Nature Cell Biology*. 2 (8), 559–562.

Xu, L., Kang, Y.B., Col, S. and Massague, J. (2002). Smad2 nucleocytoplasmic shuttling by nucleoporins CAN/Nup214 and Nup153 feeds TGFβ signaling complexes in the cytoplasm and nucleus. *Molecular Cell*. 10 (2), 271–282.

Xu, R.-H., Sampsell-Barron, T.L., Gu, F., Root, S., Peck, R.M., Pan, G., Yu, J., Antosiewicz-Bourget, J., Tian, S., Stewart, R., et al. (2008). NANOG is a direct target of TGFβ/Activin-mediated SMAD signaling in human ESCs. *Stem Cell*. 3 (2), 196–206.

Xu, R.H., Peck, R.M., Li, D.S., Feng, X.Z., Ludwig, T. and Thomson, J.A. (2005). Basic FGF and suppression of BMP signaling sustain undifferentiated proliferation of human ES cells. *Nature Methods*. 2 (3), 185–190.

Yagi, K., Goto, D., Hamamoto, T., Takenoshita, S., Kato, M. and Miyazono, K. (1999). Alternatively spliced variant of Smad2 lacking exon 3 - Comparison with wild-type Smad2 and Smad3. *The Journal of Biological Chemistry*. 274 (2), 703–709.

Yamamoto, M., Meno, C., Sakai, Y., Shiratori, H., Mochida, K., Ikawa, Y., Saijoh, Y. and Hamada, H. (2001). The transcription factor FoxH1 (FAST) mediates Nodal signaling during anterior-posterior patterning and node formation in the mouse. *Genes & Development*. 15 (10), 1242–1256.

Yang, H., Rudge, D.G., Koos, J.D., Vaidialingam, B., Yang, H.J. and Pavletich, N.P. (2013). mTOR kinase structure, mechanism and regulation. *Nature*. 497 (7448), 217–223.

Yang, Z.-Z., Tschopp, O., Di-Poï, N., Bruder, E., Baudry, A., Dümmler, B., Wahli, W.,and Hemmings, B.A. (2005). Dosage-dependent effects of Akt1/protein kinase Balpha (PKBalpha) and Akt3/PKBgamma on thymus, skin, and cardiovascular and nervous system development in mice. *Molecular and Cellular Biology*. 25 (23), 10407–10418.

Yeo, C.Y. and Whitman, M. (2001). Nodal signals to Smads through Cripto-dependent and Cripto-independent mechanisms. *Molecular Cell*. 7 (5), 949–957.

Ying, Q.-L., Wray, J., Nichols, J., Batlle-Morera, L., Doble, B., Woodgett, J., Cohen, P. and Smith, A. (2008). The ground state of embryonic stem cell self-renewal. *Nature*. 453 (7194), 519–523.

Ying, Q.L., Nichols, J., Chambers, I. and Smith, A. (2003). BMP induction of Id proteins suppresses differentiation and sustains embryonic stem cell self-renewal in collaboration with STAT3. *Cell*. 115 (3), 281–292.

Yoshizaki, T., Maegawa, H., Egawa, K., Ugi, S., Nishio, Y., Imamura, T., Kobayashi, T., Tamura, S., Olefsky, J.M. and Kashiwagi, A. (2004). Protein Phosphatase-2C alpha as a positive regulator of insulin sensitivity through direct activation of phosphatidylinositol 3-kinase in 3T3-L1 adipocytes. *The Journal of Biological Chemistry*. 279 (21), 22715–22726.

Zeng, X., Tamai, K., Doble, B., Li, S., Huang, H., Habas, R., Okamura, H., Woodgett, J. and He, X. A dual-kinase mechanism for Wnt co-receptor phosphorylation and activation. *Nature*. 438 (7069), 873-877.

Zhou, B.P., Liao, Y., Xia, W., Spohn, B., Lee, M.H. and Hung, M.C. (2001). Cytoplasmic localization of p21Cip1/WAF1 by Akt-induced phosphorylation in HER-2/neu-overexpressing cells. *Nature Cell Biology*. 3 (3), 245–252.

Zhou, J., Su, P., Wang, L., Chen, J., Zimmermann, M., Genbacev, O., Afonja, O., Horne, M.C., Tanaka, T., Duan, E., et al. (2009). mTOR supports long-term self-renewal and suppresses mesoderm and endoderm activities of human embryonic stem cells. *Proceedings of the National Academy of Sciences of the United States of America*. 106 (19), 7840–7845.

Zhou, S., Zawel, L., Lengauer, C., Kinzler, K. W. and Vogelstein., B. (199). Characterization of Human FAST-1, a TGFβ and Activin Signal Transducer. *Molecular Cell*. 2 (1), 121–127.

Zhou, X.L., Sasaki, H., Lowe, L., Hogan, B. and Kuehn, M.R. (1993). Nodal Is a Novel TGF-β-Like Gene Expressed in the Mouse Node During Gastrulation. *Nature*. 361 (6412), 543–547.

Zinzalla, V., Stracka, D., Oppliger, W. and Hall, M.N. (2011). Activation of mTORC2 by Association with the Ribosome. *Cell*. 144 (5), 757–768.

Zorn, A.M. (2008). *Liver development*. Cambridge (MA), Harvard Stem Cell Institute.

Appendix

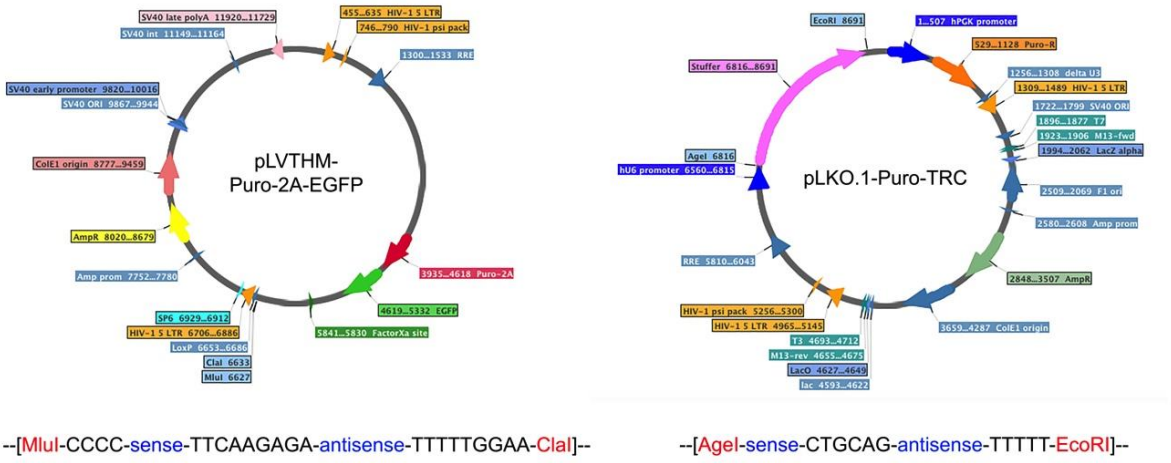

Figure A-I: Lentivectors and shRNA design

Cloning strategies and respective shRNA design templates for pLVTHM and pLKO.1 vectors used in this study. pLVTHM-Puro-2A-EGFP is a modified lentivector in which the Puro-2A-EGFP sequence from pHyg-Puro-2A-EGFP was subcloned to replace original EGFP sequence. MluI/ClaI double digestion was used to clone shRNA oligos into pLVTHM vectors whilst AgeI/EcoRI was used to clone into pLKO.1. Insertion was verified by sequencing and in the case of pLKO.1 vectors, assessed via digestion and loss of the stuffer fragment.

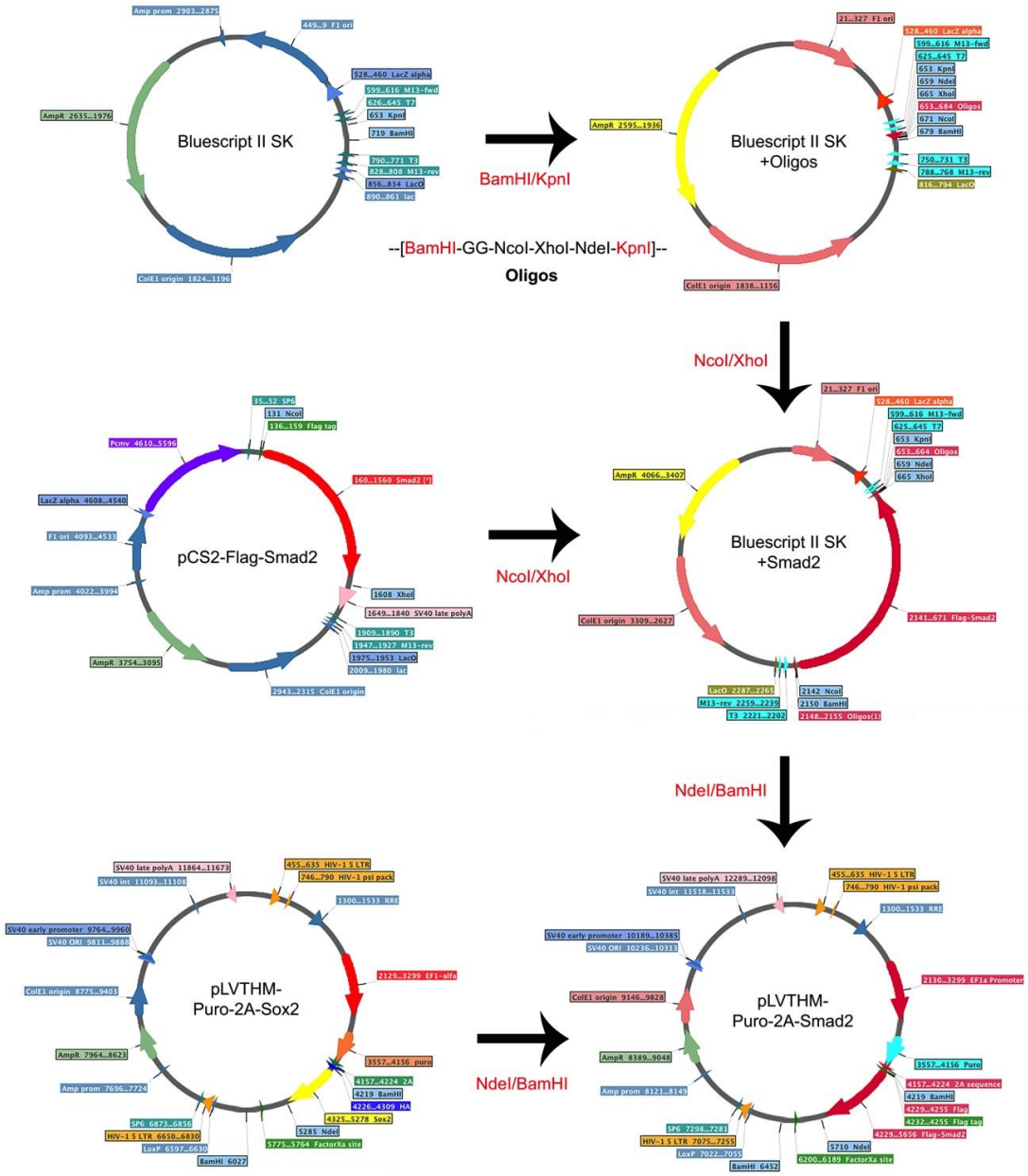

Figure A-II: Subcloning of pLVTHM-Puro-2A-Smad2-WT/T220V

Cloning strategy used to subclone Smad2-WT or Smad2-T220V coding DNA from the pCS2 expression vector into the lentiviral pLVTHM vector. Modification of the Bluescript II SK holding vector was first performed to prepare it for the insertion of the Smad2 fragment. Oligos (as indicated above) were annealed and ligated into the holding vector via BamHI/KpnI digestion. Oligos were designed contain a 2 bp GG insertion after the BamHI site to ensure the final Smad2 sequence will be in-frame after insertion into pLVTHM. After verification of oligo insertion via digestion, Smad2-WT/T220V fragment was ligated into the new holding vector following NcoI/XhoI digestion. Finally, the Smad2-WT/T220V fragment was further ligated into the pLVTHM-Puro-2A backbone via triple ligation following NdeI/BamHI digestion. Clones obtained from last step were screened for inversion using NdeI/FseI and NdeI/NotI digestion, and sequenced to ensure correct orientation of the fragments.

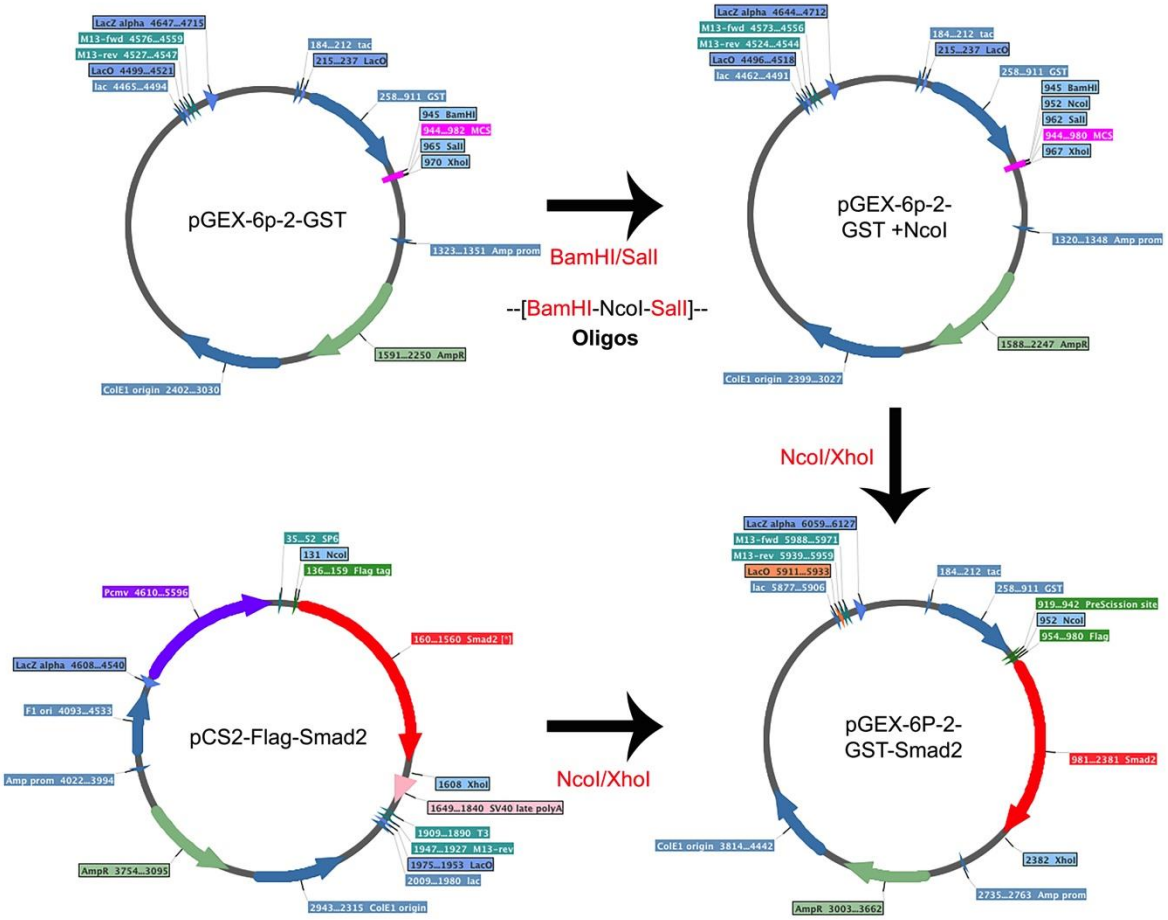

Figure A-III: Subcloning of pGEX-6p-GST-Smad2-WT/T220V

Cloning strategy used to subclone Smad2-WT or Smad2-T220V coding DNA from the pCS2 expression vector into the bacterial pGEX expression vector. Modification of the pGEX-6p-GST vector was first performed to prepare it for the insertion of the Smad2 fragment. Oligos (as indicated above) were annealed and ligated into the vector via BamHI/SalI digestion. Oligos were designed to contain an NcoI site to facilitate insertion of Smad2 fragment from pCS2 expression vector. After verification of oligo insertion via digestion, Smad2-WT/T220V fragment was ligated into the new holding vector following NcoI/XhoI digestion. Clones were screened by digestion, and sequenced to ensure correct insertion.

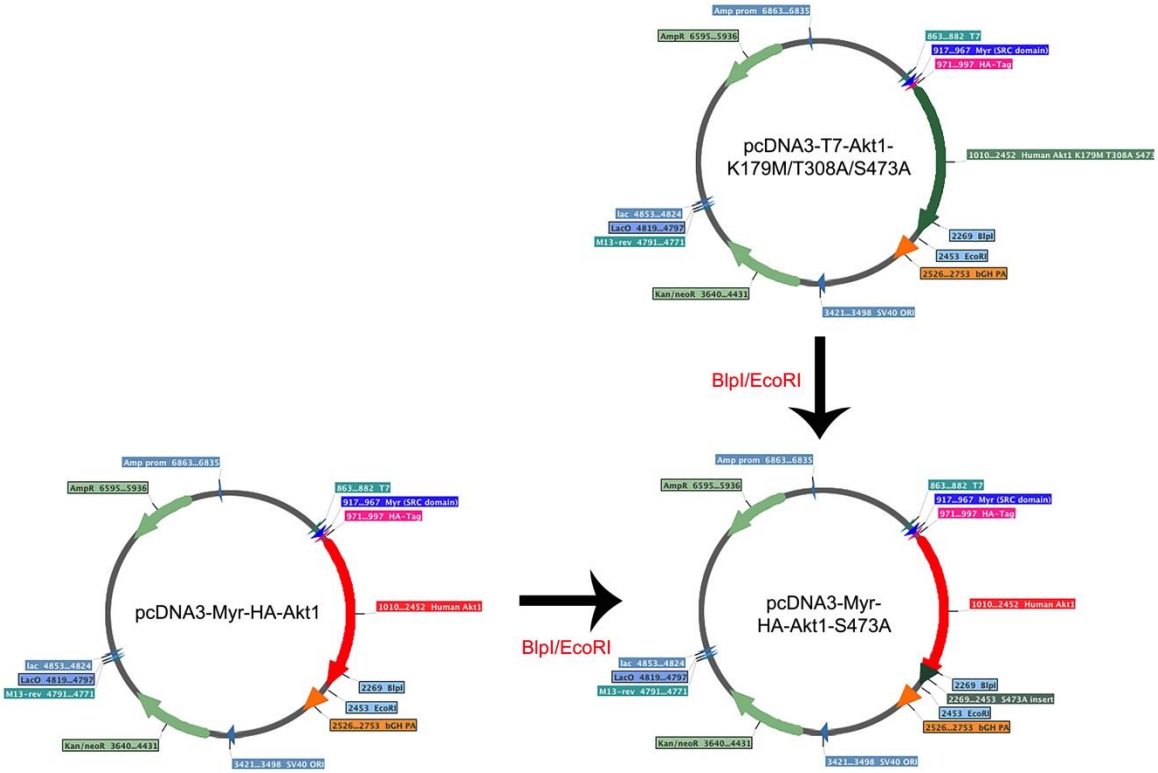

Figure A-IV: Subcloning of pcDNA3-T7-Myr-HA-AktI-S473A

Cloning strategy used to generate pcDNA-T7-Myr-HA-Akt-S473A from triple mutant and wild-type containing vector. Mutated S473 fragment was isolated from the triple mutant vector via Blp1/EcoRI digestion and switched with the opposing wild-type fragment for ligation to generate the final vector. Presence of mutated sequence was confirmed via sequencing.

Publications

Part of the work presented here has been published as follows:

Yu, J. S., Ramasamy, T. S., Murphy, N., Holt, M.K., Czapiewski, R., Wei, S. K., and Cui, W. (2015). PI3K/mTORC2 regulates TGF-β/Activin signalling by modulating Smad2/3 activity via linker phosphorylation. *Nature Communications*. 6, 7212.

nature COMMUNICATIONS

ARTICLE

Received 18 Dec 2014 | Accepted 20 Apr 2015 | Published 22 May 2015

DOI: 10.1038/ncomms8212 OPEN

PI3K/mTORC2 regulates TGF-β/Activin signalling by modulating Smad2/3 activity via linker phosphorylation

Jason S.L. Yu[1], Thamil Selvee Ramasamy[1,†], Nick Murphy[1], Marie K. Holt[1], Rafal Czapiewski[1], Shi-Khai Wei[1] & Wei Cui[1]

Crosstalk between the phosphatidylinositol 3-kinase (PI3K) and the transforming growth factor-β signalling pathways play an important role in regulating many cellular functions. However, the molecular mechanisms underpinning this crosstalk remain unclear. Here, we report that PI3K signalling antagonizes the Activin-induced definitive endoderm (DE) differentiation of human embryonic stem cells by attenuating the duration of Smad2/3 activation via the mechanistic target of rapamycin complex 2 (mTORC2). Activation of mTORC2 regulates the phosphorylation of the Smad2/3-T220/T179 linker residue independent of Akt, CDK and Erk activity. This phosphorylation primes receptor-activated Smad2/3 for recruitment of the E3 ubiquitin ligase Nedd4L, which in turn leads to their degradation. Inhibition of PI3K/mTORC2 reduces this phosphorylation and increases the duration of Smad2/3 activity, promoting a more robust mesendoderm and endoderm differentiation. These findings present a new and direct crosstalk mechanism between these two pathways in which mTORC2 functions as a novel and critical mediator.

[1] Department of Surgery and Cancer, Institute of Reproductive and Developmental Biology, Imperial College London, Du Cane Road, London W12 0NN, UK. [†] Present address: Department of Molecular Medicine, Faculty of Medicine, University of Malaya, 50603 Kuala Lumpur, Malaysia. Correspondence and requests for materials should be addressed to W.C. (email: wei.cui@imperial.ac.uk).

Cytokines of the transforming growth factor-β (TGF-β) superfamily including Nodal and Activin, control many cellular functions, such as cell growth, apoptosis and cell fate determination. These functions are not only controlled by the TGF-β pathway itself but are also extensively regulated by crosstalk between TGF-β and other signalling pathways[1–3]. TGF-β/Activin signalling is initiated upon ligand binding and activation of receptor complexes, which leads to the phosphorylation of the Smad2 and Smad3 (henceforth Smad2/3) C-terminal SxS motif, promoting their interaction with Smad4 and facilitating the translocation of the Smad2/3–Smad4 complexes to and accumulation within the nucleus where they regulate targeted gene expression in cooperation with other cofactors[4–6]. The efficacy of this pathway is not solely determined by the abundance of ligands and receptors but is also influenced by other signalling pathways[3]. Notably, the phosphatidylinositol 3-kinase (PI3K) pathway has been shown to alleviate TGF-β-induced apoptosis and cell cycle arrest in several tumour cell lines[7–10], as well as inhibiting the Activin-induced DE differentiation of human embryonic stem cells (hESCs)[11–13]. However, the molecular mechanisms behind these effects remain contentious[8–10]. Although it has recently been proposed that the negative effects of PI3K upon DE differentiation are an indirect effect attributed to the inhibition of the Wnt-β-catenin pathway[14], it is unclear how this mechanism results in enhanced Smad2/3 activity, thereby positing the existence of a more direct relationship between these two pathways[15].

In this study, we demonstrate that PI3K signalling has a direct inhibitory effect on Activin-induced Smad2/3 activity in hESCs via the activation of mechanistic target of rapamycin complex 2 (mTORC2), leading to a reduction of Smad2/3 transcriptional activity and DE differentiation efficacy. PI3K/mTORC2 negatively regulates Smad2/3 activity by modulating their degradation via phosphorylation of a particular threonine residue within the Smad2/3 linker region. Our results therefore demonstrate a new and novel mechanism underpinning the crosstalk between the PI3K/mTOR and TGF-β/Activin signalling axes and in particular, firmly establishes mTORC2 as a critical mediator in modulating Smad2/3 activity.

Results

PI3K inhibits Activin-induced DE differentiation of hESCs. To decipher the mechanisms underlying the antagonistic impact of the PI3K pathway upon TGF-β/Activin activities and the DE differentiation of hESCs, we developed a serum-free and chemically defined culture condition to convert hESCs to DE, in which high-dosage Activin A (henceforth AA) was shown to enhance the activation of Smad2/3 signalling and DE differentiation as previously reported (Supplementary Fig. 1a; Fig. 1a)[11,12,16]. Under this culture condition, treatment of hESCs with LY294002 (LY), a PI3K inhibitor, diminished Akt activation even in the presence of AA (Fig. 1b). In comparison with the differentiation using AA alone, co-treatment of hESCs with AA and LY evidently enhanced the Activin-induced DE differentiation as shown by a higher expression of mesendoderm and DE markers (Fig. 1c–f). This LY-dependent enhancement of DE differentiation was further corroborated by an increase in the generation of functional hepatocyte-like cells and in multiple hESC lines (Fig. 1g; Supplementary Fig. 1b,c). Therefore, this chemically defined culture system provides a useful platform from which to further interrogate the underlying molecular mechanisms driving the improvement of DE specification.

Inhibiting PI3K prolongs Activin-induced Smad2/3 activation. To interrogate the mechanisms through which PI3K signalling interferes with TGF-β activities, we first evaluated the activation status of Smad2/3 under AA ± LY conditions. Time-course analysis revealed that although LY treatment had no effect on the initial activation of Smad2/3 (Smad2/3-pTail), the decline of active Smad2/3 was clearly attenuated in AA–LY-treated cells compared with cells treated with AA alone (Fig. 2a), resulting in a marked increase of active Smad2/3 six hours post treatment (Fig. 2b). AA–LY-treated cells also exhibited a significant increase in Smad2/3 transcriptional activity evidenced by higher luciferase reporter activity (Fig. 2c) and a considerable upregulation of mesendoderm markers MixL1, Eomes and goosecoid and DE marker Sox17, which are known Smad2/3 targets (Fig. 2d)[1,17,18]. This finding implies preferential specification of the cells towards the mesendoderm and DE even at this early stage of differentiation. Furthermore, to rule out the possibility that these enhancements were due to any off-target effects of LY, we treated hESCs with two other PI3K inhibitors in the place of LY, the more commonly used wortmannin and the more selective Pictilisib (also known as GDC-0941). Both experiments largely replicated the changes observed using AA–LY treatment (Supplementary Fig. 2) Therefore, inhibition of PI3K directly enhances Activin-induced DE formation by extending the duration of Smad2/3 activity.

PI3K modulates ubiquitination and degradation of Smad2/3. Since inhibition of PI3K extended the duration of Smad2/3 activation rather than altering their initial response to AA, we reasoned that PI3K signalling might affect Smad2/3 activity by regulating its turnover, either via phosphatase-mediated dephosphorylation of the SxS motif or by ubiquitin-mediated proteasomal degradation of the active Smad2/3 protein[2]. Until recently, nuclear PPM1A was the only phosphatase identified to dephosphorylate Smad2/3 at the SxS motif[19], which is inhibited by CLIC4 (chloride intracellular channel 4) protein[20]. However, not only did LY treatment not affect the expression of either protein, PPM1A was also detected primarily in the cytoplasm (Supplementary Fig. 3a,b). It is therefore unlikely that Smad2/3 dephosphorylation by PPM1A is the mechanism accounting for the phenotypic changes associated with AA–LY treatment. Although one recent study has shown that PP5, a member of the PPP phosphatase family, is able to dephosphorylate active Smad2/3 upon overexpression[21], treatment of hESCs with okadaic acid, a potent inhibitor of PPP phosphatases, had no effect on the decay kinetics of active Smad2 (Supplementary Fig. 3c). Furthermore, enhanced TGF-β-induced transcriptional responses that were observed in PP5-null mice has been shown to result from increased levels of Smad3 protein rather than through any direct effect upon the duration of their activation[21]. These findings therefore further discount the involvement of phosphatases in our underlying mechanism.

Given that ubiquitin-mediated proteasomal degradation is another mechanism by which Smad2/3 activity is terminated[22], we next investigated whether LY acts to protect active Smad2 from proteasomal degradation. Similar decay kinetics for active Smad2 was observed between LY- and MG132-treated cells, albeit not with the same efficacy (Fig. 3a–c). In addition, inhibition of the Activin receptor by SB431542 did not abolish the effect of LY, but rather made it observable much earlier at 1 h post treatment (Fig. 3b). Together, this suggests that PI3K affects the TGF-β/Activin pathway independent of receptor activity and acts to promote the ubiquitin-mediated proteasomal degradation of active Smad2/3. Although Nedd4L has been previously identified as the ubiquitin ligase responsible for Smad2/3 ubiquitination[23], we observed no LY-dependent changes in its expression (Supplementary Fig. 3d). However, LY treatment substantially

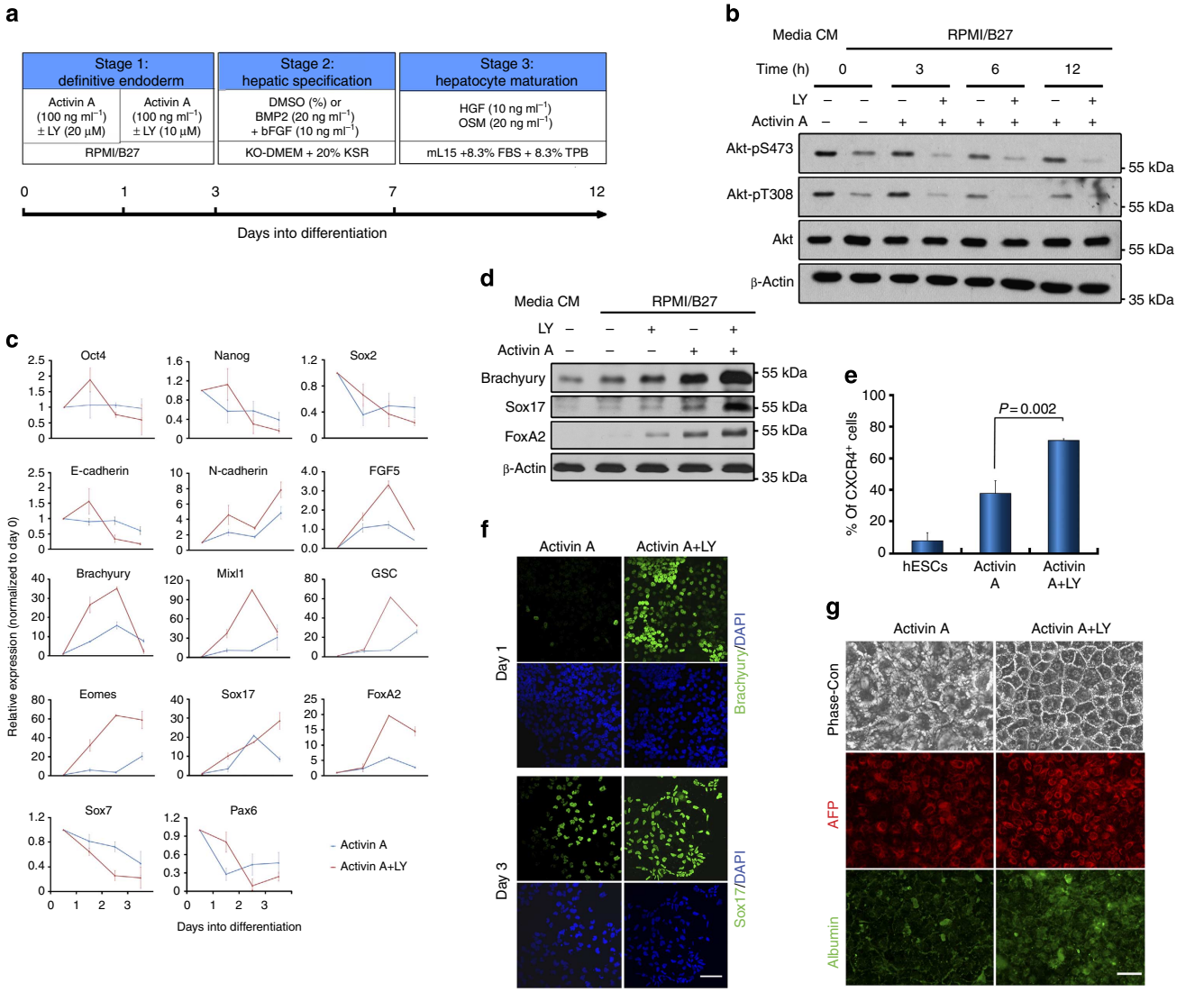

Figure 1 | Inhibition of PI3K signalling promotes differentiation of hESCs to the definitive endoderm (DE). (**a**) Schematic illustrating the DE and hepatocyte differentiation protocol. (**b**) H1 hESCs cultured in MEF-CM (CM) were transferred into defined medium, RPMI/B27, for 1 h (time 0) prior to treatment with Activin A ± LY294002 (LY). Cell lysates were collected at indicated time points and analysed by immunoblot. (**c**) Gene expression analysis by qRT–PCR in Activin A-treated hESCs with (red line) or without (blue line) LY. Data represent mean ± s.d. from six measurements of two independent differentiations. (**d**) Immunoblot showing mesendoderm marker expression in hESCs treated for 24 h with indicated factors. (**e**) Percentage of CXCR4-positive cells by flow cytometry in hESCs with or without indicated treatment for 3 days. Data represent mean ± s.d. from three independent biological samples. *P* value was calculated using the Student's *t*-test. (**f**) Immunostaining with Brachyury and Sox17 antibodies in hESCs treated as indicated. Scale bar, 50 μm. (**g**) hESCs were initially treated with Activin A ± LY and then further differentiated to hepatocytes. Phase-contrast images (Phase-con) and immunostaining with AFP and albumin antibodies are presented. Scale bar, 50 μm.

reduced its interaction with Smad2 (Fig. 3d), which was corroborated by decreased ubiquitination of Smad2 (Fig. 3e). These results therefore highlight the critical role PI3K signalling plays in regulating the association of Nedd4L with Smad2/3, which in turn, dictates the duration and efficacy of Smad2/3 activity.

PI3K primes Smad2/3 interaction with Nedd4L via pT220/T179. Although activation of TGF-β/Activin signalling is primarily determined by the receptor-mediated phosphorylation of Smad2/3 C-terminal SxS motif that induces their accumulation within the nucleus, it is increasingly apparent that the linker region of Smad2/3 serves a critical site through which their activity is regulated. This region contains multiple S/T residues, which are targeted by various S/T kinases stemming from other signalling pathways[24–28]. Phosphorylation of these residues alters the interaction of Smad2/3 with other proteins, which subsequently affects Smad2/3 stability, translocation and transcriptional activity[3,23,29,30]. Recruitment of Nedd4L to Smad2/3 was shown to be dependent on the phosphorylation status of their linker T220/T179 residue, which lies directly upstream of the PPXY-binding motif (Fig. 4a)[23]. Therefore, we anticipated that PI3K signalling might affect Smad2/3 degradation through altering the phosphorylation of this residue. Indeed, LY treatment significantly reduced the phosphorylation of T220/T179, irrespective of Smad2/3 activation, but had negligible effects on the other linker serine residues in both hESC and tumour cell lines (Fig. 4b–d; Supplementary Fig. 4a–e). This suggests that Smad2/3 linker threonine and serine residues are differentially regulated, with PI3K specifically modulating the phosphorylation of the

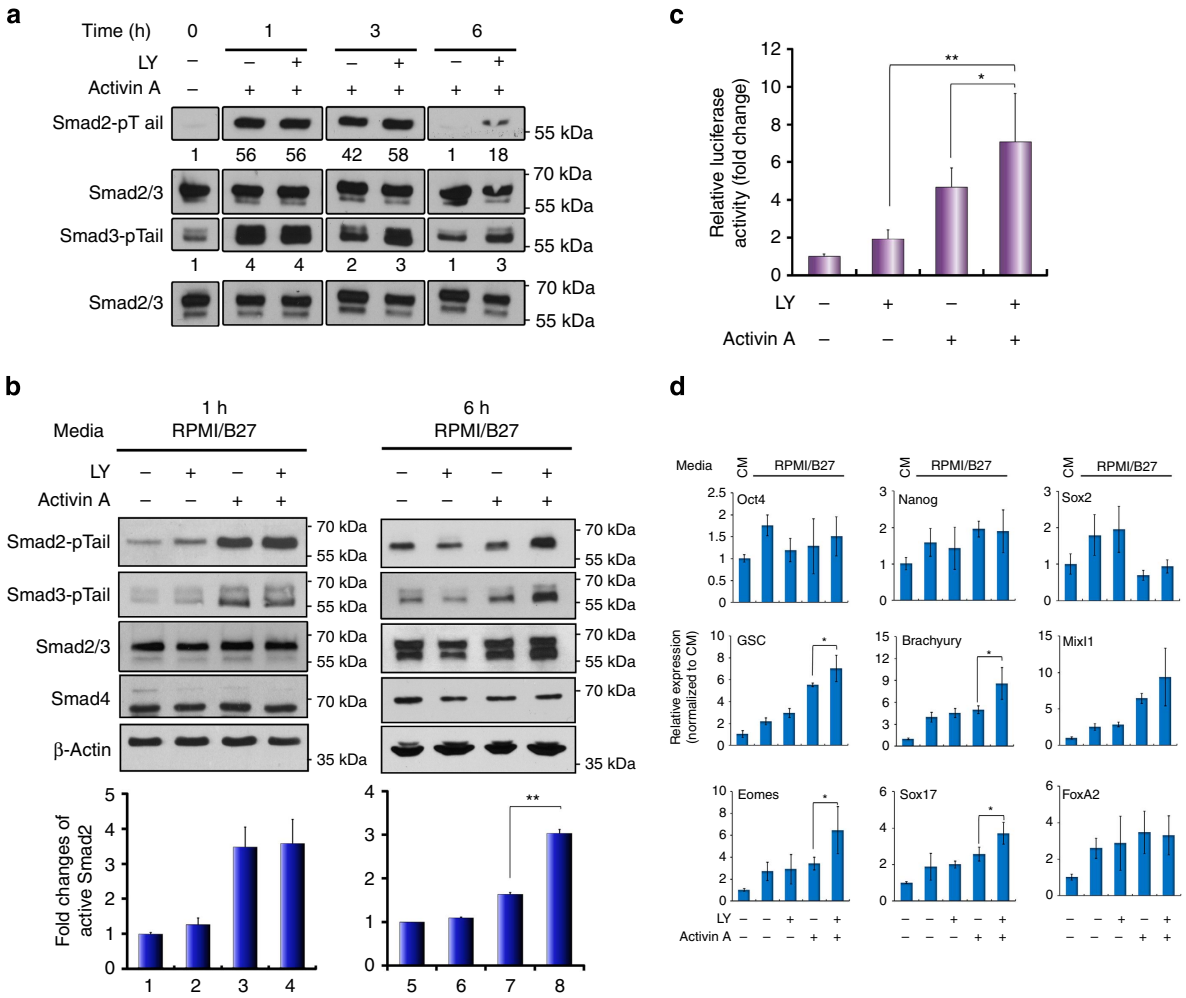

Figure 2 | Suppression of PI3K signalling prolongs Activin-induced Smad2/3 activity. (**a**,**b**) hESCs were treated with Activin A or/and LY for the indicted time points before being subjected to immunoblotting analysis. Numbers in **a** represent the quantification of activated Smad2 and Smad3. Upper panels in **b** are representative immunoblot and lower panels are histograms of densitometric measurements from three independent biological samples. (**c**) Luciferase assay in hESCs co-transfected with pGL3-CAGA$_{12}$-luc and renilla constructs and treated for 6 h. Data show mean ± s.d. of three independent transfection experiments. (**d**) Messenger RNA expression of indicated markers by qRT-PCR. Bar graphs indicate fold induction. Data represent mean ± s.d. of six measurements from two independent experiments. $^{**}P<0.001$ and $^{*}P\leq0.05$ by the Student's *t*-test. LY, LY294002.

T220/T179 linker residue. Our results also demonstrate that PI3K-mediated phosphorylation of this residue can occur in the absence of Smad2/3 activation (Fig. 5a,d), which raised the question as to whether Nedd4L binds to both active and inactive Smad2/3 or solely to the active form. To address this, PC3 cells, which retain high levels of PI3K signalling even after overnight starvation due to the presence of a PTEN mutation, were used for Nedd4L co-immunoprecipitation experiments upon treatment with AA ± LY post starvation. This showed that Nedd4L recruitment and ubiquitination of Smad2/3 occurred most effectively only when both T220/T179 and SxS residues were phosphorylated (Fig. 4e), offering an explanatory mechanism by which Nedd4L selectively targets active Smad2/3 for ubiquitination and turnover.

We hence postulated that PI3K promotes phosphorylation of Smad2/3-T220/T179 and primes Smad2/3 for the binding of Nedd4L upon activation, resulting in increased ubiquitin-mediated Smad2/3 degradation, which acts to reduce the transcriptional activation of endoderm genes. If this is correct, mutagenesis of T220/T179 to a non-phosphorylatable residue should enhance the resistance of Smad2/3 to degradation independent of LY. To test this, we ectopically expressed wild-type (WT) or T220V mutant Smad2 in hESCs and PC3 cells. PC3 cells expressing Smad2-T220V showed higher Smad2/3 activation upon AA stimulation irrespective of whether LY was present (Fig. 4f) and correspondingly, hESCs expressing Smad2-T220V exhibited improved mesendoderm differentiation in response to AA alone (Fig. 4g). In further support of the view that Nedd4L-mediated degradation of active Smad2/3 accounts for the inhibitory effect of PI3K during Activin-induced DE differentiation, Nedd4L knockdown in PC3 cells resulted in increased Smad2/3 activation in the absence of LY (Fig. 4h; Supplementary Fig. 4f), while Nedd4L-deficient hESCs expressed endoderm genes at much higher levels upon AA stimulation (Fig. 4i). Taken together, PI3K signalling therefore inhibits Activin-induced DE differentiation by phosphorylating the T220/T179 of Smad2/3, enabling the recruitment of Nedd4L upon their activation, which leads to the degradation and termination of active Smad2/3.

Smad2/3-pT220/pT179 is a direct effect of PI3K activity. Although many kinases including Erk (extracellular-signal-regulated kinases), p38 and CDK (cyclin-dependent kinase) have

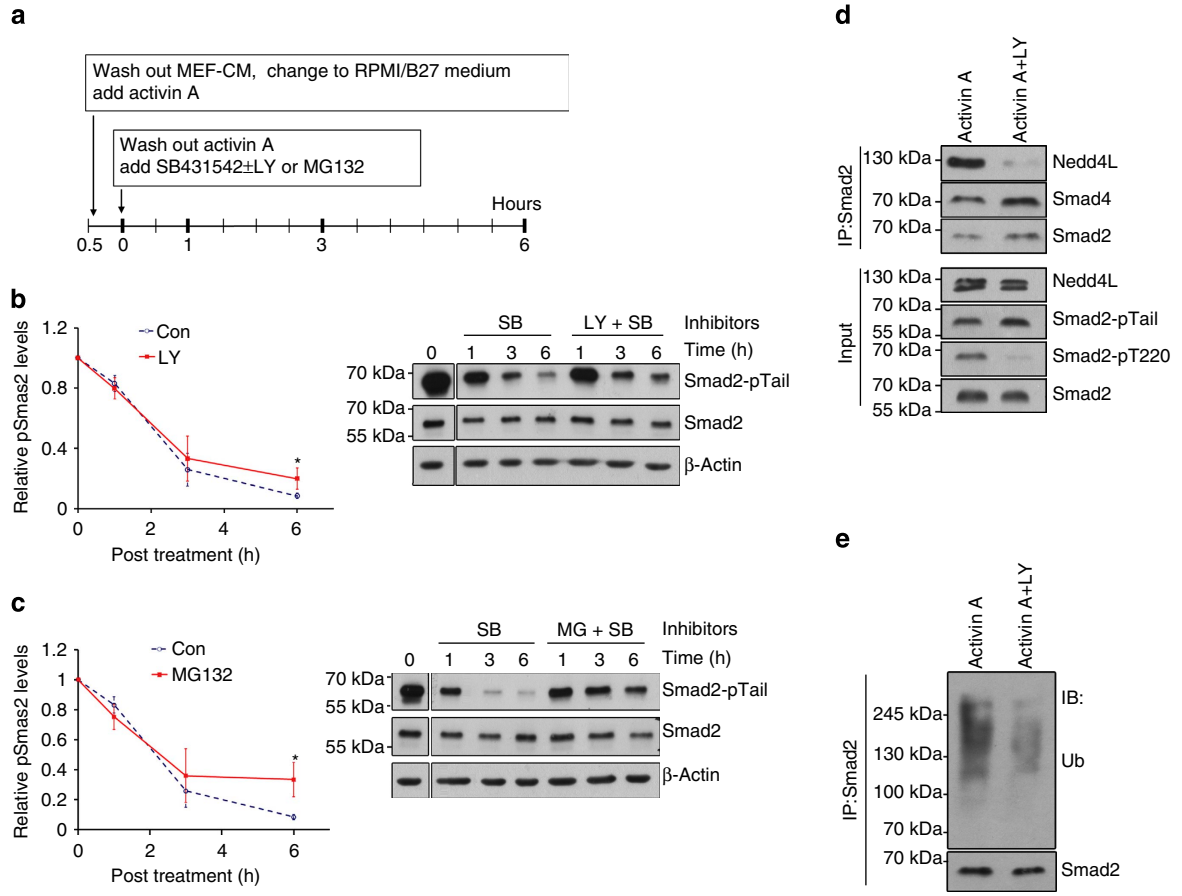

Figure 3 | Inhibition of PI3K reduces Smad2/3 interaction with Nedd4L and subsequent ubiquitination. (**a**) Scheme of treatment for **b** and **c**. (**b**,**c**) Representative immunoblot (right) and quantifications (left) of activated Smad2 (Smad2-pTail) in hESCs treated as illustrated in **a** with SB ± LY (**b**) or SB ± MG132 (**c**). Graphs represent mean ± s.d. from three independent experiments. (**d**,**e**) hESCs treated with Activin A ± LY for 1 h were analysed by Smad2 co-immunoprecipitation with indicated antibodies. *$P \leq 0.05$ by the Student's *t*-test. SB, SB431542; LY, LY294002; MG, MG132; Ub, ubiquitin.

been shown to phosphorylate Smad2/3 linker residues[24,26,27,30], inhibitors that specifically target these kinases were less effective in suppressing T220/T179 phosphorylation when compared with LY (Fig. 5a,b; Supplementary Fig. 5a). Notably, flavopiridol-mediated inhibition of CDKs only diminished the phosphorylation of the linker serine residues, whereas the T220/T179 residue was unaffected. Furthermore, PI3K-mediated phosphorylation of T220/T179 requires neither Smad2/3 activation nor nuclear localization, which thereby eliminates the direct involvement of CDK in causing this effect. Although active Erk can phosphorylate the T220/T179 residue, inhibition of PI3K elicited a greater reduction in T220/T179 phosphorylation than that of MAPK/Erk inhibition. In addition, LY treatment did not inhibit, but rather increased Erk activation under certain conditions (Fig. 5c; Supplementary Fig. 5a–c)[14], which therefore excludes the possibility of LY-induced downregulation of T220/T179 phosphorylation being an Erk-related event. Furthermore, treatment of hESCs in RPMI base media along with heregulin and IGF-1 (HI), two potent stimulators of the PI3K pathway, increased T220/T179 phosphorylation (Fig. 5d), suggesting that this phosphorylation is regulated by the PI3K pathway itself independent of Erk and CDK activity.

Since Akt is one of the principal kinases acting downstream of PI3K, we next investigated whether Akt was responsible for T220/T179 phosphorylation by ectopically expressing constitutively active (Myr-Akt-WT), partially active (S473A) and inactive (K179M/T308A/S473A) Akt in Hep3B cells, using green fluorescent protein (GFP)-expressing Hep3B as controls. In comparison with the marked upregulation and reduction of T220/T179 phosphorylation observed in control cells upon heregulin and IGF-1 and LY treatment, respectively, expression of Akt possessing varying states of activation had negligible impact on T220/T179 phosphorylation (Fig. 5e), suggesting that Akt is not directly responsible for this phosphorylation. This was further confirmed by an *in vitro* kinase assay that demonstrated the inability of fully active Akt to phosphorylate this residue (Fig. 5f), which is consistent with previous findings[8–10].

mTORC2 induces the phosphorylation of Smad2/3-T220/T179. The mTOR branches of the PI3K signalling pathway acts to regulate cell growth, differentiation and metabolism. mTOR is the kinase component of two distinct multi-protein complexes, mTORC1 and mTORC2, which differ not only in their constituent components, but also in their response to rapamycin[31]. mTORC1 contains an adaptor protein, raptor, as a key subunit, while mTORC2 comprises rictor as its novel component; while mTORC1 activity is rapidly inhibited by rapamycin, mTORC2 is more resistant to acute rapamycin exposure[32]. To investigate whether mTOR complexes are involved in Smad2/3 regulation, PC3 cells were treated with AA in the presence of rapamycin or Torin-2 (henceforth Torin), an mTOR inhibitor that inhibits both complexes. While rapamycin showed no obvious effects on both Smad2 activation and T220/T179 phosphorylation (Fig. 6a), Torin treatment mimicked that of LY in prolonging Smad2 activation and inhibiting T220/T179 phosphorylation (Fig. 6b),

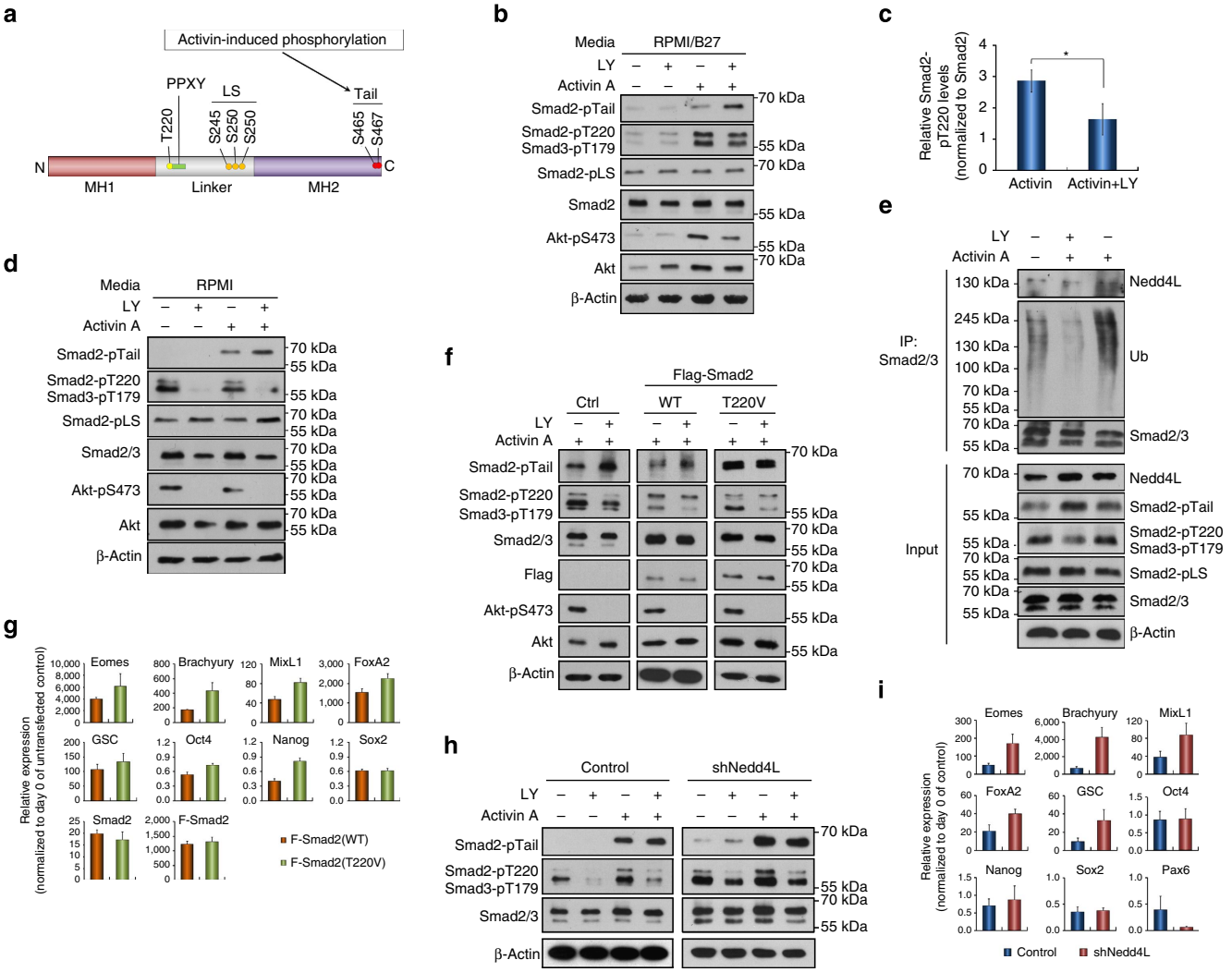

Figure 4 | PI3K regulates Nedd4L-mediated Smad2/3 degradation via phosphorylation of the T220/T179 linker residue. (**a**) A schematic illustrating structural domains of Smad2 protein. The C-terminal and linker phosphorylation sites as well as the E3 ubiquitin ligase-binding PPXY motif are indicated. (**b**,**c**) Representative immunoblot (**b**) and quantification (**c**) showing significant reduction of Smad2-pT220 in hESCs at 6 h post treatment with Activin A + LY. Data in **c** represent mean ± s.d. from three independent experiments. *$P<0.05$ (Student *t*-test). (**d**) Immunoblot showing that PC3 cells exhibited a similar pattern of Smad2 phosphorylation at various residues as that of hESCs in response to Activin ± LY treatment after overnight starvation. (**e**) Nedd4L-mediated Smad2/3 ubiquitination requires phosphorylation at both linker T220/T179 and C-terminal SxS sites. PC3 cells were treated with Activin A ± LY for 1 h, with MG132 added into the cultures 30 min prior to lysis. Smad2/3 immunoprecipitates were analysed by immunoblotting with indicated antibodies. (**f**) Immunoblot showing that Smad2-T220V mutant abolished the effect of LY on Activin-induced Smad2 activation. PC3 cells expressing Flag-tagged WT or T220V mutant (T220V) Smad2 were starved overnight, followed by treatment for 1 h with Activin A ± LY. (**g**) qRT-PCR showing that hESCs expressing Smad2-T220V gave rise to higher levels of DE gene expression in response to Activin A. (**h**) Knockdown of Nedd4L in PC3 cells abolished the effect of LY on Activin-induced Smad2 activation. (**i**) qRT-PCR showing hESCs of Nedd4L knockdown exhibiting higher DE gene expression. hESCs in **g** and **i** were treated with Activin A for 2 days before the analysis, and data represent mean ± s.d. from at least six measurements of two independent experiments.

thereby suggesting that mTORC2, rather than mTORC1, is involved in the regulation of Smad2/3 activity. In support of this notion, phosphorylation of T220/T179 was shown to be downregulated in rictor knockdown PC3 cells (Fig. 6c) and this reduction of pT220/pT179 appeared more evident in MEFs (mouse embryonic fibroblasts) that were derived from rictor null mice (Fig. 6d)[33]. The difference between rictor knockdown and rictor null cells could be due to the incomplete removal of rictor in the former as we have shown that PI3K/mTORC2-dependent phosphorylation of T220/179 is highly sensitive to any trace amount of PI3K/mTORC2 activity (Fig. 5d vs Supplementary Fig. 5b). Furthermore, this downregulation of T220/T179 phosphorylation in rictor null cells was fully rescued by the ectopic expression of human rictor (Fig. 6d), highlighting the important role mTORC2 plays in regulating Smad2/3-T220/T179 phosphorylation. Moreover, hESCs expressing rictor short hairpin RNA (shRNA) exhibited improved DE differentiation in response to AA treatment evidenced by rapid morphological changes and increased expression of DE markers, effects that are reminiscent of those observed upon AA–LY treatment (Fig. 6e,f). Therefore, these results suggest that mTORC2 plays an important role in modulating Activin-induced Smad2/3 activity by modifying the phosphorylation of the Smad2/3 linker T220/T179 residue. Intriguingly, immunoprecipitated mTORC2 was unable to phosphorylate Smad2-T220 in an *in vitro* kinase reaction (Fig. 6g), while inhibition of SGK1, one of the limited

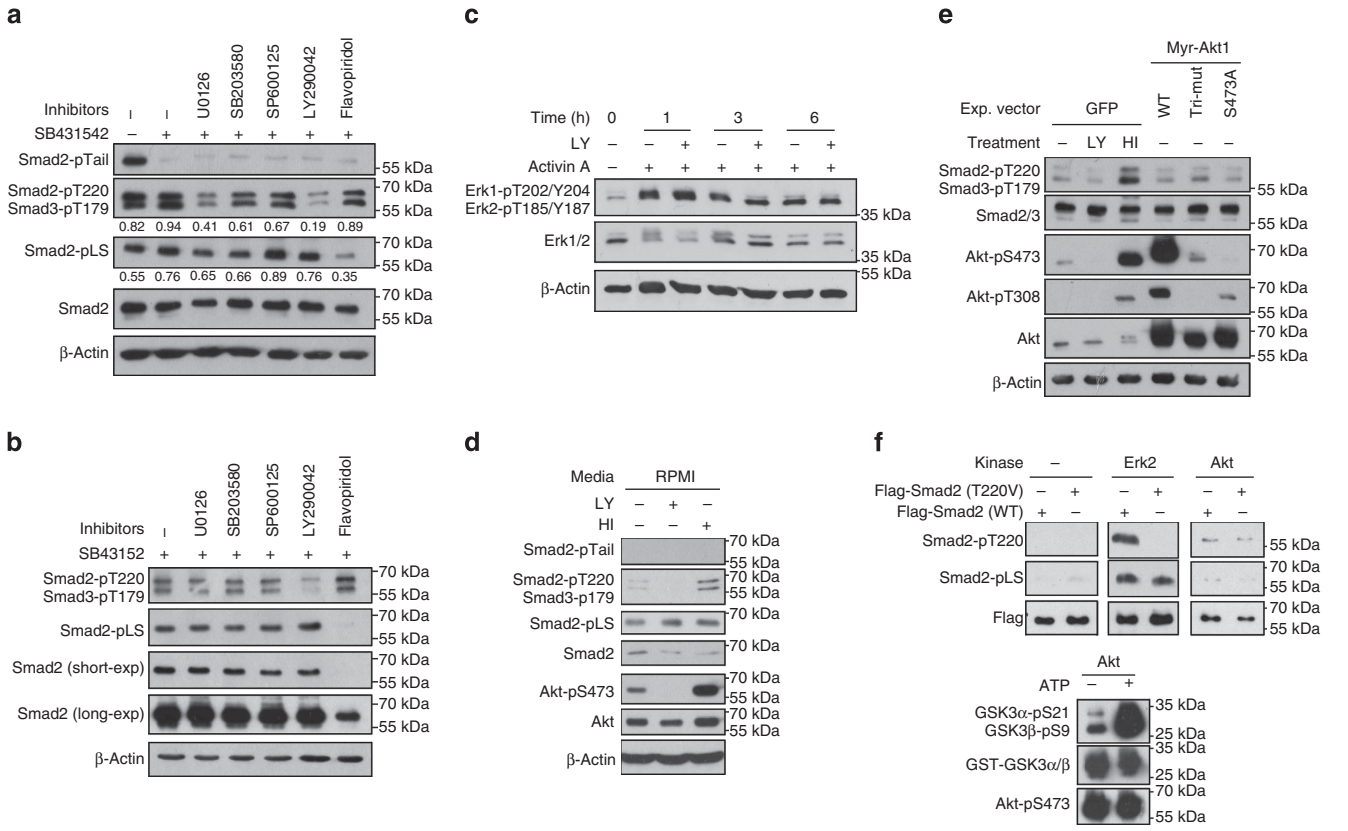

Figure 5 | Phosphorylation of Smad2/3 linker residues are differentially regulated by various signalling pathways. (**a**,**b**) Immunoblot of Smad2/3 phosphorylation in hESCs that were pre-treated with Activin A, then incubated with indicated inhibitors for 1 h (**a**) or 6 h (**b**). (**c**) Immunoblot with Erk1/2 antibodies on cell extracts from hESCs with indicated treatments. (**d**) hESCs were starved for1 h in RPMI medium followed by treatment with either LY or HI for 1 h before being analysed by immunoblotting. (**e**) Hep3B cells transiently expressing either green fluorescent protein (GFP) or the various forms of Akt as indicated were starved overnight while GFP-expressing cells were treated with either LY or HI for 1 h before harvest for immunoblot. (**f**) *In vitro* kinase assay. Active Akt was isolated from PC3 cells by immunoprecipitation and incubated with recombinant GST-Flag-tagged wild-type (WT) or T220V mutant Smad2 in the presence of ATP. The protein mixtures were then resolved by SDS–polyacrylamide gel electrophoresis and analysed by immunoblotting with indicated antibodies. Commercially bought Erk2 and GST-GSK3 were used as positive controls. HI represents co-treatment with heregulin and IGF-1.

substrates identified to be regulated by mTORC2 (refs 34,35), exhibited considerable reduction of both active and total Smad2/3 (Supplementary Fig. 6), effects that are completely different to that of either LY treatment or mTORC2 inhibition. Thus, the exact mechanisms by which mTORC2 regulates the phosphorylation of Smad2/3 linker residue await further elucidation.

Suppression of mTORC2 leads to more efficient DE formation. Consistent with the posited role for mTORC2 in regulating T220/T179 phosphorylation and inhibiting Smad2/3 activity, treatment of hESCs using a combination of AA and Torin yielded a substantial increase in the expression of endoderm genes (Fig. 7a,b), recapitulating the effects of AA–LY treatment, but with noticeably less cell death. Consequently, this led to both a more efficient DE differentiation and hepatocyte generation (Fig. 7c,d). Thus, the greater yield of DE cells in combination with the reduction in cytotoxicity makes AA–Torin a superior alternative to AA–LY treatment and provides compelling evidence to suggest that the mTORC2-mediated regulation of Smad2/3 linker phosphorylation is a critical mechanism accounting for the inhibitory effect of PI3K on Activin-induced DE differentiation.

Discussion

In the present study, we have identified a novel and direct role for PI3K/mTORC2 signalling in regulating the phosphorylation status of the Smad2/3 linker T220/T179 residue. This phosphorylation permits the recruitment of the E3 ubiquitin ligase Nedd4L to Smad2/3 upon their activation, which subsequently promotes the ubiquitin-mediated proteasomal degradation of active Smad2/3. PI3K/mTORC2-mediated degradation of active Smad2/3 curtails the duration and intensity of the Activin-Smad2/3 signal, which ultimately leads to the attrition of Activin-induced DE differentiation in hESCs.

Our results are in line with previous findings, in that ubiquitin-mediated proteasomal degradation of active Smad2/3 plays an important role in the regulation of TGF-β/Smad2/3 activity[22,23] and that the phosphorylation of Smad2/3 linker T220/T179 is critical for the recruitment of the E3 ubiquitin ligase Nedd4L[23]. However, we have found that the T220/T179 residue can be readily phosphorylated by PI3K/mTORC2 signalling in the absence of Smad2/3 activation and is thus independent of AA-induced CDK or Erk activation. Furthermore, this phosphorylation can only recruit Nedd4L efficiently upon Smad2/3 activation, thereby offering a mechanism by which preferential selectivity for active Smad2/3 degradation is established. In addition, TGF-β ligands are able to activate PI3K signalling through non-canonical means concurrently with the canonical activation of Smad2/3 (ref. 36), which may act as an internal regulative mechanism that prevents overactivation of Smad2/3. However, given that the majority of active Smad2/3 is still able to translocate into the nucleus despite the presence of

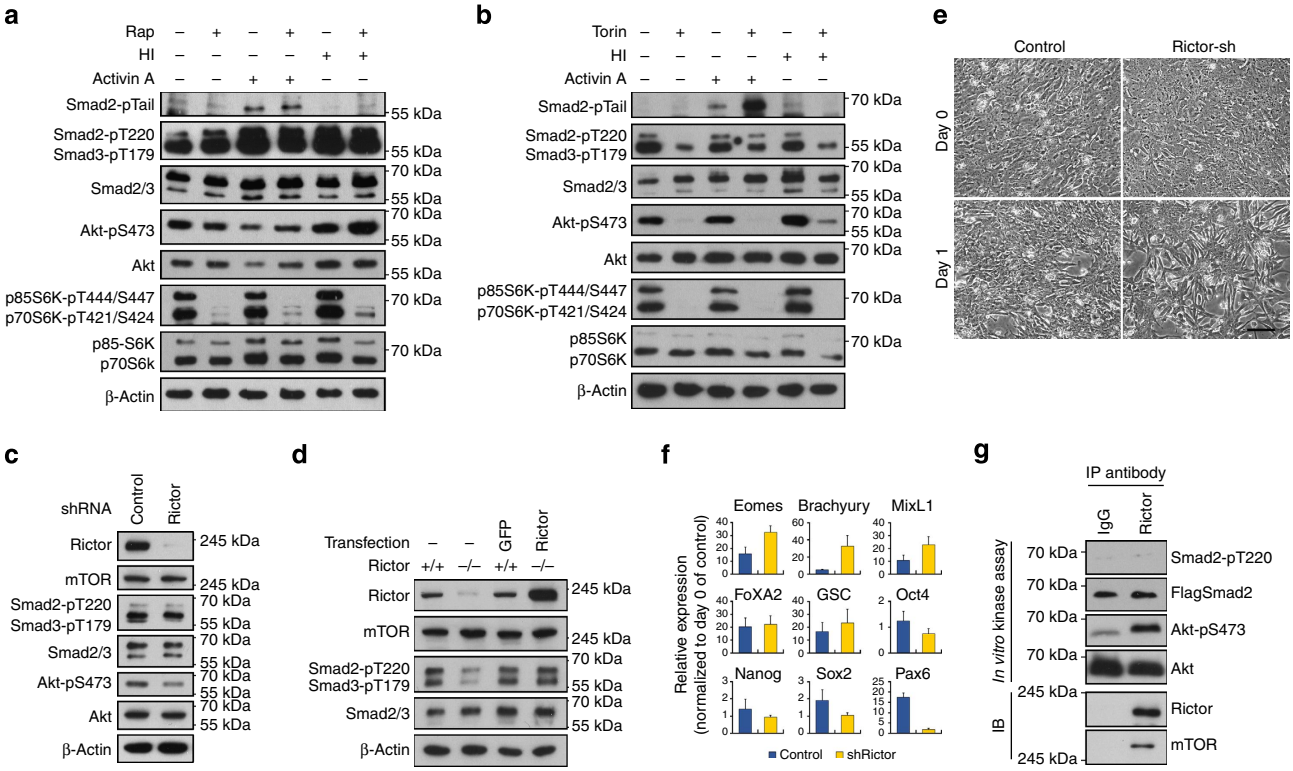

Figure 6 | mTORC2 regulates Smad2/3 activity by modulating the phosphorylation of T220/T179 residue. (**a**) Effect of rapamycin on Smad2/3 signalling. PC3 cells were treated with rapamycin in the presence of Activin A or HI for 6 h and then harvested for immunoblot with indicated antibodies. (**b**) Effect of Torin treatments on Activin-Smad2/3 signalling. Immunoblot of PC3 cells treated similar as in **a** but replacing rapamycin with Torin-2 (Torin). (**c**,**d**) Reduction of Smad2/3-pT220/T179 in rictor-shRNA knockdown PC3 cells (**c**) and in rictor null MEF (**d**). Ectopic expression of human rictor in rictor null MEF reverted the levels of Smad2/3-pT220/T179. (**e**,**f**) Knockdown of rictor in hESCs accelerated morphological changes associated with DE specification (**e**) and increased expression of DE markers (**f**) in response to Activin A. Scale bar, 100 μm. hESCs in **f** were treated with Activin A for 2 days before the analysis and data represent mean ± s.d. from at least six measurements of two independent experiments. (**g**) *In vitro* kinase assay of mTORC2 on Smad2-T220 phosphorylation. mTORC2 complexes were isolated by immunoprecipitation with rictor antibody and incubated with recombinant GST-Flag-Smad2 or inactive Akt in the presence of ATP. The protein mixtures were then resolved by SDS-polyacrylamide gel electrophoresis and analysed by immunoblot.

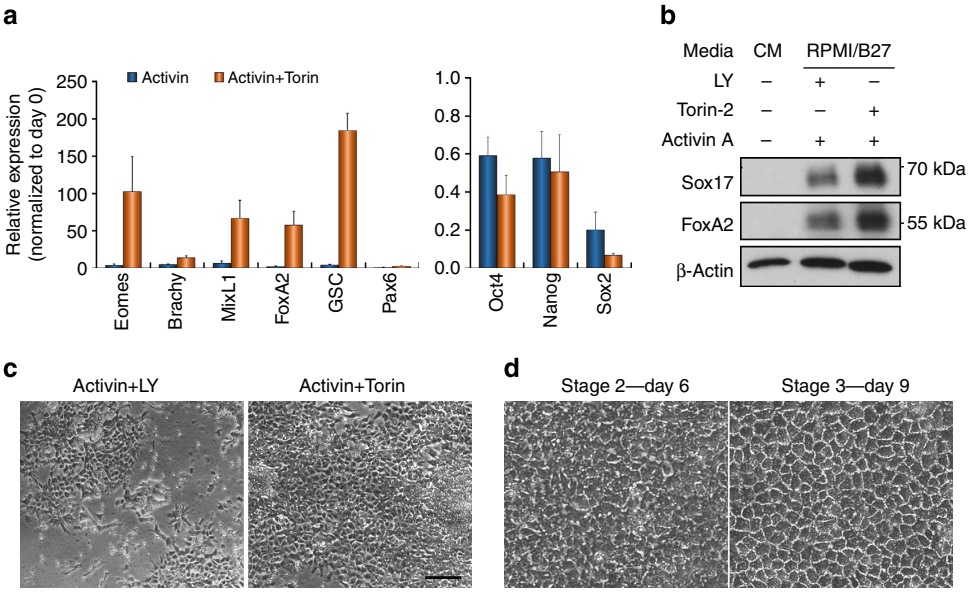

Figure 7 | Inhibition of mTOR enhances DE differentiation of hESCs. (**a**) qRT-PCR showing gene expression in hESCs treated with Activin A ± Torin for 2 days. Data represent mean ± s.d. of six measurements from two independent experiments. (**b**) Immunoblot showing protein expression in hESCs treated as in **a**. (**c**) Phase-contrast images of hESCs treated for 3 days with Activin A together with either LY or Torin. Scale bar, 100 μm. (**d**) Phase-contrast images of the cells from **c** that were further differentiated by a hepatic differentiation protocol as shown in Fig. 1. Days of differentiation are indicated. Scale bar, 50 μm.

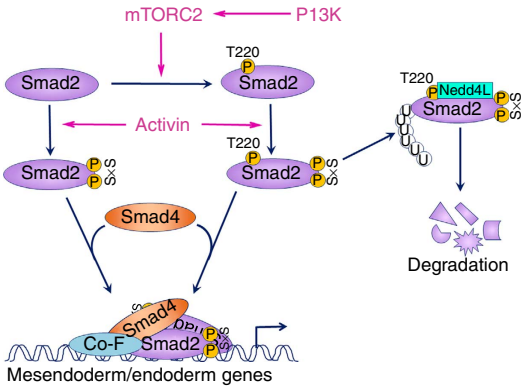

Figure 8 | Model depicting a possible mechanism accounting for the inhibitory effect of PI3K/mTORC2 on the Activin-induced DE differentiation of hESCs.

T220/T179 phosphorylation (Supplementary Fig. 4e), this suggests that additional factors that interact with active Smad2/3 may hinder the recruitment of Nedd4L and prevent their degradation. Receptor-mediated activation of Smad2/3 has been well characterized for inducing conformational changes that enable the homo- and heterodimerization of R-Smads, as well as interaction with Smad4. However, whether or not such interactions between the Smad2/3 and other factors can act to impede the recruitment of Nedd4L awaits further investigation. In any case, despite only a small proportion of the activated R-Smads being targeted for degradation, this appears to be sufficient in impeding the proper formation of DE from hESCs. To definitively establish that Smad2/3 linker phosphorylation mediates the mTORC2-dependent inhibition of DE differentiation of hESCs, one would need to generate hESCs with knock-ins of linker phospho-deficient or phospho-mimetic mutants of Smad2/3.

As shown in our experiments, AA–LY-induced enhancement of Smad2/3 activation in hESCs is only apparent at 3 h post treatment, despite the effectiveness of LY in reducing T220/T179 phosphorylation by 1 h of treatment. In explaining this discrepancy, it is probable that initially in the presence of abundant ligand (100 ng ml^{-1} AA) and persistent receptor activation[37], the rate of Smad2/3 activation outpaces that of its Nedd4L-mediated degradation, which consequently obscures the effect of LY-induced downregulation of T220/T179 phosphorylation in prolonging Smad2/3 activation. However, as the ligand availability diminishes with increasing time, the proportion of the active Smad2/3 that is targeted for Nedd4L-mediated degradation becomes increasingly higher relative to the total active Smad2/3 pool, which ultimately promotes the rapid downregulation of Smad2/3 activity (Fig. 8). In support of this, the LY-dependent effect on active Smad2/3 was shown to be evident at 1 h post treatment when a lower dose of ligand (10 ng ml^{-1} AA) is applied or when receptor activation is blocked by SB431542. Putting this in a biological context, during embryonic development where TGF-β/Nodal/Activin are at physiological levels, this PI3K/mTOR/Nedd4L-mediated degradation mechanism may act as an internal thermostat that regulates the amplitude of Smad2/3 induction and thereby allowing proper readout of the morphogenic gradient *in vivo*.

One important finding of this study is the identification of mTORC2 as a modulator of TGF-β signalling, specifically by regulating the phosphorylation of the Smad2/3 linker T220/T179 residue. In assessing the contribution of the previously identified linker kinases, Erk1/2 and CDK[24,26,27], we showed that when inhibited, neither could replicate the effects of PI3K inhibition. Furthermore, under certain conditions, LY-mediated inhibition of PI3K did not reduce, but rather enhanced the activation of Erk1/2. As such, enhancement of DE differentiation via downregulation T220/T179 phosphorylation and enhancement of Smad2/3 activity does not appear to be solely through an Erk/Wnt/β-catenin-mediated mechanism as outlined in a recent study[14], but is rather through a more distinct and direct mechanism. The PI3K pathway bifurcates at many points and constitutes a large family of serine/threonine kinases of which the best characterized are the Akt and mTOR branches. Our data have shown that Akt does not affect phosphorylation of Smad2/3-T220/T179, which is consistent with previous findings[8–10]. In manipulating mTORC2 activity using both inhibitor-based and genetic means, we have identified mTORC2 as a key player in the regulation of the linker T220/T179 phosphorylation opposed to mTORC1. Although it has been reported that inhibition of mTORC1 by rapamycin can enhance the DE specification of hESCs[38], chronic exposure of hESCs to rapamycin over several days will also inhibit mTORC2 activity[32], which may ultimately be the reason for the reported improvement in DE specification. Furthermore, since mTORC2 activation is mediated by PI3K[39], it is not surprising that the inhibition of PI3K signalling could lead to a cessation of mTORC2 kinase activity. Although mTORC2 immunoprecipitates could not phosphorylate the T220/T179 residue in an *in vitro* kinase reaction, this cannot completely exclude the possibility of mTORC2 being the direct kinase responsible for this phosphorylation, as the substrate recognition mechanisms of mTORC2 are still poorly defined[39,40]. Alternatively, mTORC2 may indeed act via indirect means through activation of downstream kinases that in turn regulate Smad2/3 linker phosphorylation; however, such kinases remain to be identified.

As a whole and to the best of our knowledge, we have for the first time identified a role for mTORC2 in mediating TGF-β/Activin signalling activities, and established a plausible mechanism through which mTORC2 activity directly impacts the Activin-induced DE differentiation of hESCs. Identification of mTORC2 as a key component of this mechanism not only provides new avenues through which hESC differentiation protocols can be improved, but also warrants the initiation of further studies into the impact of this mechanism on other TGF-β activities, adding to the growing repertoire of novel mTORC2 functions.

Methods

Cell culture and differentiation. H1 and H9 hESCs from WiCell were routinely cultured on Matrigel-coated plates in MEF conditioned medium (MEF-CM) supplemented with 10 ng ml^{-1} of bFGF[41]. DE differentiation was carried out as summarized in Fig. 1a[12]. When hESCs were grown to 70–80% confluency, MEF-CM was replaced with RPMI-1,640 supplemented with 1 × B27 (RPMI/B27 medium) containing Activin (100 ng ml^{-1}, PeproTech) and LY294002 (20 μM day 1 and 10 μM day 2 and 3, Sigma) or Torin-2 (15 nM, Tocris) or wortmannin (300 nM, Sigma) for 2–3 days with daily medium change (Supplementary Fig. 1b). For hepatocyte differentiation, cells were further cultured in knockout-DMEM (KO-DMEM) containing 20% KO serum replacement, 1 mM glutamine, 1% non-essential amino acids, 0.1 mM β-mercaptoethanol (all from Life Technologies) with either DMSO (1%, Sigma) or BMP2 (20 ng ml^{-1}, PeproTech) and bFGF (10 ng ml^{-1}, R&D systems) for another 4 days, followed by 3–5 days culture in L15 medium supplemented with 8.3% foetal bovine serum (FBS), 8.3% tryptose phosphate broth, 10 μM hydrocortisone 21-hemisuccinate, 1 μM insulin (all from Sigma), 50 μg ml^{-1} ascorbic acid and 2 mM glutamine containing 10 ng ml^{-1} hepatocyte growth factor (PeproTech) and 20 ng ml^{-1} oncostatin M (R&D systems). In the experiments using various inhibitors, hESCs were cultured in RPMI/B27 medium containing Activin (100 ng ml^{-1}) for 20 min following MEF-CM removal and 2 × PBS wash (Fig. 3a). The Activin-containing medium was then replaced with fresh RPMI/B27 containing the indicated inhibitors, and cells were harvested 1–6 h later as indicated. The following inhibitors were used: MG132 (10 μM) and okadaic acid (5 nM) from Merck/Millipore; SB431542 (10 μM) from Sigma; U0126 (10 μM) and SP600125 (500 nM) from Reagents

Direct; SB203580 (20 μM) from R&D systems, flavopiridol (1 μM) and GDC-0941 (200 nM), both from Selleck Bio.

PC3 cells were kindly provided by Dr Kypta of Imperial College London. Hep3B and HEK293T tumour cell lines were obtained from ATCC (HB8064 and CRL-3216, respectively). Rictor null and corresponding control MEF were a gift from Professor Magnuson, VUMC, Tennessee[33]. PC3 cells were cultured in RPMI-1,640 medium containing 10% FBS. Hep3B, HEK293T and transgenic MEF cells were cultured in DMEM containing 10% FBS. All reagents for tumour cell cultures are from Sigma. Treatment of PC3 cells were performed by starving the cells overnight in RPMI-1,640 medium and then treating them for 1 h with Activin (10 ng ml^{-1}) ± LY (20 μM) or indicated factors, including rapamycin (100 nM), LongR^3 IGF-1 (I, 200 ng ml^{-1}, both from Sigma), Heregulin (H, 10 ng ml^{-1}, PeproTech) and SGK inhibitor, GSK650394 (100 μM, Sigma).

All cell lines have been regularly checked for the absence of mycoplasma.

Plasmids. Expression vectors for WT Smad2 (pCS2-Flag-Smad2, #14042), active Akt (pcDNA3 Myr-HA-Akt1, #9008) Akt triple mutant (pcDNA3-T7-Akt-K179M/T308A/S473A, #9031) and Rictor (pRK-myc-Rictor #11367) were obtained from Professor J. Massague[42], Professor W. Sellers[43] and Professor D. Sabatini[44] through Addgene. Smad2 mutant T220V was generated by site-directed mutagenesis of pCS2-Flag-Smad2 using the Q5 Site-Directed Mutagenesis Kit (NEB) following the manufacturer's protocol, with the following oligonucleotides: forward primer 5′-GAGTAATTATATTCCAGAAGTGCCACCTCCTGGA TATATC-3′ and reverse primer 5′-TGTGGCTCAATTCCTGCTGG-3′. The resulting sequences were validated by bidirectional sequencing. Partially active Akt (S473A) plasmid was generated by subcloning to replace the *Blp*I/*Eco*RI fragment of pcDNA3-Myr-HA-Akt1 containing S473 with A473 from pcDNA3-T7-Akt1-K179M/T308A/S473A. Lentivector containing shNedd4L was generated by cloning shNedd4L oligonucleotides into modified pLVTHM expressing puro-2A-GFP complementary DNA (cDNA)[45]. The sequence of shNedd4L was as previously published[23]:
5′-GCTAGACTGTGGATTGAGTttcaagagaACTCAATCCACAGTCTAGCtttttgg aaa-3′. Lentivectors that contained two different shRNAs targeting Rictor within a pLKO.1 backbone were obtained from Addgene and used in combination to generate Rictor deficient lines. The sequences are as previously published[46]: 5′-ccggtCAGCCTTGAACTGTTTAActcgagTTAAACAGTTCAAGGCTGtttttg-3′ and 5′-ccggtACTTGTGAAGAATCGTATCTTctcgagAAGATACGATTCTTCACA AGTttttg-3′. Lentivectors containing non-targeting shGFP was used to generate control cells. GST-Flag-Smad2/Smad2-T220V plasmids were generated by inserting NcoI/XhoI fragment containing Flag-Smad2 or Flag-Smad2-T220V from their respective expression vectors into the pGEX-6p2 vector (GE Healthcare).

Transfection and lentiviral transduction. Hep3B cells and transgenic MEFs were grown to 70–90% confluency on the day of transfection. Akt or GFP expression plasmids were transfected using Lipofectamine LTX with PLUS reagent (Life Technologies) with modifications. In brief, for 1 × 10^6 tumour cells, 1.6 μg of kit-purified plasmid DNA was suspended in 50 μl of OptiMEM supplemented with 1.6 μl of PLUS reagent. In another tube, 4 μl of Lipofectamine LTX reagent was resuspended in another 50 μl of OptiMEM. Both tubes were incubated at room temperature for 5 min before being mixed together and incubated for a further 25 min. During this time, target cells were trypsinized, counted and pelleted before being directly resuspended in the transfection mix and incubated for 15 min. The transfection process was stopped upon the addition of growth media and cells were allowed to plate down overnight in the appropriate culture vessel. Cells were typically split 1:2–1:3 following transfection. Reagents were scaled up accordingly depending on the number of cells to be transfected. For hESCs and MEFs, lipofection was conducted following the accompanying manufacturer's instructions with a DNA to Lipofectamine LTX ratio of 1:3 and 1:10, respectively. Transfected Hep3B cells were starved overnight the following day and then treated with the appropriate reagents for 1 h before being harvested for analysis. Transfected MEFs were allowed to recover and proliferate for 48 h before being harvested for immunoblot.

Lentiviruses were produced by transient transfection of HEK293T cells with a lentivector containing the desired transgenic cDNA or shRNA, as well as pCMVΔ8.91 helper and pVSV-G envelope plasmids using standard protocols[47]. hESCs were split 1:3 the day of transduction by being dissociated with accutase (Sigma) into single cells and resuspended in MEF-CM supplemented with 10 μM ROCKi (Y-27632 or ROCK inhibitor, Reagents Direct) to prevent apoptosis induced by the loss of cell–cell contact[48]. The cells were incubated overnight with concentrated viral particles and consequently became infected as they were plating down. Forty-eight hours post infection, cells were selected with puromycin (2 μg ml^{-1}) and upon stable passaging, assessed for transgene expression or knockdown via immunoblot and quantitative reverse transcription (qRT–PCR), which was phenotypically assessed via DE differentiation.

Quantitative reverse transcription–PCR (qRT–PCR). Total RNAs were isolated from cells with TRI reagent (Sigma) and cDNA samples were synthesized with Protoscript II Reverse Transcriptase (NEB). qRT–PCR was performed in a DNA Engine Opticon (Bio-Rad) or Step One thermocycler (Applied BioSystems) using SYBR Green Jumpstart Taq Ready Mix (Sigma). Two housekeeping genes were used as normalizer. Two independent biological samples were used and multiple measurements were carried out for each treatment. Data were presented as mean ± s.d. for six measurements. A list of primers used in this study are provided in Supplementary Table 1.

Cytoplasmic/nuclear fractionation. Cells were harvested in cytoplasmic buffer (10 mM HEPES pH 7.9, 0.1 mM EDTA, 0.1 mM EGTA, 10 mM KCl and 0.5 mM dithiothreitol (DTT)) supplemented with phosphatase and protease inhibitors and allowed to swell on ice for 20 min after which Nonidet-P40 was added to a final concentration of 0.5%. Samples were quickly vortexed and centrifuged to pellet the cell nuclei. The supernatant was extracted and retained as the cytoplasmic fraction. The nuclear pellet was washed three times with cytoplasmic buffer to remove residual cytoplasmic contamination and resuspended in nuclear buffer (20 mM HEPES pH 7.9, 1 mM EDTA, 1 mM EGTA, 1 mM DTT and 0.4 M NaCl) before a final centrifugation at 15,000*g* to extract the nuclear fraction. Samples were quantified using bicinchoninic acid assay kit (Thermo Fisher Scientific) before being analysed by immunoblot.

Antibodies. The following are the primary antibodies used in this study; indicated dilutions refer to use in immunoblotting, unless otherwise stated: anti-Akt (#9727, 1:2,000), pAkt-S473 (#4060, 1:2,000), pAkt-T308 (#9275, 1:1,000), Erk1/2 (#9102, 1:1,000), pErk1/2-T202/Y204 (#9106, 1:1,000), mTOR (#2972, 1:1,000), pNedd4L-S448 (#8063, 1:1,000), P70S6K (#9202, 1:1,000), pP70S6K-T421/S424 (#9204, 1:1,000), pGSK3α/β-S21/9 (#9331, 1:1,000), pRb-S780 (#9307, 1:1,000), pSAPK/JNK-T183/Y185 (#4668, 1:1,000), Smad2 (#3122, 1:1,000), Smad2/3 (#3102, 1:1,000), pSmad2-S245/250/255 (#3104, 1:1,000), pSmad2-S465/467 (#3122, 1:1,000), Smad4 (#9515, 1:1,000) and Ubiquitin (#3936, 1:1,000) were from Cell Signalling/New England Biolabs; anti-Brachyury (AF2085, 1:500, IF:1:50), CXCR4-PE (FAB170P, 1:25) and Sox17 (MAB1924, 1:500, IF:1:100) were from R&D systems; anti-CLIC4 (sc-130723, 1:500), Lamin B (sc-365962, 1:500) and PPM1A (sc-56956, 1:500) were from Santa Cruz; anti-AFP (A8452, 1:500), β-actin (A5316, 1:5,000), Flag (F1804, 1:1,000) and GST (G7781, 1:1,000) were from Sigma; anti-pSmad2/3-T220/179 (AP3675a, 1:500) and pSmad3-S423/425 (EP823Y, #04-1042, 1:1,000) were from Abgent and Millipore, respectively; anti-β-tubulin (ab6046, 1:1,000), FoxA2 (ab60721, 1:200) and Nedd4L (ab131167, 1:5,000) were from Abcam; anti-albumin (A0001, 1:500) was from DAKO and anti-Rictor (A300-459A, 1:5,000) was from Bethyl Labs.

Secondary antibodies for immunostaining used were as follows: Alexa Fluor goat anti-mouse IgG 488, 1:400, Alexa Fluor goat anti-mouse IgG 568, 1:400, Alexa Fluor goat anti-rabbit IgG 488, 1:400 and Alexa Fluor donkey anti-goat IgG 488, 1:400 were from Life Technologies. For immunoblotting: goat anti-rabbit IgG-HRP, 1:2,000, goat anti-mouse IgG-HRP, 1:5,000, donkey anti-goat IgG-HRP, 1:5,000 were from Santa Cruz and goat anti-rabbit or mouse IgG-HRP (light-chain specific), 1:10,000 were from Jackson ImmunoResearch Laboratories. Isotope controls: normal mouse IgG2a and normal rabbit IgG were from Santa Cruz.

Immunostaining of hESCs. hESCs were split and cultured on Matrigel-coated Thermanox coverslips (Thermo Fisher Scientific) until the desired confluency was reached. Cells were then washed with Dulbecco's PBS (DPBS) and fixed for 10–20 min with 4% fresh paraformaldehyde solution. Excess paraformaldehyde was removed by washing three times with DPBS and the coverslips were then incubated with blocking/permeabilization buffer for 1 h followed by an overnight incubation with primary antibody at the appropriate dilution at 4 °C with tilting. The following day, coverslips were subjected to 10-min washes three times with DPBS, followed by a 40-min incubation with the appropriate fluorophore-conjugated secondary antibody in the dark. Coverslips were then subjected to two further 10 min washes with DPBS followed by a 10-min DPBS/4′,6 diamidino-2-phenylindole (DAPI) wash, with DAPI at a final concentration of 1 μg ml^{-1} to counterstain the nuclei. All washes were carried out in dark. Slides were mounted onto microscope slides using Mowiol 4–88 solution and allowed to dry overnight. Slides were visualized using a Leica SP5 II confocal fluorescent microscope typically at × 64 magnification.

Immunoblotting. Cells were harvested using RIPA (radio immunoprecipitation assay) buffer (50 mM Tris-HCl, pH 8.0, 150 mM NaCl, 1% Nonidet-P40, 0.5% sodium deoxycholate and 0.5% SDS) supplemented with phosphatase (Na_3VO_4, 1:100, NaF, 1:200 or phosphatase inhibitor cocktail 2, Sigma, 10 μl ml^{-1}) and protease inhibitors (phenylmethylsulphonyl fluoride in ethanol or protease inhibitor cocktail, Sigma). Proteins were purified by centrifugation at 15,000*g* at 4 °C for 20 min and then quantified using bicinchoninic acid assay kit (Thermo Fisher Scientific) and resolved on 7.5% Bis-Tris polyacrylamide gels, before being transferred onto polyvinylidene fluoride membranes via electroblotting. Blots were probed with primary antibody overnight followed by horseradish peroxidise (HRP)-conjugated secondary antibodies before being developed via enhanced chemiluminescent substrate and exposure onto CL-XPosure film (Thermo Fisher Scientific). Molecular weight markers (Thermo Fisher Scientific 11832124 or New England BioLab #7712) were run alongside all samples and values are as indicated in both the main and uncropped scans (Supplementary Fig. 7).

Co-immunoprecipitation of Nedd4L with Smad2. Cells were harvested in HEPES lysis buffer (40 mM HEPES pH 7.4, 10 mM EDTA and 10% glycerol) supplemented with phosphatase and protease inhibitors as per immunoblotting. Cell lysis was induced mechanically by repeatedly passing lysate through a 23-G needle on ice. Protein within lysates were purified by centrifugation at 13,000*g* at 4 °C for 10 min and quantified, with 1 mg used in the subsequent immunoprecipitation with Smad2 antibody for 90 min at 4 °C with rotation. Immunocomplexes were isolated with the lysates using Protein-G conjugated Dynabeads (Life Technologies) through a further 1 h incubation under the same conditions. Beads were then washed 3 times with cold HEPES lysis buffer to remove nonspecific binding prior to protein elution with 2 × Laemmli buffer. Elutes were subjected to immunoblotting and the co-immunoprecipitation assessed using relevant primary antibodies.

Smad2 ubiquitination assay. Cells were harvested in non-denaturing lysis buffer (20 mM Tris-HCl, pH 7.5, 150 mM NaCl, 1 mM EDTA, pH 8.0, 1 mM EGTA, pH 8.0 and 0.5% Nonidet-P40) supplemented with phosphatase and protease inhibitors as per immunoblotting. Lysates were additionally supplemented with 2 μM ubiquitin aldehyde (Boston Biochem) to prevent the action of deubiquitinating enzymes. Protein within lysates were purified and quantified, with 1 mg used in the subsequent immunoprecipitation with Smad2 antibody for 90 min at 4 °C with rotation. Immunocomplexes were isolated from the lysates using Protein-G conjugated Dynabeads through a further 1 h incubation under the same conditions. Beads were then washed 3 times with cold non-denaturing lysis buffer to remove nonspecific binding prior to protein elution with 2 × Laemmli buffer. Elutes were subjected to immunoblotting and the degree of ubiquitination was assessed using an anti-ubiquitin antibody.

Generation of recombinant GST-Flag-Smad2/Smad2-T220V. pGEX-6p2 vectors containing Flag-Smad2/Smad2-T220V cDNAs were transformed into BL-21 *E. coli* strain. Upon ampicillin selection, single colonies were used to inoculate overnight cultures, which were then subsequently used to inoculate new cultures the following day. Expression of GST-Flag-Smad2/Smad2-T220V was induced in these cultures using 0.1 M isopropyl β-D-1-thiogalactopyranoside (Sigma) once they reached mid-log phase growth ($OD_{550-600}$ ~ 0.6–1.0). Proteins were harvested via centrifugation and sonication, followed by immunoprecipitation with glutathione-conjugated magnetic beads (Thermo Fisher Scientific). Recombinant proteins were eluted from the beads in 50 mM Tris-HCl containing 10 mM reduced glutathione. Proteins were then taken for immunoblotting with the relevant antibodies to check for successful expression and then used as substrate for subsequent kinase assays.

Akt/Erk2 kinase assay. HEK293T or PC3 cells were harvested using non-denaturing lysis buffer (as per the Smad2 ubiquitination assay) to retain kinase activity and supplemented with phosphatase and protease inhibitors as per immunoblotting. Active Akt was immunoprecipitated using anti-pAkt (S473) antibody and was tested for kinase activity via incubation with recombinant GST-GSK3α/β fusion protein (NEB) as a substrate in kinase assay buffer (25 mM Tris-HCl, pH 7.5, 5 mM β-glycerophosphate, 2 mM DTT, 10 mM $MgCl_2$ and 200 mM ATP) for 40 min at 30 °C. Kinase assay was repeated using GST-Flag-Smad2/Smad2-T220V as substrate and phosphorylation of the linker region was analysed via immunoblotting with the appropriate primary antibody. As a positive control, GST-Flag-Smad2/Smad2-T220V proteins were incubated with Erk2 kinase (NEB) in the supplied buffer supplemented with 200 mM ATP and assessed for phosphorylation via immunoblotting.

mTORC2 kinase assay. The assay was carried out using previously described methods[46] with the following modifications. HEK293T or PC3 cells were harvested in mTORC lysis buffer (40 mM HEPES pH 7.5, 120 mM NaCl, 1 mM EDTA, 10 mM $Na_4P_2O_7$, 50 mM NaF and 0.5% Nonidet-P40) supplemented with phosphatase and protease inhibitors as per immunoblotting. Cells were gently lysed with rotation for 20 min at 4 °C after which 1 mg of total protein was used in the subsequent immunoprecipitation with Rictor antibody to selectively isolate mTORC2 over mTORC1. Immunoprecipitated complexes were washed 3 times with mTORC lysis buffer followed by washing with mTOR kinase assay buffer (25 mM HEPES, 100 mM potassium acetate, 1 mM $MgCl_2$ and 500 mM ATP) twice to remove residual detergent. mTORC2 complexes were incubated with λ-phosphatase-treated His6-tagged-Akt1 (Millipore) protein or GST-Flag-Smad2/Smad2-T220V recombinant proteins in mTORC kinase assay buffer for 40 min at 37 °C. Reactions were stopped upon the addition of 2 × Laemmli buffer, and the phosphorylation on Akt-S473 or SmadT220 residues was assessed by immunoblotting with the appropriate primary antibodies.

Luciferase assay. hESCs were split 1:6 into 12-well plates using the accutase/ROCKi method as above and allowed to reach 70–80% confluence prior to transfection. Both firefly pGL3-CAGA[12]-luc and renilla pRL-T7-renilla (Promega) plasmids were transfected at a ratio of 10:1 using Lipofectamine 2000 following the manufacturer's protocol. Forty-two hours post transfection, hESCs were differentiated for 6 h, harvested using accutase and dispensed into a 96-well luminometer plate. Luciferase assay was performed using the Dual-Glo luciferase assay kit (Promega) following the accompanying protocol. Both firefly and renilla luminescence was recorded using a Victor II luminometer (Perkin Elmer). Firefly luminescence readings were normalized with corresponding renilla luminescence readings to give representative luciferase expression values that are independent of transfection efficiency and cell number. Data presented are mean ± s.d. from three independent transfection experiments.

References

1. Massague, J. & Wotton, D. Transcriptional control by the TGF-beta/Smad signaling system. *EMBO J.* **19,** 1745–1754 (2000).
2. Schmierer, B. & Hill, C. S. TGFbeta-SMAD signal transduction: molecular specificity and functional flexibility. *Nat. Rev. Mol. Cell Biol.* **8,** 970–982 (2007).
3. Guo, X. & Wang, X. F. Signaling cross-talk between TGF-beta/BMP and other pathways. *Cell Res.* **19,** 71–88 (2009).
4. Feng, X. H. & Derynck, R. Specificity and versatility in tgf-beta signaling through Smads. *Annu. Rev. Cell Dev. Biol.* **21,** 659–693 (2005).
5. Massague, J. TGFbeta signalling in context. *Nat. Rev. Mol. Cell Biol.* **13,** 616–630 (2012).
6. Ross, S. & Hill, C. S. How the Smads regulate transcription. *Int. J. Biochem. Cell Biol.* **40,** 383–408 (2008).
7. Chen, R. H., Su, Y. H., Chuang, R. L. & Chang, T. Y. Suppression of transforming growth factor-beta-induced apoptosis through a phosphatidylinositol 3-kinase/Akt-dependent pathway. *Oncogene* **17,** 1959–1968 (1998).
8. Conery, A. R. *et al.* Akt interacts directly with Smad3 to regulate the sensitivity to TGF-beta induced apoptosis. *Nat. Cell Biol.* **6,** 366–372 (2004).
9. Remy, I., Montmarquette, A. & Michnick, S. W. PKB/Akt modulates TGF-beta signalling through a direct interaction with Smad3. *Nat. Cell Biol.* **6,** 358–365 (2004).
10. Song, K., Wang, H., Krebs, T. L. & Danielpour, D. Novel roles of Akt and mTOR in suppressing TGF-beta/ALK5-mediated Smad3 activation. *EMBO J.* **25,** 58–69 (2006).
11. D'Amour, K. A. *et al.* Efficient differentiation of human embryonic stem cells to definitive endoderm. *Nat. Biotechnol.* **23,** 1534–1541 (2005).
12. Hay, D. C. *et al.* Efficient differentiation of hepatocytes from human embryonic stem cells exhibiting markers recapitulating liver development in vivo. *Stem Cells* **26,** 894–902 (2008).
13. McLean, A. B. *et al.* Activin a efficiently specifies definitive endoderm from human embryonic stem cells only when phosphatidylinositol 3-kinase signaling is suppressed. *Stem Cells* **25,** 29–38 (2007).
14. Singh, A. M. *et al.* Signaling network crosstalk in human pluripotent cells: a Smad2/3-regulated switch that controls the balance between self-renewal and differentiation. *Cell Stem Cell* **10,** 312–326 (2012).
15. Chen, Y. G., Li, Z. & Wang, X. F. Where PI3K/Akt meets Smads: the crosstalk determines human embryonic stem cell fate. *Cell Stem Cell* **10,** 231–232 (2012).
16. Kubo, A. *et al.* Development of definitive endoderm from embryonic stem cells in culture. *Development* **131,** 1651–1662 (2004).
17. Teo, A. K. *et al.* Pluripotency factors regulate definitive endoderm specification through eomesodermin. *Genes Dev.* **25,** 238–250 (2011).
18. Brown, S. *et al.* Activin/Nodal signaling controls divergent transcriptional networks in human embryonic stem cells and in endoderm progenitors. *Stem Cells* **29,** 1176–1185 (2011).
19. Lin, X. *et al.* PPM1A functions as a Smad phosphatase to terminate TGFbeta signaling. *Cell* **125,** 915–928 (2006).
20. Shukla, A. *et al.* TGF-beta signalling is regulated by Schnurri-2-dependent nuclear translocation of CLIC4 and consequent stabilization of phospho-Smad2 and 3. *Nat. Cell Biol.* **11,** 777–784 (2009).
21. Bruce, D. L., Macartney, T., Yong, W., Shou, W. & Sapkota, G. P. Protein phosphatase 5 modulates SMAD3 function in the transforming growth factor-beta pathway. *Cell Signal.* **24,** 1999–2006 (2012).
22. Lo, R. S. & Massague, J. Ubiquitin-dependent degradation of TGF-beta-activated smad2. *Nat. Cell Biol.* **1,** 472–478 (1999).
23. Gao, S. *et al.* Ubiquitin ligase Nedd4L targets activated Smad2/3 to limit TGF-beta signaling. *Mol. Cell* **36,** 457–468 (2009).
24. Alarcon, C. *et al.* Nuclear CDKs drive Smad transcriptional activation and turnover in BMP and TGF-beta pathways. *Cell* **139,** 757–769 (2009).
25. Kamaraju, A. K. & Roberts, A. B. Role of Rho/ROCK and p38 MAP kinase pathways in transforming growth factor-beta-mediated Smad-dependent growth inhibition of human breast carcinoma cells in vivo. *J. Biol. Chem.* **280,** 1024–1036 (2005).
26. Kretzschmar, M., Doody, J., Timokhina, I. & Massague, J. A mechanism of repression of TGFbeta/ Smad signaling by oncogenic Ras. *Genes Dev.* **13,** 804–816 (1999).
27. Matsuura, I. *et al.* Cyclin-dependent kinases regulate the antiproliferative function of Smads. *Nature* **430,** 226–231 (2004).
28. Yamagata, H. *et al.* Acceleration of Smad2 and Smad3 phosphorylation via c-Jun NH(2)-terminal kinase during human colorectal carcinogenesis. *Cancer Res.* **65,** 157–165 (2005).

29. Grimm, O. H. & Gurdon, J. B. Nuclear exclusion of Smad2 is a mechanism leading to loss of competence. *Nat. Cell Biol.* **4,** 519–522 (2002).
30. Wrighton, K. H., Lin, X. & Feng, X. H. Phospho-control of TGF-beta superfamily signaling. *Cell Res.* **19,** 8–20 (2009).
31. Lamming, D. W. & Sabatini, D. M. A central role for mTOR in lipid homeostasis. *Cell Metab.* **18,** 465–469 (2013).
32. Sarbassov, D. D. *et al.* Prolonged rapamycin treatment inhibits mTORC2 assembly and Akt/PKB. *Mol. Cell* **22,** 159–168 (2006).
33. Shiota, C., Woo, J. T., Lindner, J., Shelton, K. D. & Magnuson, M. A. Multiallelic disruption of the rictor gene in mice reveals that mTOR complex 2 is essential for fetal growth and viability. *Dev. Cell* **11,** 583–589 (2006).
34. Garcia-Martinez, J. M. & Alessi, D. R. mTOR complex 2 (mTORC2) controls hydrophobic motif phosphorylation and activation of serum- and glucocorticoid-induced protein kinase 1 (SGK1). *Biochem. J.* **416,** 375–385 (2008).
35. Heikamp, E. B. *et al.* The AGC kinase SGK1 regulates TH1 and TH2 differentiation downstream of the mTORC2 complex. *Nat. Immunol.* **15,** 457–464 (2014).
36. Derynck, R. & Zhang, Y. E. Smad-dependent and Smad-independent pathways in TGF-beta family signalling. *Nature* **425,** 577–584 (2003).
37. Inman, G. J., Nicolas, F. J. & Hill, C. S. Nucleocytoplasmic shuttling of Smads 2, 3, and 4 permits sensing of TGF-beta receptor activity. *Mol. Cell* **10,** 283–294 (2002).
38. Zhou, J. *et al.* mTOR supports long-term self-renewal and suppresses mesoderm and endoderm activities of human embryonic stem cells. *Proc. Natl Acad. Sci. USA* **106,** 7840–7845 (2009).
39. Zinzalla, V., Stracka, D., Oppliger, W. & Hall, M. N. Activation of mTORC2 by association with the ribosome. *Cell* **144,** 757–768 (2011).
40. Oh, W. J. *et al.* mTORC2 can associate with ribosomes to promote cotranslational phosphorylation and stability of nascent Akt polypeptide. *EMBO J.* **29,** 3939–3951 (2010).
41. Gerrard, L., Zhao, D., Clark, A. J. & Cui, W. Stably transfected human embryonic stem cell clones express OCT4-specific green fluorescent protein and maintain self-renewal and pluripotency. *Stem Cells* **23,** 124–133 (2005).
42. Hata, A., Lo, R. S., Wotton, D., Lagna, G. & Massague, J. Mutations increasing autoinhibition inactivate tumour suppressors Smad2 and Smad4. *Nature* **388,** 82–87 (1997).
43. Ramaswamy, S. *et al.* Regulation of G1 progression by the PTEN tumor suppressor protein is linked to inhibition of the phosphatidylinositol 3-kinase/Akt pathway. *Proc. Natl Acad. Sci. USA* **96,** 2110–2115 (1999).
44. Sarbassov, D. D. *et al.* Rictor, a novel binding partner of mTOR, defines a rapamycin-insensitive and raptor-independent pathway that regulates the cytoskeleton. *Curr. Biol.* **14,** 1296–1302 (2004).
45. Ovando-Roche, P., Yu, J. S., Testori, S., Ho, C. & Cui, W. TRF2-mediated stabilization of hREST4 is critical for the differentiation and maintenance of neural progenitors. *Stem Cells* **32,** 2111–2122 (2014).
46. Sarbassov, D. D., Guertin, D. A., Ali, S. M. & Sabatini, D. M. Phosphorylation and regulation of Akt/PKB by the rictor-mTOR complex. *Science* **307,** 1098–1101 (2005).
47. Szulc, J., Wiznerowicz, M., Sauvain, M. O., Trono, D. & Aebischer, P. A versatile tool for conditional gene expression and knockdown. *Nat. Methods* **3,** 109–116 (2006).
48. Watanabe, K. *et al.* A ROCK inhibitor permits survival of dissociated human embryonic stem cells. *Nat. Biotechnol.* **25,** 681–686 (2007).

Acknowledgements

We thank Professor M.A. Magnuson, VUMC, Tennessee, for kindly providing rictor null MEFs. We also thank our colleagues here at Imperial College London: Professor V. Episkopou for the pGL3-CAGA$_{12}$-luc construct; Professor E. Lam for the p70S6K antibodies, Dr R. Kypta for PC3 cells; Professors V. Episkopou, M. Parker and Dr R. Kypta for their helpful discussions. The work was supported by UK MRC and Genesis Research Trust. T.S.R. was supported by a studentship from University of Malaya/Ministry of Higher Education, Malaysia.

Author contributions

J.S.L.Y. and W.C. conceived the study and designed experiments. T.S.R. and J.S.L.Y. performed hESC differentiation experiments and analysis. N.M. and R.C. generated mutant Smad2 construct and recombinant Smad2 protein. M.K.H. characterized the response of PC3 cells to PI3K/TGF-β. J.S.L.Y. and S.-K.W. analysed the molecular mechanisms between Smad2/3 and Nedd4L, Akt and mTORC2. W.C. and J.S.L.Y. wrote the manuscript.

Additional information

Supplementary Information accompanies this paper at http://www.nature.com/naturecommunications

Competing financial interests: The authors declare no competing financial interests.

Reprints and permission information is available online at http://npg.nature.com/reprintsandpermissions/

How to cite this article: Yu, J. S. L. *et al.* PI3K/mTORC2 regulates TGF-β/Activin signalling by modulating Smad2/3 activity via linker phosphorylation. *Nat. Commun.* 6:7212 doi: 10.1038/ncomms8212 (2015).